Universität Potsdam
Lehrstuhl Für Wahrscheinlichkeitstheorie

Université de Lille 1
École doctorale Sciences pour l'Ingénieur
Laboratoire de Mathématiques Paul Painlevé

RTG 1845, Stochastic Analysis with Applications
in Biology, Finance and Physics

On the Exact Simulation of (Skew) Brownian Diffusions with Discontinuous Drift

Dissertation eingereicht von

Thèse de Doctorat présentée par

Sara Mazzonetto

zur Erlangung des akademischen Grades
"doctor rerum naturalium"
(Dr. rer. nat.)
in der Wissenschaftsdisziplin Stochastik

pour obtenir le grade de
"Docteur en Mathématiques Appliquées"

Defended on November, 8th 2016 in Potsdam,
in front of a committee composed by:

Antoine	Lejay	Université de Lorraine	Rapporteur
Arnulf	Jentzen	ETH Zürich	Rapporteur
Gilles	Blanchard	Universität Potsdam	President
Noemi	Kurt	Technische Universität Berlin	Examinatrice
Michael	Scheutzow	Technische Universität Berlin	Examinateur
Thomas	Simon	Université Lille 1	Examinateur
David	Dereudre	Université Lille 1	Directeur
Sylvie	Rœlly	Universität Potsdam	Directrice

Published online at the
Institutional Repository of the University of Potsdam:
URN urn:nbn:de:kobv:517-opus4-102399
http://nbn-resolving.de/urn:nbn:de:kobv:517-opus4-102399

Summary

This thesis is focused on the study and the *exact simulation* of two classes of real-valued Brownian diffusions: *multi-skew* Brownian motions with constant drift and Brownian *diffusions whose drift admits a finite number of jumps*.

The skew Brownian motion was introduced in the sixties by Itô and McKean, who constructed it from the reflected Brownian motion, flipping its excursions from the origin with a given probability. Such a process behaves as the original one except at the point 0, which plays the role of a semipermeable barrier. More generally, a skew diffusion with several semipermeable barriers, called multi-skew diffusion, is a diffusion everywhere except when it reaches one of the barriers, where it is partially reflected with a probability depending on that particular barrier. Clearly, a multi-skew diffusion can be characterized either as solution of a stochastic differential equation involving weighted local times (these terms providing the semi-permeability) or by its infinitesimal generator as Markov process.

In this thesis we first obtain a contour integral representation for the transition semigroup of the multi-skew Brownian motion with constant drift, based on a fine analysis of its complex properties. Thanks to this representation we write explicitly the *transition densities of the two-skew Brownian motion with constant drift* as an infinite series involving, in particular, Gaussian functions and their tails.

Then we propose a new useful application of a generalization of the known rejection sampling method. Recall that this basic algorithm allows to sample from a density as soon as one finds an - easy to sample - instrumental density verifying that the ratio between the goal and the instrumental densities is a bounded function. The *generalized rejection sampling* method allows to sample *exactly* from densities for which indeed only an approximation is known. The originality of the algorithm lies in the fact that one finally samples directly from the law without any approximation, except the machine's.
As an application, we sample from the transition density of the two-skew Brownian motion with or without constant drift. The instrumental density is the transition density of the Brownian motion with constant drift, and we provide an useful uniform bound for the ratio of the densities. We also present numerical simulations to study the efficiency of the algorithm.

The second aim of this thesis is to develop an exact simulation algorithm for a Brownian diffusion whose *drift admits several jumps*. In the literature, so far only the case of a continuous drift (resp. of a drift with one finite jump) was treated. The theoretical method we give allows to deal with any finite number of discontinuities. Then we focus on the case of two jumps, using the transition densities of the two-skew Brownian motion obtained before. Various examples are presented and the efficiency of our approach is discussed.

Zusammenfassung

Über die exakte Simulation (skew) Brownsche Diffusionen mit unstetiger Drift

In dieser Dissertation wird die *exakte Simulation* zweier Klassen reeller Brownscher Diffusionen untersucht: die *multi-skew Brownsche Bewegung mit konstanter Drift* sowie die *Brownsche Diffusionen mit einer Drift mit endlich vielen Sprüngen*.

Die skew Brownsche Bewegung wurde in den sechzigern Jahren von Itô and McKean als eine Brownsche Bewegung eingeführt, für die die Richtung ihrer Exkursionen am Ursprung zufällig mit einer gegebenen Wahrscheinlichkeit ausgewürfelt wird. Solche asymmetrischen Prozesse verhalten sich im Wesentlichen wie der Originalprozess außer bei 0, das sich wie eine semipermeable Barriere verhält. Allgemeiner sind skew Diffusionsprozesse mit mehreren semipermeablen Barrieren, auch multi-skew Diffusionen genannt, Diffusionsprozesse mit Ausnahme an den Barrieren, wo sie jeweils teilweise reflektiert wird. Natürlich ist eine multi-skew Diffusion durch eine stochastische Differentialgleichung mit Lokalzeiten (diese bewirken die Semipermeabilität) oder durch ihren infinitesimalen Generator als Markov Prozess charakterisiert.

In dieser Arbeit leiten wir zunächst eine Konturintegraldarstellung der Übergangshalbgruppe der multi-skew Brownschen Bewegung mit konstanter Drift durch eine feine Analyse ihrer komplexen Eigenschaften her. Dank dieser Darstellung wird eine explizite Darstellung der Übergangswahrscheinlichkeiten der zweifach-skew Brownschen Bewegung mit konstanter Drift als eine unendliche Reihe Gaußscher Dichten erhalten.

Anschließend wird eine nützliche Verallgemeinerung der bekannten Verwerfungsmethode vorgestellt. Dieses grundlegende Verfahren ermöglicht Realisierungen von Zufallsvariablen, sobald man eine leicht zu simulierende Zufallsvariable derart findet, dass der Quotient der Dichten beider Zufallsvariablen beschränkt ist. Unsere *verallgmeinerte Verwerfungsmethode* erlaubt eine *exakte Simulation* für Dichten, die nur approximiert werden können. Die Originalität unseres Verfahrens liegt nun darin, dass wir, abgesehen von der rechnerbedingten Approximation, exakt von der Verteilung ohne Approximation simulieren.
In einer Anwendung simulieren wir die zweifach-skew Brownsche Bewegung mit oder ohne konstanter Drift. Die Ausgangsdichte ist dabei die der Brownschen Bewegung mit konstanter Drift, und wir geben gleichmäßige Schranken des Quotienten der Dichten an. Dazu werden numerische Simulationen gezeigt, um die Leistungsfähigkeit des Verfahrens zu demonstrieren.

Das zweite Ziel dieser Arbeit ist die Entwicklung eines exakten Simulationsverfahrens für Brownsche Diffusionen, deren Drift mehrere Sprünge hat. In der Literatur wurden bisher nur Diffusionen mit stetiger Drift bzw. mit einer Drift mit höchstens einem Sprung behandelt. Unser Verfahren erlaubt den Umgang mit jeder endlichen Anzahl von Sprüngen. Insbesondere wird der Fall zweier Sprünge behandelt, da unser Simulationsverfahren mit den bereits erhaltenen Übergangswahrscheinlichkeiten der zweifach-skew Brownschen Bewegung verwandt ist. An mehreren Beispielen demonstrieren wir die Effizienz unseres Ansatzes.

Résumé

Simulation exacte de diffusions browniennes (biaisées) avec dérive discontinue

Cette thèse de doctorat consiste en l'étude et en la *simulation exacte* de deux classes de diffusions browniennes à valeurs réelles: le mouvement brownien *biaisé en plusieurs points* et les diffusions browniennes avec *dérive admettant un nombre fini de sauts*.

Le *mouvement brownien biaisé* a été construit dans les années soixantes par Itô et McKean à partir du mouvement brownien réfléchi, en retournant chacune de ses excursions indépendamment et avec une probabilité donnée. Ce processus markovien admet un comportement semblable au processus original, excepté au point 0 où le biais se produit, et qui joue le rôle de barrière semi-perméable. Plus généralement, on appelle diffusion *biaisée en plusieurs points* une diffusion évoluant entre plusieurs barrières semi-perméables. Lorsqu'une telle diffusion atteint l'une de ces barrières, elle est partiellement réfléchie, avec une probabilité dépendant de la barrière. Une diffusion biaisée peut être caractérisée comme solution d'une équation différentielle stochastique incluant des temps locaux pondérés (en relation avec les coefficients de semi-perméabilité) ou par son générateur infinitésimal.

Dans cette thèse nous obtenons tout d'abord une représentation du semi-groupe de transition du mouvement brownien biaisé avec dérive constante sous la forme d'une intégrale de contour, grâce à l'étude fine des propriétés complexes de ce semi-groupe. Cette représentation nous fournit alors une formule explicite et novatrice pour la *densité de transition du mouvement brownien avec dérive constante biaisé en deux points*. L'expression de cette densité consiste en une série de fonctions gaussiennes et spéciales.
Nous proposons dans un deuxième temps une nouvelle application d'une *méthode généralisée de simulation par rejet*. La méthode classique permet de simuler à partir d'une densité f. Elle s'applique lorsque l'on peut identifier une densité facilement simulable, dite instrumentale, par rapport à laquelle la densité f est bornée. La généralisation offre la possibilité d'échantilloner *de façon exacte* à partir d'une densité, même si elle n'est connue que par approximation, sans aucune autre erreur que celles de l'ordinateur.
Nous appliquons ensuite ce schéma à la simulation d'un mouvement brownien avec dérive constante, biaisé en deux points. La densité instrumentale choisie est alors celle du mouvement brownien (non biaisé) avec dérive constante. Chemin faisant, nous obtenons une borne uniforme pour le quotient de ces deux densités. Nous présentons également des simulations numériques qui permettent d'étudier l'efficacité de l'algorithme.

Un autre objectif de la thèse est de développer un algorithme de simulation exacte pour les diffusions browniennes avec dérive admettant plusieurs sauts. Dans la littérature mathématique actuelle seul le cas de dérives continues (respectivement dérives admettant un seul saut) a été traité. La méthode théorique proposée permet d'étendre l'étude à un nombre quelconque de discontinuités. Nous nous concentrons sur le cas de dérives à deux sauts, car pour la simulation nous utilisons l'expression explicite de la densité de transition du mouvement brownien biaisé en deux points obtenue précédemment. Des exemples variés sont présentés et l'efficacité de la méthode est discutée.

Acknowledgments

First of all I would like to thank my advisors Sylvie Rœlly and David Dereudre. I am extremely grateful to you for sharing with me your intuitions. You are remarkably patient, encouraging and above all inspiring. I have spent more time with Sylvie Rœlly who is a person of extraordinary humanity, and I can recognize her trademark in David Dereudre. I am every day more glad to have had such advisors and I will keep taking inspirations from you and the way you work.
I will tell myself, all the time, *"il faut prendre le lecteur par la main"*.

During these three years I had the occasions to encounter and present my work to various mathematicians. I appreciated their suggestions and comments, I would like to thank them all. Thanks to Markus Klein, who gave me a nice and useful overview of functional analysis, and who has patiently answered all my questions and doubts together with Elke Rosenberger. Thanks to Patrick Cattiaux, Pierre Étoré and Andrej Pilipenko for food for thought and references. Lionel Lenôtre too pointed out lots of references and have organized many helpful discussions about open problems. I want to thank him for his contagious mathematical energy and the help with the code style.
I owe my gratitude to the referees Arnulf Jentzen and Antoine Lejay for reading carefully this document and discussing some key points with me. Since I have met them I have always had the occasion to profit from their precious advises and their mathematical experience. Thank you very much.

I am grateful to the *RTG 1845 Stochastic Analysis and Applications in Biology, Finance and Physics*, the *Deutsch-Französische Hochschüle/Université Franco-Allemande*, the *Berlin Mathematical School*, the *Laboratoire Paul Painlevé* and the *Labex Centre Européenne pour le Mathématique, la Physique et leurs Interactions (ANR-11-LABX-0007-01)*, for the financial support me and my advisors have enjoyed during this research period and the opportunity to conduct my research in such a stimulating environment.

I consider myself lucky to have met so many people who I value professionally and personally. I think most of you know how happy I am to have shared with you the last years and that if they were the best years of my life it is also because I have met you.

In the RTG group I already knew Giuseppe and Massimo, but other compatriots from Padua have surprisingly been among the most important person for me: Alessandra, Alberto and Giovanni. I am glad to have shared with them times of work and leisure, as I have done with Jenny, Mathias and Matti who are, as I use to say, "my favorite Germans". I am not forgetting the others super nice guys Alexandra, Marzia, Alexandros, Ammar, Eugenio, Florian, Moritz...

I shared the office with many other people and each one of them has left me a joyous mark. In particular in Potsdam Tania, Laure, Maksym and Giovanni again and in Lille Simon, Faicel and (unofficially) Pierre.

I have always felt welcome and comfortable in the Laboratoire Paul Painlevé. I have enjoyed the *group de travail* in stochastic geometry and the company of Charlotte, Pierre, Simon and Geoffrey have made every moment entertaining. I am looking forward to coming back in Lille for another year with Simon et Pierre, Celine, Emilie, Ha...

A special thank to my nurses Giorgia, Leila, Nadia and Oliver who are always there for me to cure dance mishaps and mathematical moods. You are the reason why I feel at home in Potsdam, I love you so much.

My dear Chiara, Valentina and Veronica... Trieste, Vazzola or Birmingham or New Zeland, Padua or Bruxelles, wherever we are we have always been close. Every time I talk to you, even if only by phone or Skype, my day brightens a little. I hope we will see each other in person more often.

A hug to Silvia and Stefano, Serena, Diana and Anna, you always cheered me up when I came back in Zero Branco and you have always reminded me how important is to relax from time to time.

I cannot forget Gas, Anna and Bepi, Marisa for being close to my mum and for having reminded me the importance of family together with Alessio, all uncles, aunts and cousins from my mother's side.

Thanks Denis! It is useless telling you how grateful I am to you for your helpfulness and understanding in every aspects of my life. On a less poetic note if the reader will not find so many typos or grammar mistakes it is also thanks to you. Thank you for your unconditional love, in the last more than nine years I have felt it in any moment in which you were not far away from me...

Finally I would like to thank my mum, Marita, who always supports, encourages and puts up with me. Mum, every time I realize how much you are proud of me I feel the need to tell you how much I am proud of you. Everything in my thesis, my life, my whole being is dedicated to you.

Contents

Introduction **i**

1 The one-skew Brownian motion with constant drift: various approaches to compute its transition density **1**
1.1 The framework . . . 1
1.1.1 The one-skew Brownian motion . . . 1
1.1.2 The (one-)skew Brownian motion with constant drift . . . 3
1.2 An approach via the path decomposition of the SBM and its local time . . . 4
1.3 An approach via the Laplace transform of the resolvent of the infinitesimal generator . . . 4
1.3.1 About the infinitesimal generator . . . 4
1.3.2 Integral representation of the semigroup through Green's function of the resolvent . 8
1.3.3 Explicit computation of Green's function in our framework . . . 9
1.3.4 First method: computing the residues . . . 11
1.3.5 Second method: contour integral . . . 14
1.4 About the case of piecewise constant drift . . . 17

2 The multi-skew Brownian diffusions **19**
2.1 The framework . . . 19
2.2 The transition density of the two-skew Brownian motion . . . 20
2.2.1 Green's function of the resolvent . . . 21
2.2.2 The explicit representation of the transition density . . . 22
2.2.3 Interpretation as an additive perturbation of the transition density of the Brownian motion . . . 25
2.3 The transition density of the two-SBM with constant drift . . . 25
2.3.1 Green's function of the resolvent . . . 25
2.3.2 Some preliminary lemmas . . . 27
2.3.3 The main result . . . 29
2.3.4 Degenerate cases and special cases . . . 35
2.4 Towards the transition density of the multi-skew Brownian diffusions . . . 36
2.5 Simulations . . . 39
2.5.1 Generalized rejection sampling method . . . 39
2.5.2 A Gaussian bound for the transition density . . . 42
2.5.3 Sampling from the density: the two-skew Brownian motion . . . 46

3 Brownian diffusions with drift admitting several jumps: an exact simulation **49**
3.1 The framework . . . 49
3.1.1 The measures involved: definitions and notations . . . 50
3.1.2 Useful theorems . . . 50
3.1.3 Assumptions on the drift . . . 52
3.2 Existing results for drifts admitting a unique jump . . . 52
3.2.1 Retrospective rejection sampling scheme . . . 52
3.2.2 Looking for the instrumental measure $\mathfrak{Q}$ . . . 53

3.2.3 Sampling via a convergence of schemes for skew Brownian motions 54
3.2.4 Sampling from the joint distribution of Brownian motions and its local times 54
3.3 On the way: the exact simulation scheme of a multi-skew Brownian diffusion whose drift admits jumps 55
3.3.1 The instrumental measure 56
3.3.2 Simulation of $\mathfrak{Q}^{(\beta_1,\dots,\beta_n)}$ 57
3.4 A drift with two or more jumps: exact simulation scheme for the associated Brownian diffusion 58
3.4.1 The exact simulation scheme of $\mathbb{P}_b$ as a limit scheme 58
3.4.2 The limit of the SBM 59
3.4.3 A uniform bound for $v^{(\theta_1,\theta_2)}$ 60
3.4.4 Sampling from the instrumental measure $\mathfrak{Q}$ 63
3.5 Simulations 65
3.5.1 The generalized rejection sampling for sampling under $\mathfrak{Q}$ (GRS) 65
3.5.2 The retrospective rejection sampling 66
3.5.3 Numerical results 67

4 Possible extensions and open questions **71**
4.1 More on the transition density of general skew diffusions 71
4.1.1 Towards an explicit expression 71
4.1.2 Its Gaussian bound 73
4.1.3 The Brownian motion with piecewise constant drift 73
4.2 Exact simulation of skew diffusions 73
4.2.1 The multi-skew Brownian motion, a new method for drawing a path 73
4.2.2 Possible improvements of the exact simulation of the Brownian motion with discontinuous drift 74
4.2.3 Skew Brownian diffusions with discontinuous drift 74
4.2.4 Numerical comparisons with other recent methods 74
4.3 ... and other unexplored dimensions! 75

A Codes **77**

Bibliography **96**

Introduction

Many applications in Applied Sciences require simulations of random diffusions, in particular when the complexity of the models makes impossible a theoretical analysis. For this reason, properties of the models are mainly studied using massive Monte Carlo methods. Diffusions whose coefficients are discontinuous emerged recently in geophysics or medical imaging, when the medium is very rough (or shows a high heterogeneity). Indeed, when the local properties of the matter or tissues change abruptly, it leads to discontinuous parameters in the diffusions. Moreover, such discontinuities appear also in financial modeling, due to the strong increase in the reactivity of markets.

The first classic algorithms for such simulations are the Euler-Maruyama one and all its variants. These approximation algorithms provide non exact simulations whose error one needs to control. It is well known that, in the case of diffusions with Lipschitz coefficients, the approximations converge to the original process, but this is no longer the case when the coefficients are not regular. Moreover the rate of convergence may depend on the nature of the singularities. For a nice summary of the state of the art of approximation methods in case of non-globally Lipschitz coefficients, we refer the reader to the introduction of Ankirchner, Kruse and Urusov [1] or to a comprehensive and easy-to-follow memoir by Hutzenthaler and Jentzen [26].

The point of view of *exact simulation* is quite different. The challenge is to simulate directly from the law of the diffusion, sampling exactly from its finite-dimensional distributions without approximations (beyond the machine's). The advantage of these algorithms is obvious since it allows to avoid the fine analysis of approximation errors. The disadvantage lies in the theoretical and computational complexity inherent in such algorithms. Notice also the existence of mixed method like the quasi-exact one proposed by Lenôtre [40].
The exact simulation is a quite popular topic in many domains. Recall the famous "coupling from the past" method by Propp and Wilson ('96), which provided a perfect sampling of statistical mechanics models. The exact approach is a new topic in the setting of diffusions. It is quite unexplored and not the object of comparison with other methods yet. There are only a few results available in case of real-valued Brownian diffusions (i.e. diffusions with unitary diffusion coefficient): either for drift which are continuous (see Beskos, Papaspiliopoulos and Roberts [9]) or for drift admitting only one jump (treated recently by Étoré and Martinez [20] or by Papaspiliopoulos, Roberts and Taylor [48]).
We think that exact simulation schemes for diffusions are going to be more and more useful in the future, therefore a systematic analysis is needed. The aim of this thesis is producing a step in this direction.

The scheme provided in Chapter 3, which is inspired by [20], gives a theoretical simulation method for a real-valued Brownian *diffusion whose drift admits a finite number of jumps*. As will be explained in Section 3.3, it is based on properties of a process, called *multi-skew Brownian motion*, which describes a Brownian particle moving in a field force and skewed by the presence of several semipermeable barriers. In the first section of Chapter 1 and Chapter 2 we give precise definitions and a short historical introduction. Let us just recall, for the moment, that these processes are solutions to a stochastic differential equation involving symmetric local times of the process such as

$$\begin{cases} dX_t = dW_t + b(X_t)\,dt + \displaystyle\int_{\mathbb{R}} \nu(dy) dL_t^y(X), \\ X_0 = x, \quad L_t^y(X) = \displaystyle\int_0^t \mathbb{1}_{\{X_s = y\}} dL_s^y, \ y \in \mathbb{R}, \end{cases}$$

where $\nu = \sum_{j=1}^{n} \beta_j \delta_{z_j}$ is a weighted sum of Dirac measures with $\beta_j \in (-1, 1)$ for all $j = 1, \dots, n$, and b is the drift function which is measurable and bounded. For ν a general finite measure, and in presence of a non constant diffusion coefficient $\sigma(X_t)$, this kind of SDE describes a wide class of processes (see Le Gall [31, 32]). The weighted local time acts as a semipermeable barrier and skews the motion.

The multi-skew Brownian motion (with possibly discontinuous drift) is interesting on its own and has emerged in various contexts during the last years. As first example, in mathematical finance, Gairat and Shcherbakov [23] apply its distribution to obtain explicit analytical formulas for pricing European options following the local volatility model (a natural extension of the Black-Scholes model). In the latter model the discontinuity appears in the diffusion coefficient which is two-valued. The skew Brownian motion appeared even earlier in finance, see for example Decamps et al. [12, 13, 14] and Rossello [55]. There are also many applications in geophysics related to advection-dispersion phenomenon across layered porous medium, see Ramirez et al. [52]. We refer the reader to Appuhamillage and Sheldon in [2] and Lejay and Pichot [37] for a more exhaustive list of references to the main applications for skew Brownian diffusions.

The main ingredient we need to produce exact algorithms of (skew) Brownian diffusions with discontinuous drifts is an *explicit expression of the transition density of the skew Brownian motion with constant drift*. The number of jumps in the drift induces the number of barriers for the skew diffusion. Therefore such an explicit expression is required for any number of barriers. Up to now, the most advanced explicit expression of the transition density was limited to the case of one barrier [19, 20]. Note also the result by Lejay, Lenôtre and Pichot [35] in the case of skew Brownian motion with one barrier but a two-valued drift. In the setting of multi-skew Brownian diffusions, the only existing explicit formula deals with the case of two reflecting (that is impermeable) barriers, treated by Svennson [59], Veestraeten [63], and Linetsky [41]. In Chapter 1 we propose a new method to compute the transition density of the one-skew Brownian motion with constant drift (Proposition 1.1.1). This approach is sufficiently general to allow us to extend it in Chapter 2 to the case of the multi-skew Brownian motion, see Theorem 2.3.7.

Let us give a chapter-by-chapter description of the content of this document.

In the first chapter we give an historical introduction to the real-valued skew Brownian motion with and without (constant) drift. We focus on its equivalent definitions with the purpose of finding its transition density. At first we mention existing techniques, in particular the one proposed by Étoré and Martinez [19]. Then we present a new method based on the properties of the divergence form operator associated to the process. Briefly, the transition density is equal to the inverse Laplace transform of the resolvent kernel. We interpret the Laplace transform as a contour integral and exploit this structure to get an explicit formula.

In the second chapter we define properly the multi-skew Brownian motion and apply to this process the method introduced in the first chapter. The latter yields a new explicit expression for the two-skew Brownian motion with and without constant drift. We detail all the computations, in particular the representation of its transition density as a series of Fourier transforms. The latter allows us to bound it uniformly in space and time, which provides an indispensable estimate for the exact simulation. We also provide a practical and easy exact method to sample from densities for which we know only an approximation. We call it *Generalized Rejection Sampling*.

In the third chapter we obtain an exact simulation scheme for real-valued Brownian diffusions whose drift admits several jumps. This is based on the knowledge of some asymptotic properties of the transition density of the multi-skew Brownian motion, as the skewness approaches zero. In particular, in the case of the Brownian motion with drift admitting two jumps, we detail the scheme and provide numerical simulations. In this way, we have paved the way to the exact simulation of diffusions with drift admitting several jumps.

In Appendix A the reader can find extracts of the Python code used in the simulations.

Chapter 1

The one-skew Brownian motion with constant drift: various approaches to compute its transition density

Outline of the chapter: In this chapter, we present various techniques to compute the transition densities of the real-valued skew Brownian motion with *one* semipermeable barrier (also called one-skew) with constant drift. Our personal contribution consists in developing a particular way which is suitable for the extension to the case of the multi-skew Brownian motion moving through *several* semipermeable barriers, which will be treated in Chapter 2 and Chapter 3. The method we propose relies on the representation of the transition densities (resp. semigroup) as the inverse Laplace transform of Green's function of the resolvent (resp. of the resolvent). The last section discusses the applicability of our method to one-skew Brownian diffusions with more general drifts. A particular attention is given to the case of a piecewise constant drift.

1.1 The framework

1.1.1 The one-skew Brownian motion

Heuristically, the real-valued (*one*)-Skew Brownian Motion (SBM) is a Brownian motion showing a particular behavior when it reaches *one* point, say the origin 0, where it is partially reflected.

A. Lejay wrote a full and comprehensive survey paper [33] on that topic, to which we will refer at several places in this section. In particular, he presents various equivalent representations of the associated semigroup.

This process was first introduced by Itô and McKean in [27], as a Wiener process transformed by flipping its excursions from the origin with probability $\frac{1-\beta}{2}$, for a certain $\beta \in [-1, 1]$. If $\beta = 0$ one recognizes the usual Brownian motion. If $\beta = 1$ (resp. $\beta = -1$) one obtains the reflected Brownian motion on the positive (resp. negative) semi-axis. This is a trajectorial construction.
Throughout this chapter we will denote this process by (β)-SBM if the permeability coefficient β does matter, and by one-SBM otherwise.

The one-SBM can be characterized in several ways: for example as the solution of a stochastic differential equation involving a weighted local time, or by its infinitesimal generator.
The first one is a path construction based on the semimartingale decomposition of the process. Let us denote by $(W_t)_{t>0}$ a real-valued Brownian motion, and $x_0 \in \mathbb{R}$. It was proved by Harrison and Shepp in [25] that if $|\beta| \leq 1$, there is a unique strong solution to the following stochastic differential equation

involving $(L_t^0)_{t\geq 0}$, the symmetric local time at the point 0:

$$\begin{cases} dX_t = dW_t + \beta\, dL_t^0(X), \\ X_0 = x_0, \quad L_t^0 = \int_0^t \mathbb{1}_{\{X_s=0\}} dL_s^0, \end{cases} \tag{1.1.1}$$

which is indeed the (β)-SBM starting in x_0. Harrison and Shepp also proved that if $|\beta| > 1$ there is no solution to (1.1.1).

The Markovianity of the SBM, as solution to the latter SDE, is not a trivial fact. Zaitseva, after having underlined in [69] the specific difficulties to prove this property, shows it in [70] in a more general multi-dimensional context. Her technique is based on the paper by Kulik [30].

The identification of the SBM through its infinitesimal generator can be attributed to Portenko who introduced in [49] and [50] even more-dimensional skew processes moving through semipermeable surfaces. He wrote down the following *formal* differential operator $\frac{1}{2}\frac{d^2}{dx^2} + \beta\delta_0\frac{d}{dx}$, involving a singular term given by the Dirac measure at 0. And he developed links with the partial differential equation the transition semigroup has to solve. In fact, the interplay between SDE, infinitesimal generator and PDE can provide various methods to find explicitely the semigroup of the SBM. Let $f \in \mathcal{C}_b$, then the transition semigroup $\mathbb{E}_x\left[f(X_t)\right]$, as function of t and x, solves (uniquely) the following PDE:

$$\begin{cases} (t,x) \mapsto u(t,x) \in \mathcal{C}^{1,2}\left(\mathbb{R}_+^* \times \mathbb{R}^*; \mathbb{R}\right) \cap \mathcal{C}\left(\mathbb{R}_+^* \times \mathbb{R}; \mathbb{R}\right) & \\ \dfrac{\partial}{\partial t}u(t,x) = \dfrac{1}{2}\dfrac{\partial^2}{\partial x^2}u(t,x) & t \in \mathbb{R}_+^*,\ x \in \mathbb{R}^*, \\ (1+\beta)\ \dfrac{\partial}{\partial x}u(t,0^+) = (1-\beta)\ \dfrac{\partial}{\partial x}u(t,0^-) & t \in \mathbb{R}_+^*, \\ u(t,0^+) = u(t,0^-) & t \in \mathbb{R}_+^*, \\ u(0,x) = f(x) & x \in \mathbb{R}, \end{cases} \tag{1.1.2}$$

(see Proposition 1 in [33]). The boundary condition involving the skewness parameter β at the point 0 is called *transmission condition*. It makes it hard to solve directly (1.1.2). To avoid this difficulty one can equivalently consider a weak solution to the following problem (see Section 3 in [33]):

$$\begin{cases} t \mapsto u(t,\cdot) \in \mathcal{C}(\mathbb{R}_+; L^2(\mathbb{R}, dx)) \cap L^2(\mathbb{R}_+; H^1(\mathbb{R}, dx)), \\ \partial_t u = Lu, \\ u(0,x) = \varphi(x) \in L^2(\mathbb{R}, dx), \end{cases} \tag{1.1.3}$$

where L is the divergence form operator on $L^2(\mathbb{R}, dx)$

$$\begin{cases} L = \dfrac{1}{2k(x)}\dfrac{d}{dx}\left(k(x)\dfrac{d}{dx}\right) \quad \text{with} \quad k(x) := \dfrac{1-\beta}{2}\mathbb{1}_{\mathbb{R}_-^*}(x) + \dfrac{1+\beta}{2}\mathbb{1}_{\mathbb{R}_+}(x), \\ \mathcal{D}(L) = \left\{\psi \in H^1(\mathbb{R}, dx) :\ k(x)\psi'(x) \in H^1(\mathbb{R}, dx)\right\}. \end{cases} \tag{1.1.4}$$

The function space $H^1(\mathbb{R}, dx)$ is as usual the set of $L^2(\mathbb{R}, dx)$-functions whose weak derivative exists and belongs to $L^2(\mathbb{R}, dx)$ too. The two-valued function $k(x)$ is unique up to a multiplicative constant.
The solution of (1.1.3) is also a solution to the problem (1.1.2) and vice versa. Indeed, one proves that the unique solution of (1.1.3) is the semigroup of the (β)-SBM, solution of (1.1.1).

Let us comment the operator $(L, \mathcal{D}(L))$ on $L^2(\mathbb{R}, dx)$. Notice that, if $|\beta| < 1$ then $L^2(\mathbb{R}, k(x)dx) = L^2(\mathbb{R}, dx)$ and $H^1(\mathbb{R}, k(x)dx) = H^1(\mathbb{R}, dx)$.
Moreover the latter operator is symmetric on $L^2(\mathbb{R}, dx)$: let $f, g \in \mathcal{D}(L)$ then, since L coincides with $\frac{1}{2}\frac{d^2}{dx^2}$ on $\mathbb{R}^*$, one has

$$\begin{aligned} \int_{\mathbb{R}} L\,f(x)\,g(x)\,dx &= \int_{\mathbb{R}_-} L\,f(x)\,g(x)\,dx + \int_{\mathbb{R}_+} L\,f(x)\,g(x)\,dx = \\ &= \int_{\mathbb{R}_-} \frac{1}{2}f''(x)\,g(x)\,dx + \int_{\mathbb{R}_+} \frac{1}{2}f''(x)\,g(x)\,dx = -\int_{\mathbb{R}_-} \frac{1}{2}f'(x)\,g'(x)\,dx - \int_{\mathbb{R}_+} \frac{1}{2}f'(x)\,g'(x)\,dx = \\ &= \int_{\mathbb{R}_-} \frac{1}{2}f(x)\,g''(x)\,dx + \int_{\mathbb{R}_+} \frac{1}{2}f(x)\,g''(x)\,dx = \int_{\mathbb{R}} f(x)\,Lg(x)\,dx. \end{aligned}$$

The advantage of considering the divergence form operator L as infinitesimal generator is twofold. One has at one's disposal the theory of the associated bilinear form (which is a Dirichlet form) and of the self-adjoint operators. More precisely, one knows that L is the infinitesimal generator of a Feller semigroup associated to a continuous Markov process. Once one proves that the associated process is the one-SBM, one gets directly its Markovianity. (See [36] for this kind of approach, which is applicable to more general skew processes).
Since it can be shown that the operator is self-adjoint one can use a spectral analysis approach to give a complex integral representation for the transition densities following the Green's function method or Titchmarsh-Kodaira-Yosida method (see for example Yosida et al. [67]). In particular, Gaveau, Okada and Okada recover in this way the transition density of the (β)-SBM without drift, see Section 5 of Chapter II in [24]. The transition density (first computed by Walsh in [64]) has the following form:

$$p^{(\beta)}(t,x,y) = p(t,x,y) + \beta\left(\mathbb{1}_{\mathbb{R}_+}(y) - \mathbb{1}_{\mathbb{R}_-^*}(y)\right)p(t,-x,y),$$

where $y \mapsto p(t,x,y)$ is the transition density of the Brownian motion (without skew) at time t starting in $x \in \mathbb{R}$. It solves the Fokker-Planck equation

$$\begin{cases} \dfrac{\partial}{\partial t}p^{(\beta)}(t,x,y) = \dfrac{1}{2}\dfrac{\partial^2}{\partial y^2}p^{(\beta)}(t,x,y) & \mathbb{R}_+^*,\ y \in \mathbb{R}^*, \\ \dfrac{\partial}{\partial y}p^{(\beta)}(t,x,0^+) = \dfrac{\partial}{\partial y}p^{(\beta)}(t,x,0^-) & t \in \mathbb{R}_+^*, \\ (1+\beta)\,p^{(\beta)}(t,x,0^-) = (1-\beta)\,p^{(\beta)}(t,x,0^+) & t \in \mathbb{R}_+^* \\ p^{(\beta)}(0,x,y) = \delta_x(y) & y \in \mathbb{R}. \end{cases} \tag{1.1.5}$$

Let us mention that interesting properties (like laws of functionals) of the (β)-SBM can be found in the compendium written by Borodin and Salminen [11].

1.1.2 The (one-)skew Brownian motion with constant drift

We are now interested in the transition density of a slightly more general process, that is the one-SBM perturbed by an additional constant drift μ, with semipermeable barrier at the point $z \in \mathbb{R}$. It is the unique strong solution to the following SDE ($\mathcal{E}(\beta,\mu)$) involving the weighted local time:

$$\begin{cases} X_t = X_0 + W_t + \mu\, t + \beta L_t^z(X), \\ L_t^z = \displaystyle\int_0^t \mathbb{1}_{\{X_s = z\}} dL_s^z. \end{cases} \tag{$\mathcal{E}(\beta,\mu)$}$$

Pathwise uniqueness and weak existence are guaranteed by (the more general) Theorem 2.3 by Le Gall [32]. The solution is a Markov process, as in the driftless case (Zaitseva [70]), and its transition probability admits a density, which we denote by $p_\mu^{(\beta)}$:

$$\begin{array}{rccc} p_\mu^{(\beta)} & : \mathbb{R}_+^* \times \mathbb{R} \times \mathbb{R} & \to & (0,+\infty) \\ & (t,x,y) & \mapsto & p_\mu^{(\beta)}(t,x,y). \end{array}$$

Its specific decomposition is given in the next proposition.

Proposition 1.1.1. *The transition density for the SBM with constant drift μ and semipermeable barrier in z satisfies*

$$p_\mu^{(\beta)}(t,x,y) = p_\mu(t,x,y)v_\mu^{(\beta)}(t,x,y),$$

where $p_\mu(t,x,y)$ is the transition density of the Brownian motion with constant drift μ (without skew), and

$$\begin{aligned} v_\mu^{(\beta)}(t,x,y) := &\left(1 - \exp\left(-\frac{2x_1y_1}{t}\right)\right)\mathbb{1}_{\{x_1y_1>0\}} \\ &+ \left(1 + \beta\left(2\mathbb{1}_{[z,+\infty)}(y) - 1\right)\right)\exp\left(-\frac{2x_1y_1}{t}\mathbb{1}_{\{x_1y_1>0\}}\right) \\ &\cdot\left[1 - \beta\mu\sqrt{2\pi t}\,\exp\left(\frac{(|x_1|+|y_1|+t\beta\mu)^2}{2t}\right)\Phi^c\left(\frac{|x_1|+|y_1|+t\beta\mu}{\sqrt{t}}\right)\right], \end{aligned}$$

where $x_1 := x - z$, $y_1 := y - z$ *and* $\Phi^c(y) := \dfrac{1}{\sqrt{2\pi}} \displaystyle\int_y^\infty e^{-\frac{u^2}{2}} du$ *is the tail of a standard Gaussian law.*

This formula has been recently obtained by various authors using different methods.
The first one was given by Appuhamillage et al. in [4], followed by their correction of a computational mistake in [3]. There, the authors compute the joint density of the one-SBM with constant drift, its local time at the barrier and its occupation time on the positive half-line as follows: first they obtain a Feynman-Kac formula for the SBM with drift and then they compute the Laplace transform of the joint density of the triplet (as Karatzas and Shreve have done for the Brownian motion in [29]).
In the next two sections, we propose other - old and new - proofs of this result. We will first sketch in Section 1.2 the method of Étoré and Martinez (see [19]) as an example of proof based on the trajectorial construction of the one-SBM via Brownian excursions. Then we provide in Section 1.3 two new alternative proofs, both based on the identification of the infinitesimal generator of the (β)-SBM with drift μ and the resulting integral representation of the associated transition semigroup. These alternative proofs are our starting point for the generalization in Chapter 2.

1.2 An approach via the path decomposition of the SBM and its local time

We now recall briefly the method proposed by Étoré and Martinez to prove Proposition 1.1.1 (see Proposition 4.7 in [19]). Their proof consists of computing $\mathbb{E}_x\left[f(X_t)\right]$ for any continuous and bounded function f and any fixed starting point $x \in \mathbb{R}$ and time $t > 0$. Thanks to Girsanov theorem they reduce the problem to compute the joint density of the SBM without drift starting from x and the Brownian motion. To do this they consider the bijection

$$\begin{aligned} \Phi_x : \mathbb{R} \times \mathbb{R}_+ &\to D_x \\ (y, \ell) &\mapsto (y, y - x - \beta\ell), \end{aligned}$$

where $D_x := \{(v, w) \in \mathbb{R}^2 : \ v - x \geq w\}$. In particular the image through Φ_x of the pair of processes (skew Brownian motion, its local time in 0) is the pair (skew Brownian motion, $W_t - x$), where $(W_t)_{t\geq 0}$ is the Wiener process. Let us denote by $\nu(dx, d\ell)$ the law on $\mathbb{R} \times [0, +\infty)$ of the pair (skew Brownian motion with initial condition x, its local time in 0) at time t. For $x > 0$, ν is the sum of two components $\nu(dx, d\ell) = \nu_1(dx, d\ell) + \nu_2(dx)\delta_0(d\ell)$. The first one $\nu_1(dx, d\ell)$ is absolutely continuous with respect to the Lebesgue measure $dxd\ell$ and concentrated on $\mathbb{R} \times (0, +\infty)$, and the second one $\nu_2(dx)\delta_0(d\ell)$ is concentrated on $\mathbb{R} \times \{0\}$, and $\nu_2(dx)$ is absolutely continuous with respect to the Lebesgue measure dx (see Lemma 1 in Zaitseva, [71]). Étoré and Martinez give explicitly the densities, relying on the definition of the one-SBM as randomly flipped excursion of the reflected Brownian motion (see Proposition 4.5 in Section 4.2 of [19]). They then define $\Delta_x := \{(v, w) \in \mathbb{R}_+ \times \mathbb{R} : \ v = w + x\}$ and, using the bijection Φ_x, they compute the joint density of the skew BM starting in x and $W_t - x$ on $D_x \setminus \Delta_x = \Phi_x(\mathbb{R} \times \mathbb{R}_+^*)$ and on Δ_x. This completes the proof in the case of $x > 0$ and $\beta > 0$. The other cases can be derived from this case.

1.3 An approach via the Laplace transform of the resolvent of the infinitesimal generator

The goal of this section is to derive an integral representation of the semigroup (resp. transition density) of the one-SBM as inverse Laplace transform of the resolvent (resp. Green's function of the resolvent) of the infinitesimal generator of the process. It will be the key point for the two different proofs of Proposition 1.1.1 that we will present in Section 1.3.4 and Section 1.3.5.

1.3.1 About the infinitesimal generator

Let us recall that in the case of the (β)-SBM with one semipermeable barrier in z *without drift*, the infinitesimal generator on $L^2(\mathbb{R}, dx)$ is the operator $(L, D(L))$ given by (1.1.4). Naturally the infinitesimal

generator on $L^2(\mathbb{R}, dx)$, in the case of a non-vanishing drift μ, is a slight modification of the operator (1.1.4):

$$\begin{cases} A = \frac{1}{2k(x)} \frac{d}{dx} \left(k(x) \frac{d}{dx} \right) + \mu \frac{d}{dx} \text{ with } k(x) = \frac{1}{2} \left(1 + \beta \left(2 \mathbb{1}_{[z,+\infty)} - 1 \right) \right) \\ \mathcal{D}(A) := \left\{ \psi \in H^1(\mathbb{R}, dx) : \ k\psi' \in H^1(\mathbb{R}, dx) \right\}. \end{cases}$$

The proof that this is the infinitesimal generator in the classical sense can be found in Étoré's PhD thesis [18] (through an argument similar to Theorem 3.1 in [32]) and in Lejay and Martinez [36].
However A is not self-adjoint on $L^2(\mathbb{R}, dx)$ because it is not even symmetric.

Inspired by the Green's function method used by Gaveau Okada and Okada (see [24]) we provide an infinitesimal generator which is self-adjoint and a similar representation of the transition density function associated to the (β)-SBM *with constant drift* $\mu \in \mathbb{R}$. Let us consider the following operator on the Banach space $L^2(\mathbb{R}, h(x)dx)$

$$\begin{cases} L = \dfrac{1}{2h(x)} \dfrac{d}{dx} \left(h(x) \dfrac{d}{dx} \right) \quad \text{with} \quad h(x) := e^{2\mu x} \left(\dfrac{1}{2} + \beta \left(\mathbb{1}_{[z,+\infty)}(x) - \dfrac{1}{2} \right) \right), \\ \mathcal{D}(L) = \left\{ \psi \in H_0^1(\mathbb{R}, h(x)dx) : \ h(x)\psi'(x) \in H^1(\mathbb{R}, h^{-1}(x)dx) \right\}, \end{cases} \tag{1.3.1}$$

where

$$H^1(\mathbb{R}, \nu) := \left\{ u \in H^1_{loc}(\mathbb{R}, dx) : \ \|u\|_{H^1(\mathbb{R},\nu)} := \|u\|_{L^2(\mathbb{R},\nu)} + \|u'\|_{L^2(\mathbb{R},\nu)} < +\infty \right\},$$
$$\text{and } H_0^1(\mathbb{R}, \nu) := \mathcal{C}\ell_{H^1(\mathbb{R},\nu)} \left(\mathcal{C}_c^\infty \right).$$

Notice that $h(x)$ is positive but not bounded from above.

Let us first analyze this operator and its domain. The function ψ in the domain are in particular continuous functions such that they satisfy the transmission condition $h\,\psi$ continuous (by Sobolev embedding theorem). Let us explicit the transmission condition in this case: $(1-\beta)\psi'(z^-) = (1+\beta)\psi'(z^+)$. Moreover the operator coincides with $\frac{1}{2}\frac{d^2}{dx^2} + \mu \frac{d}{dx}$ in $\mathbb{R} \setminus \{z\}$.

Lemma 1.3.1. *The operator $(L, \mathcal{D}(L))$ defined by* (1.3.1) *is self-adjoint in $L^2(\mathbb{R}, h(x)dx)$ and its spectrum $\sigma(L)$ is a closed subset of $(-\infty, 0]$ containing 0.*

Proof. First of all notice that the measure $\nu(dx) := h(x)dx$ is not a finite measure, therefore it is not normalizable into a probability measure. The bilinear form

$$\begin{array}{rccc} q : & H_0^1(\mathbb{R}, h(x)dx) \times H_0^1(\mathbb{R}, h(x)dx) & \to & \mathbb{R} \\ & (f, g) & \longmapsto & q(f,g) = \int_{\mathbb{R}} f'(x)g'(x)h(x)dx, \end{array} \tag{1.3.2}$$

is symmetric, semibounded and closed with domain $\mathcal{Q}(q) = H_0^1(\mathbb{R}, h(x)dx) \subseteq L^2(\mathbb{R}, h(x)dx)$. Therefore there exists a unique operator T with $\mathcal{D}(T) \subseteq \mathcal{Q}(q)$ such that $q(u, v) = -\langle u, Tv \rangle_{L^2(\mathbb{R},h(x)dx)}$ (see for example Corollary 1.3.1 in [22], from the point of view of functional analysis this is a Riesz representation theorem for Hilbert spaces). Moreover the operator T is self-adjoint.
Let us now prove the identity $(2L, \mathcal{D}(L)) = (T, \mathcal{D}(T))$.
Riesz representation theorem provides an implicit characterization of the domain of T as

$$\begin{aligned} \mathcal{D}(T) &:= \left\{ \psi \in H^1(\mathbb{R}, h(x)dx) : \ \exists g \in L^2(\mathbb{R}, h(x)dx) \ \ \langle \cdot, g \rangle_{L^2(\mathbb{R},h(x)dx)} = \langle \cdot, \psi \rangle_{L^2(\mathbb{R},h(x)dx)} + q(\cdot, \psi) \right\} \\ &= \left\{ \psi \in H^1(\mathbb{R}, h(x)dx) : \ \exists f \in L^2(\mathbb{R}, h(x)dx) \ \ \langle \cdot, f \rangle_{L^2(\mathbb{R},h(x)dx)} = q(\cdot, \psi) \right\}. \end{aligned}$$

We first prove that $\mathcal{D}(T) \subseteq \mathcal{D}(L)$ and that $2L$ coincides with T on $\mathcal{D}(T)$.
Take $v \in \mathcal{D}(T)$. We want to show that the weak derivative $(hv')'$ exists in $L^2(\mathbb{R}, h^{-1}(x)dx)$. But by the previous characterization of the domain, there exists $f \in L^2(\mathbb{R}, h(x)dx)$ such that $q(\cdot, v) = \langle \cdot, f \rangle_{L^2(h(x)dx)}$ (indeed $f = -Tv$ since $q(\cdot, v) = -\langle \cdot, Tv \rangle_{L^2(\mathbb{R},h(x)dx)}$). Hence, for all $u \in \mathcal{C}_c^\infty(\mathbb{R})$

$$\int_{\mathbb{R}} h(x)u'(x)v'(x)dx = \int_{\mathbb{R}} h(x)u(x)f(x)dx,$$

and by the definition of weak derivative $(hv')' = -hf$. This implies that $(hv')' \in L^2(\mathbb{R}, h^{-1}(x)dx)$ and also that $2Lv = Tv$, since $f = -Tv$.
Then one can prove that $q(u,v) = -\langle u, 2Lv\rangle_{L^2(\mathbb{R},h(x)dx)}$ for any $u \in H^1(\mathbb{R}, h(x)dx)$ and $v \in \mathcal{D}(L)$, just showing that the equality holds for $u \in \mathcal{C}_c^\infty(\mathbb{R})$ and passing to the limit for a sequence converging to u in $H^1(\mathbb{R}, h(x)dx)$. If one supposes $\mathcal{D}(L) \neq \mathcal{D}(T)$, there would be a contradiction: we have shown that $2L$ is an extension of T such that $\mathcal{D}(L) \subseteq \mathcal{Q}(q)$ and $q(u,v) = - < u, Lv >_{L^2(\mathbb{R},h(x)dx)}$, but T is the unique operator with these properties.
Since the operator is self-adjoint, it has spectrum $\sigma(L) \subseteq \mathbb{R}$ and one can easily check that the spectrum is contained in $(-\infty, 0]$ since for each $u \in \mathcal{D}(L)$ $\langle L\,u,\, u\rangle_{L^2(\mathbb{R},h(x)dx)} \leq 0$. □

Lemma 1.3.2. *The operator $(L, \mathcal{D}(L))$ defined on $L^2(\mathbb{R}, h(x)dx)$ by (1.3.1) is the infinitesimal generator of the (β)-SBM with drift μ.*

Proof. One possible (quick but indirect) way to identify L as the infinitesimal generator we are looking for, is to apply results related to (more general) Dirichlet forms obtained by Ouknine, Russo and Trutnau in [47]. The Hunt process whose semigroup is associated to the closed form $(q, \mathcal{Q}(q))$ in (1.3.2) is the (β)-SBM with drift with semipermeable barrier in z. By uniqueness of the self-adjoint operator associated to the form, we conclude that the operator $(L, \mathcal{D}(L))$ is nothing but the infinitesimal generator of this SBM.
We now sketch a direct proof based on showing the convergence, when t vanishes, of $\frac{1}{t}(P_t\phi - \phi)$ to $L\phi$ in $L^2(\mathbb{R}, h(x)dx)$ for $\phi \in \mathcal{D}(L)$. We denote by J the set of discontinuities of h. In our framework, $J = \{z\}$. The space $\mathcal{C}_c^\infty(\mathbb{R} \setminus J)$ of smooth functions with compact support in $\mathbb{R} \setminus J$ is dense in $L^2(\mathbb{R}, h(x)dx)$ and contained in $\mathcal{D}(L)$.
The Itô-Tanaka formula applies to any function $\phi \in \mathcal{C}_c^\infty(\mathbb{R} \setminus J)$ and one gets:

$$\begin{aligned} P_t\phi(x) - \phi(x) &= \mathbb{E}_x\left[\phi(X_t) - \phi(x)\right] \\ &= \mathbb{E}_x\left[\int_0^t \frac{1}{2}\left(\phi'(X_s^+) + \phi'(X_s^-)\right) dX_t + \frac{1}{2}\int_{\mathbb{R}} L_t^a(X)\phi''(a)da\right]. \end{aligned}$$

Using the occupation time formula and the fact that the SBM satisfies $\mathcal{E}(\beta, \mu)$, one obtains

$$\begin{aligned} &\mathbb{E}_x\left[\int_0^t \frac{1}{2}\left(\phi'(X_s^+) + \phi'(X_s^-)\right)(dB_s + \mu\, ds + \beta\, dL_s^z(X)) + \frac{1}{2}\int_0^t \phi''(X_s)ds\right] \\ &= \mathbb{E}_x\left[\int_0^t \frac{1}{2}\left(\phi'(X_s^+) + \phi'(X_s^-)\right) dB_s\right] + \mu\mathbb{E}_x\left[\int_0^t \frac{1}{2}\left(\phi'(X_s^+) + \phi'(X_s^-)\right) ds\right] \\ &\quad + \mathbb{E}_x\left[\beta\int_0^t \frac{1}{2}\left(\phi'(X_s^+) + \phi'(X_s^-)\right) \mathbb{1}_{\{X_s = z\}}\, dL_s^z(X) + \frac{1}{2}\int_0^t \phi''(X_s)ds\right] \\ &= \mathbb{E}_x\left[\int_0^t \phi'(X_s)\mathbb{1}_{\{X_s \neq z\}} dB_s + \mu\int_0^t \phi'(X_s)\mathbb{1}_{\{X_s \neq z\}} ds + 0 + \frac{1}{2}\int_0^t \phi''(X_s)ds\right] \\ &= 0 + \mathbb{E}_x\left[\int_0^t \frac{1}{2}\phi''(X_s) + \mu\,\phi'(X_s)ds\right]. \end{aligned}$$

Hence

$$\frac{P_t\phi(x) - \phi(x)}{t} = \mathbb{E}_x\left[\mu\int_0^t \phi'(X_s)ds + \frac{1}{2}\int_0^t \phi''(X_s)ds\right].$$

Notice that $L\phi(x) = \frac{1}{2}\phi''(x) + \mu\phi'(x)$ for all $x \in \mathbb{R} \setminus J$. Let us now check the convergence of $\frac{P_t\phi(x) - \phi(x)}{t}$

in $L^2(\mathbb{R}, h(x)dx)$:

$$\begin{aligned}
&\lim_{t\to 0}\int_{\mathbb{R}}\left(\frac{1}{t}\mathbb{E}_x\left[\frac{1}{2}\int_0^t \phi''(X_s)ds + \mu\int_0^t \phi'(X_s)ds\right] - L\phi(x)\right)^2 h(x)dx\\
&\quad= \int_{\mathbb{R}}\lim_{t\to 0}\left(\frac{1}{t}\mathbb{E}_x\left[\frac{1}{2}\int_0^t \phi''(X_s)ds + \mu\int_0^t \phi'(X_s)ds\right] - \frac{1}{2}\phi''(x) - \mu\phi'(x)\right)^2 h(x)dx\\
&\quad= \int_{\mathbb{R}}\mathbb{E}_x\left[\lim_{t\to 0}\int_0^t\left(\frac{1}{2}\phi''(X_s) + \mu\phi'(X_s)\right)ds - \frac{1}{2}\phi''(x) - \mu\phi'(x)\right]^2 h(x)dx\\
&\quad= \int_{\mathbb{R}}\mathbb{E}_x\left[\frac{1}{2}\phi''(X_0) + \mu\phi'(X_0) - \frac{1}{2}\phi''(x) - \mu\phi'(x)\right]^2 h(x)dx\\
&\quad= 0,
\end{aligned}$$

where we could exchange integrals and limit by dominated convergence, thanks to the compactness of the support of ϕ. □

Now, for any fixed initial condition $x \in \mathbb{R}$, the transition density $(t, y) \mapsto p_\mu^{(\beta)}(t, x, y)$ of the (β)-SBM with drift μ, given in Proposition 1.1.1, solves the Fokker-Plank equation:

$$\begin{cases}
\dfrac{\partial}{\partial t}p(t,x,y) = \dfrac{1}{2}\dfrac{\partial^2}{\partial y^2}p(t,x,y) - \mu\dfrac{\partial}{\partial y}p(t,x,y) & t>0,\ y\in\mathbb{R}\setminus\{z\},\\
p(0,x,y) = \delta_x(y) & y\in\mathbb{R}\\
\dfrac{1}{2}\dfrac{\partial}{\partial y}p(t,x,z^+) - \mu\, p(t,x,z^+) = \dfrac{1}{2}\dfrac{\partial}{\partial y}p(t,x,z^-) - \mu\, p(t,x,z^-) & t\in\mathbb{R}_+,\\
(1+\beta)\, p(t,x,z^-) = (1-\beta)\, p(t,x,z^+) & t\in\mathbb{R}_+,
\end{cases} \tag{1.3.3}$$

The transmission conditions are obtained using the continuity of $y \mapsto \dfrac{1}{h^{-1}(y)}p(t,x,y)$ and $y \mapsto h(y)(h(y)p(t,x,y))'$, where h is given in (1.3.1).

Remark 1.3.3. Since the SBM is a one-dimensional process, following Feller's approach, one can characterize it by its scale function s and its speed measure m. In the driftless case, $\mu = 0$, Itô and McKean did it in [27]. In presence of a drift, we obtain the following explicit expressions for the scale function and the speed measure of the (β)-SBM with constant drift μ and barrier in z:

$$s(x) = \frac{e^{2\mu x} - 1}{2\mu\, h(x)}, \qquad m(dx) = 2h(x)dx,$$

where $h(x)$ is given by (1.3.1).

The infinitesimal generator can also be written through s and m. Lejay, Lenôtre and Pichot show in Section 1.2 of [35] that the infinitesimal generator is given by

$$Af = D_m D_s f \quad \text{where } \mathcal{D}(A) := \{f \in \mathcal{C}_b(\bar{\mathbb{R}}) :\ D_m D_s f \in \mathcal{C}_b(\bar{\mathbb{R}})\}, \tag{1.3.4}$$

as soon as D_m and D_s have a sense. Hence A is formally of the same shape than L, but associated to the domain

$$\mathcal{D}(A) = \{f \in \mathcal{C}_b(\bar{\mathbb{R}}) :\ h(z^+)f(z^+) = h(z^-)f(z^-),\ f \in \mathcal{C}^2(\mathbb{R}\setminus\{z\})\}.$$

They provide the result for the skew diffusions which is a larger class of processes, containing the $(\beta) - SBM$. It is composed by the Feller processes associated to the divergence form operator

$$\tilde{L}u(x) := \frac{\rho}{2}\nabla(a(x)\nabla u) + b(x)\nabla u(x)$$

for measurable real functions ρ, a and b such that a, ρ are have positive bounds from below and above and $|b|$ is bounded.

1.3.2 Integral representation of the semigroup through Green's function of the resolvent

Any self-adjoint operator in a Banach space with spectrum which is bounded from above generates a strongly continuous semigroup P_t satisfying $\|P_t\| \leq e^{-\omega t}$ for some $\omega \in \mathbb{R}$, see Lumer and Phillips [42]. We apply this result to the operator $(L, \mathcal{D}(L))$ defined on the Hilbert space $L^2(\mathbb{R}, h(x)dx)$. As a consequence, the assumptions of the Hille-Yosida theorem are satisfied. Therefore the differential operator $(L, \mathcal{D}(L))$ is closed, its domain is dense in $L^2(\mathbb{R}, h(x)dx)$ and for any $\lambda \in (\omega, +\infty)$ the resolvent operator $\mathcal{R}_\lambda := (\lambda - L)^{-1}$ has a norm bounded by $\frac{M}{\lambda - \omega}$ for some constant $M > 0$. From Hille-Yosida theorem one also deduces that the resolvent exists more generally for any $\lambda \in \mathbb{C}$ such that $\Re e(\lambda) > \omega$, and in this case its norm admits a similar bound as above.
Now, under these conditions the associated semigroup is analytic and admits the below integral representation (1.3.5). (All these results are available in [53], see Theorem 12.22 for Lumer-Phillips Theorem, Theorem 12.17 for Hille-Yosida Theorem and Theorem 12.31 for the analyticity and the integral representation of the semigroup.)

The transition semigroup P_t associated to the one-SBM with drift can be represented as follows: for all bounded function $\varphi \in L^2(\mathbb{R}, h(x)dx)$,

$$P_t\varphi(x) = \frac{1}{2\pi i}\int_\Gamma e^{\lambda t}\,\mathcal{R}_\lambda\varphi(x)\,d\lambda \tag{1.3.5}$$

where Γ is a contour in the complex plane around the spectrum $\sigma(L)$ (see Figure 1.2) and $\mathcal{R}_\lambda$ is the resolvent. Recall that for $\lambda \notin \sigma(L)$, $R_\lambda\varphi$ is equal to $(\lambda - L)^{-1}\varphi$.

Therefore P_t admits a transition density which satisfies

$$p(t, x, y) = \frac{1}{2\pi i}\int_\Gamma e^{\lambda t}\,G(x, y; \lambda)\,d\lambda \tag{1.3.6}$$

where $G(x, y; \lambda)$ is Green's function of the resolvent, that is, for any fixed $y \in \mathbb{R}$ and $\lambda \in \mathbb{C}\backslash\sigma(L)$, $x \mapsto G(x, y; \lambda)$ solves in $\mathcal{D}(L)$ the equation

$$(\lambda - L)G(\cdot, y; \lambda) = \delta_y. \tag{1.3.7}$$

Let us notice that, for fixed λ, the solution $x \mapsto G(x, y; \lambda)$ belongs to $\mathcal{D}(L)$, in particular it is continuous, vanishing at infinity, and its first derivative satisfies the transmission conditions: $h(x)\frac{d}{dx}G(x, y; \lambda)$ is continuous. Moreover $y \mapsto \frac{1}{h(y)}G(x, y; \lambda) \in \mathcal{D}(L)$ or equivalently $y \mapsto G(x, y; \lambda) \in \mathcal{D}(L^*)$ where $L^*g := hL\left(\frac{g}{h}\right)$ is the formal adjoint of L in $L^2(\mathbb{R}, dx)$.

Lemma 1.3.4. *For each $\lambda \in \mathbb{C} \setminus \mathbb{R}_-$ Green's function is given by*

$$G(x, y; \lambda) = -2h(y)\frac{U_+(y, \lambda)U_-(x, \lambda)\mathbb{1}_{\{x \leq y\}} + U_+(x, \lambda)U_-(y, \lambda)\mathbb{1}_{\{y < x\}}}{h(x_0)W(U_-, U_+)(x_0, \lambda)}$$

where the functions $U_\pm \in \mathcal{D}(L)$ are respectively solution to:

$$(\lambda - L)U_\pm(x, \lambda) = 0, \qquad \lim_{x \to +\infty} U_+(x, \lambda) = 0, \quad \lim_{x \to -\infty} U_-(x, \lambda) = 0, \tag{1.3.8}$$

while $W(U_-, U_+)(x_0, \lambda) = U_-(x_0, \lambda)U_+'(x_0, \lambda) - U_-'(x_0, \lambda)U_+(x_0, \lambda)$ is the Wronskian in $x_0 \in \mathbb{R}$.

Proof. One can easily prove that the function $x \mapsto h(x)W(U_-, U_+)(x, \lambda)$ is constant, since its derivative vanishes. The function $x \mapsto G(x, y; \lambda)$ belongs to $\mathcal{D}(L)$ because so do the functions U_- and U_+ and is a solution to (1.3.7). Since the latter equation admits a unique solution for any fixed y, λ, the proof is completed. □

The remaining work is to obtain explicitly the functions $U_\pm$ solutions to (1.3.8) and it will be done in the following section.

In [35] Lejay, Lenôtre and Pichot show in a different way that the transition densities are the inverse Laplace transform of the resolvent kernel for a wider class of Feller processes, the skew diffusions. In Section 1.3 they give a detailed description of the resolvent kernel, including the functions $U_\pm$, as the solution to a Sturm-Liouville problem. Their proof is based on the identification of the infinitesimal generator of the skew diffusions as the operator $D_m D_s$ (see (1.3.4)). We will give some more details on that in Section 1.4.

1.3.3 Explicit computation of Green's function in our framework

This section is devoted to Green's function in the case of the (β)-SBM with one barrier in z, and in particular to the computation of the functions $U_\pm(x,\lambda)$ solutions to (1.3.8). Actually they are linear combinations of

$$\begin{aligned} u_\pm :&\mathbb{R}\times\mathbb{C}\setminus[0,+\infty)\to\mathbb{R}\\ &(x,\lambda)\mapsto u_\pm(x,\lambda)=\exp\left(-\mu x\mp\sqrt{\mu^2+2\lambda}\,x\right), \end{aligned}$$

the two (continuous) eigenfunctions of the operator $\frac{1}{2}\frac{d^2}{dx^2}+\mu\frac{d}{dx}$ associated to the eigenvalue λ, and satisfying $u_\pm(0)=1$ (Sturm-Liouville problem). Notice that the functions u_+ and u_- vanish at $+\infty$ and $-\infty$ respectively. One sets

$$U_-(x,\lambda)=\begin{cases} u_-(x,\lambda) & x\in(-\infty,z),\\ A(\lambda)u_-(x,\lambda)+B(\lambda)u_+(x,\lambda) & x\in(z,+\infty),\end{cases}$$

and

$$U_+(x,\lambda)=\begin{cases} E(\lambda)u_-(x,\lambda)+F(\lambda)u_+(x,\lambda) & x\in(-\infty,z),\\ u_+(x,\lambda) & x\in(z,+\infty),\end{cases}$$

as in Figure 1.1.

Figure 1.1: The functions U_- and U_+.

The coefficients A, B, E, F are uniquely determined by the fact that $U_\pm$ belongs to the domain $\mathcal{D}(L)$; therefore they have to be continuous in z and to satisfy the transmission condition (continuity of $x\mapsto h(x)'U_\pm(x,\lambda)$).

$$\begin{cases} A(\lambda)=\frac{1}{\beta+1}\left(1+\frac{\beta\mu}{\sqrt{\mu^2+2\lambda}}\right), & B(\lambda)=(1-A(\lambda))e^{2\sqrt{\mu^2+2\lambda}z},\\ F(\lambda)=\frac{1}{(1-\beta)}\left(1+\frac{\beta\mu}{\sqrt{\mu^2+2\lambda}}\right), & E(\lambda)=(1-F(\lambda))e^{-2\sqrt{\mu^2+2\lambda}z}.\end{cases}$$

One compute the Wronskian at any point, exploiting the fact that $x\mapsto h(x)W(U_-,U_+)(x,\lambda)$ is constant, and obtain

$$W(U_-,U_+)(x,\lambda)\equiv -2\sqrt{\mu^2+2\lambda}\,F(\lambda)\exp(-2\mu x).$$

This leads to the following result.

Lemma 1.3.5. *Green's function satisfy*

$$\begin{aligned} G(x,y;\lambda)&=2h(y)\frac{U_-(x\wedge y,\lambda)U_+(x\vee y,\lambda)}{\beta\mu+\sqrt{2\lambda+\mu^2}}\\ &=\frac{e^{\mu(y-x)}e^{-\sqrt{2\lambda+\mu^2}|y-x|}}{2\lambda+\mu^2+\beta\mu\sqrt{2\lambda+\mu^2}}\left(\sum_{j=1}^{2}c_j(y,\mu;\sqrt{2\lambda+\mu^2})e^{-\sqrt{2\lambda+\mu^2}a_j(x,y)}\right)\end{aligned}\tag{1.3.9}$$

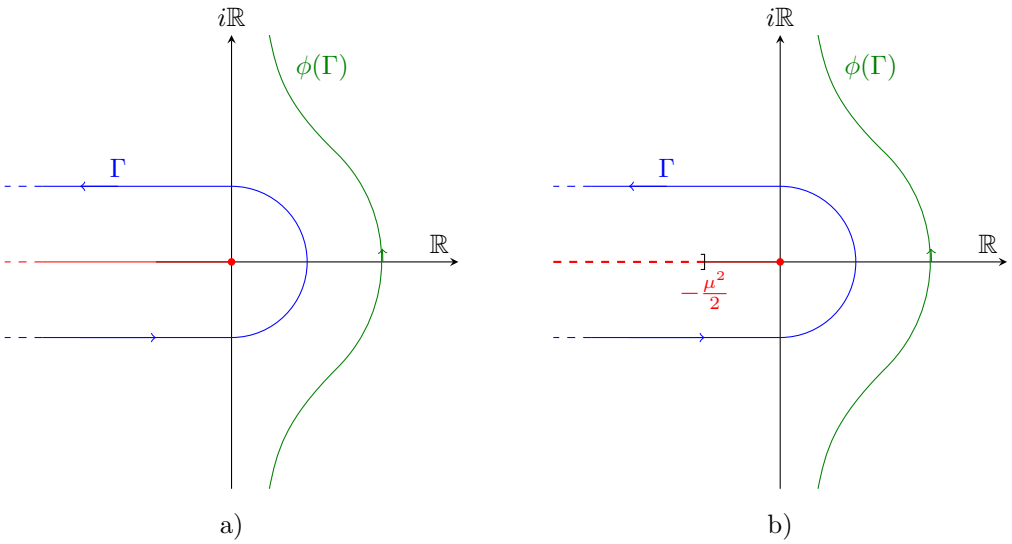

Figure 1.2:

a) Let $\mu = 0$. The picture shows the (green) image of the (blue) contour Γ under $\phi : \lambda \mapsto \sqrt{2\lambda}$. The spectrum of the operator $(L, \mathcal{D}(L))$ is contained in the (red) semi-axis $(-\infty, 0]$, which coincides with the complement of the domain of ϕ.

b) Let $\mu \in \mathbb{R}$. The picture shows the image of the contour Γ under $\phi : \lambda \mapsto \sqrt{2\lambda + \mu^2}$. The line $(-\infty, 0]$ contains the spectrum of the operator $(L, \mathcal{D}(L))$ and the dashed line $(-\infty, -\frac{\mu^2}{2}]$ is the complement of the domain of ϕ.

where

$$\begin{cases} c_1(y,\mu;\xi) = \beta\mu + \xi \\ c_2(y,\mu;\xi) = \beta\xi\left(2\mathbb{1}_{[z,+\infty)}(y) - 1\right) - \beta\mu, \end{cases} \quad \textit{and} \quad \begin{cases} a_1(x,y) \equiv 0 \\ a_2(x,y) = |y-z| + |x-z| - |y-x|. \end{cases} \tag{1.3.10}$$

Notice that $a_2(x, y) \geq 0$ for all $x, y \in \mathbb{R}$.
The dependence on λ of Green's function given by (1.3.9) is actually a dependence on $\phi(\lambda)$ where

$$\begin{aligned} \phi : \mathbb{C} \setminus (-\infty, -\frac{1}{2}\mu^2] &\to \{\zeta \in \mathbb{C} : \Re e(\zeta) > 0\} \\ \lambda &\mapsto \phi(\lambda) := \sqrt{2\lambda + \mu^2}. \end{aligned}$$

Let us consider the integral representation of the density (1.3.6); the contour integral Γ contains $(-\infty, 0]$ (see Figure 1.2.b), hence the change of variables $\xi := \phi(\lambda)$ is allowed and one has

$$\begin{aligned} p_\mu^{(\beta)}(t,x,y) &= \frac{1}{2\pi i}\int_\Gamma e^{\lambda t} G(x,y;\lambda)\, d\lambda \\ &= e^{\mu(y-x)-\frac{\mu^2}{2}t}\frac{1}{2\pi i}\int_{\phi(\Gamma)} e^{\frac{\xi^2}{2}t}\frac{e^{-\xi|y-x|}}{\xi+\beta\mu}\left(\sum_{j=1}^{2} c_j(y,\mu;\xi)e^{-\xi a_j(x,y)}\right) d\xi. \end{aligned} \tag{1.3.11}$$

In the next two sections, starting from the latter integral on the curve $\phi(\Gamma)$, we compute the transition density of the (β)-SBM with drift μ in two different ways.

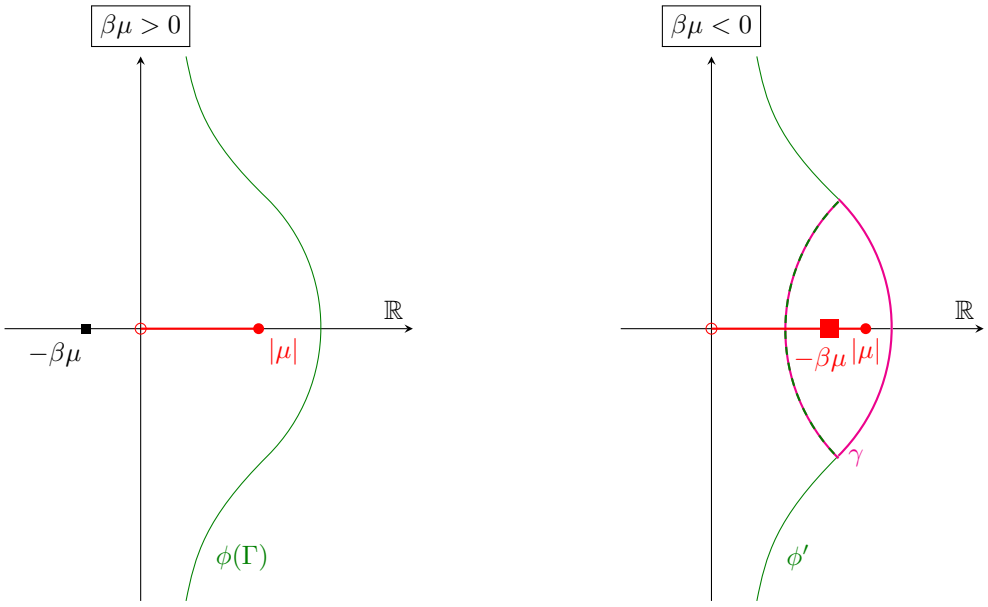

Figure 1.3:

a) Case $\beta\mu > 0$: The red segment $(0, |\mu|]$ is the image under ϕ of $(-\frac{\mu^2}{2}, 0]$.

b) Case $\beta\mu < 0$: The curve $\phi(\Gamma)$ is decomposed as the union of a green curve ϕ' that avoids the unique pole $-\beta\mu \in (0, |\mu|]$ and the cycle γ containing it.

1.3.4 First method: computing the residues

If $\beta\mu > 0$ the integrand in (1.3.11) is holomorphic as a function of ξ on the region between the contour $\phi(\Gamma)$ and the imaginary line. If $\beta\mu < 0$ the integrand has exactly one pole of order one in $\xi = -\beta\mu$. We then decompose the curve $\phi(\Gamma)$ as the union of a curve ϕ' and γ, where γ is a loop around the pole and ϕ' avoids the pole (see Figure 1.3).
Both $\phi(\Gamma)$ and ϕ' can be deformed to the imaginary line (through $H : [0,1] \times \mathbb{R} \to \mathbb{R}^2$ given by $H(t,u) = U(1-t) + tU'$) as in Figure 1.4, if the following Lemma is satisfied.

Lemma 1.3.6.

$$\lim_{|u|\to+\infty} \int_{\rho_U} e^{\frac{\xi^2}{2}t} \, \frac{e^{-\xi|y-x|}}{\xi + \beta\mu} \left(\sum_{j=1}^{2} c_j(y,\mu;\xi) e^{-\xi a_j(x,y)} \right) d\xi = 0,$$

where ρ_U is the segment in Figure 1.4 connecting the points U and U'.

Proof. First of all notice that the integral is equal to

$$I_u := \int_{\rho_U} e^{\frac{\xi^2}{2}t} \, e^{-\xi|y-x|} \left(1 + \frac{c_2(y,\mu;\xi)}{\xi + \beta\mu} e^{-\xi a_2(x,y)} \right) d\xi.$$

Let $\ell(u) := |UU'|$, then notice that $\lim_{u\to\infty} \ell(u) = 0$. The segment ρ_U can be parametrized as $\rho_U = \{U + w;\ w \in (0, \ell(u))\}$ and

$$|I_u| \le \int_0^{\ell(u)} e^{-\frac{(u^2-w^2)}{2}t} e^{-w|y-x|} \left(1 + \left| \frac{c_2(y,\mu;w+iu)}{w+iu+\beta\mu} \right| e^{-w\, a_2(x,y)} \right) dw.$$

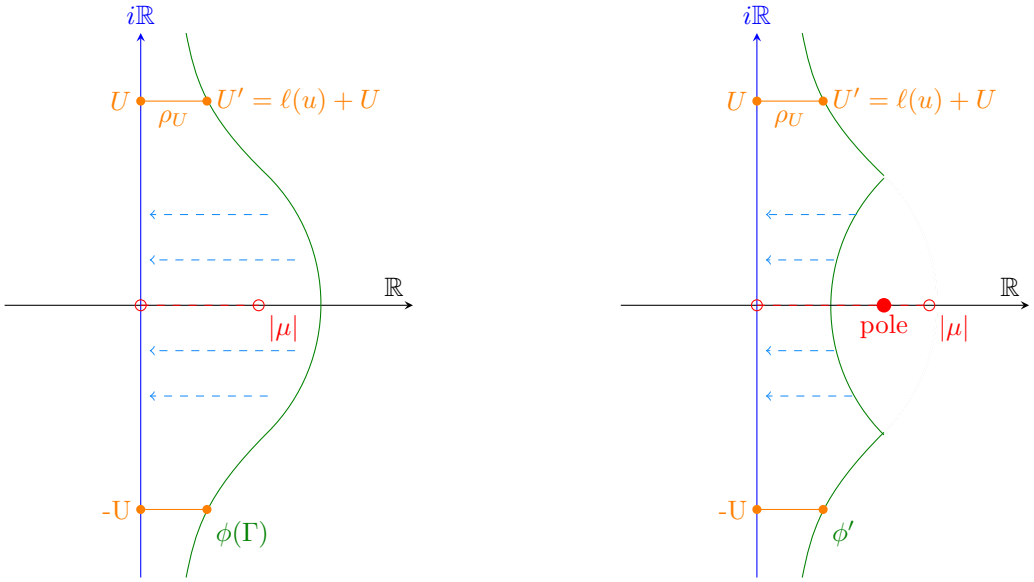

Figure 1.4:

a) The picture shows the contour $\phi(\Gamma)$ which shrinks to the imaginary line (in blue). The segment ρ_U connects the unique point $U' \in \phi(\Gamma)$ with imaginary part u to its projection U on the imaginary line.

b) The picture shows the contour ϕ' which shrinks to the imaginary line (in blue). The segment ρ_U connects the point $U = iu$ to its unique projection $U' \in \phi'$.

For u large enough

$$\left|\frac{c_2(y,\mu;w+iu)}{w+iu+\beta\mu}\right| = |\beta|\sqrt{\frac{\left(w\left(2\mathbb{1}_{[z,+\infty)}(y)-1\right)-\mu\right)^2+u^2}{(w+\beta\mu)^2+u^2}} \leq 1,$$

therefore

$$|I_u| \leq \int_0^{\ell(u)} e^{-\frac{(u^2-w^2)}{2}t} e^{-w|y-x|}\left(1+e^{-w\,a_2(x,y)}\right)dw,$$

that converges to zero if $|u|$ goes to infinity. □

The expression (1.3.11) can be written, for any value of $\beta\mu \in \mathbb{R}$, as follows

$$\begin{aligned} p_\mu^{(\beta)}(t,x,y) &= e^{\mu(y-x)-\frac{\mu^2}{2}t}\frac{1}{2\pi i}\int_{\phi'} e^{\frac{\xi^2}{2}t}\frac{e^{-\xi|y-x|}}{\xi+\beta\mu}\Big(\sum_{j=1}^{2} c_j(y,\mu;\xi)e^{-\xi a_j(x,y)}\Big)d\xi \\ &+ \mathbb{1}_{\mathbb{R}^-}(\beta\mu)\, e^{\mu(y-x)-\frac{\mu^2}{2}t}\frac{1}{2\pi i}\int_{\gamma} e^{\frac{\xi^2}{2}t}\frac{e^{-\xi|y-x|}}{\xi+\beta\mu}\Big(\sum_{j=1}^{2} c_j(y,\mu;\xi)e^{-\xi a_j(x,y)}\Big)d\xi \\ &= e^{\mu(y-x)-\frac{\mu^2}{2}t}\sum_{j=1}^{2}\frac{1}{2\pi}\int_{\mathbb{R}} e^{-\frac{w^2}{2}t}\frac{1}{iw+\beta\mu}c_j(y,\mu;iw)e^{-iw(a_j(x,y)+|x-y|)}dw \\ &\underbrace{-\beta\mu\,\mathbb{1}_{\mathbb{R}^-}(\beta\mu)\left(1+\beta\,\left(2\mathbb{1}_{[z,+\infty)}(y)-1\right)\right)\, e^{\mu(y-x)-\frac{\mu^2}{2}t}e^{\frac{\beta^2\mu^2}{2}t}e^{\beta\mu(|y-z|+|x-z|)}}_{(*)}. \end{aligned} \tag{1.3.12}$$

The last equality is obtained by shrinking $\int_{\phi'}$ towards $\int_{i\mathbb{R}}$, changing variable $\xi := iw$ and computing the integral on the loop γ in Figure 1.3.b through the method of residues.
We interpret the last equality of equation (1.3.12) as the sum of $(*)$ and two Fourier transforms computed at the value $(a_j(x,y)+|x-y|)$ of the two functions

$$\begin{aligned} w \mapsto \frac{e^{-\frac{w^2}{2}t}}{iw+\beta\mu}c_j(y,\mu;iw) &= \begin{cases} e^{-\frac{w^2}{2}t} & \text{if } j=1 \\ \beta\left(\left(2\mathbb{1}_{[z,+\infty)}(y)-1\right)+\mu\left(1+\beta\,\left(2\mathbb{1}_{[z,+\infty)}(y)-1\right)\right)\frac{i}{w-i\beta\mu}\right)e^{-\frac{w^2}{2}t} & \text{if } j=2. \end{cases} \end{aligned}$$

By Fourier transform of f, we mean $\mathcal{F}(f)(\omega)(=\hat{f}(\omega)) = \frac{1}{\sqrt{2\pi}}\int_{\mathbb{R}} e^{-i\omega y}f(y)\,dy$.
In both cases, these functions are integrable in w, so the transition density can now be written as

$$\begin{aligned} p_\mu^{(\beta)}(t,x,y) =& \frac{1}{\sqrt{2\pi}}e^{\mu(y-x)-\frac{\mu^2}{2}t}\sum_{j=1}^{2}\mathcal{F}\left(e^{-\frac{w^2}{2}t}\frac{1}{iw+\beta\mu}c_j(y,\mu;iw)\right)(a_j(x,y)+|x-y|) \\ &-\beta\mu\,\left(1+\beta\left(2\mathbb{1}_{[z,+\infty)}(y)-1\right)\right)\, e^{\mu(y-x)-\frac{\mu^2}{2}t}e^{\frac{\beta^2\mu^2}{2}t}e^{\beta\mu(|y-z|+|x-z|)}\mathbb{1}_{\mathbb{R}^-}(\beta\mu). \end{aligned}$$

It is straightforward to see that if $\beta = 0$ we get the simple Brownian motion with drift (without skew), and if $\mu = 0$ we get the (β)-SBM whose transition density is already known.
Therefore we now focus only on the case $\beta\mu \neq 0$.

Lemma 1.3.7. *If $a \in \mathbb{R}^*$, then*

$$\mathcal{F}\left(w \mapsto \frac{1}{w-ia}\right)(\omega) = i\sqrt{2\pi}\,\left(2\mathbb{1}_{\mathbb{R}^+}(a)-1\right)\, e^{a\omega}\,\mathbb{1}_{\mathbb{R}^-}\left(a\,\omega\right).$$

Proof. It is true since

$$\begin{aligned} \frac{1}{w-ia} &= \mathcal{F}^{-1}\left(i\sqrt{2\pi}\,\left(2\mathbb{1}_{\mathbb{R}^+}(a)-1\right)\, e^{a\omega}\,\mathbb{1}_{\mathbb{R}^-}\left(a\,\omega\right)\right)(w) \\ &= \frac{1}{\sqrt{2\pi}}\int_{\mathbb{R}}\left(i\sqrt{2\pi}\,\left(2\mathbb{1}_{\mathbb{R}^+}(a)-1\right)\, e^{a\omega}\,\mathbb{1}_{\mathbb{R}^-}\left(a\,\omega\right)\right)\, e^{i\,\omega\,w}\,d\omega. \end{aligned}$$

□

Using $\mathcal{F}\left(e^{-\frac{w^2}{2}t}\right)(\omega) = \frac{1}{\sqrt{t}}e^{-\frac{\omega^2}{2t}}$ and Lemma 1.3.7, we get

$$\begin{aligned} \mathcal{F}\left(e^{-\frac{w^2}{2}t}\frac{c_2(y,\mu;iw)}{iw+\beta\mu}\right)(\omega) =& \frac{\beta}{\sqrt{t}}\left(2\mathbb{1}_{[z,+\infty)}(y)-1\right)e^{-\frac{\omega^2}{2t}} \\ &-\frac{1}{\sqrt{t}}|\beta\mu|\left(1+\beta\left(2\mathbb{1}_{[z,+\infty)}(y)-1\right)\right)\cdot\left(e^{w\,\beta\mu}\mathbb{1}_{\mathbb{R}^-}\left(\beta\mu w\right)*e^{-\frac{w^2}{2t}}\right)(\omega). \end{aligned}$$

We compute the convolution as

$$\left(e^{w\,\beta\mu}\mathbb{1}_{\mathbb{R}^-}(\beta\mu w) * e^{-\frac{w^2}{2t}}\right)(\omega) = \sqrt{t}e^{\frac{(\beta\mu)^2}{2}t+\beta\mu\omega}\sqrt{2\pi}\left(\underbrace{\mathbb{1}_{\mathbb{R}^-}(\beta\mu)}_{(**)} + \left(2\mathbb{1}_{\mathbb{R}^+}(\beta\mu)-1\right)\Phi^c\left(\frac{\omega}{\sqrt{t}}+\beta\mu\sqrt{t}\right)\right).$$

The term $(**)$ arising from the convolution is actually the opposite to the term $(*)$ in (1.3.12) arising from the integration on the cycle γ containing the pole. Therefore the transition density becomes

$$\begin{aligned} p_\mu^{(\beta)}(t,x,y) =& \frac{1}{\sqrt{2\pi t}}e^{\mu(y-x)-\frac{\mu^2}{2}t}\left(e^{-\frac{(a_1(x,y)+|x-y|)^2}{2t}} + \beta\left(2\mathbb{1}_{[z,+\infty)}(y)-1\right)e^{-\frac{(a_2(x,y)+|x-y|)^2}{2t}}\right) \\ & - \left(1+\beta\left(2\mathbb{1}_{[z,+\infty)}(y)-1\right)\right)\beta\mu \\ & \cdot e^{\mu(y-x)-\frac{\mu^2}{2}t}e^{\frac{(\beta\mu)^2}{2}t+\beta\mu(a_2(x,y)+|x-y|)}\Phi^c\left(\frac{a_2(x,y)+|x-y|}{\sqrt{t}}+\beta\mu\sqrt{t}\right). \end{aligned}$$

Isolating the density of the Brownian motion with drift μ without skew, we recognize the expected expression, that is,

$$\begin{aligned} p_\mu^{(\beta)}(t,x,y) =& p_\mu(t,x,y)\left(e^{-\frac{(|x-y|)^2-|x-y|^2}{2t}} + \beta\left(2\mathbb{1}_{[z,+\infty)}(y)-1\right)e^{-\frac{(|x-z|+|y-z|)^2-|x-y|^2}{2t}}\right) \\ & - p_\mu(t,x,y)\sqrt{2\pi t}\beta\mu\left(1+\left(2\mathbb{1}_{[z,+\infty)}(y)-1\right)\beta\right) \\ & \cdot e^{\beta\mu a_2(x,y)}e^{\frac{(\beta\mu t+|x-y|)^2}{2t}}\Phi^c\left(\frac{|x-z|+|y-z|+\beta\mu t}{\sqrt{t}}\right), \end{aligned}$$

which completes the proof of Proposition 1.1.1.

1.3.5 Second method: contour integral

The method we develop here differs from the previous in the tricky way to deal with the integral (1.3.11). It has the advantage to prove Proposition 1.1.1 without distinguish between the different cases $\beta\mu<0$, $\beta\mu=0$ or $\beta\mu>0$, and in particular without computing explicitly the residue.

The idea is based on the fact that the integrand of the contour integral given by (1.3.11) is holomorphic on the curves $\phi(\Gamma)$ and $\mathfrak{a}+i\mathbb{R}$, where $\mathfrak{a}>0$ is as in Figure 1.5.a, and on the region between the two curves. It is indeed clear that the integrand is holomorphic everywhere except at the pole on $-\beta\mu$. In addition it is easy to show that the analogous to Lemma 1.3.6 for the segment $[iu,\mathfrak{a}+iu]$ holds, which implies that the integral on ρ_U in Figure 1.5.a is vanishing if $|U|\to\infty$ as well.
Let us state the announced lemma, which actually implies Lemma 1.3.6.

Lemma 1.3.8.

$$\lim_{|u|\to+\infty}\int_{\rho'_U} e^{\frac{\xi^2}{2}t}\,\frac{e^{-\xi|y-x|}}{\xi+\beta\mu}\left(\sum_{j=1}^{2}c_j(y,\mu;\xi)e^{-\xi a_j(x,y)}\right)d\xi = 0$$

where ρ'_U is the segment connecting $U=iu$ and $\mathfrak{a}+U$.

Proof. Let us consider the integral

$$I_u := \int_{\rho'_U} e^{\frac{\xi^2}{2}t}\,e^{-\xi|y-x|}\left(1+\frac{c_2(y,\mu;\xi)}{\xi+\beta\mu}e^{-\xi a_2(x,y)}\right)d\xi$$

and the following parametrization of the segment $\rho'_U=\{U+w;\ w\in(0,\mathfrak{a})\}$. Then

$$|I_u| \le \int_0^{\mathfrak{a}} e^{-\frac{(u^2-w^2)}{2}t}e^{-w|y-x|}\left(1+\left|\frac{c_2(y,\mu;w+iu)}{w+iu+\beta\mu}\right|e^{-w\,a_2(x,y)}\right)dw.$$

For u large enough

$$\left|\frac{c_2(y,\mu;w+iu)}{w+iu+\beta\mu}\right| = |\beta|\sqrt{\frac{\left(w\left(2\mathbb{1}_{[z,+\infty)}(y)-1\right)-\mu\right)^2+u^2}{(w+\beta\mu)^2+u^2}} \leq 1,$$

so

$$|I_u| \leq e^{-\frac{u^2}{2}t}e^{\frac{\mathfrak{a}^2}{2}t}\int_0^{\mathfrak{a}} 2dw = 2\mathfrak{a}e^{\frac{\mathfrak{a}^2}{2}t}e^{-\frac{u^2}{2}t}$$

which vanishes if u tends to infinity. □

As shown in Figure 1.5.a, the integral on the contour $\phi(\Gamma)$ in (1.3.11) shrinks to the integral on the line $\mathfrak{a}+i\mathbb{R}$ and the transition density can be written as

$$p_\mu^{(\beta)}(t,x,y) = e^{\mu(y-x)-\frac{\mu^2}{2}t}\frac{1}{2\pi i}\int_{\mathfrak{a}+i\mathbb{R}} e^{\frac{\xi^2}{2}t}\frac{e^{-\xi|y-x|}}{\xi+\beta\mu}\left(\sum_{j=1}^{2} c_j(y,\mu;\xi)e^{-\xi a_j(x,y)}\right)d\xi,$$

where $a_j(x,y)$ and $c_j(y,\mu;\xi)$ are given by (1.3.10).

A priori the integral does not depend on the choice of $\mathfrak{a}$, as soon as the latter has been chosen bigger than any pole, and (as a consequence of Lemma 1.3.8 for ρ'_U) one can choose to shrink the integral to any line $\mathfrak{a}'+i\mathbb{R}$ as in Figure 1.5.b. In particular, if $\beta\mu > 0$ there is no pole, hence one can choose directly $\mathfrak{a}=0$, and obtain the case of Figure 1.3.a.

Let us do the following change of variable: $\xi := \mathfrak{a}+iw$. Then $v_\mu^{(\beta)}(t,x,y) := \dfrac{p_\mu^{(\beta)}(t,x,y)}{p_\mu(t,x,y)}$ is equal to

$$v_\mu^{(\beta)}(t,x,y) = e^{\frac{1}{2t}(|y-x|-\mathfrak{a}t)^2}\frac{\sqrt{t}}{\sqrt{2\pi}}\int_{\mathbb{R}} e^{-\frac{w^2}{2}t}e^{iw\mathfrak{a}t}\sum_{j=1}^{2} e^{-iw(a_j(x,y)+|x-y|)}e^{-\mathfrak{a}\,a_j(x,y)}p_j(w)dw,$$

where the ratio $p_j(w) := \dfrac{c_j(y,\mu;\mathfrak{a}+iw)}{iw+\mathfrak{a}+\beta\mu}$, $j=1,2$, is given by

$$p_1(w)=1, \quad p_2(w) = \left(2\mathbb{1}_{\{y\geq z\}}-1\right)\beta + \beta\mu\left(1+\left(2\mathbb{1}_{\{y\geq z\}}-1\right)\beta\right)\frac{i}{w-i(\mathfrak{a}+\beta\mu)}.$$

We expect that the dependence on $\mathfrak{a}$ cancels. Let us make the computations explicitly.

$$\begin{aligned}
v_\mu^{(\beta)}(t,x,y) &= 1 + e^{\frac{1}{2t}(|y-x|-\mathfrak{a}t)^2}e^{-\mathfrak{a}\,a_2(x,y)}\frac{\sqrt{t}}{\sqrt{2\pi}}\int_{\mathbb{R}} e^{-\frac{w^2}{2}t}e^{-iw(a_2(x,y)+|x-y|-\mathfrak{a}t)}p_2(w)dw \\
&= 1 + \left(2\mathbb{1}_{\{y\geq z\}}-1\right)\beta\, e^{\frac{1}{2t}(|y-x|-\mathfrak{a}t)^2}e^{-\mathfrak{a}\,a_2(x,y)}e^{-\frac{(a_2(x,y)+|x-y|-\mathfrak{a}t)^2}{2t}} \\
&\quad + \beta\mu\left(1+\left(2\mathbb{1}_{\{y\geq z\}}-1\right)\beta\right)\sqrt{t}\,e^{\frac{1}{2t}(|y-x|-\mathfrak{a}t)^2}e^{-\mathfrak{a}\,a_2(x,y)}\mathcal{F}\left(w\mapsto e^{-\frac{w^2}{2}t}\frac{i}{w-i(\mathfrak{a}+\beta\mu)}\right)(\bar\omega) \\
&= 1 + \left(2\mathbb{1}_{\{y\geq z\}}-1\right)\beta\, e^{-\frac{1}{t}|y-x|a_2(x,y)-\frac{1}{2t}a_2(x,y)^2} \\
&\quad + \beta\mu\left(1+\left(2\mathbb{1}_{\{y\geq z\}}-1\right)\beta\right)\frac{\sqrt{t}}{\sqrt{2\pi}}\,e^{\frac{1}{2t}(|y-x|-\mathfrak{a}t)^2}e^{-\mathfrak{a}\,a_2(x,y)}\mathcal{F}\left(e^{-\frac{w^2}{2}t}\right)*\mathcal{F}\left(\frac{i}{w-i(\mathfrak{a}+\beta\mu)}\right)(\bar\omega),
\end{aligned}$$

where

$$\bar\omega := a_2(x,y)+|x-y|-\mathfrak{a}\,t = |x-z|+|y-z|-\mathfrak{a}\,t. \tag{1.3.13}$$

Thanks to Lemma 1.3.7, the convolution of the Fourier transforms can be explicit as

$$\begin{aligned}
&\mathcal{F}\left(w\mapsto e^{-\frac{w^2}{2}t}\right)*\mathcal{F}\left(w\mapsto\frac{i}{w-i(\mathfrak{a}+\beta\mu)}\right)(\bar\omega) \\
&\qquad = -\frac{1}{\sqrt{t}}e^{-\frac{1}{2t}w^2} * \left(\sqrt{2\pi}e^{(a+\beta\mu)w}\mathbb{1}_{(-\infty,0)}(w)\right)(\bar\omega) \\
&\qquad = -\frac{2\pi}{\sqrt{t}}\exp\left(-\frac{\bar\omega^2}{2t}+\frac{(\bar\omega+(\mathfrak{a}+\beta\mu)t)^2}{2t}\right)\Phi^c\left(\frac{\bar\omega+(\mathfrak{a}+\beta\mu)t}{\sqrt{t}}\right),
\end{aligned}$$

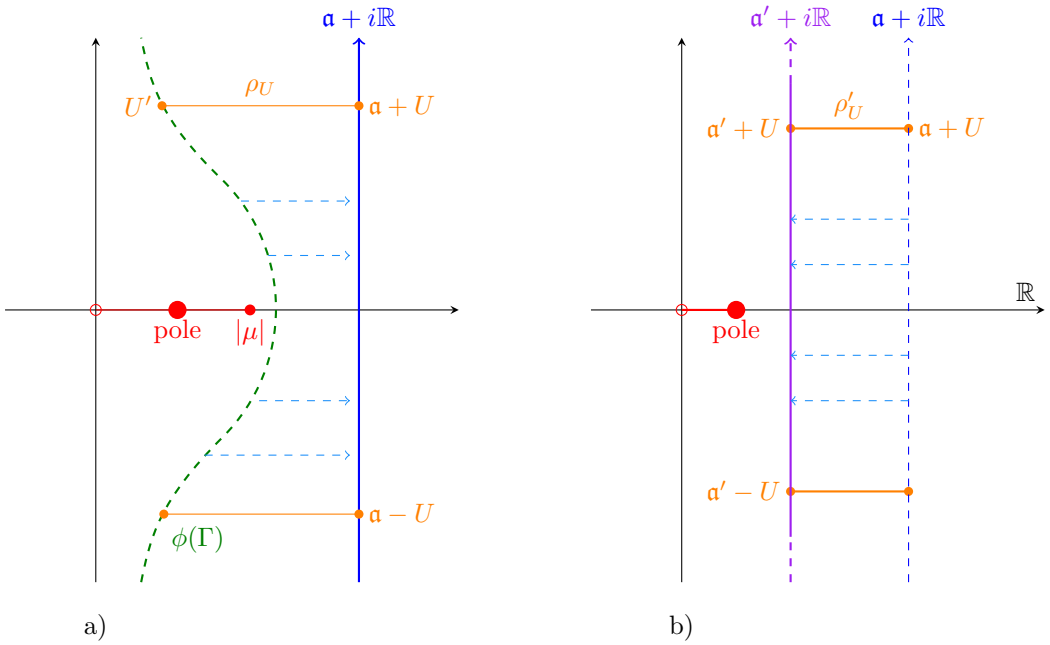

Figure 1.5:

a) The figure represents the vertical line $\mathfrak{a} + i\mathbb{R}$ on the right of the curve $\phi(\Gamma)$ and the segment ρ_U connecting the point $U = \mathfrak{a} + iu$ to its unique projection on $\phi(\Gamma)$. The segment $(0, |\mu|]$ contains all possible singularities (poles) with positive real part. It is the image under ϕ of $(-\frac{\mu^2}{2}, 0]$ (see Figure 1.2.b).

b) The segment ρ'_U connects here the point $\mathfrak{a} + U$ with its projection on $\mathfrak{a}' + i\mathbb{R}$. The real number $\mathfrak{a}'$ is chosen smaller than $\mathfrak{a}$ but larger than any pole.

where $\Phi^c(w) = \frac{1}{2\pi}\int_w^{+\infty} e^{-\frac{u^2}{2}}\,du$.
One can then conclude

$$v_\mu^{(\beta)}(t,x,y) = 1 + \left(2\mathbb{1}_{\{y\geq z\}} - 1\right)\beta\, e^{-\frac{1}{t}|y-x|a_2(x,y) - \frac{1}{2t}a_2(x,y)^2} - \beta\mu\left(1 + \left(2\mathbb{1}_{\{y\geq z\}} - 1\right)\beta\right)\sqrt{2\pi}\cdot \cdot \exp\left(\frac{(|y-x| - \mathfrak{a}t)^2 - 2t\mathfrak{a}\,a_2(x,y) - \bar{\omega}^2 + (\bar{\omega} + (\mathfrak{a}+\beta\mu)t)^2}{2t}\right)\Phi^c\left(\frac{\bar{\omega} + (\mathfrak{a}+\beta\mu)t}{\sqrt{t}}\right).$$

Let $\bar{\omega}$ as in (1.3.13) and recall that $a_2(x,y) = |x-z| + |y-z| - |x-y|$. To conclude the proof of Proposition 1.1.1, one just needs to notice that $\bar{\omega} + \mathfrak{a}t + \beta\mu t = a_2(x,y) + |x-y| + \beta\mu t$ does not depend on $\mathfrak{a}$ and neither the following sum.

$$\begin{aligned}(|y-x| - \mathfrak{a}\,t)^2 - 2\,t\,\mathfrak{a}\,a_2(x,y) - \bar{\omega}^2 + (\bar{\omega} + (\mathfrak{a}+\beta\mu)t)^2 \\ = (|y-x| - \mathfrak{a}\,t)^2 - 2\,t\,\mathfrak{a}\,a_2(x,y) + (\mathfrak{a}+\beta\mu)^2t^2 + 2t(\mathfrak{a}+\beta\mu)(a_2(x,y) + |x-y| - \mathfrak{a}\,t) \\ = -a_2(x,y)\,(a_2(x,y) + 2|x-y|) + (\beta\mu t + a_2(x,y) + |x-y|)^2.\end{aligned}$$

1.4 About the case of piecewise constant drift

The purpose of this section is to identify the difficulties in finding the transition densities of the one-SBM when the drift is not constant anymore.

Let us first consider the case of a piecewise constant drift.
The assertions at the beginning of Section 1.3 do not depend on the fact that the drift is constant. Thus, if b is a two-valued drift (i.e $b(x) := b_-\,\mathbb{1}_{(-\infty,z)}(x) + b_+\,\mathbb{1}_{[z,\infty)}(x)$), the infinitesimal generator of the (β)-SBM with drift b is, as in (1.3.1),

$$\begin{cases} L = \dfrac{1}{2h(x)}\dfrac{d}{dx}\left(h(x)\dfrac{d}{dx}\right) \text{ where } h(x) := \dfrac{1}{2}\left(1 + \beta\left(2\mathbb{1}_{[z,+\infty)} - 1\right)\right)e^{2B(x)}, \\ \mathcal{D}(L) = \left\{\psi \in H_0^1(\mathbb{R}, h(x)dx) :\ h(x)\psi'(x) \in H^1(\mathbb{R}, h^{-1}(x)dx)\right\}, \end{cases}$$

where $B(x) := \displaystyle\int_0^x b(u)\,d\,u$ is a primitive of b.
The integral representation of the transition density presented in (1.3.6), Section 1.3, holds in this case as well. Actually it holds in the larger context of skew diffusions with discontinuous but piecewise regular coefficients (their finite jumps should form a subset of $\mathbb{R}$ without accumulation points). In that case, Green's function can be computed, through a space transformation, from the one of a SBM with unitary diffusion coefficient; see Lejay, Lenôtre, and Pichot [35].

For a two valued drift $b \in \{b_-, b_+\}$ as above, they compute explicitly the transition density in two special cases.

- The *Bang-Bang SBM*: $b_+ = -b_-$. The transition density has been first obtained by Fernholz, Ichiba and Karatzas, see formulas (6.8),(6.9) and (6.10) in [21]. In [35], the authors recover this result computing the resolvent kernel and its inverse Laplace transforms. Since the resolvent kernel depends on λ only through $\sqrt{2\lambda + b_+^2}$, one could also follow the procedure developed in Section 1.3.4. For the same reason, in the case $\beta = 0$, our method recovers the formula given by Karatzas and Shreve (through a stochastic calculus approach, see Proposition 5.1 in [29]).

- The *constant Péclet case*: $b_- = \dfrac{1+\beta}{1-\beta}\,b_+$,$|\beta| \in (0,1)$. In this case the resolvent kernel depends on λ trough two functions $\phi_\pm(\lambda) := \sqrt{2\lambda + b_\pm^2}$. The combination of these functions is non trivial, which makes more difficult to transform the contour integral as we did in Section 1.3. In [35], the authors obtain an integral representation of the transition density. It may be that the integral involved there leads to transcendental functions different from the cumulative distribution function of a Gaussian.

If the drift b is not piecewise constant, in general it is difficult to compute Green's function of the resolvent, i.e to find the regular eigenfunctions $u_\pm$ of the operator $\frac{1}{2}\frac{d^2}{d^2x} + b(x)\frac{d}{dx}$ associated to the eigenvalue $\lambda \in \mathbb{C} \setminus (-\infty, 0]$ and such that $u_\pm(0) = 1$.

In conclusion: if b is piecewise constant one can compute Green's function, but it can involve some combination of terms which makes highly non trivial the computation of the inverse Laplace transform. If b is not piecewise constant, even the computation of Green's function is difficult.

Chapter 2

The multi-skew Brownian diffusions

Outline of the chapter: In this chapter we obtain an explicit representation of the transition density of the skew Brownian motion with constant drift and two semipermeable barriers in terms of Gaussian transition densities and of cumulative distribution functions (Theorem 2.3.7). We illustrate also a generalization of the rejection sampling method for sampling from densities which are expressed as a sum of series (Proposition 2.5.2). In particular the latter method can be applied to obtain samples from the two-skew Brownian motion. We devote then the last section (Section 2.5) to some numerical simulations for showing the performance of our sampling method. The main results in this chapter, together with the method proposed in Section 1.3, have been the object of the publication [16]. The latter paper includes a version of Theorem 2.3.7 which is only valid in some particular cases. The final version of the theorem, as it appears in this document, has been given in [15].

2.1 The framework

There are many possible generalizations of the skew Brownian motion presented in the first chapter: one-dimensional skew Brownian motion with more semipermeable barriers (Le Gall [32], Ouknine [46], Ramirez [51]), d-dimensional skew BM with one permeable barrier, as it is called by Ouknine [46] (referring to Portenko [49] and [50]), and distorted Brownian motion which is the Hunt process associated to a Dirichlet form studied by Ouknine, Russo and Trutnau [47]. We devote this chapter to the extension of the skew Brownian motion by considering several semipermeable barriers and we find an explicit expression of the transition density following the method illustrated in Section 1.3.

Let us denote by $(\beta_1, \beta_2, \dots, \beta_n)$-SBM the skew Brownian motion with n semipermeable barriers of permeability coefficients respectively $(\beta_1, \beta_2, \dots, \beta_n)$. For simplicity we denote it multi-SBM if the skewness coefficients do not matter.

The existence of several barriers does not allow anymore a trajectorial interpretation as randomly flipped excursions as for the (β)-SBM. Nevertheless one can define the process as the unique strong solution to a slight modification of equation (1.1.1). The stochastic differential equation satisfied by the $(\beta_1, \beta_2, \dots, \beta_n)-$SBM with drift $\mu \in \mathbb{R}$ and starting at $x_0 \in \mathbb{R}$ is

$$\begin{cases} dX_t = dW_t + \mu dt + \beta_1 dL_t^{z_1}(X) + \beta_2 dL_t^{z_2}(X) + \ldots + \beta_n dL_t^{z_n}(X), \\ X_0 = x_0, \\ L_t^{z_j} = \int_0^t \mathbb{1}_{\{X_s = z_j\}} dL_s^{z_j}, \ j = 1, 2, \dots, n, \end{cases} \qquad \mathcal{E}((\beta_1, \beta_2, \dots, \beta_n), \mu)$$

where the coefficients $\beta_j \in [-1, 1]$ and barriers $z_1 < z_2 < \cdots < z_n$. In the case $\mu = 0$, Ramirez [51] constructed the solution process through a Brownian time change using the scale function and the speed measure. A general proof of the existence and uniqueness of the solution, even in the case $\mu \neq 0$ is due to Le Gall [31, 32].

If for some $j \in \{1, \dots, n\}$, $|\beta_j| = 1$ there is a complete reflection at the barrier z_j: to the right if $\beta_j = 1$ (resp. to the left if $\beta_j = -1$). Therefore, if the starting point x_0 is in $(z_j, +\infty)$ (resp. $(-\infty, z_j)$), the

process will almost surely do not reach the barriers $z_1, \dots, z_{j-1}$ (resp. $z_{j+1}, \dots, z_n$). This kind of process is called skew-reflected Brownian motion. Song, Wang and Wang consider in [56] the case of two barriers ($n = 2$) without drift ($\mu = 0$): one reflecting and the other semipermeable.

Let us first notice that it is not possible to find the transition density of the two-SBM (i.e. $n = 2$) by following the approach recalled in Section 1.2. That's because the latter approach is based on the trajectorial interpretation (i.e. through excursions) of the one-SBM.
However one can find the transition densities using the method presented in Section 1.3. In particular the infinitesimal generator of the multi-SBM with constant drift μ is the self-adjoint operator $(L, \mathcal{D}(L))$ on $L^2(\mathbb{R}^2, h(x))$, generalizing the expression (1.3.1):

$$\begin{cases} L = \dfrac{1}{2h(x)} \dfrac{d}{dx} \left(h(x) \dfrac{d}{dx} \right) \text{ with } h(x) := k(x) e^{2\mu x}, \\ \mathcal{D}(L) = \left\{ \psi \in H_0^1(\mathbb{R}, h(x)dx) : \ h(x)\psi'(x) \in H^1(\mathbb{R}, h^{-1}(x)dx) \right\}, \end{cases} \tag{2.1.1}$$

with

$$k(x) := \prod_{j=1}^{n} \frac{1}{2} \left(1 + \beta_j \left(2 \mathbb{1}_{[z_j, +\infty)}(x) - 1 \right) \right) \tag{2.1.2}$$

(unique up to a multiplicative constant). Moreover the transition density of the multi-SBM with or without drift satisfies the contour integral representation (1.3.6)

$$p(t, x, y) = \frac{1}{2\pi i} \int_{\Gamma} e^{\lambda t} G(x, y; \lambda) d\lambda$$

where $G(x, y; \lambda)$ is Green's function of the resolvent $(\lambda - L)^{-1}$ and Γ is a complex contour around the spectrum $\sigma(L)$. Then, following the method presented in Section 1.3.5, one can compute Green's function of the resolvent, which satisfies Lemma 1.3.4.

Let us first focus on the transition density of the two-SBM. To the best of our knowledge, the transition density of the real-valued two-SBM with constant drift was not yet given as a closed formula, not even for the driftless version. In Section 5, Chapter II of [24], Gaveau, Okada and Okada have given a *non explicit formula* for the transition density of the two-skew Brownian motion without drift. They just identify it through a "kind of θ-function"

$$h(t, \xi, C, \alpha) = \frac{1}{2\pi} \int_{-\infty}^{+\infty} e^{-w^2 t} e^{iw\xi} \left(1 + C e^{iw\alpha} \right)^{-1} dw. \tag{2.1.3}$$

Here we obtain in Proposition 2.2.4 a closed formula for the transition density of the two-SBM without drift, and with drift in Theorem 2.3.7, as series of Gaussian transition densities and cumulative distribution functions.

2.2 The transition density of the two-skew Brownian motion

In this section we treat only the two-SBM *without drift*. Let us explicit the infinitesimal generator (2.1.1) in this driftless case with two semipermeable barriers z_1, z_2:

$$L = \frac{1}{2k(x)} \frac{d}{dx} \left(k(x) \frac{d}{dx} \right), \qquad \mathcal{D}(L) = \left\{ \psi \in H^1(\mathbb{R}, dx) : \ k(x)\psi'(x) \in H^1(\mathbb{R}, dx) \right\},$$

where the function $k(x)$ assumes three different values:

$$\begin{aligned} k(x) &= \left(\frac{1}{2} + \beta_1 \left(\mathbb{1}_{[z_1, +\infty)}(x) - \frac{1}{2} \right) \right) \left(\frac{1}{2} + \beta_2 \left(\mathbb{1}_{[z_2, +\infty)}(x) - \frac{1}{2} \right) \right) \\ &= \begin{cases} \frac{1}{4}(1 - \beta_1)(1 - \beta_2) & x < z_1, \\ \frac{1}{4}(1 + \beta_1)(1 - \beta_2) & z_1 \le x < z_2, \\ \frac{1}{4}(1 + \beta_1)(1 + \beta_2) & x \ge z_2. \end{cases} \end{aligned} \tag{2.2.1}$$

Notice that it is a straightforward generalization of (1.1.4). We refer again to Étoré's PhD thesis [18] and Lejay and Martinez [36] for the proof that this is actually the infinitesimal generator in the classical sense.

2.2.1 Green's function of the resolvent

In this section we compute explicitly Green's function of the resolvent, whose generic form is given in Lemma 1.3.4. One has to find the eigenfunctions $U_\pm$ of L associated to the eigenvalue λ, i.e. solution to (1.3.8). The two semi-permeable barriers z_1, z_2 divide the real line into three intervals over which the functions $U_\pm$ are linear combinations of $u_-(x) = \exp\left(\sqrt{2\lambda}x\right)$, $u_+(x) = \exp\left(-\sqrt{2\lambda}x\right)$. The functions $u_\pm$ are the fundamental solutions of the homogeneous problem $(\lambda - L)u = 0$ (Sturm-Liouville): the eigenfunctions of L for the eigenvalue $\lambda \in \mathbb{C} \setminus (-\infty, 0]$ and vanish either at $+\infty$ or $-\infty$.

Figure 2.1: The functions U_- (on the left) and U_+ (on the right).

Therefore, as in Figure 2.1,

$$U_- = \begin{cases} u_- & x \le z_1, \\ A(\lambda)u_- + B(\lambda)u_+ & z_1 \le x \le z_2, \\ C(\lambda)u_- + D(\lambda)u_+ & x \ge z_2; \end{cases} \qquad U_+ = \begin{cases} G(\lambda)u_- + H(\lambda)u_+ & x \le z_1, \\ E(\lambda)u_- + F(\lambda)u_+ & z_1 \le x \le z_2, \\ u_+ & x \ge z_2, \end{cases} \tag{2.2.2}$$

with eight coefficients to be determined. Notice that since $U_\pm \in \mathcal{D}(L)$, they

- are continuous functions and
- have to satisfy the so-called *transmission conditions* derived from the continuity of $x \mapsto k(x)U'_\pm(x,\lambda)$.

These conditions determine the eight coefficients:

$$\begin{cases} A(\lambda) = (1+\beta_1)^{-1}; \\ B(\lambda) = A(\lambda)\beta_1 e^{2\sqrt{2\lambda}z_1}; \\ C(\lambda) = \left(\beta_1\beta_2 e^{-2\sqrt{2\lambda}(z_2-z_1)} + 1\right)((1+\beta_1)(1+\beta_2))^{-1}; \\ D(\lambda) = \left(\beta_1 e^{2\sqrt{2\lambda}z_1} + \beta_2 e^{2\sqrt{2\lambda}z_2}\right)((1+\beta_1)(1+\beta_2))^{-1}; \end{cases}$$

$$\begin{cases} G(\lambda) = -\left(\beta_2 e^{-2\sqrt{2\lambda}z_2} + \beta_1 e^{-2\sqrt{2\lambda}z_1}\right)((1-\beta_1)(1-\beta_2))^{-1}; \\ H(\lambda) = \left(\beta_1\beta_2 e^{-2\sqrt{2\lambda}(z_2-z_1)} + 1\right)((1-\beta_1)(1-\beta_2))^{-1}; \\ E(\lambda) = -F(\lambda)\beta_2 e^{-2\sqrt{2\lambda}z_2}; \\ F(\lambda) = (1-\beta_2)^{-1}. \end{cases}$$

The second step is to compute *the Wronskian*. Let k as in (2.2.1). Since for each λ fixed $x \mapsto k(x)W(U_-, U_+)(x,\lambda)$ is constant, one can compute it choosing a favorite point.

$$x \mapsto W(U_-, U_+)(x,\lambda) \equiv -2\sqrt{2\lambda}H(\lambda).$$

This leads to the following lemma.

Lemma 2.2.1. *Green's function is given by*

$$G(x,y;\lambda) = \frac{1}{\phi(\lambda)} e^{-\phi(\lambda)\,|x-y|} \frac{\sum_{j=1}^4 c_j(y) e^{-\phi(\lambda)\,a_j(x,y)}}{\beta_1\beta_2 e^{-2\,\phi(\lambda)\,z} + 1},$$

where $\phi(\lambda) := \sqrt{2\lambda}$, $z := z_2 - z_1$ *is the distance between the barriers, and*

$$\begin{cases} c_1(y) \equiv 1 \\ c_2(y) = \left(2\mathbb{1}_{[z_1,+\infty)}(y) - 1\right)\beta_1 \\ c_3(y) = \left(2\mathbb{1}_{[z_2,+\infty)}(y) - 1\right)\beta_2 \\ c_4(y) = \left(1 - 2\mathbb{1}_{[z_1,z_2)}(y)\right)\beta_1\beta_2, \end{cases} \tag{2.2.3}$$

$$\begin{cases} a_1(x,y) \equiv 0 \\ a_2(x,y) = |y - z_1| + |x - z_1| - |y - x| \\ a_3(x,y) = |y - z_2| + |y - z_2| - |y - x| \\ a_4(x,y) = 2\left(z_2 - \max(x,y,z_1)\right)^+ + 2\left(\min(x,y,z_2) - z_1\right)^+. \end{cases} \tag{2.2.4}$$

Proof. We present the computations just in one case, since the other cases are similar. Let $x < z_1 < z_2 < y$. Since there is no drift ($\mu = 0$), $h \equiv k$ where k is the function given in (2.2.1). From Lemma 1.3.4, Green's function has the following form

$$\begin{aligned} G(x,y;\lambda) &= -2k(y)\frac{U_+(y,\lambda)U_-(x,\lambda)}{-2\sqrt{2\lambda}H(\lambda)} = -2k(y)\frac{u_+(y,\lambda)u_-(x,\lambda)}{-\frac{1}{2}\sqrt{2\lambda}(1+\beta_1\beta_2 e^{-2\sqrt{2\lambda}z})} \\ &= \frac{1}{\sqrt{2\lambda}}\frac{4k(y)e^{-\sqrt{2\lambda}(y-x)}}{1+\beta_1\beta_2 e^{-2\sqrt{2\lambda}z}}. \end{aligned}$$

Noticing that $a_j(x,y) = 0$ for $j \in \{1,2,3,4\}$ and that $\sum_{j=1}^4 c_j(y) = 4k(y)$, one concludes the proof. □

Remark 2.2.2. Let us notice some useful facts

(i) The function ϕ is a well defined biholomorphism between $\mathbb{C} \setminus (-\infty, 0]$ and $\{\zeta \in \mathbb{C};\ \Re e(\zeta) > 0\}$.

(ii) The function at the denominator $\lambda \mapsto 1 + \beta_1\beta_2 e^{-2\,\phi(\lambda)\,z}$ has no zero in $\mathbb{C} \setminus (-\infty, 0]$.

(iii) $a_j(x,y) \geq 0$ for $j \in \{1,2,3,4\}$.

2.2.2 The explicit representation of the transition density

Since the dependence on λ of Green's function is given only through $\phi(\lambda) = \sqrt{2\lambda}$, one can apply the change of variable $\lambda \mapsto \phi(\lambda) =: \xi$ to the contour integral representation in equation (1.3.6):

$$\int_\Gamma e^{\frac{\phi(\lambda)^2}{2}t}\,\overline{G}(x,y;\phi(\lambda))\,d\phi(\lambda) = \int_{\phi(\Gamma)} e^{\frac{\xi^2}{2}t}\,\overline{G}(x,y;\xi)\,d\xi$$

where $\overline{G}(x,y;\phi(\lambda)) := \phi(\lambda)G(x,y;\lambda)$ and $G(x,y,\lambda)$ is given in Lemma 2.2.1. See Figure 2.2.a.
Since the integrand $e^{\frac{\xi^2}{2}t}\overline{G}(x,y;\xi)$ is holomorphic on the closed subset of the complex plane between $i\mathbb{R}$ and $\phi(\Gamma)$, we deform (shrink) the contour $\phi(\Gamma)$ to the imaginary line by an homotopy, see Figure 2.2.b. One still needs to check that the following lemma holds.

Lemma 2.2.3. *Consider the function*

$$\overline{G}(x,y,\xi) = e^{-\xi|x-y|}\frac{\sum_{j=1}^4 c_j(y)e^{-\xi a_j(x,y)}}{\beta_1\beta_2 e^{-2\xi z} + 1},$$

where the functions c_j and a_j are given respectively by (2.2.3) and (2.2.4), and $z := z_2 - z_1$.
Let $u \in \mathbb{R}$. Let U' be the unique point with imaginary part u in $\phi(\Gamma)$ and ρ_U be the segment connecting U' with its projection $U = i\,u$ on $i\mathbb{R}$ (see Figure 2.2.b), then

$$\lim_{u\to\pm\infty}\int_{\rho_U} e^{\frac{\xi^2}{2}t}\,\overline{G}(x,y;\xi)\,d\xi = 0.$$

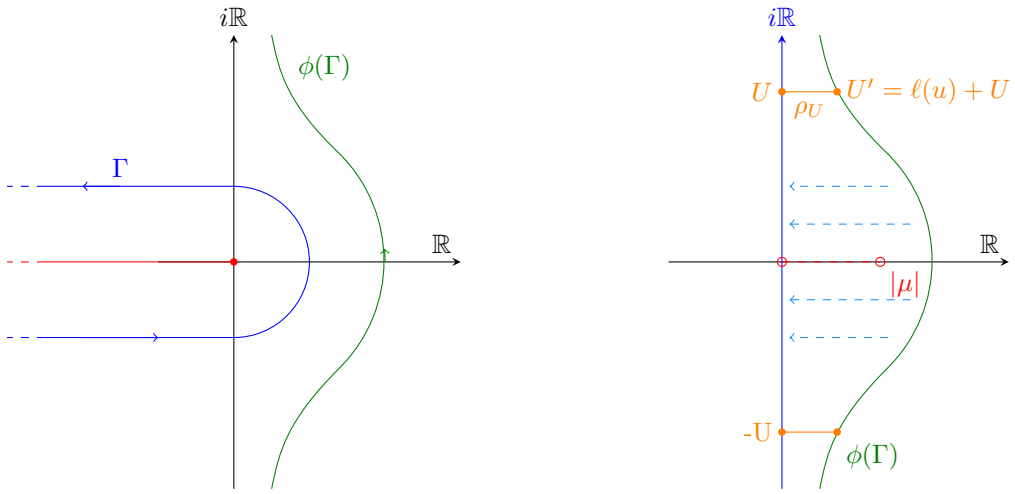

Figure 2.2:

a) Let $\mu = 0$. The picture shows the (green) image of the (blue) contour Γ under $\phi : \lambda \mapsto \sqrt{2\lambda}$. The spectrum of the operator $(L, \mathcal{D}(L))$ is contained in the (red) semi-axis $(-\infty, 0]$, which coincides with the complement of the domain of ϕ.

b) The picture shows the contour $\phi(\Gamma)$ which shrinks to the imaginary line (in blue). The segment ρ_U connects the unique point $U' \in \phi(\Gamma)$ with imaginary part u to its projection U on the imaginary line.

Proof. Let us show that the absolute value converges to zero.

$$\left| \int_{\rho_U} e^{\frac{\xi^2}{2}t}\, \overline{G}(x,y;\xi)\, d\xi \right| \leq \int_{\rho_U} \left| e^{\frac{\xi^2}{2}t}\, \overline{G}(x,y;\xi) \right| d\xi = \int_0^{\ell(u)} e^{\frac{(w^2-u^2)}{2}t} \left| \overline{G}(x,y;iu+w) \right| dw$$

with $\ell(u) := |U - U'|$ (hence $U' = \ell(u) + U$) and $\lim_{u\to\infty} \ell(u) = 0$. Let us notice that

$$\left| \overline{G}(x,y;iu+w) \right| \leq e^{-w|x-y|} \frac{\sum_{j=1}^4 |c_j(y)|\, e^{-wa_j(x,y)}}{\left| \beta_1\beta_2 e^{-2(iu+w)z} + 1 \right|},$$

therefore

$$\left| \int_{\rho_U} e^{\frac{\xi^2}{2}t}\, \overline{G}(x,y;\xi)\, d\xi \right| \leq e^{-\frac{u^2}{2}t} \int_0^{\ell(u)} e^{\frac{w^2}{2}t}\, e^{-w|x-y|} \frac{\sum_{j=1}^4 |c_j(y)|\, e^{-wa_j(x,y)}}{1 - |\beta_1\beta_2|\, e^{-2wz}}\, dw$$

that clearly converges to zero if $|u|$ goes to infinity. □

Therefore the integral in (1.3.6) becomes (with $\xi = iw$)

$$p^{(\beta_1,\beta_2)}(t,x,y) = \frac{1}{2\pi} \int_{\mathbb{R}} e^{-\frac{w^2}{2}t} \frac{\sum_{j=1}^4 c_j(y) e^{-iw(a_j(x,y)+|x-y|)}}{\beta_1\beta_2 e^{-2iwz} + 1} dw. \tag{2.2.5}$$

One can also rewrite it using the function h defined by equation (2.1.3):

$$p^{(\beta_1,\beta_2)}(t,x,y) = \sum_{j=1}^4 c_j(y) h\left(\frac{t}{2}, -\left(a_j(x,y) + |x-y|\right), \beta_1\beta_2, -2z \right),$$

which is the integral representation given by Gaveau, Okada and Okada in [24].
Nevertheless, since $|\beta_1\beta_2| \leq 1$, we can explicit further the expression (2.2.5) and write it as a series of Fourier transforms.

Proposition 2.2.4. *The transition density of the (β_1, β_2)-SBM admits the following expansion*

$$\begin{aligned} &p^{(\beta_1,\beta_2)}(t,x,y) = p(t,x,y)v^{(\beta_1,\beta_2)}(t,x,y) \\ &\text{with } v^{(\beta_1,\beta_2)}(t,x,y) = \sum_{k=0}^{\infty}(-\beta_1\beta_2)^k \sum_{j=1}^{4} c_j(y) e^{-\frac{(a_j(x,y)+2\,z\,k)^2}{2t}} e^{-|x-y|\frac{a_j(x,y)+2\,z\,k}{t}}, \end{aligned} \tag{2.2.6}$$

where $p(t,x,y)$ is the usual transition density function from x to y of the Brownian motion and the functions c_j and a_j are given respectively by (2.2.3) and (2.2.4), and $z := z_2 - z_1$.

Proof. First let us do the case $|\beta_1\beta_2| < 1$. Let us consider the expression (2.2.5). The denominator can be seen as the sum of a geometric series

$$\frac{1}{1+\beta_1\beta_2 e^{-2\,i\,w\,z}} = \sum_{k=0}^{\infty}(-\beta_1\beta_2 e^{-2\,i\,w\,z})^k\,.$$

Therefore the density can be written as

$$p^{(\beta_1,\beta_2)}(t,x,y) = \frac{1}{2\pi}\int_{\mathbb{R}} \sum_{k=0}^{\infty}(-\beta_1\beta_2)^k e^{-\frac{w^2}{2}t} e^{-iw|x-y|} \sum_{j=1}^{4} c_j(y) e^{-iw(a_j(x,y)+2\,z\,k)} dw.$$

We can exchange integral and series, because the series of absolute values $e^{-\frac{w^2}{2}t}\frac{1}{1-|\beta_1\beta_2|}$ is integrable.
We conclude that the transition density is a series of Fourier transforms:

$$\begin{aligned} p^{(\beta_1,\beta_2)}(t,x,y) &= \sum_{k=0}^{\infty}(-\beta_1\beta_2)^k \sum_{j=1}^{4} \frac{c_j(y)}{2\pi} \int_{\mathbb{R}} e^{-\frac{w^2}{2}t} e^{-iw(a_j(x,y)+2\,z\,k+|x-y|)} dw \\ &= \frac{1}{\sqrt{2\pi}} \sum_{k=0}^{\infty}(-\beta_1\beta_2)^k \sum_{j=1}^{4} c_j(y)\hat{g}_t(a_j(x,y)+2\,z\,k+|x-y|) \\ &= \frac{1}{\sqrt{2\pi t}} \sum_{k=0}^{\infty}(-\beta_1\beta_2)^k \sum_{j=1}^{4} c_j(y) g_1\left(\frac{a_j(x,y)+2\,z\,k+|x-y|}{\sqrt{t}}\right) \end{aligned} \tag{2.2.7}$$

where $g_t(w) := e^{-\frac{w^2}{2}t} = g_1(w\sqrt{t})$ and its Fourier transform satisfies $\hat{g}_t(\omega) = \frac{1}{\sqrt{t}} g_t(\frac{\omega}{t}) = \frac{1}{\sqrt{t}} g_1\left(\frac{\omega}{\sqrt{t}}\right)$. We notice that $g_1(a+b) = g_1(a)g_1(b)e^{-ab}$ hence we can write the density as

$$\begin{aligned} p^{(\beta_1,\beta_2)}(t,x,y) &= \frac{1}{\sqrt{2\pi t}}\, g_1\left(\frac{|x-y|}{\sqrt{t}}\right) v^{(\beta_1,\beta_2)}(t,x,y) \\ v^{(\beta_1,\beta_2)}(t,x,y) &= \sum_{k=0}^{\infty}(-\beta_1\beta_2)^k \sum_{j=1}^{4} c_j(y) g_1\left(\frac{a_j(x,y)+2\,z\,k}{\sqrt{t}}\right) e^{-\frac{|x-y|}{t}(a_j(x,y)+2\,z\,k)}. \end{aligned}$$

Using the identity $p(t,x,y) = \frac{1}{\sqrt{2\pi t}} g_1\left(\frac{|x-y|}{\sqrt{t}}\right)$ we conclude and obtain (2.2.6).

Now let us do the remaining case $|\beta_1\beta_2| = 1$. Here we need to adopt a trick: instead of pushing the contour integral on the imaginary axis, we push it on the line $\mathfrak{a} + i\mathbb{R} = \{z \mid \Re e(z) = \mathfrak{a}\}$ for some $\mathfrak{a} > 0$. The same proof as in Lemma 2.2.3 shows that we are allowed to do so and we are reduced to compute the integral (by substituting ξ with $\mathfrak{a} + iw$ in (1.3.6)

$$p^{(\beta_1,\beta_2)}(t,x,y) = \frac{1}{2\pi}\int_{\mathbb{R}} e^{(-\frac{w^2}{2}+iw\mathfrak{a}+\frac{\mathfrak{a}^2}{2})t} \frac{\sum_{j=1}^{4} c_j(y) e^{-(iw+\mathfrak{a})(a_j(x,y)+|x-y|)}}{\beta_1\beta_2 e^{-2\mathfrak{a}z-2iwz}+1} dw.$$

Since $|\beta_1\beta_2 e^{-2\mathfrak{a}z-2iwz}| = e^{-2\mathfrak{a}z} < 1$ we can expand the denominator as a geometric series and obtain

$$p^{(\beta_1,\beta_2)}(t,x,y) = \frac{1}{2\pi}\int_{\mathbb{R}} \sum_{k=0}^{\infty} (-\beta_1\beta_2)^k e^{(-\frac{w^2}{2}+iwa+\frac{a^2}{2})t} e^{-(a+iw)|x-y|} \sum_{j=1}^{4} c_j(y) e^{-(a+iw)(a_j(x,y)+2\,z\,k)} dw.$$

Since the sum of the series of the absolute values $e^{-\frac{1}{2}w^2 t}\,\frac{e^{\left(\frac{1}{2}\mathfrak{a}^2 t+\mathfrak{a}(|x-y|+a_j(x,y))\right)}}{2\pi(1-e^{-2z\mathfrak{a}t})}$ is integrable in w, one can exchange the integral and the series. After interpreting the sum of integrals as a sum of Fourier transforms, one has

$$p^{(\beta_1,\beta_2)}(t,x,y) = \frac{1}{\sqrt{2\pi t}} \sum_{k=0}^{\infty} (-\beta_1\beta_2)^k \sum_{j=1}^{4} c_j(y) e^{\frac{\mathfrak{a}^2}{2}t-\mathfrak{a}(a_j(x,y)+2zk+|x-y|)} g_1\left(\frac{a_j+2zk+|x-y|+\mathfrak{a}t}{\sqrt{t}}\right).$$

After simplifying the latter sum becomes equal to (2.2.7) which does not depend on $\mathfrak{a}$. □

2.2.3 Interpretation as an additive perturbation of the transition density of the Brownian motion

One can notice that the transition density of the two-SBM is a multiplicative perturbation (by $v^{(\beta_1,\beta_2)}$) of the transition density of the Brownian motion. Actually we can interpret it as an additive perturbation, writing $v^{(\beta_1,\beta_2)}$ as $1+V^{(\beta_1,\beta_2)}$. Indeed Green's function can be rewritten as

$$G(x,y;\lambda) = \frac{1}{\phi(\lambda)} e^{-\phi(\lambda)\,|x-y|}\left(1+\frac{\sum_{j=1}^{4}\bar{c}_j(y)e^{-\phi(\lambda)\,\bar{a}_j(x,y)}}{\beta_1\beta_2 e^{-2\,\phi(\lambda)\,z}+1}\right).$$

where $\phi(\lambda) := \sqrt{2\lambda}$ and $z := z_2 - z_1$ is the distance between the barriers. For $j = 2,3,4$, $\bar{a}_j(x,y)$ and $\bar{c}_j(y)$ are given by (2.2.4) and (2.2.3) respectively, and

$$\bar{c}_1(y) := -\left(1-2\mathbb{1}_{[z_1,z_2)}(y)\right)c_4(y) = -\beta_1\beta_2, \qquad \bar{a}_1(x,y) := 2z.$$

Therefore, following the proof of Proposition 2.2.4, one obtains the following new version of (2.2.6):

$$\begin{aligned} &p^{(\beta_1,\beta_2)}(t,x,y) = p(t,x,y)v^{(\beta_1,\beta_2)}(t,x,y),\\ &\text{where } v^{(\beta_1,\beta_2)}(t,x,y) = 1+\sum_{k=0}^{\infty}(-\beta_1\beta_2)^k \sum_{j=1}^{4}\bar{c}_j(y)e^{-\frac{(\bar{a}_j(x,y)+2\,z\,k)^2}{2t}} e^{-|x-y|\frac{\bar{a}_j(x,y)+2\,z\,k}{t}}. \end{aligned} \tag{2.2.8}$$

In particular, in case x and y are both on the same unbounded side of the barriers, one gets that $\bar{c}_4 = -\bar{c}_1$ and $\bar{a}_4 = \bar{a}_1 = 2\,z$, and each term of the infinite series is a sum of only two terms (j=2,3).

2.3 The transition density of the two-SBM with constant drift

In this section we provide the transition density for the (β_1,β_2)-SBM with constant drift μ, in terms of Gaussians and the transcendental cumulative distribution function of Gaussians. To simplify the notations, without loss of generality we assume that the barriers are located in 0 and $z > 0$.

Its infinitesimal generator on $L^2(\mathbb{R}, h(x)dx)$ is the self-adjoint operator given by (2.1.1) where $h(x) = e^{2\mu x}k(x)$ with $k(x)$ given by (2.2.1).

2.3.1 Green's function of the resolvent

Let us define four non negative functions

$$\begin{cases} a_1(x,y) \equiv 0\\ a_2(x,y) = |x|+|y|-|y-x|\\ a_3(x,y) = |x-z|+|y-z|-|y-x|\\ a_4(x,y) = 2\,(z-\max(x,y,0))^+ + 2\min(x,y,z)^+. \end{cases} \tag{2.3.1}$$

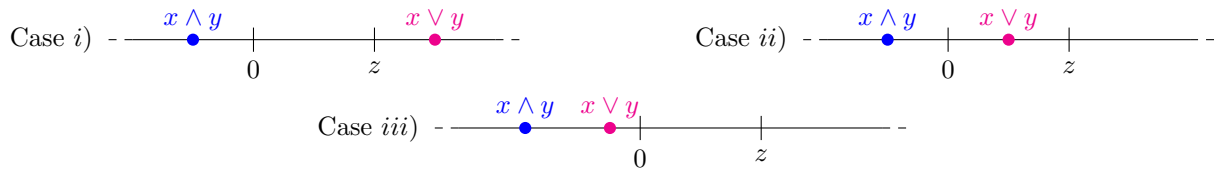

Figure 2.3: The different values of $a_j, j = 1, 2, 3, 4$, according to the relative positions of x, y and z:

Case i) For all $j = 1, 2, 3, 4$, $a_j = 0$

Case ii) $a_1 = a_2 = 0$ and $a_3 = a_4 = 2\,(z - x \vee y)$

Case iii) $a_1 = 0, a_2 = -2\,x \vee y, a_3 = 2\,(z - x \vee y), a_4 = 2z$.

Let us also introduce polynomials of second order in ξ setting

$$c_j(y, \mu; \xi) := \xi^2\, c_{j,0}(y) + \xi\, \mu c_{j,1}(y) + \mu^2 c_{j,2}(y), j \in \{1, 2, 3, 4\},$$

where

$$\begin{cases} c_{1,0}(y) = 1, \\ c_{2,0}(y) = \left(2\mathbb{1}_{\{y>0\}} - 1\right)\beta_1 \\ c_{3,0}(y) = \left(2\mathbb{1}_{\{y>z\}} - 1\right)\beta_2 \\ c_{4,0}(y) = \left(1 - 2\mathbb{1}_{[0,z)}(y)\right)\beta_1\beta_2 \end{cases}, \begin{cases} c_{1,1}(y) = \beta_1 + \beta_2 \\ c_{2,1}(y) = -\beta_1 - c_{4,0}(y) \\ c_{3,1}(y) = -\beta_2 + c_{4,0}(y) \\ c_{4,1}(y) = 0 \end{cases}, \begin{cases} c_{1,2}(y) = \beta_1\beta_2 \\ c_{2,2}(y) = \beta_1 c_{3,0}(y) \\ c_{3,2}(y) = -\beta_2 c_{2,0}(y) \\ c_{4,2}(y) = -c_{4,0}(y). \end{cases} \tag{2.3.2}$$

The polynomials c_j can be rewritten as

$$\begin{cases} c_1(y, \mu; \xi) = (\xi + \beta_1\mu)(\xi + \beta_2\mu) \\ c_2(y, \mu; \xi) = \left(2\mathbb{1}_{\{y>0\}} - 1\right)\left(\beta_1\xi - \left(2\mathbb{1}_{\{y>0\}} - 1\right)\beta_1\mu\right)\left(\xi - \left(2\mathbb{1}_{\{y>z\}} - 1\right)\beta_2\mu\right) \\ c_3(y, \mu; \xi) = \left(2\mathbb{1}_{\{y>z\}} - 1\right)\left(\beta_2\xi - \left(2\mathbb{1}_{\{y>z\}} - 1\right)\beta_2\mu\right)\left(\xi + \left(2\mathbb{1}_{\{y>0\}} - 1\right)\beta_1\mu\right) \\ c_4(y, \mu; \xi) = \left(1 - 2\mathbb{1}_{\{0\le y<z\}}\right)\left(\beta_1\beta_2\xi^2 - \beta_1\beta_2\mu^2\right). \end{cases}$$

Let $\mathfrak{a}$ be a fixed real number and define

$$C_{j,0} := c_{j,0}, \quad C_{j,1} := \mu c_{j,1} + 2c_{j,0}\mathfrak{a}, \quad C_{j,2} := c_{j,2}\mu^2 + c_{j,1}\mu\mathfrak{a} + c_{j,0}\mathfrak{a}^2, \tag{2.3.3}$$

which are y-dependent.

Lemma 2.3.1. *Green's function is given by*

$$G(x, y; \xi) = \frac{1}{\xi} e^{\mu(y-x)} e^{-\xi|x-y|} \frac{\sum_{j=1}^4 c_j(y, \mu; \xi) e^{-\xi a_j(x,y)}}{\beta_1\beta_2 e^{-2\,\xi\, z}(\xi^2 - \mu^2) + (\xi + \beta_1\mu)(\xi + \beta_2\mu)},$$

where z is the distance between the barriers and $\xi := \sqrt{2\lambda + \mu^2} \in \{\zeta \in \mathbb{C}\ s.t.\ \Re e(\zeta) > 0\}$ $(\lambda \in \mathbb{C}\backslash(-\infty, 0])$. The functions $a_j(x, y)$ are the non negative functions defined by (2.3.1), and $c_j(y, \mu; \xi) = \xi^2 c_{j,0}(y) + \xi\mu c_{j,1}(y) + \mu^2 c_{j,2}(y)$ are given by (2.3.2).

Proof. The form of Green's function is given by Lemma 1.3.4, hence one has to compute the functions $U_\pm$. They are linear combinations of

$$u_-(x) = e^{-\mu x + \sqrt{\mu^2 + 2\lambda}\, x}, \qquad u_+(x) = e^{-\mu x - \sqrt{\mu^2 + 2\lambda}\, x},$$

generalizing (2.2.2). One finds $U_\pm$ imposing the continuity of $U_\pm$ and of $h\,U'_\pm$. The latter condition yields the transmission conditions

$$k(0^-)U'_\pm(0^-) = k(0^+)U'_\pm(0^+), \qquad k(z^-)U'_\pm(z^-) = k(z^+)U'_\pm(z^+),$$

where k is given by (2.2.1). One computes then the Wronskian, using the fact that $w \mapsto h(w)W(U_-, U_+)(w, \lambda)$ is constant. □

2.3.2 Some preliminary lemmas

Before presenting our main result, let us develop some useful technical lemmas.

About Green's function

Let $x, y \in \mathbb{R}$ be fixed. We first study the singularities of Green's function $\xi \mapsto G(x, y; \xi)$ for $\xi \in \mathbb{C}$ such that the real part $\Re e(\xi)$ is non negative. Since Green's function is a ratio of holomorphic functions, it is meromorphic and the singularities are poles.

Lemma 2.3.2 (Possible singularities of Green's function)**.** *Let $\beta_1, \beta_2 \in [-1, 1]$, $\mu \in \mathbb{R}$ and $z > 0$.*

- *If $2z\beta_1\beta_2\mu + \beta_1 + \beta_2 \neq 0$ then 0 is an erasable singularity for Green's function. Moreover*
  - *If $\beta_1\mu > 0$ and $\beta_2\mu > 0$ or if $\beta_1\beta_2 < 0$ but $2z\beta_1\beta_2\mu^2 + \beta_1\mu + \beta_2\mu > 0$, there are no poles.*
  - *If $2z\beta_1\beta_2\mu^2 + \beta_1\mu + \beta_2\mu < 0$, there is a pole of the first order.*
  - *If $\beta_1\mu < 0, \beta_2\mu < 0$ and $2\,z\,\beta_1\beta_2\mu^2 + \beta_1\mu + \beta_2\mu > 0$, there are two poles of the first order.*
- *If $2z\beta_1\beta_2\mu+\beta_1+\beta_2 = 0$, then 0 is either erasable singularity (for example in Case i) of Figure 2.3) or a pole of order 1 and it may be a pole of order two for a special choice of the parameters z, μ, β_1, β_2. And there is a positive pole of the first order only if $\beta_1\mu < 0, \beta_2\mu < 0$.*

Proof. Let us consider the denominator of Green's function, which is

$$D(\xi) := \beta_1\beta_2(\xi^2 - \mu^2)e^{-2\,\xi\,z} + (\xi + \beta_1\mu)(\xi + \beta_2\mu)$$

and let us study its zeros on $\{\zeta \in \mathbb{C} \text{ s.t. } \Re e(\zeta) \geq 0\}$.
Clearly $D(0) = 0$, the others zeros of $\xi \mapsto D(\xi)$ can only be on $\mathbb{R}_+^*$, actually on the interval $(0, |\mu|]$. Indeed fix the $u := \Im m(\xi) \in \mathbb{R}^*$ and consider the function on $\mathbb{R}_+^*$ $w \mapsto D(w + iu)$. One can check that the real part and the imaginary part of this function do not have the same zeros. This proves that the zeros of D have to be real (i.e. $u = 0$). Therefore we can identify the location and the number of the solutions $\xi \in (0, |\mu|)$ of the equation $e^{-2z\xi} = \frac{(\xi+\beta_1\mu)(\xi+\beta_2\mu)}{\beta_1\beta_2(\mu^2-\xi^2)}$ on $(0, |\mu|)$ through a simple study of variations of a real function. In particular one sees that the zeros cannot be greater than $|\mu|$ and localize the zeros in $[0, \mu]$. If the curves are tangent in 0 one gets the condition $2z\beta_1\beta_2\mu^2 + \beta_1\mu + \beta_2\mu = 0$. The order of the poles can be verified directly.
Moreover, comparing case by case the denominator with a convenient function, we show that if $\bar{\xi}$ is a non negative zero of the function $\xi \mapsto D(\xi)$, then

$$\bar{\xi} \leq \max(0, -2\beta_1\mu, -2\beta_2\mu). \tag{2.3.4}$$

□

The following lemma implies that the integral over ρ_U in Figure 2.4.b (resp. over ρ'_U in Figure 2.5.a.) vanishes if $U \to \infty$.

Lemma 2.3.3. *Let $\mathfrak{a} \geq 0$, and assume $|\beta_1\beta_2| \leq 1$. Then the integral of the function*

$$\xi \mapsto e^{\frac{\xi^2}{2}t}e^{-\xi|x-y|}\frac{\sum_{j=1}^4 c_j(y, \mu; \xi)e^{-\xi a_j(x,y)}}{\beta_1\beta_2 e^{-2\xi z}(\xi^2 - \mu^2) + (\xi + \beta_1\mu)(\xi + \beta_2\mu)}$$

on the segment $\rho_U = [iu; \mathfrak{a} + iu]$ vanishes if $|u| \to \infty$.

Proof. One should prove that $\lim_{|u|\to\infty} I_u = 0$ where

$$I_u := \int_0^{\mathfrak{a}} e^{\frac{(w+iu)^2}{2}t}e^{-(w+iu)|x-y|}\frac{\sum_{j=1}^4 c_j(y, \mu; w + iu)e^{-(w+iu)a_j(x,y)}}{\beta_1\beta_2 e^{-2(w+iu)z}((w + iu)^2 - \mu^2) + (iu + w + \beta_1\mu)(iu + w + \beta_2\mu)}dw.$$

First

$$|I_u| \leq e^{-\frac{1}{2}u^2} \int_0^{\mathfrak{a}} \frac{e^{\frac{w^2}{2}t} \sum_{j=1}^4 |c_j(y,\mu;w+iu)| e^{-w(|x-y|+a_j(x,y))}}{|\beta_1\beta_2 e^{-2(w+iu)z}((w+iu)^2-\mu^2)+(iu+w+\beta_1\mu)(iu+w+\beta_2\mu)|} dw.$$

Let us consider separately the numerator and the denominator appearing in the integrand. It is straightforward to prove that the numerator is smaller than $K_{\mathfrak{a}} \sum_{j=1}^4 \sum_{h=0}^2 |\mu^{2-h}| \left(\mathfrak{a}^2+u^2\right)^{\frac{h}{2}}$, where $K_{\mathfrak{a}}$ is a positive constant.
If $|\beta_1\beta_2| < 1$, the denominator is greater or equal than

$$\sqrt{(u^2+(w+\beta_1\mu)^2)(u^2+(w+\beta_2\mu)^2)} - |\beta_1\beta_2|(u^2+w^2+\mu^2) \geq (1-|\beta_1\beta_2|)u^2 - |\beta_1\beta_2|(\mu^2+\mathfrak{a}^2),$$

which does not depend on w and is positive for u large enough. Therefore, since

$$\int_0^{\mathfrak{a}} e^{\frac{w^2}{2}t} e^{-w(|x-y|+a_{j,k}(x,y))} dw \leq \mathfrak{a} e^{\frac{1}{2}\mathfrak{a}^2},$$

one has

$$\lim_{|u|\to\infty} |I_u| \leq \mathfrak{a} e^{\frac{1}{2}\mathfrak{a}^2} \lim_{|u|\to\infty} e^{-\frac{1}{2}u^2} \frac{K_{\mathfrak{a}} \sum_{j=1}^4 \sum_{h=0}^2 |\mu^{2-h}| \left(\mathfrak{a}^2+u^2\right)^{\frac{h}{2}}}{(1-|\beta_1\beta_2|)u^2 - |\beta_1\beta_2|(\mu^2+\mathfrak{a}^2)} = 0.$$

If $|\beta_1\beta_2| = 1$, then one considers separately the cases $\beta_1\beta_2 = -1$ and $\beta_1\beta_2 = 1$ and the proof is similar. If $\beta_1\beta_2 = -1$ the denominator $\left((w+iu)^2-\mu^2\right)\left(1-e^{-2\,z\,(iu+w)}\right)$ has absolute value bigger than $2|u\mu|$. If $\beta_1\beta_2 = 1$ instead, the denominator is $(\xi+\mu)\left((\xi+\mu)+e^{-2\,z\,(iu+w)}(\xi-\mu)\right)$ and its absolute value is, at least for large u, bigger than $\sqrt{\mu^2+u^2}\left(|u|\left(1-e^{-2\,z\,\mathfrak{a}}\right)-2|\mu|\right)$. □

Useful Fourier transforms and integrals

Let us define

$$\begin{array}{rccl} g & : & \mathbb{R}\times\mathbb{R} & \to & [0,+\infty) \\ & & (\omega,a) & \mapsto & g(\omega,a) := e^{a\omega}\mathbb{1}_{(-\infty,0)}(\omega), \end{array} \tag{2.3.5}$$

and, for $a_1, a_2 \in \mathbb{R}$ such that $a_1 \neq a_2$ and $k \in \mathbb{N}$,

$$f_{k+1}(\omega,a_1,a_2) := \frac{\sqrt{2\pi}}{(a_1-a_2)^{2k+1}k!} \cdot \sum_{n=0}^k \frac{(2k-n)!}{n!(k-n)!}(a_1-a_2)^n\omega^n \left[g(\omega,a_2)-(-1)^n g(\omega,a_1)\right]. \tag{2.3.6}$$

Lemma 2.3.4 (Partial fractional decomposition)**.** *Let $a, b \in \mathbb{R}^*$, $a \neq b$ and $k \in \mathbb{N}$, then*

$$\begin{aligned} &\frac{1}{(w-ia)^{k+1}(w-ib)^{k+1}} \\ &= i\sum_{j=0}^k \frac{1}{(a-b)^{2k+1-j}} \binom{2k-j}{k-j} \left(\frac{i^j}{(w-ib)^{j+1}} - (-1)^j \frac{i^j}{(w-ia)^{j+1}}\right). \end{aligned}$$

Proof. The function $f(x) = \frac{1}{(w-ia)^{k+1}(w-ib)^{k+1}}$ is a rational function with two poles $x_1 = ia, x_2 = ib$ of order $k+1$. We follow a standard method for computing the decomposition: there exist coefficients $\alpha_{i,j}$ such that the function can be written as $f(x) = \sum_{i=1}^2 \sum_{j=1}^{k+1} \frac{\alpha_{i,j}}{(x-x_i)^j}$. Since the $\alpha_{i,j}$ are the residues in x_i of the function $g_{i,j}(x) = (x-x_i)^{j-1}f(x)$, we computed them explicitly. □

Lemma 2.3.5. *If $a > 0$ and $k \in \mathbb{N}$, then*

$$\mathcal{F}\left(w \mapsto \frac{1}{(w-ia)^{k+1}}\right)(\omega) = i^{k+1}\sqrt{2\pi}\,\frac{(-\omega)^k}{k!}\,g(\omega,a),$$

where $g(\omega,a)$ is defined in (2.3.5)*. More generally if $a \in \mathbb{R}^*$ and $k \in \mathbb{N}$ then*

$$\mathcal{F}\left(w \mapsto \frac{1}{(w-ia)^{k+1}}\right)(\omega) = i^{k+1}\sqrt{2\pi}\,\left(2\mathbb{1}_{(-\infty,0)}(a)-1\right)\,\frac{(-\omega)^k}{k!}\,e^{a\omega}\,\mathbb{1}_{\mathbb{R}^-}(a\,\omega).$$

Proof. If $k = 0$ it coincides with Lemma 1.3.7, otherwise the function $\frac{1}{(w-ia)^{k+1}} \in L^1(\mathbb{R}, dx) \cap L^2(\mathbb{R}, dx)$ and one computes its Fourier transform at the point ω through the method of residues. □

Lemmas 2.3.4 and 2.3.5 imply that the function $f_k(\omega, a_1, a_2)$ defined by (2.3.6), for any $\omega \in \mathbb{R}$ and $a_1 > 0, a_2 > 0$, is equal to

$$f_k(\omega, a_1, a_2) = \mathcal{F}\left(w \mapsto \frac{-1}{(w - ia_1)^k (w - ia_2)^k}\right)(\omega).$$

Let us give the last useful lemma.

Lemma 2.3.6. *Let $q \in \mathbb{N}$. The function*

$$\begin{array}{rccc} I_q(\textit{resp. } \tilde{I}_q): & \mathbb{R} & \to & \mathbb{R} \\ & w & \mapsto & \displaystyle\int_{-\infty}^{w} u^q\, e^{-\frac{u^2}{2}}\, du \quad \left(\textit{resp. } -\int_{w}^{+\infty} u^q\, e^{-\frac{u^2}{2}}\, du\right) \end{array}$$

satisfies

$$\begin{cases} I_0(w) := \sqrt{2\pi}\Phi(w) = \sqrt{2\pi}\Phi^c(-w) \quad (\textit{resp. } -\sqrt{2\pi}\Phi^c(w)) & q = 0, \\ I_1(w) := -e^{-\frac{w^2}{2}} & q = 1, \\ I_q(w) = I_0(w)(q-1)!! + I_1(w)\sum_{k=0}^{\frac{q}{2}-1} w^{q-2k-1}\frac{(q-1)!!}{(q-2k-1)!!} & q \geq 2 \textit{ even}, \\ I_q(w) = I_1(w)\sum_{k=0}^{\frac{q-1}{2}} w^{(q-1-2k)} 2^k \frac{(\frac{q-1}{2})!}{(\frac{q-1}{2}-k)!} & q \geq 3 \textit{ odd }, \end{cases}$$

where $(2n+1)!! = (2n+1)\cdot(2n-1)\cdot\ldots\cdot 3\cdot 1$, $n \in \mathbb{N}$.

Proof. Straightforward for $q = 0, q = 1$, and for $q \geq 2$ one can use the integration by parts for the integral $\int w^q e^{-\frac{w^2}{2}} dw = -\int w^{q-1}\frac{d}{dw}\left(e^{-\frac{w^2}{2}}\right) dw$ and obtain the recursive formula

$$I_q(w) = w^{q-1} I_1(w) + (q-2) I_{q-2}(w)$$

that yields the conclusion. □

2.3.3 The main result

Let us now define some functions which will be used in our main result. For any $K, m, n \in \mathbb{N}$, $\omega \geq 0$, and $\mathfrak{a}, \tau \in \mathbb{R}$:

$$\mathscr{G}_{K,m,n}(\omega, \mathfrak{a}, \tau) := (-1)^K (K+m)! \sum_{\ell=0}^{\lfloor \frac{K+m}{2} \rfloor} \frac{(-1)^\ell}{2^\ell} \frac{1}{\ell!(K+m-2\ell)!} \mathcal{S}_{K+m-2\ell,n}(\omega, \mathfrak{a}, \tau) \tag{2.3.7}$$

where

$$\mathcal{S}_{L,n}(\omega, \mathfrak{a}, \tau) = \sum_{n'=0}^{n}\sum_{L'=0}^{L} \binom{n}{n'}\binom{L}{L'} (\omega+\tau)^{n-n'} (\mathfrak{a}+\tau)^{L-L'} \mathcal{J}_{n'+L'}(\omega, \tau),$$

and

$$\mathcal{J}_q(\omega, \tau) := e^{-\frac{1}{2}\omega^2} e^{\frac{1}{2}(\omega+\tau)^2} I_q(\omega+\tau), \tag{2.3.8}$$

where I_q is defined in Lemma 2.3.6. The latter function satisfies the recursive relationship

$$\mathcal{J}_q(\omega, \tau) = (q-1)\mathcal{J}_{q-2}(\omega, \tau) + (-1)^{q-1}(\omega+\tau)^{q-1}\mathcal{J}_1(\omega, \tau),$$

hence, following Lemma 2.3.6,

$$\mathcal{J}_q(\omega, \tau) := \begin{cases} \sqrt{2\pi} e^{-\frac{1}{2}\omega^2} e^{\frac{1}{2}(\omega+\tau)^2} \Phi^c(\omega+\tau) & q = 0, \\ -e^{-\frac{1}{2}\omega^2} & q = 1, \\ \mathcal{J}_0(\omega, \tau)(q-1)!! - \mathcal{J}_1(\omega, \tau)\sum_{k=0}^{\frac{q}{2}-1}(\omega+\tau)^{q-2k-1}\frac{(q-1)!!}{(q-2k-1)!!} & q \geq 2 \text{ even}, \\ \mathcal{J}_1(\omega, \tau)\sum_{k=0}^{\frac{q-1}{2}}(\omega+\tau)^{(q-1-2k)} 2^k \frac{(\frac{q-1}{2})!}{(\frac{q-1}{2}-k)!} & q \geq 3 \text{ odd }, \end{cases}$$

where $(2n+1)!! = (2n+1)\cdot(2n-1)\cdot\ldots\cdot 3\cdot 1$, $n \in \mathbb{N}$.

Theorem 2.3.7. *Let $\beta_1, \beta_2 \in [-1,1]$, $\mu \in \mathbb{R}$ and $\mathfrak{a} \geq \max(0, -2\beta_1\mu, -2\beta_2\mu)$. The transition density of the (β_1,β_2)-SBM with constant drift μ and barriers in 0 and $z>0$ decomposes as*

$$p_\mu^{(\beta_1,\beta_2)}(t,x,y) = p_\mu(t,x,y) v_\mu^{(\beta_1,\beta_2)}(t,x,y) \tag{2.3.9}$$

where the function $v_\mu^{(\beta_1,\beta_2)}$, which does not depend on $\mathfrak{a}$, admits the following series representation

$$v_\mu^{(\beta_1,\beta_2)}(t,x,y) = \sum_{k=0}^{\infty} (-\beta_1\beta_2)^k \sum_{j=1}^{4} F_{j,k}(\omega_{j,k}, \mathfrak{a}), \tag{2.3.10}$$

where

$$F_{j,k}(\omega_{j,k},\mathfrak{a}) := \begin{cases} (-1)^{k+1} \dfrac{\mathfrak{C}_{j,k}(\mathfrak{a})}{(2k+1)!} \mathscr{G}_{k+h-s,m,2k+1}(\omega_{j,k}, \mathfrak{a}\sqrt{t}, \beta_1\mu\sqrt{t}), & \text{if } \beta_1\mu = \beta_2\mu; \\ \displaystyle\sum_{n=0}^{k} \binom{2k-n}{k} \frac{\mathfrak{C}_{j,k}(\mathfrak{a})}{n!(\beta_1\mu\sqrt{t} - \beta_2\mu\sqrt{t})^{2k+1-n}} \mathscr{F}_{k+h-s,m,n}(\omega_{j,k}, \mathfrak{a}), & \text{if } \beta_1\mu \neq \beta_2\mu; \end{cases} \tag{2.3.11}$$

$$\omega_{j,k}(x,y) := \frac{a_j(x,y) + 2zk + |y-x|}{\sqrt{t}}, \quad j = 1,2,3,4, \quad k \in \mathbb{N}; \tag{2.3.12}$$

$$\mathfrak{C}_{j,k}(\mathfrak{a}) := e^{\frac{1}{2}\omega_{1,0}^2} \sum_{m=0}^{k} \sum_{s=0}^{k-m} \sum_{h=0}^{2} C_{j,2-h}(y) \binom{k-m}{s} \binom{k}{m} (-2\mathfrak{a}\sqrt{t})^{k-m-s} (\mu^2 - \mathfrak{a}^2)^s t^s$$

with $C_{j,h}(y)$ given in (2.3.3), $a_j(x,y)$ in (2.3.1) and the function $\mathscr{G}_{K,m,n}$ given by (2.3.7). The function $\mathscr{F}_{K,m,n}$ is defined by

$$\mathscr{F}_{K,m,n}(\omega,\mathfrak{a}) := \mathscr{G}_{K,m,n}(\omega, \mathfrak{a}\sqrt{t}, \beta_2\mu\sqrt{t}) - (-1)^n \mathscr{G}_{K,m,n}(\omega, \mathfrak{a}\sqrt{t}, \beta_1\mu\sqrt{t}).$$

Let us notice that $F_{j,k}(\omega_{j,k},\mathfrak{a})$ is actually a function depending on (t,x,y). This is the case of $\omega_{j,k}(x,y)$ and $\mathfrak{C}_{j,k}(\mathfrak{a})$ as well. The latter functions should be written $\omega_{j,k}(t,x,y)$ and $\mathfrak{C}_{j,k}(t,x,y,\mathfrak{a})$ respectively.

We now present a proof of Theorem 2.3.7 which is quite technical and divided in several steps. Nevertheless, some ideas are derived from the proof of Proposition 2.2.4 (recognize a geometric sum) and from the proof of Proposition 1.1.1 presented in Section 1.3.5 (there is no need to compute the possible residues).

Proof of Theorem 2.3.7. In Section 2.1 we have seen that the transition density of the (β_1,β_2)-SBM with constant drift μ admits the contour integral representation (1.3.6), i.e.

$$p_\mu^{(\beta_1,\beta_2)}(t,x,y) = \frac{1}{2\pi i} \int_\Gamma e^{\lambda t} G(x,y;\lambda) d\lambda,$$

where Γ is a contour of $(-\infty, 0]$ and $G(x,y;\lambda)$ is Green's function of the resolvent. Let us consider the explicit expression of Green's function, given by Lemma 2.3.1. We have already noticed that it depends on λ though the function $\phi(\lambda) = \sqrt{2\lambda + \mu^2}$ which is defined on $\lambda \in \mathbb{C} \setminus (-\infty, -\frac{\mu^2}{2}]$ (see Figure 2.4.a). Therefore a change of variable is possible, and one obtains the following expression for $v_\mu^{(\beta_1,\beta_2)}(t,x,y)$:

$$\frac{p_\mu^{(\beta_1,\beta_2)}(t,x,y)}{p_\mu(t,x,y)} = \frac{\sqrt{t}}{\sqrt{2\pi}i} e^{\frac{(y-x)^2}{2t}} \int_{\phi(\Gamma)} e^{\frac{\xi^2}{2}t} e^{-\xi|x-y|} \frac{\sum_{j=1}^{4} c_j(y,\mu;\xi) e^{-\xi a_j(x,y)}}{\beta_1\beta_2 e^{-2\xi z}(\xi^2 - \mu^2) + (\xi + \beta_1\mu)(\xi + \beta_2\mu)} d\xi. \tag{2.3.13}$$

Let us assume for the moment that the integrand has no poles on the region between the imaginary line and the contour $\phi(\Gamma)$ (i.e. it does not have poles in $[0,\mu^2]$, see Lemma 2.3.2) and that the integrand is also holomorphic on the entire imaginary line. Being in the case of Figure 1.3.a, let ρ_U as in the figure,

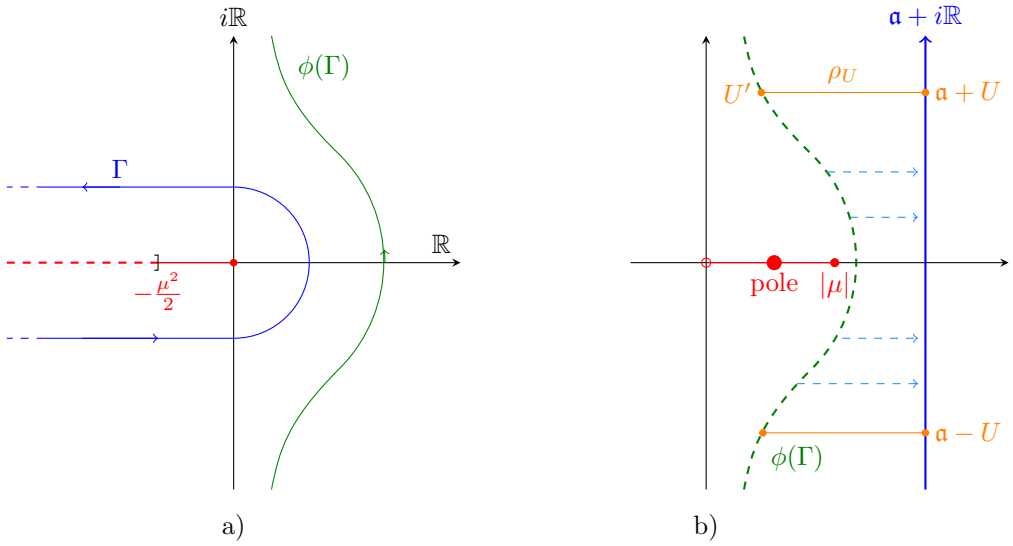

Figure 2.4:

a) Let $\mu \in \mathbb{R}$. The picture shows the image of the contour Γ under $\phi : \lambda \mapsto \sqrt{2\lambda+\mu^2}$. The line $(-\infty, 0]$ contains the spectrum of the operator $(L, \mathcal{D}(L))$ and the dashed line $(-\infty, -\frac{\mu^2}{2}]$ is the complement of the domain of ϕ.

b) The figure represents the vertical line $\mathfrak{a}+i\mathbb{R}$ on the right of the curve $\phi(\Gamma)$ and the segment ρ_U connecting the point $U = \mathfrak{a}+iu$ to its unique projection on $\phi(\Gamma)$. The segment $(0, |\mu|]$ contains all possible singularities (poles) with positive real part. It is the image under ϕ of $(-\frac{\mu^2}{2}, 0]$.

since the integral on this segment vanishes if U goes to infinity (see Lemma 2.3.3), one can deform the contour $\phi(\Gamma)$ to the imaginary line, obtaining the transition density as

$$v_\mu^{(\beta_1,\beta_2)}(t,x,y) = e^{-\frac{(x-y)^2}{2t}+\mu(y-x)}\frac{\sqrt{t}}{\sqrt{2\pi}}\int_{\mathbb{R}} e^{-\frac{w^2}{2}t}\frac{\sum_{j=1}^4 -c_j(y,\mu;iw)e^{-iwa_j(x,y)}e^{-iw|x-y|}}{\beta_1\beta_2 e^{-2iwz}(w^2+\mu^2)+(w-i\beta_1\mu)(w-i\beta_2\mu)}dw.$$

On one hand one recognizes that this is a Fourier transform (of a complicated function), on the other hand one wants to shrink to a contour that allows the computations even if there are some poles (i.e. for any possible choice of the parameters β_1, β_2, μ as in the hypotheses). As we have seen in Lemma 2.3.2, the possible singularities with positive real part could only be located in $[0, |\mu|]$ (which is the image through ϕ of $[-\mu^2/2, 0]$, see Figure 2.4.b) and have to be smaller than $\max(0, -2\beta_1\mu, -2\beta_2\mu)$.

Let us fix a non negative real number $\mathfrak{a}$ as in Figure 2.4.b. In particular it is bigger than any pole of the integrand, because the poles are smaller than the minimum between $|\mu|$ and $\max(0, -2\beta_1\mu, -2\beta_2\mu)$ (see inequality (2.3.4)).

One can deform the contour $\phi(\Gamma)$ to the line $\mathfrak{a}+i\mathbb{R}$ because the integrand is holomorphic on the region between the two curves, continuous on the curves and on the segment ρ_U where the integral is vanishing if $|U| \to \infty$ (by Lemma 2.3.3).

Noticing that $\omega_{j,0} = \frac{a_j(x,y)+|x-y|}{\sqrt{t}}$, one has

$$v_\mu^{(\beta_1,\beta_2)}(t,x,y) = \frac{\sqrt{t}}{\sqrt{2\pi}i}e^{\frac{1}{2}\omega_{1,0}^2}\int_{\mathfrak{a}+i\mathbb{R}} e^{\frac{\xi^2}{2}t}e^{-\xi|x-y|}\frac{\sum_{j=1}^4 c_j(y,\mu;\xi)e^{-\xi a_j(x,y)}}{\beta_1\beta_2 e^{-2\xi z}(\xi^2-\mu^2)+(\xi+\beta_1\mu)(\xi+\beta_2\mu)}d\xi$$

$$\overset{\eta=\xi\sqrt{t}}{=} \frac{1}{\sqrt{2\pi}i}e^{\frac{\omega_{1,0}^2}{2}}\int_{\mathfrak{a}\sqrt{t}+i\mathbb{R}} e^{\frac{\eta^2}{2}}\frac{\sum_{j=1}^4 c_j(\mu\sqrt{t},y;\eta)e^{-\eta\frac{a_j(x,y)+|x-y|}{\sqrt{t}}}}{\beta_1\beta_2 e^{-2\eta\frac{z}{\sqrt{t}}}(\eta^2-\mu^2 t)+(\eta+\beta_1\mu\sqrt{t})(\eta+\beta_2\mu\sqrt{t})}d\eta.$$

Setting $\eta = iw + \mathfrak{a}\sqrt{t}$ one gets

$$v_\mu^{(\beta_1,\beta_2)}(t,x,y) = \frac{1}{\sqrt{2\pi}} \int_{\mathbb{R}} \frac{e^{\frac{1}{2}\omega_{1,0}^2} e^{\frac{(iw+\mathfrak{a}\sqrt{t})^2}{2}} \sum_{j=1}^4 c_j(\mu\sqrt{t}, y; iw+\mathfrak{a}\sqrt{t}) e^{-(iw+\mathfrak{a}\sqrt{t})\frac{a_j(x,y)+|x-y|}{\sqrt{t}}}}{\beta_1\beta_2 e^{-2(iw+\mathfrak{a}\sqrt{t})\frac{z}{\sqrt{t}}}((iw+\mathfrak{a}\sqrt{t})^2 - \mu^2 t) + ((iw+\mathfrak{a}\sqrt{t}) + \beta_1\mu\sqrt{t})((iw+\mathfrak{a}\sqrt{t}) + \beta_2\mu\sqrt{t})} dw.$$

Taking $\mathfrak{a} = 0$ one obtains the same integral that one would obtain in the case without poles.

For simplicity (but without loss of generality) we continue the computation supposing $t = 1$. Let us define the non negative constants

$$\mathfrak{a}_\mathfrak{i} := \mathfrak{a} + \beta_\mathfrak{i}\mu, \qquad \mathfrak{i} = 1, 2.$$

$$v_\mu^{(\beta_1,\beta_2)}(1,x,y) = \frac{1}{\sqrt{2\pi}} e^{\frac{1}{2}(\omega_{1,0}^2+\mathfrak{a}^2)} \int_{\mathbb{R}} \frac{e^{-\frac{w^2}{2}} \sum_{j=1}^4 \sum_{h=0}^2 \left(-c_{j,2-h}(y)\mu^{2-h}(iw+\mathfrak{a})^h\right) e^{-iw(\omega_{j,0}-\mathfrak{a})} e^{-\mathfrak{a}\omega_{j,0}}}{(w-i\mathfrak{a}_1)(w-i\mathfrak{a}_2)\left(1 + e^{-i2zw} e^{-2z\mathfrak{a}} \frac{\beta_1\beta_2(w^2-\mathfrak{a}^2+\mu^2-2iw\mathfrak{a})}{(w-i\mathfrak{a}_1)(w-i\mathfrak{a}_2)}\right)} dw. \tag{2.3.14}$$

Since we assume $\mathfrak{a} \geq 0, \mathfrak{a} \geq -2\beta_1\mu, \mathfrak{a} \geq -2\beta_2\mu$, it is easy to prove that

$$\left| -e^{-2z\mathfrak{a}} \beta_1\beta_2 \frac{(w^2 - \mathfrak{a}^2 + \mu^2 - 2iw\mathfrak{a})}{(w-i\mathfrak{a}_1)(w-i\mathfrak{a}_2)} \right| < 1.$$

Therefore one factor of the integrand is a geometric series:

$$\frac{1}{1 + e^{-i2zw} e^{-2z\mathfrak{a}} \frac{\beta_1\beta_2(w^2-\mathfrak{a}^2+\mu^2-2iw\mathfrak{a})}{(w-i\mathfrak{a}_1)(w-i\mathfrak{a}_2)}} = \sum_{k=0}^\infty \left(-e^{-i2zw} e^{-2z\mathfrak{a}} \frac{\beta_1\beta_2(w^2 - \mathfrak{a}^2 + \mu^2 - 2iw\mathfrak{a})}{(w-i\mathfrak{a}_1)(w-i\mathfrak{a}_2)} \right)^k.$$

Hence, exchanging integral and series one obtains the series of Fourier transforms

$$\begin{cases} v_\mu^{(\beta_1,\beta_2)}(1,x,y) = \sum_{k=0}^\infty (-\beta_1\beta_2)^k \sum_{j=1}^4 F_{j,k}(\omega_{j,k}, \mathfrak{a}), \\ F_{j,k}(\omega_{j,k}, \mathfrak{a}) := e^{\frac{1}{2}(\omega_{1,0}^2+\mathfrak{a}^2)} e^{-\mathfrak{a}\omega_{j,k}} \mathcal{F}\left(w \mapsto e^{-\frac{w^2}{2}} c_j(y, \mu; iw+\mathfrak{a}) \frac{-(w^2 - \mathfrak{a}^2 + \mu^2 - 2iw\mathfrak{a})^k}{(w-i\mathfrak{a}_1)^{k+1}(w-i\mathfrak{a}_2)^{k+1}} \right)(\omega_{j,k} - \mathfrak{a}), \end{cases} \tag{2.3.15}$$

where $\omega_{j,k}$ is given by (2.3.12). We could exchange the integral and the series since there exists a bound for the absolute value of the $k-th$ term of the series, such that the series of these bounds converges (see Proposition 2.5.3 for an explicit bound).

The Fourier transform in $F_{j,k}$ can be rewritten as the following convolution of Fourier transforms

$$\frac{1}{\sqrt{2\pi}\mu^{2k}} \underbrace{\mathcal{F}\left(e^{-\frac{w^2}{2}} \left(\sum_{h=0}^2 c_{j,2-h}(y)\mu^{2-h}(iw+\mathfrak{a})^h \right) (w^2 - \mathfrak{a}^2 + \mu^2 - 2iw\mathfrak{a})^k \right)}_{(1)} * \underbrace{\mathcal{F}\left(\frac{-1}{[(w-i\mathfrak{a}_1)(w-i\mathfrak{a}_2)]^{k+1}} \right)}_{(2)}. \tag{2.3.16}$$

Let us first study the term (2). This Fourier transform is computed using Lemma 2.3.5 if $\beta_1\mu = \beta_2\mu$, otherwise using jointly Lemma 2.3.4 and Lemma 2.3.5 we obtain the function $f_{k+1}(\omega, \mathfrak{a}_1, \mathfrak{a}_2)$ given by (2.3.6).

Let us now consider the term (1) in (2.3.16). One uses the properties of the iterated derivatives of Gaussian densities, and the functions $\mathscr{G}$ given by (2.3.7).

The coefficients defined in (2.3.3) are such that $\sum_{h=0}^2 c_{j,2-h}(y)\mu^{2-h}(iw+\mathfrak{a})^h = \sum_{h=0}^2 C_{j,2-h}(y) i^h w^h$, hence the first term of the Fourier transform becomes

$$\mathcal{F}\left(e^{-\frac{w^2}{2}} \left(\sum_{h=0}^2 C_{j,2-h}(y) i^h w^h \right) (w^2 - \mathfrak{a}^2 + \mu^2 - 2iw\mathfrak{a})^k \right).$$

Developing the power of binomials one obtains

$$\sum_{h=0}^{2} C_{j,2-h}(y) \sum_{m=0}^{k} \binom{k}{m} \sum_{s=0}^{k-m} \binom{k-m}{s} (-2\mathfrak{a})^{k-m-s} (\mu^2 - \mathfrak{a}^2)^s \; i^{k-m-s+h} \mathcal{F}\left(e^{-\frac{w^2}{2}} w^{k+m-s+h}\right).$$

Finally one computes the Fourier transforms $\mathcal{F}\left(e^{-\frac{w^2}{2}} w^n\right)(w) = i^n \frac{d^n}{dw^n} e^{-\frac{w^2}{2}}$ and concludes that

$$\begin{aligned}
&\frac{1}{\mu^{2k}} \mathcal{F}\left(e^{-\frac{w^2}{2}} \left(\sum_{h=0}^{2} C_{j,2-h}(y) i^h w^h\right) (w^2 - \mathfrak{a}^2 + \mu^2 - 2iw\mathfrak{a})^k\right) \\
&\quad = \sum_{m=0}^{k} \binom{k}{m} \sum_{s=0}^{k-m} \binom{k-m}{s} (-2\mathfrak{a})^{k-m-s} \frac{(\mu^2 - \mathfrak{a}^2)^s}{\mu^{2k}} \; \sum_{h=0}^{2} C_{j,2-h}(y) \; (-1)^{k+h-s} \frac{d^{k+m+h-s}}{dw^{k+m+h-s}} e^{-\frac{w^2}{2}}.
\end{aligned}$$

Define now

$$\mathscr{G}_{K,m,n}(\omega, \mathfrak{a}, \beta_{\mathfrak{i}}\mu) := e^{\frac{1}{2}\mathfrak{a}^2} e^{-\mathfrak{a}\omega} (-1)^K \left(\frac{d^{K+m}}{dw^{K+m}} e^{-\frac{w^2}{2}} * w^n g(w, \mathfrak{a}_{\mathfrak{i}})\right)(\omega - \mathfrak{a}) \quad \mathfrak{i} = 1, 2.$$

One has to show that this function coincides with the expression given in (2.3.7).
Let $(H_n(w))_n$ be the Hermite polynomials, then

$$\frac{d^n}{dw^n} e^{-\frac{w^2}{2}} = (-1)^n e^{-\frac{w^2}{2}} H_n(w).$$

Hence

$$\begin{aligned}
\mathscr{G}_{K,m,n}(\omega, \mathfrak{a}, \beta_{\mathfrak{i}}\mu) &= e^{\frac{1}{2}\mathfrak{a}^2} e^{-\mathfrak{a}\omega} (-1)^m \left(w^n g(w, \mathfrak{a}_{\mathfrak{i}}) * H_{K+m}(w) e^{-\frac{w^2}{2}}\right)(\omega - \mathfrak{a}) \\
&= (-1)^m e^{-\frac{1}{2}\omega^2} e^{\frac{1}{2}(\omega + \beta_{\mathfrak{i}}\mu)^2} \int_{-\infty}^{-(\omega + \beta_{\mathfrak{i}}\mu)} (w + \omega + \beta_{\mathfrak{i}}\mu)^n e^{-\frac{w^2}{2}} H_{K+m}(-\mathfrak{a}_{\mathfrak{i}} - w) dw.
\end{aligned}$$

One then uses the explicit expression of the Hermite polynomials

$$H_n(w) = n! \sum_{\ell=0}^{\lfloor \frac{n}{2} \rfloor} (-1)^\ell \frac{1}{2^\ell} \frac{1}{\ell!(n-2\ell)!} w^{n-2\ell}.$$

Replacing the polynomials inside the integral and defining

$$\mathcal{S}_{L,n}(\omega, \mathfrak{a}, \beta_{\mathfrak{i}}\mu) := e^{-\frac{1}{2}\omega^2} e^{\frac{1}{2}(\omega + \beta_{\mathfrak{i}}\mu)^2} \int_{-\infty}^{-(\omega + \beta_{\mathfrak{i}}\mu)} (w + \omega + \beta_{\mathfrak{i}}\mu)^n e^{-\frac{w^2}{2}} (\mathfrak{a}_{\mathfrak{i}} + w)^L dw,$$

one recovers the expression in (2.3.7).
The final step consists in checking the formula giving the function $S_{L,n}$. Let us expand the $n-th$ power with the help of the binomial formula,

$$\mathcal{S}_{L,n}(\omega, \mathfrak{a}, \beta_{\mathfrak{i}}\mu) = e^{-\frac{1}{2}\omega^2} e^{\frac{1}{2}(\omega + \beta_{\mathfrak{i}}\mu)^2} \sum_{n'=0}^{n} \sum_{L'=0}^{L} \binom{n}{n'} \binom{L}{L'} (\omega + \beta_{\mathfrak{i}}\mu)^{n-n'} \mathfrak{a}_{\mathfrak{i}}^{L-L'} \int_{-\infty}^{-(\omega + \beta_{\mathfrak{i}}\mu)} w^{n'+L'} e^{-\frac{w^2}{2}} dw.$$

Recognizing the function $\mathcal{J}_q(\omega, \beta_{\mathfrak{i}}\mu)$ given by (2.3.8) one concludes. □

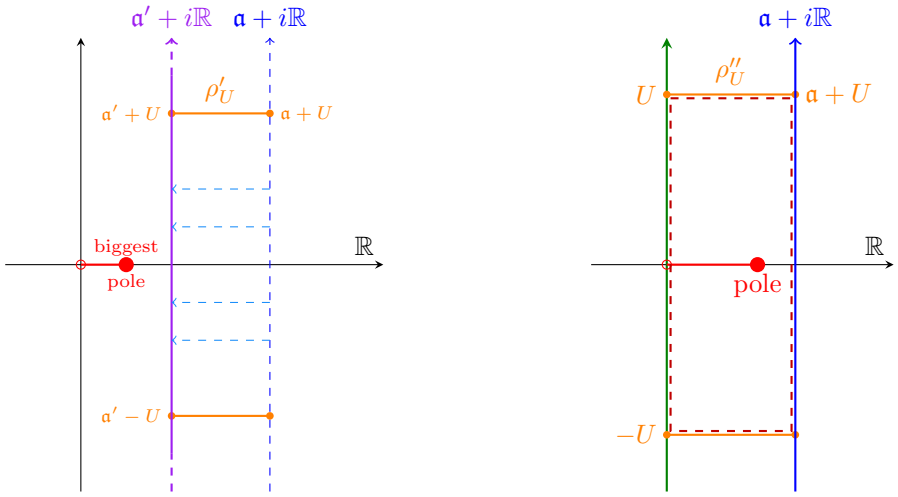

Figure 2.5:

a) The segment ρ'_U connects here the point $\mathfrak{a} + U$ with its projection on $\mathfrak{a}' + i\mathbb{R}$. The real number $\mathfrak{a}'$ is chosen smaller than $\mathfrak{a}$ but larger than any pole.

b) The figure represents the imaginary line (in green), the line $\mathfrak{a} + i\mathbb{R}$ on the right of any pole and the rectangular cycle (in red dashed) around a pole situated in $(0, |\mu|]$. The segment ρ''_U connects here the point $\mathfrak{a} + U$ with $U = iu$.

2.3.4 Degenerate cases and special cases

In this section we give some comments on the main result, Theorem 2.3.7.

- In [16], we have provided the transition density assuming both $\beta_1\mu$ and $\beta_2\mu$ to be positive, because in this simpler case there is no residue to compute (see Section 1.3.4). Later in [15], we have proved the complete formula presented in this document, following the approach in Section 1.3.5, which does not require an explicit knowledge of the singularities of Green's function. Indeed, if there is no singularity located on the interval $[0, |\mu|]$, the two approaches coincides: one can choose $\mathfrak{a} = 0$ and shrink the contour $\phi(\Gamma)$ to the imaginary line (see Figure 2.2.b).

- If there are poles in $[0, |\mu|]$ (see Lemma 2.3.2 for a summary of the possible cases), the situation is much more delicate. In Figure 2.5.b we illustrate the link of the "$\mathfrak{a}$-method" (Section 1.3.5) with the "residues-method" used in Section 1.3.4.
  If $2z\mu\beta_1\beta_2 + \beta_1 + \beta_2 \neq 0$, thanks to Lemma 2.3.3 one can easily show that $\int_{\mathfrak{a}+i\mathbb{R}} = \int_{i\mathbb{R}} +$ residues. However, the computation of the residue is usually not trivial at all, but one can give an explicit series expression making the difference of the explicit series expressions coming from the integrals on the curves $\mathfrak{a}' + i\mathbb{R}$ and $i\mathbb{R}$. The integral on the imaginary line gives formula (2.3.11) with $\mathfrak{a} := 0$ and the function $(\omega, \tau) \mapsto J_0(\omega, \tau)$ in (2.3.8) redefined as $\mathcal{J}_0(\omega, \tau) := \sqrt{2\pi} e^{-\frac{1}{2}\omega^2} e^{\frac{1}{2}(\omega+\tau)^2} \left(\Phi^c(\omega + \tau) - \mathbb{1}_{\{\tau<0\}}\right)$ (see Lemma 2.3.6).

- The transition density is independent from $\mathfrak{a}$ once $\mathfrak{a}$ is larger than any pole of the integrand in (2.3.13) (the inequality (2.3.4) give a lower bound for $\mathfrak{a}$). The left hand side of (2.3.10) does not depend on $\mathfrak{a}$, even if each term (2.3.11) of the series does depend on it. One can then choose to integrate on a particular vertical line $\mathfrak{a}' + i\mathbb{R}$, as in Figure 2.5.a. A choice that simplifies some terms is $\mathfrak{a} = |\mu|$.

- The transition density of the two-SBM with constant drift can be seen as an additive perturbation of the transition density of the Brownian motion with the same constant drift. This means that the analogous of equation (2.2.8) holds. To prove it we consider Green's function given in Lemma 2.3.1 and we write it as

$$G(x, y; \xi) = \frac{1}{\xi} e^{\mu(y-x)} e^{-\xi|x-y|} \left(1 + \frac{\sum_{j=1}^{4} \bar{c}_j(y, \mu; \xi) e^{-\xi \bar{a}_j(x,y)}}{\beta_1\beta_2 e^{-2\,\xi\, z}(\xi^2 - \mu^2) + (\xi + \beta_1\mu)(\xi + \beta_2\mu)}\right),$$

  where z is the distance between the barriers and $\xi := \sqrt{2\lambda + \mu^2} \in \{\zeta \in \mathbb{C}\ s.t.\ \Re e(\zeta) > 0\}$ since $\lambda \in \mathbb{C} \setminus (-\infty, 0]$. For $j = 2, 3, 4$, the functions $\bar{a}_j(x, y)$ are the non negative functions $a_j(x, y)$ defined by (2.3.1), and $\bar{c}_j(y, \mu; \xi) = \xi^2 \bar{c}_{j,0}(y) + \xi\mu\bar{c}_{j,1}(y) + \mu^2\bar{c}_{j,2}(y)$ are the polynomials $c_j(y, \mu; \xi) = \xi^2 c_{j,0}(y) + \xi\mu c_{j,1}(y) + \mu^2 c_{j,2}(y)$ with coefficients $c_{j,h}$ given by (2.3.2). Moreover

$$\bar{a}_1(x, y) := 2z \qquad \bar{c}_1(y, \mu; \xi) = -\left(1 - 2\mathbb{1}_{[z_1,z_2)}(y)\right) c_4(y, \mu; \xi) = -\beta_1\beta_2(\xi^2 - \mu^2)$$

  and the latter is equal to $\xi^2\bar{c}_{1,0}(y) + \xi\mu\bar{c}_{1,1}(y) + \mu^2\bar{c}_{1,2}(y)$, with $\bar{c}_{1,h}(y) = -\left(1 - 2\mathbb{1}_{[z_1,z_2)}(y)\right) c_{4,h}(y)$ for $h = 0, 1, 2$.
  Equation (2.3.10) is then equal to

$$v_\mu^{(\beta_1,\beta_2)}(t, x, y) = 1 + \sum_{k=0}^{\infty} (-\beta_1\beta_2)^k \sum_{j=1}^{4} \bar{F}_{j,k}(\omega_{j,k}, \mathfrak{a}),$$

  where $\bar{F}_{j,k}$ is defined by (2.3.11) with the functions $C_{j,h}$ given by (2.3.3) replaced by their analogous with $\bar{c}_{j,h}$, instead of $c_{j,h}$ $(h = 0, 1, 2)$.

For particular choices of the parameters and shrinking the two barriers, formulas (2.3.10) and (2.3.11) reduce to simpler cases.

- For $\beta_2 = 0$, the correspondent barrier z_2 is completely permeable, so it is like if it disappears, and one obtains, as expected, the transition density of the β_1-SBM with drift μ. (The analogous holds if $\beta_1 = 0$.)
  One can notice that expression (2.3.10) is not a series anymore since $(\beta_1\beta_2)^k$ is a factor of the $k-th$ term. Moreover only $F_{j,0}(\omega_{j,0})$ for $j \in \{1,2\}$ do not vanish.

- For $\mu = 0$ one recovers the formula (2.2.6) of the two-SBM without drift.

- If $z \to +\infty$ one expects to obtain the density of the β_1-SBM with drift. In fact, if the second barrier is really far from the starting point of the process, at every finite time the trajectory has no way to see the latter barrier and is effected only by the reflection coefficient β_1.
  More precisely: First notice that, since $z \to +\infty$, the functions $a_3(x,y), a_4(x,y)$ go to $+\infty$ which implies $\omega_{j,k} \to \infty$ as soon as $k \neq 0$ or $j \neq \{1,2\}$. Consider the expression for $F_{j,k}$: in (2.3.16), it is a Fourier transform of a $L^2(\mathbb{R}, dx)$-function, hence it is in $L^2(\mathbb{R}, dx)$. It admits a limit at infinity (implied by Proposition 2.5.3) and a fortiori the limit is zero. Therefore the unique non vanishing terms are again given by $j = 1, 2$ and $k = 0$.

- If $z \to 0$ one obtain the transition density of a one-SBM with drift μ. The skewness coefficient is given by $\frac{\beta_1+\beta_2}{1+\beta_1\beta_2}$ (see Proposition 2.4.1 for a proof).
  To check that the transition density we propose fulfills this property, one notices that the limits of the functions in (2.3.1) satisfy $a_1(x,y) = a_4(x,y) = 0$ and $a_2(x,y) = a_3(x,y) = |x| + |y| - |x-y|$ and the limit of $\omega_{j,k}$, given by (2.3.12), is actually independent from k and is $\omega_j = \frac{a_j(x,y)+|x-y|}{\sqrt{t}}$, $j = 1, 2, 3, 4$.

- If $|\beta_1\beta_2| = 1$ the most interesting case is of course the reflected Brownian motion with constant drift, i.e. $\beta_1 = 1, \beta_2 = -1$. The transition density in that case has been computed by Svensson [59], Veestraeten [63] and Linetzky [41] with different techniques. Notice that formula (11) in [63] is an infinite sum of Gaussian densities as ours.

2.4 Towards the transition density of the multi-skew Brownian diffusions

In this section we discuss the possibilities to find the transition density of the multi-SBM using the techniques developed above. In the drifted case, we continue the reasoning given in Section 1.4. Moreover, we give a convergence result when n barriers shrinks to a unique barrier.

The multi-skew Brownian motion without drift

The representation of the density as contour integral of Green's function holds and one can compute Green's function of the resolvent, given by Lemma 1.3.4, starting from the functions $u_\pm(x) = e^{\mp\sqrt{2\lambda}\,x}$ as in Figure 2.6.

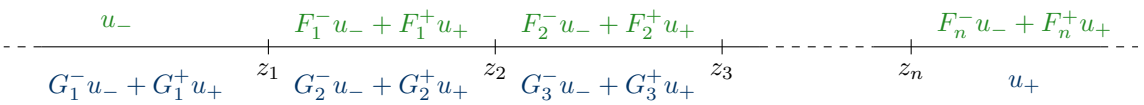

Figure 2.6: The functions U_- and U_+.

The change of variable $\xi := \sqrt{2\lambda}$ is still possible and one reduces to integrate on the curve $\phi(\Gamma)$ as in Figure 2.2.a.

The key point to shrink the integral is the nature of the denominator of Green's function, i.e the numerator of the Wronskian. Actually the denominator is the numerator of the constant function $w \mapsto k(x)W(U_-, U_+)(w, \lambda)$, i.e. the numerator of G_1^+ in Figure 2.6.

Let us consider the easiest example not yet considered: the three-SBM ($n = 3$). In this case the denominator of Green's function is

$$1 + \beta_1\beta_2 e^{-2\xi(z_2-z_1)} + \beta_1\beta_3 e^{-2\xi(z_3-z_1)} + \beta_2\beta_3 e^{-2\xi(z_3-z_2)}\,, \qquad \xi \in \mathbb{C},\, \Re e(\xi) > 0$$

for $\beta_1, \beta_2, \beta_3 \in [-1, 1]$. We need to localize the zeros of this function. For example there is no zero between $\phi(\Gamma)$ and $i\mathbb{R}$ if the coefficients $\beta_1, \beta_2, \beta_3$ have a small absolute value. Hence one can shrink the contour $\phi(\Gamma)$ to the imaginary line as in Figure 2.2.b. Moreover one can identify the sum of a geometric series and explicit the integral as a series of Fourier transforms if $|\beta_1\beta_2 e^{-2\,i\,w(z_2-z_1)} + \beta_1\beta_3 e^{-2\,i\,w(z_3-z_1)} + \beta_2\beta_3 e^{-2\,i\,w(z_3-z_2)}| < 1$ for all $w > 0$.

In conclusion we may notice that, possibly under additional condition on the parameters (such as large distances between the barriers, or for small skewness parameters), Green's function

- is holomorphic on the region between the imaginary line and $\phi(\Gamma)$, or between $\phi(\Gamma)$ and $\mathfrak{a} + i\mathbb{R}$ for some $\mathfrak{a} > 0$,
- has a factor which is the sum of a geometric series.

Therefore, it may be possible to obtain an explicit expression of the transition density.

The multi-skew Brownian motion with constant drift

It may be possible to obtain an explicit expression also in the case of the multi-skew Brownian motion with constant drift μ, at least for some choices of skewness coefficients close to 0 and/or large distances between the barriers (or equivalently small times).

The situation is similar to the one discussed in Section 1.4. Green's function satisfies Lemma 1.3.4 and is constructed as in Figure 2.6 using

$$u \pm (x, \lambda) := \exp\left(-\mu x \mp \sqrt{2\lambda + \mu^2}\, x\right),$$

for $\lambda \in \mathbb{C}\backslash(-\infty, -\frac{1}{2}\mu^2]$. The functions $U_\pm$ are then obtained imposing the continuity and the transmission conditions at the barriers. One has then the following system for $j = 1, \dots, n$:

$$\begin{cases} G_j^- u_-(z_j) + G_j^+ u_+(z_j) = G_{j+1}^- u_-(z_j) + G_{j+1}^+ u_+(z_j) \\ k(z_j^-)\left(G_j^- u'_-(z_j) + G_j^+ u'_+(z_j)\right) = k(z_j^+)\left(G_{j+1}^- u'_-(z_j) + G_{j+1}^+ u'_+(z_j)\right) \end{cases}$$

where $G_{n+1}^- := 0$, $G_{n+1}^+ = 1$ and k is the $(n+1)$-valued function given by (2.1.2). Hence one has the recursive relationship:

$$\begin{cases} G_j^+ \frac{u_+(z_j)}{u_-(z_j)} = \frac{1}{2} G_{j+1}^- \left(1 - \frac{\sqrt{2\lambda+\mu^2}}{\mu}\right)\left(1 - \frac{k(z_j^+)}{k(z_j^-)}\right) + \frac{1}{2} G_{j+1}^+ \frac{u_+(z_j)}{u_-(z_j)} \left(\left(1 + \frac{k(z_j^+)}{k(z_j^-)}\right) - \frac{\sqrt{2\lambda+\mu^2}}{\mu}\left(1 - \frac{k(z_j^+)}{k(z_j^-)}\right)\right) \\ G_j^- = \frac{1}{2} G_{j+1}^- \left(\left(1 + \frac{k(z_j^+)}{k(z_j^-)}\right) - \frac{\sqrt{2\lambda+\mu^2}}{\mu}\left(1 - \frac{k(z_j^+)}{k(z_j^-)}\right)\right) + \frac{1}{2} G_{j+1}^+ \frac{u_+(z_j)}{u_-(z_j)} \left(1 - \frac{\sqrt{2\lambda+\mu^2}}{\mu}\right)\left(1 - \frac{k(z_j^+)}{k(z_j^-)}\right). \end{cases}$$

Let us notice that $\frac{u_+(z_j)}{u_-(z_j)} = e^{-2\sqrt{2\lambda+\mu^2}\, z_j}$. One can impose the analogous conditions on $F_j^\pm$. There is no obstacle in computing the coefficients $G_j^\pm, F_j^\pm$ and with them, Green's function. The transition density could nevertheless be difficult to obtain as an explicit series of Gaussians and other transcendent functions.

The limit of the multi-skew Brownian motion for several barriers converging to one

Proposition 2.4.1. *Let $\beta_1, \beta_2 \in [-1, 1]$, $\mu \in \mathbb{R}$ and $z_2^{(m)} = z_1 + \frac{1}{m}$, $m \in \mathbb{N}$. Let*

$$\beta := \frac{\beta_1 + \beta_2}{1 + \beta_1\beta_2}.$$

Let us denote by $(X_t^{(m)})_t$ the $(\beta_1,\beta_2)-SBM$ with drift μ and barriers in z_1 and $z_2^{(m)}$, and $(Y_t)_t$ the $(\beta)-SBM$ with drift μ and barrier in z_1. Let us assume $X_0^{(m)}=Y_0$, then $X^{(m)}$ converges to Y in the following sense:

$$\mathbb{E}\left(\sup_{s\in[0,t]}|X_s^{(m)}-Y_s|\right)\overset{m\to\infty}{\to}0 \text{ for all } t\geq 0.$$

The same holds in the case of $n\geq 3$ barriers merging. In this case $(X_t^{(m)})_t$ is the $(\beta_1,\beta_2\ldots,\beta_n)-SBM$ with drift $\mu\in\mathbb{R}$, skewness parameters $\beta_1,\beta_2,\ldots,\beta_n\in[-1,1]$ and barriers $z_1\in\mathbb{R}$, $z_{j+1}:=j\frac{1}{m}+z_1$ for all $j=1,\ldots,n-1$. The skewness parameter of the limit one-SBM is given by

$$\beta:=\frac{\prod_{j=1}^n(1+\beta_j)-\prod_{j=1}^n(1-\beta_j)}{\prod_{j=1}^n(1+\beta_j)+\prod_{j=1}^n(1-\beta_j)}.$$

In particular

$$\beta=\frac{\sum_{j=1}^n\beta_j+\sum_{j_1<j_2<j_3}\beta_{j_1}\beta_{j_2}\beta_{j_3}+\ldots+\sum_{j_1<\ldots<j_{n-1}}\beta_{j_1}\cdots\beta_{j_{n-1}}}{1+\sum_{j_1<j_2}\beta_{j_1}\beta_{j_2}+\sum_{j_1<\ldots<j_4}\beta_{j_1}\beta_{j_2}\beta_{j_3}\beta_{j_4}+\ldots+\beta_1\beta_2\cdots\beta_n},$$

if n is even, and

$$\beta=\frac{\sum_{j=1}^n\beta_j+\sum_{j_1<j_2<j_3}\beta_{j_1}\beta_{j_2}\beta_{j_3}+\ldots+\beta_{j_1}\cdots\beta_{j_n}}{1+\sum_{j_1<j_2}\beta_{j_1}\beta_{j_2}+\sum_{j_1<\ldots<j_4}\beta_{j_1}\beta_{j_2}\beta_{j_3}\beta_{j_4}+\ldots+\sum_{j_1<\ldots<j_{n-1}}\beta_{j_1}\cdots\beta_{j_{n-1}}}$$

if n is odd.

Proof. The result in the case of two barriers is due to Zaitseva [68]. For any $n\geq 2$, we propose a proof based on a straightforward application of Theorem 3.1 by LeGall [32] which ensures the convergence of Brownian diffusions under some assumptions on their skewness. Let $(W_t)_t$ be a Brownian motion. The $(\beta_1,\ldots,\beta_n)-$SBM with drift μ is the continuous semimartingale such that:

$$X_t^{(m)}=X_0+\mu\,t+W_t+\int_{\mathbb{R}}L_t^w(X^{(m)})\nu_m(dw)\quad\text{ with }\quad\nu_m(dw):=\sum_{j=1}^n\beta_j\delta_{z_j}(dw).$$

On the other hand the $(\beta)-SBM$ with drift μ and semipermeable barrier z_1 is given by

$$Y_t=Y_0+\mu\,t+W_t+\int_{\mathbb{R}}L_t^w(Y)\nu(dw)\quad\text{ with }\quad\nu(dw):=\beta\delta_{z_1}(dw).$$

Clearly the measures ν and ν_m are discrete finite measures concentrated on the barriers z_1 and $z_1<z_2<\ldots<z_n$ respectively. Since these measures are finite, one can define f_m and f, functions of bounded variation such that $\lim_{w\to-\infty}f(w)=1$ and $f'(dx)+(f(x^+)+f(x^-))\,\nu(dx)=0$ (and similarly for f_m and ν_m). Thus

$$\begin{aligned}f_m(w)&:=\mathbb{1}_{(-\infty,z_1)}(w)+\prod_{j=1}^{n-1}\frac{1-\beta_j}{1+\beta_j}\mathbb{1}_{[z_j,z_{j+1})}(w)+\prod_{j=1}^{n}\frac{1-\beta_j}{1+\beta_j}\mathbb{1}_{[z_n,+\infty)}(w),\\ f(w)&:=\mathbb{1}_{(-\infty,z_1)}(w)+\frac{1-\beta}{1+\beta}\mathbb{1}_{[z_1,+\infty)}(w).\end{aligned}$$

It is straightforward to prove that, for any $K>0$, $\int_{-K}^K|f_m(w)-f(w)|\,dw\overset{m\to\infty}{\longrightarrow}0$, hence Theorem 3.1 in [32] can be applied, which means that $(X^{(m)})_m$ converges to Y in the desired sense. □

2.5 Simulations

In this section we illustrate an *exact* simulation scheme to sample the two-SBM (with constant drift) at time $t > 0$. The scheme is *exact* in the sense that it generates random variates distributed according to the desired law. Usually, an *exact* sampling of a random variable can be achieved using the rejection sampling method, introduced by Neumann in [45].

The rejection method allows to sample a random variable X with density h (w.r.t. the Lebesgue measure) from a sample variate of an instrumental random variable Y with density g if for all $x \in \mathbb{R}$, $h(x) \leq mg(x)$ where m is a finite positive constant. Let us denote by f the function ratio $f(x) := \frac{1}{m}\frac{h(x)}{g(x)}$. The sample variates y of Y is accepted as a sample of X if and only if $u < f(y)$, where u is a draw of a uniform random variable $U \sim \mathcal{U}_{[0,1]}$. Therefore the acceptance-rejection corresponds to a sample of a Bernoulli random variable with random parameter $f(Y)$: $\mathbb{1}_{\{U<f(Y)\}}$. Notice that the densities $h(x)$ and $g(x)$ do not need to be normalized.

In our framework, the one-dimensional projection at time t of a (β_1, β_2)-SBM (resp. with drift μ) starting at x has a density whose ratio with respect to the well known transition probability density of the Brownian motion (resp. with drift μ) is a series, as we saw in equation (2.2.6) (resp. (2.3.10)). The technique we propose allows to evaluate only a finite number of terms of the series, and at the same time, to maintain the exactness of the sampling.

2.5.1 Generalized rejection sampling method

Let us introduce the method by explaining a toy example for simulating *exactly* a Bernoulli random variable $X \sim \mathcal{B}_p$ with unknown parameter $p \in [0, 1]$. If the parameter is known, then clearly $X \overset{(d)}{=} \mathbb{1}_{\{U\leq p\}}$, hence an *exact* simulation consists of sampling the uniform random variable $U \sim \mathcal{U}_{[0,1]}$ and checking if the sample is smaller (or bigger) than p to decide if $X = 1$ (or $X = 0$).

Lemma 2.5.1. *Suppose p is an unknown parameter which is approximated by a sequence $(p_n)_n$. Suppose the rate of convergence is $(\delta_n)_n$ where $(\delta_n)_n$ is a vanishing sequence (i.e. for all n $|p - p_n| < \delta_n$, and $\delta_n \overset{n\to\infty}{\to} 0$). Then it is possible to simulate exactly a Bernoulli random variable of parameter p since*

$$X := \mathbb{1}_{\{\exists n;\ |U-p_n|>\delta_n,\ U<p_n\}} \sim \mathcal{B}_p.$$

Proof. One needs to show that $\mathbb{P}(X = 1) = p$. It is sufficient to show that the following equality holds

$$\{U < p\} = \{\exists n \in \mathbb{N};\ |U - p_n| > \delta_n,\ U < p_n\}.$$

Let us show the inclusion ($\subseteq$): Let $\omega \in \{U < p\}$ then $u < p$ where u denotes the draw $U(\omega)$. Let us notice that the sequence $(p_n - 2\delta_n)_n$ converges to p and each term is smaller than p, hence there exists an n such that $u < p_n - 2\delta_n < p$. In particular $|u - p_n| > \delta_n$ and $u < p_n$.
Let us show the other inclusion: Let $\omega \in \{\exists n \in \mathbb{N};\ |U - p_n| > \delta_n,\ U < p_n\}$ and let us denote by u the draw $U(\omega)$ then $|u - p_n| > \delta_n$ which implies $u < p_n - \delta_n$ which implies $u < p$ since $p \in (p_n - \delta_n, p_n + \delta_n)$.

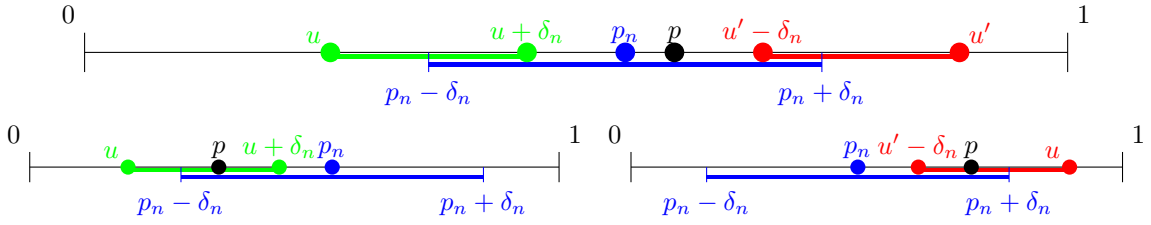

Figure 2.7: How to sample a Bernoulli random variable X of unknown parameter p: if $u < p$ then $X := 1$, otherwise $X := 0$. In the first image $u < p_n - \delta_n$ hence $u < p$ (resp. $u' > p_n + \delta_n$ hence $u' > p$). The second (resp. third) image shows that, if $u < p_n - \delta_n < u + \delta_n < p_n$ (resp. $p_n < u' - \delta_n < p_n + \delta_n < u$) then $u < p$ (resp. $u' > p$) anyway.

The scheme of the algorithm is:

1. sample from $\mathcal{U}$, obtain u
2. find n such that $|u - p_n| > \delta_n$,
3. if $u < p_n$, then $u < p$ hence $X := 1$ otherwise $X := 0$ (see Figure 2.7).

□

This idea allows an extension of the rejection sampling method for sampling $X \sim h(x)dx$ knowing just an approximation of the density h, and therefore of f.

Proposition 2.5.2 (Generalized rejection sampling method: GRS)**.** *Let Y be the instrumental random variable with (unnormalized) density $x \mapsto g(x)$. Then one can sample the random variable X with (unnormalized) density $x \mapsto h(x)$ under the following assumptions:*

(i) the ratio between the functions g and h is bounded:

$$\exists m > 0 \text{ such that } 0 < f(y) := \frac{1}{m}\frac{h(y)}{g(y)} \leq 1 \text{ for all } y \in \mathbb{R};$$

(ii) there exists a sequence of explicitly computable functions $(f_n)_n$ converging pointwise to f at a vanishing and explicitly computable rate $(\mathfrak{R}_n^f)$ (i.e. $\forall y \in \mathbb{R}\ |f_n(y) - f(y)| \leq \mathfrak{R}_n^f(y)$ for all n).

Then $X \sim \big(Y \,|\, \exists n;\ U < f_n(Y) - \mathfrak{R}_n^f(Y)\big)$ i.e. an exact simulation is possible.

Proof. It is well known from the standard rejection sampling that $X \sim (Y|U < f(Y))$ (see for example [54]). Lemma 2.5.1 ensures that we can simulate exactly without knowing $f(Y)$ with complete accuracy. The acceptability of the draw $y = Y$ as a sample from X is a Bernoulli r.v. with parameter $f(y)$ and we can compute explicitly a sequence converging to this quantity $f_n(y)(=: p_n)$ and its rate of convergence $\mathfrak{R}_n^f(y)\,(=: \delta_n)$. □

An analogous version of the sampling method in Proposition 2.5.2 has been first introduced by Devroye in [17] with the name of *Series method for random variate generation*. The generalized rejection sampling (GRS) allows in particular to sample from a density h from an instrumental density g (both w.r.t. the Lebesgue measure), once the ratio between the densities h/g is an *infinite* bounded series. Let us recall that $f(x) := \frac{1}{m}\frac{h(x)}{g(x)}$, where m is an upper bound of the ratio, is a series.
In Algorithm 1 we propose a pseudo-code referring to this particular case. Let us first notice that with probability one the algorithm terminates itself in a finite number of steps and yet delivers draws which are exactly from the desired density. We introduce the quantity $N_{max} \in \mathbb{N}$ in order to prevent the zero-probability event that the algorithm keeps turning.

The implementation of the algorithm that we propose requires the following quantities and functionals:

- g: instrumental density under which it is known how to sample,
- N_{max}: the maximal number of terms of the series one decides to consider ($N_{max} \geq 1$),
- $(f_N)_{N=0,\dots,N_{max}}$: the partial sums of the series f,
- $(\mathfrak{R}_N^f)_{N=0\dots,N_{max}}$: sequence of bounds for the absolute value of the remainder $f - f_N$,
- $I_{\mathfrak{R}}^f$: the inverse function of $\mathfrak{R}_N^f$

$$\begin{array}{rccl} I_{\mathfrak{R}}^f: & (0,1) & \to & \{0,\dots,N_{max}\} \\ & u & \mapsto & I_{\mathfrak{R}}^f(u) = \inf\{N \leq N_{max} : \mathfrak{R}_N^f \leq u\}\,, \end{array}$$

with the convention that $\inf \emptyset = N_{max}$.

Let us notice that, a priori, the sequence of bounds for the remainder may be a function which is a vanishing sequence for each y fixed: $\left(\mathfrak{R}_N^f(y)\right)_N$ is the sequence of bound for $|f(y) - f_N(y)|$. If this is the case, then the function $u \mapsto I_{\mathfrak{R}}^f(u)$ has to be defined, for each y, as the inverse of $\mathfrak{R}_N^f(y)$. In the cases we consider, $\mathfrak{R}_N^f$ is a simple sequence independent from y.

Algorithm 1: The generalized rejection sampling **GRS**

Input : g, N_{max}, $(f_N)_N$; $(\mathfrak{R}_N^f)_N$, $I_{\mathfrak{R}}^f$.
Output: x, `exact`: x is a sample from the desired density and `exact` is True if the sample is *exact* (obtained considering less than N_{max} f_N, $N = 0, \ldots, N_{max}$) or False if it is a good approximation.

```
reject ← True;
while reject do
    sample a standard uniform u;
    sample y from g;
    N ← 0;
    while |f_N(y) − u| < ℜ_N^f(y) and N < N_max do
        N ← I_ℜ^f(|f_N(y) − u|);
    if N == N_max then
        reject ← False;
        x ← y and exact ← False;
    else if f_N > u then
        reject ← False ;
        x ← y and exact ← True;
return x and exact
```

The function $I_{\mathfrak{R}}^f(u)$ has a special role in the above algorithm. It provides an alternative to the natural approach and, in some cases, it speeds up the rejection step in the algorithm. More precisely, once $|f_N(y) - u|$ is smaller than $\mathfrak{R}_N^f(y)$, the natural approach consists in taking as next index $\hat{N} = n + 1$ and check again the same condition. Instead, one can choose to take $I_{\mathfrak{R}}^f(|f_N(y) - u|)$. Intuitively this choice improves the chances to conclude the acceptance/rejection at the immediate next step. Indeed it is easy to show that $I_{\mathfrak{R}}^f(|f_N(y) - u|) \in N + 1, \ldots, N_{max}$. In particular if $n \mapsto \mathfrak{R}_n^f(y)$ is decreasing quickly enough the two ways are equivalent.

One is drawing *exactly* form the desired law if each sample has been accepted or rejected considering less than N_{max} terms of the series f_N. Therefore one may have to consider a big number of terms of the series f_N, but we can control the maximal number N_{max} fixing it to $N_{max} = \inf\{N \in \mathbb{N} : \mathfrak{R}_N^f \leq 0.00005\}(= I_{\mathfrak{R}}^f(0.00005))$, i.e. the smallest integer N such that $2\mathfrak{R}_N^f$ is smaller than 0.0001. Indeed the probability that for all $N \leq N_{max}$ one has not been able to accept or reject a sample is smaller than twice the bound $\mathfrak{R}_{N_{max}}^f$. In this unfortunate case, our strategy would be to accept the variate as a good approximation of the real one, but the outputs inform that the variate is not necessarily "exact".

All sequences of functions $y \mapsto (\mathfrak{R}_N^f(y))_N$ considered in this document are in fact independent from y and exponentially decreasing in N. In particular $I_N^f(u)$ is the first integer greater or equal than $\dfrac{\log|f_N(y) - u|}{\log(\mathfrak{R}_N^f)}$ and it is at least $N + 1$. Moreover all simulations turn out to be exact, i.e. one takes the decision to accept or reject without the need to consider N_{max}) and the procedure to accept or reject is really fast since usually it is done by computing only f_0, f_1 and f_2.

2.5.2 A Gaussian bound for the transition density

In this section we check that the hypotheses of Proposition 2.5.2 are satisfied in order to provide random variates of the (β_1, β_2)-SBM (with constant drift μ) at time t, starting at x.

The case of the two-SBM without drift

We already noticed in Proposition 2.2.4 that the density $y \mapsto p^{(\beta_1,\beta_2)}(t,x,y)$ is absolutely continuous with respect to the one of the Brownian motion $y \mapsto p(t,x,y)$ with ratio given by equation (2.2.6):

$$v^{(\beta_1,\beta_2)}(t,x,y) = \sum_{k=0}^{\infty}(-\beta_1\beta_2)^k \sum_{j=1}^{4} c_j(y) e^{-\frac{(a_j(x,y)+2zk)^2}{2t}} e^{-|x-y|\frac{a_j(x,y)+2zk}{t}}.$$

Let us denote by $(v^{(\beta_1,\beta_2)})_k(t,x,y)$ the $k-th$ term of the series $v^{(\beta_1,\beta_2)}(t,x,y)$.

For each $k \in \mathbb{N}$, there exists an upper bound uniform in y for $(v^{(\beta_1,\beta_2)})_k$:

$$\sup_{y\in\mathbb{R}} \left|(v^{(\beta_1,\beta_2)})_k(t,x,y)\right| \leq (1+|\beta_1|)(1+|\beta_2|)|\beta_1\beta_2|^k e^{-2\frac{z^2}{t}k} =: v_k(t).$$

In fact the bound $v_k(t)$ is uniform in x as well. Moreover for each $t>0$, $v_k(t) \leq v_k(0) := (1+|\beta_1|)(1+|\beta_2|)|\beta_1\beta_2|^k$ which is uniform in $t \in \mathbb{R}_+^*$.

The proof is straightforward, one just need to notice that $\frac{1}{2}(a_j(x,y)+2zk)^2+|x-y|(a_j(x,y)+2zk) \geq 2z^2k$, hence

$$\left|\left(v^{(\beta_1,\beta_2)}\right)_k(t,x,y)\right| \leq |\beta_1\beta_2|^k e^{-2\frac{z^2}{t}k}\left(\sum_{j=1}^{4}|c_j(y)|\right) = (1+|\beta_1|)(1+|\beta_2|)\,|\beta_1\beta_2|^k e^{-2\frac{z^2}{t}k}.$$

Let us denote by $\left[v^{(\beta_1,\beta_2)}\right]_N(t,x,y)$ and $R_N v^{(\beta_1,\beta_2)}(t,x,y)$ the truncated series up to the term N and its remainder:

$$\left[v^{(\beta_1,\beta_2)}\right]_N(t,x,y) = \sum_{k=0}^{N}(-\beta_1\beta_2)^k \sum_{j=1}^{4} c_j(y) e^{-\frac{(a_j(x,y)+2zk)^2}{2t}} e^{-|x-y|\frac{a_j(x,y)+2zk}{t}},$$

$$R_N v^{(\beta_1,\beta_2)}(t,x,y) = v^{(\beta_1,\beta_2)}(t,x,y) - v_N^{(\beta_1,\beta_2)}(t,x,y).$$

Let us then define

$$\bar{v}(t) := \frac{(1+|\beta_1|)(1+|\beta_2|)}{1-|\beta_1\beta_2|e^{-2\frac{z^2}{t}}} < \frac{(1+|\beta_1|)(1+|\beta_2|)}{1-|\beta_1\beta_2|}. \tag{2.5.1}$$

One can easily check that for any fixed t, $\bar{v}(t)$ is a bound for $v^{(\beta_1,\beta_2)}(t,x,y)$ uniform in x and y:

$$v^{(\beta_1,\beta_2)}(t,x,y) \leq \bar{v}(t) \quad \text{and} \quad |R_N v^{(\beta_1,\beta_2)}(t,x,y)| \leq \bar{v}(t)\,|\beta_1\beta_2|^{N+1} e^{-2\frac{z^2}{t}(N+1)}.$$

For the Algorithm 1, we choose the functions

$$\begin{aligned} f(y) &:= \frac{1}{\bar{v}(t)} v^{(\beta_1,\beta_2)}(t,x,y), \\ f_N(y) &:= \frac{1}{\bar{v}(t)}\left[v^{(\beta_1,\beta_2)}\right]_N(t,x,y), \quad \mathfrak{R}_N^f := |\beta_1\beta_2|^{N+1} e^{-2\frac{z^2}{t}(N+1)}, \end{aligned} \tag{2.5.2}$$

with $x \in \mathbb{R}$, $t>0$, $z>0$, $N \in \mathbb{N}$ and $\bar{v}(t)$ given by (2.5.1).

The case of the two-SBM with constant drift μ

We already noticed in Theorem 2.3.7 that the density $y \mapsto p_\mu^{(\beta_1,\beta_2)}(t,x,y)$ is absolutely continuous with respect to the one of the Brownian motion with constant drift μ $y \mapsto p_\mu(t,x,y)$ with ratio given in (2.3.15) as series of Fourier transforms.

Proposition 2.5.3. *Let us denote by $(v_\mu^{(\beta_1,\beta_2)})_k(t,x,y)$ the $k-th$ term of the series $v_\mu^{(\beta_1,\beta_2)}(t,x,y)$ in (2.3.15). For each $k \in \mathbb{N}$, there exists an upper bound uniform in y for $(v^{(\beta_1,\beta_2)})_k$:*

$$\sup_{y\in\mathbb{R}} \left|(v_\mu^{(\beta_1,\beta_2)})_k(t,x,y)\right| \leq C(\beta_1,\beta_2,k)\, e^{-2\,\frac{z^2}{t}\,k} =: v_k(t).$$

If $\beta_1 > 0, \beta_2 > 0$ the constant $C(\beta_1,\beta_2)$ does not depend on k.

Proof. The proof is quite laborious and divided into several steps. For simplicity, but without loss of generality, let us fix $t = 1$. Let us consider then the representation as series of Fourier transforms (2.3.15):

$$\begin{cases} v_\mu^{(\beta_1,\beta_2)}(1,x,y) = \displaystyle\sum_{k=0}^{\infty}(-\beta_1\beta_2)^k \sum_{j=1}^{4} F_{j,k}(\omega_{j,k},\mathfrak{a}), \\ F_{j,k}(\omega_{j,k},\mathfrak{a}) := e^{\frac{1}{2}(\omega_{1,0}^2+\mathfrak{a}^2)}e^{-\mathfrak{a}\omega_{j,k}}\mathcal{F}\left(w \mapsto e^{-\frac{w^2}{2}} c_j(y,\mu;iw+\mathfrak{a})\,\frac{-(w^2-\mathfrak{a}^2+\mu^2-2iw\mathfrak{a})^k}{(w-i\mathfrak{a}_1)^{k+1}(w-i\mathfrak{a}_2)^{k+1}}\right)(\omega_{j,k}-\mathfrak{a}), \end{cases}$$

where $\omega_{j,k}$ and $\mathfrak{a}$ are defined as in Theorem 2.3.7, and let us recall that $\mathfrak{a}_i = \mathfrak{a} + \beta_i\mu$.
Let us rewrite the functions $F_{j,k}$:

$$\begin{cases} F_{j,k}(\omega_{j,k},\mathfrak{a}) := e^{\frac{1}{2}(\omega_{1,0}^2+\mathfrak{a}^2)}e^{-\mathfrak{a}\omega_{j,k}}\Psi_{j,k}(\omega_{j,k},\mathfrak{a}) \\ \Psi_{j,k}(\omega_{j,k},\mathfrak{a}) := \mathcal{F}\left(w \mapsto e^{-\frac{w^2}{2}} p_j(w)\,\frac{(w^2-\mathfrak{a}^2+\mu^2-2iw\mathfrak{a})^k}{(w-i\mathfrak{a}_1)^k(w-i\mathfrak{a}_2)^k}\right)(\omega_{j,k}-\mathfrak{a}) \end{cases}$$

where

$$p_j(w) := \frac{-c_j(y,\mu;iw+\mathfrak{a})}{(w-i\mathfrak{a}_1)(w-i\mathfrak{a}_2)}.$$

The latter functions are equal to

$$\begin{cases} p_1(w) = 1 \\ p_2(w) = \left(2\mathbb{1}_{\{y>0\}}-1\right)\beta_1 - \frac{\beta_1\mu(1+\left(2\mathbb{1}_{\{y>0\}}-1\right)\beta_1)}{iw+\mathfrak{a}_1} - 2\mathbb{1}_{\{y>z\}}\frac{\beta_1\beta_2\mu}{iw+\mathfrak{a}_2} + 2\mathbb{1}_{\{y>z\}}\frac{\beta_1\beta_2\mu^2(1+\beta_1)}{(iw+\mathfrak{a}_1)(iw+\mathfrak{a}_2)} \\ p_3(w) = \left(2\mathbb{1}_{\{y>z\}}-1\right)\beta_2 - \frac{\beta_2\mu(1+\left(2\mathbb{1}_{\{y>z\}}-1\right)\beta_2)}{iw+\mathfrak{a}_2} + 2\mathbb{1}_{\{y\leq 0\}}\frac{\beta_1\beta_2\mu}{iw+\mathfrak{a}_1} + 2\mathbb{1}_{\{y\leq 0\}}\frac{\beta_1\beta_2\mu^2(1-\beta_2)}{(iw+\mathfrak{a}_1)(iw+\mathfrak{a}_2)} \\ p_4(w) = \left(1-2\mathbb{1}_{\{0\leq y<z\}}\right)\beta_1\beta_2\left(1+\frac{\mu(1-\beta_1)}{iw+\mathfrak{a}_1} - \frac{\mu(1+\beta_2)}{iw+\mathfrak{a}_2} - \frac{\mu^2(1-\beta_1)(1+\beta_2)}{(iw+\mathfrak{a}_1)(iw+\mathfrak{a}_2)}\right). \end{cases}$$

Let us notice that the proof is over once one shows for each $j = 1,2,3,4$ that there exists a positive constant $C_j(\beta_1,\beta_2,k)$ such that

$$|\Psi_{j,k}(\omega)| \leq \frac{C_j(\beta_1,\beta_2,k)}{|\beta_1\beta_2|^k}\, e^{-\frac{1}{2}\omega^2} \tag{2.5.3}$$

and $\sum_k C_j(\beta_1,\beta_2,k)\, e^{\omega_{1,0}^2-\omega_{j,k}^2}$ is finite.

Let us now prove the statement (2.5.3) for the function $\Psi_{1,k}$. $\Psi_{1,k}$ is the Fourier transform of the product of a Gaussian and the $k-th$ power of the fractional function

$$\frac{(w^2+\mu^2)}{(w-i\mathfrak{a}_1)(w-i\mathfrak{a}_2)} = 1 - \frac{\mu^2(1-\beta_1)(1-\beta_2)}{(w-i\mathfrak{a}_1)(w-i\mathfrak{a}_2)} - i\frac{(1-\beta_1)\mu}{w-i\mathfrak{a}_2} - i\frac{(1-\beta_2)\mu}{w-i\mathfrak{a}_2}.$$

Let

$$\Psi_{0,k}(w) := \frac{(w^2+\mu^2)^k}{(w-i\mathfrak{a}_1)^k(w-i\mathfrak{a}_2)^k}.$$

Using the binomial formula the latter quantity can be expressed as follows.

$$\begin{aligned}\Psi_{0,k}(w) &= \sum_{n=0}^{k}\binom{k}{n}\left(1-\frac{\mu^2(1-\beta_1)(1-\beta_2)}{(w-i\mathfrak{a}_1)(w-i\mathfrak{a}_2)}\right)^{k-n}\left(-i\frac{(1-\beta_2)\mu}{w-i\beta_2\mu}-i\frac{(1-\beta_1)\mu}{w-i\mathfrak{a}_2}\right)^{n}\\ &= \sum_{n=0}^{k}\sum_{n_1=0}^{k-n}\sum_{n_2=0}^{n}\binom{k}{n}\binom{k-n}{n_1}\binom{n}{n_2}\left(-\frac{\mu^2(1-\beta_1)(1-\beta_2)}{(w-i\mathfrak{a}_1)(w-i\mathfrak{a}_2)}\right)^{n_1}\left(\frac{(1-\beta_2)\mu}{iw+\mathfrak{a}_2}\right)^{n_2}\left(\frac{(1-\beta_1)\mu}{iw+\mathfrak{a}_1}\right)^{n-n_2}\\ &= \sum_{n=0}^{k}\sum_{n_1=0}^{k-n}\sum_{n_2=0}^{n}\binom{k}{n}\binom{k-n}{n_1}\binom{n}{n_2}\frac{(-1)^{n_1}\left((1-\beta_2)\mu\right)^{n_1+n_2}\left((1-\beta_1)\mu\right)^{n-n_2+n_1}}{(iw+\mathfrak{a}_2)^{n_1+n_2}(iw+\mathfrak{a}_1)^{n-n_2+n_1}}.\end{aligned}$$

Notice that the latter function is a sum of constants (when $n_1=0,n_2=0,n=0$) and of square integrable complex functions. In particular, let $n_1,n_2\in\mathbb{N}$, the Fourier transform of $(iw+\mathfrak{a}_1)^{-n_1}(iw+\mathfrak{a}_2)^{-n_2}$ has support on $(-\infty,0]$ because is the convolution of two functions supported on $(-\infty,0]$ (see Lemma 2.3.5). Hence, since

$$\Psi_{1,k}=\frac{1}{\sqrt{2\pi}}\left(w\mapsto e^{-\frac{1}{2}\omega^2}\right)*\mathcal{F}\left(w\mapsto\Psi_{0,k}\right),$$

we have

$$|\Psi_{1,k}(\omega_{j,k}-\mathfrak{a})|\leq\frac{1}{\sqrt{2\pi}}\int_{\mathbb{R}}e^{-\frac{1}{2}(\omega_{j,k}-\mathfrak{a}-y)^2}\left|\hat{\Psi}_{0,k}(y)\right|dy\leq e^{-\frac{1}{2}(\omega_{j,k}-\mathfrak{a})^2}\|e^{-\mathfrak{a}\cdot}\,\hat{\Psi}_{0,k}(\cdot)\|_{L^1(\mathbb{R},dx)}.$$

The $L^1(\mathbb{R},dx)$-norm of $e^{-\omega\mathfrak{a}}\mathcal{F}\left(w\mapsto(iw+\mathfrak{a}_1)^{-n_1}(iw+\mathfrak{a}_2)^{-n_2}\right)$ is equal to $|\beta_1\mu|^{-n_1}|\beta_2\mu|^{-n_2}$ (see Lemma 3.4.5), hence

$$\begin{aligned}\|e^{-\mathfrak{a}\cdot}\,\hat{\Psi}_{0,k}(\cdot)\|_{L^1(\mathbb{R},dx)} &\leq \sum_{n=0}^{k}\sum_{n_1=0}^{k-n}\sum_{n_2=0}^{n}\binom{k}{n}\binom{k-n}{n_1}\binom{n}{n_2}\left(\frac{1-\beta_2}{|\beta_2|}\right)^{n_1+n_2}\left(\frac{1-\beta_1}{|\beta_1|}\right)^{n-n_2+n_1}\\ &= \sum_{n=0}^{k}\binom{k}{n}\left(\frac{1-\beta_1}{|\beta_1|}+\frac{1-\beta_2}{|\beta_2|}\right)^{n}\left(1+\frac{(1-\beta_1)(1-\beta_2)}{|\beta_1\beta_2|}\right)^{k-n}\\ &= \left(1+\frac{(1-\beta_1)(1-\beta_2)}{|\beta_1\beta_2|}+\frac{1-\beta_1}{|\beta_1|}+\frac{1-\beta_2}{|\beta_2|}\right)^{k}\\ &= \frac{(1-\beta_1+|\beta_1|)^k(1-\beta_2+|\beta_2|)^k}{|\beta_1\beta_2|^k}.\end{aligned}$$

Let $C_1(\beta_1,\beta_2,k):=(1-\beta_1+|\beta_1|)^k(1-\beta_2+|\beta_2|)^k$. Notice that this quantity is equal to 1 if $\beta_1>0,\beta_2>0$. We have proven (2.5.3) for $j=1$.

Let us check (2.5.3) for $j=2,3,4$. Notice that the functions $p_j(w)$, $j=2,3,4$ are sums of constants and functions whose Fourier transforms have support on $(-\infty,0)$. Let us define $\hat{p}_j$, $j=2,3,4$ as

$$\begin{cases}\hat{p}_2(w)=\sqrt{2\pi}\left(2\mathbb{1}_{\{y>0\}}-1\right)\beta_1-\beta_1\mu(1+\left(2\mathbb{1}_{\{y>0\}}-1\right)\beta_1)\mathcal{F}\left(\frac{1}{iw+\mathfrak{a}_1}\right)\\ \qquad -2\mathbb{1}_{\{y>z\}}\beta_1\beta_2\mu\mathcal{F}\left(\frac{1}{iw+\mathfrak{a}_2}\right)+2\mathbb{1}_{\{y>z\}}\beta_1\beta_2\mu^2(1+\beta_1)\mathcal{F}\left(\frac{1}{(iw+\mathfrak{a}_1)(iw+\mathfrak{a}_2)}\right)\\ \hat{p}_3(w)=\sqrt{2\pi}\left(2\mathbb{1}_{\{y>z\}}-1\right)\beta_2-\beta_2\mu(1+\left(2\mathbb{1}_{\{y>z\}}-1\right)\beta_2)\mathcal{F}\left(\frac{1}{iw+\mathfrak{a}_2}\right)\\ \qquad +2\mathbb{1}_{\{y\leq 0\}}\beta_1\beta_2\mu\mathcal{F}\left(\frac{1}{iw+\mathfrak{a}_1}\right)+2\mathbb{1}_{\{y\leq 0\}}\beta_1\beta_2\mu^2(1-\beta_2)\mathcal{F}\left(\frac{1}{(iw+\mathfrak{a}_1)(iw+\mathfrak{a}_2)}\right)\\ \hat{p}_4(w)=\left(1-2\mathbb{1}_{\{0\leq y<z\}}\right)\beta_1\beta_2\left(\sqrt{2\pi}+\mu(1-\beta_1)\mathcal{F}\left(\frac{1}{iw+\mathfrak{a}_1}\right)-\mu(1+\beta_2)\mathcal{F}\left(\frac{1}{iw+\mathfrak{a}_2}\right)\right.\\ \qquad \left.-\mu^2(1-\beta_1)(1+\beta_2)\mathcal{F}\left(\frac{1}{(iw+\mathfrak{a}_1)(iw+\mathfrak{a}_2)}\right)\right).\end{cases}$$

Hence one has

$$\begin{aligned}|\Psi_{j,k}|(\omega_{j,k}-\mathfrak{a}) &\leq \frac{|\hat{p}_j|}{\sqrt{2\pi}}*|\Psi_{1,0}|(\omega_{j,k}-\mathfrak{a})\\ &= \int_{\mathbb{R}}\frac{|\hat{p}_j(y)|}{\sqrt{2\pi}}|\Psi_{1,k}(\omega_{j,k}-a-y)|dy\leq\frac{C_1(\beta_1,\beta_2,k)}{|\beta_1\beta_2|^k}\int_{\mathbb{R}}\frac{|\hat{p}_j(y)|}{\sqrt{2\pi}}e^{-\frac{1}{2}(\omega_{j,k}-a-y)^2}dy.\end{aligned}$$

The latter inequality holds because $\Psi_{1,k}$ satisfies (2.5.3). For the constant term of p_j we do not actually compute the convolution, we keep the formal presentation anyway, for the sake of simplicity. One now notices that the Fourier transforms involved in p_j have support on the negative semi-line, hence

$$|\Psi_{j,k}|(\omega_{j,k}-\mathfrak{a}) \leq \frac{C_1(\beta_1,\beta_2,k)}{|\beta_1\beta_2|^k} e^{-\frac{1}{2}(\omega_{j,k}-a)^2} \int_{-\infty}^{0} \frac{|\hat{p}_j(y)|}{\sqrt{2\pi}}\, e^{a\,y}\, e^{-\frac{1}{2}y^2} dy.$$

Hence (2.5.3) holds, with $C_j(\beta_1,\beta_2,k) \geq C_1(\beta_1,\beta_2,k)\int_{-\infty}^{0} \frac{|\hat{p}_j(y)|}{\sqrt{2\pi}}\, e^{a\,y}\, e^{-\frac{1}{2}y^2} dy$ for example

$$\begin{cases} C_2(\beta_1,\beta_2,k) = C_1(\beta_1,\beta_2,k)\left(1+2|\beta_1|+2\mathbb{1}_{\{y>z\}}(1+\beta_1+|\beta_1|)\right) \\ C_3(\beta_1,\beta_2,k) = C_1(\beta_1,\beta_2,k)\left(1+2|\beta_2|+2\mathbb{1}_{\{y\leq 0\}}(1-\beta_2+|\beta_2|)\right) \\ C_4(\beta_1,\beta_2,k) = C_1(\beta_1,\beta_2,k)\left(1-\beta_1+|\beta_1|\right)\left(1+\beta_2+|\beta_2|\right). \end{cases}$$

To conclude the proof, we need to show that

$$\sum_{k=0}^{\infty}\sum_{j=1}^{4} C_j(\beta_1,\beta_2,k) e^{\omega_{1,0}^2-\omega_{j,k}^2} < +\infty.$$

It is easy to check that $\omega_{1,0}^2-\omega_{j,k}^2 < -2\frac{z^2}{t}k^2$, therefore if $C(\beta_1,\beta_2,k) := \sum_{j=1}^{4} C_j(\beta_1,\beta_2,k)$, one has

$$\sum_{k=0}^{\infty}\sum_{j=1}^{4} C_j(\beta_1,\beta_2,k) e^{\omega_{1,0}^2-\omega_{j,k}^2} \leq \sum_{k=0}^{\infty} C(\beta_1,\beta_2,k) e^{-2\frac{z^2}{t}k^2}.$$

If $\beta_1 > 0, \beta_2 > 0$, then $C_1(\beta_1,\beta_2,k) = 1$ and $C(\beta_1,\beta_2,k)$ do not depend on k. Moreover the sum $\sum_{k=0}^{\infty} e^{-2\frac{z^2}{t}k^2}$ is finite because it is controlled by the geometric sum $\sum_{k=0}^{\infty} e^{-2\frac{z^2}{t}k} = \frac{1}{1-e^{-2\frac{z^2}{t}}}$.
Instead, at least for small t or big distance between the barriers z, it is always true that $C_1(\beta_1,\beta_2,k)e^{-\frac{2z^2}{t}k^2} \leq |\beta_1\beta_2|^k e^{-\frac{z^2}{t}k}$ which yields a geometric sum as well.
If z and t are fixed, than one exploits the fact that for k big enough one has again a geometric sum. □

The bound $v_k(t)$, which is not sharp, is uniform in x.
Denote by $\left[v_\mu^{(\beta_1,\beta_2)}\right]_N(t,x,y)$ and $R_N v_\mu^{(\beta_1,\beta_2)}(t,x,y)$ the truncated series up to the term N and its remainder. Let us consider the case $\beta_1 > 0, \beta_2 > 0$, in that case $C(\beta_1,\beta_2,k)$ does not depend on k hence we will denote it by $C(\beta_1,\beta_2)$. Then let

$$\bar{v}_\mu(t) := \frac{C(\beta_1,\beta_2)}{1-e^{-2\frac{z^2}{t}}}.$$

(Removing the previous assumption, for t or z appropriate one can take $\bar{v}_\mu(t) = \frac{C(\beta_1,\beta_2)}{1-|\beta_1\beta_2|e^{-\frac{z^2}{t}}}$.)
One can easily check that

$$v_\mu^{(\beta_1,\beta_2)}(t,x,y) \leq \bar{v}_\mu(t) \quad \text{and} \quad |R_N v_\mu^{(\beta_1,\beta_2)}(t,x,y)| \leq \bar{v}_\mu(t)\, e^{-2\frac{z^2}{t}(N+1)}.$$

For the Algorithm 1, we choose the functions

$$\begin{aligned} f(y) &:= \frac{1}{\bar{v}_\mu(t)} v_\mu^{(\beta_1,\beta_2)}(t,x,y), \\ f_N(y) &:= \frac{1}{\bar{v}_\mu(t)} \left[v_\mu^{(\beta_1,\beta_2)}\right]_N(t,x,y), \qquad \mathfrak{R}_N^f := e^{-2\frac{z^2}{t}(N+1)}. \end{aligned} \tag{2.5.4}$$

$x \in \mathbb{R}$, $t > 0$, $z > 0$ and $N \in \mathbb{N}$.

Let $\mathfrak{N}$ be the random number of steps necessary to take the decision in the generalized rejection sampling. Using Wald's equation one can easily show that $\mathbb{E}[\mathfrak{N}] \leq \sum_{n=0}^{\infty} \mathfrak{R}_n^f = \frac{e^{-2\frac{z^2}{t}}}{1-e^{-2\frac{z^2}{t}}}$.

2.5.3 Sampling from the density: the two-skew Brownian motion

Let $x \in \mathbb{R}$, $t > 0$, $z > 0$ be fixed, one can apply the GRS Algorithm 1 (given by Proposition 2.5.2) with the functions given by equation (2.5.2) and sample from the density $y \mapsto p^{(\beta_1,\beta_2)}(t,x,y)$ in equation (2.2.6). One can then simulate exactly the Markov process (β_1,β_2)-SBM starting at x, up to a time $T > 0$ simply taking a discretization of the time interval $[0,T]$ (see for example Figure 2.8).
The same holds for the transition density $y \mapsto p_\mu^{(\beta_1,\beta_2)}(t,x,y)$ using the functions given by (2.5.4).

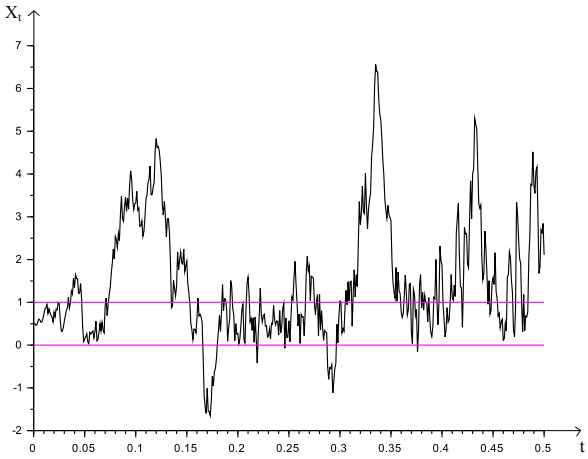

Figure 2.8: Exact simulation of a path of the $(0.7,-0.2)$-SBM starting at time 0 in $x = 0.5$. The barriers are $z_1 = 0$ and $z_2 = 1$. The time discretization is $\delta t = 0.001$.

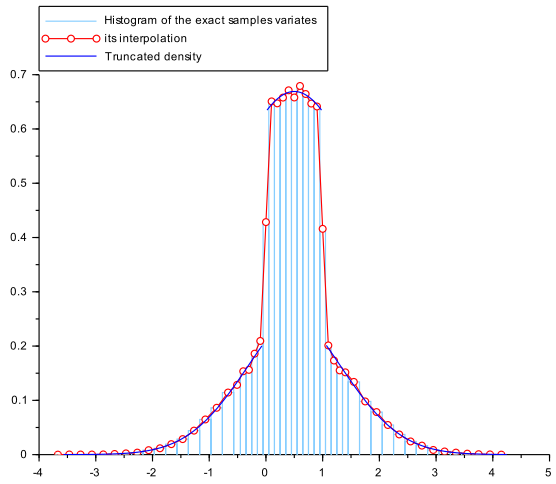

Figure 2.9: Comparison between the function $y \mapsto p^{(\frac{1}{2},-\frac{1}{2})}(1,0.5,y)$ obtained from 50000 exact simulations through generalized rejection sampling method and the plot of its truncated version at the tenth term ($N_{max} = 10$). The barriers are $z_1 = 0$ and $z_2 = 1$.

For simplicity, we always take time $t = 1$, starting point $x = 0.5$ and we assume that the barriers are fixed in $z_1 = 0$ and $z_2 = 1$. Let us compare now the approximation of the density $y \mapsto p^{(\beta_1,\beta_2)}(t,x,y)$ in equation (2.2.6) obtained truncating the series at the $N_{max}-th$ term and an histogram of a large number of *exact* samples from the untruncated density computed through the generalized rejection sampling method.

We represent in Figure 2.9, as typical situation, the function $y \mapsto p^{(\frac{1}{2},-\frac{1}{2})}(1,0.5,y)$. In this case, 100% of the 50000 simulations are exact. The average number of terms of the series that are necessary in order to decide if to accept or reject the simulations is slightly larger than 1, actually it is 1.19 (it would have been around 2 with the rougher bound $\bar{v}(0)$). From now on we will denote this number as N_{ac}.
The transition density in this case is mainly concentrated inside of the interval between the barriers (z_1,z_2) since $\beta_1 > 0$ and $\beta_2 < 0$. Choosing $N_{max} = 10$ the truncated series differs from the untruncated one at most of $\overline{v}\,|\beta_1\beta_2|^{11} \sim 6 \cdot 10^{-7}$.

In Figure 2.10 and 2.11 we propose skewness parameters with different absolute values and pointing respectively inward and outward. All our simulations are exact and $N_{ac} \sim 1.15$ is low as expected. In these cases $\delta_n = 0.028^{n+1}$, $\overline{v} = 2.8$ and $\overline{v}_1 = 2.3$. We can observe in Figure 2.10 that the process tends to stay between the barriers because when it reaches the barrier z_1 it has probability $\frac{1+\beta_1}{2} = 0.65$ to be reflected to this region and when it reaches z_2 the probability is $\frac{1-\beta_2}{2} = 0.85$. If the process leaves (z_1,z_2), then the probability to be before z_1 is larger than to be after z_2 because $1-\beta_1 > 1+\beta_2$.
In Figure 2.11 the parameters $\beta_1 = -0.7$ and $\beta_2 = 0.3$ induce that the process is more likely to be outside the region between the barriers because it is reflected outside this region with probability $\frac{1-\beta_1}{2} = 0.85$ in z_1 and with probability 0.65 in z_2.

Figure 2.12 represents a case where $\beta_1\beta_2 > 0$. From the simulated density function the behavior we

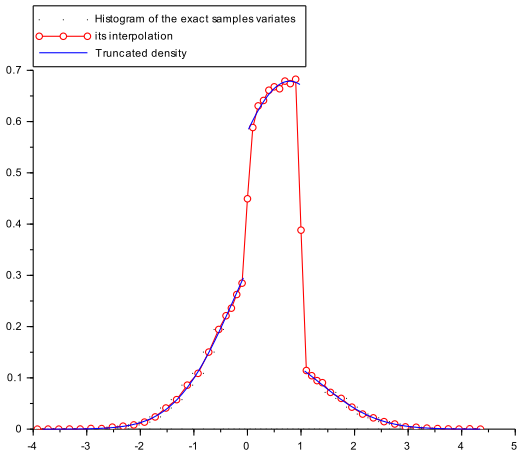

Figure 2.10: Comparison between the truncation at the $10-th$ term of the series expression of $y \mapsto p^{(0.3,-0.7)}(1, 0.5, y)$ given in (2.2.6) and the histogram resulting from 50000 exact simulations obtained through generalized rejection sampling. The barriers are $z_1 = 0$ and $z_2 = 1$. The average acceptance number is $N_{ac} = 1.15$.

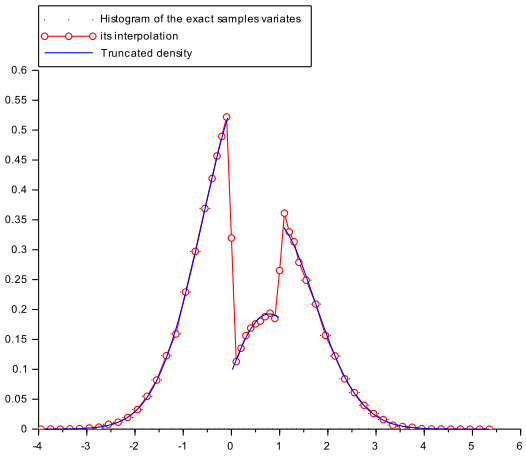

Figure 2.11: Comparison between the truncation at the $10-th$ term of the series expression of $y \mapsto p^{(-0.7,0.3)}(1, 0.5, y)$ given in (2.2.6) and the histogram resulting from 50000 exact simulations obtained through generalized rejection sampling. The barriers are $z_1 = 0$ and $z_2 = 1$. The average acceptance number is $N_{ac} = 1.15$.

expected is confirmed: the process after a time t will be more likely to stay on the left (respectively right if the parameters are positive) side of the barriers. We chose the parameters $\beta_1 < \beta_2$ in such a way that the process would more likely stay in $(-\infty, z_1)$.

Another interesting example is the case of a completely reflecting barrier and a partially reflecting one: in Figure 2.13 we choose $\beta_1 = 1$ and $\beta_2 < 0$, i.e. z_1 totally reflecting and z_2 semipermeable with semipermeabiliy coefficient $\beta_2 = -0.4$. The process shows the tendency to stay between the barriers (z_1, z_2), while it will have probability zero to be in $(-\infty, z_1)$.

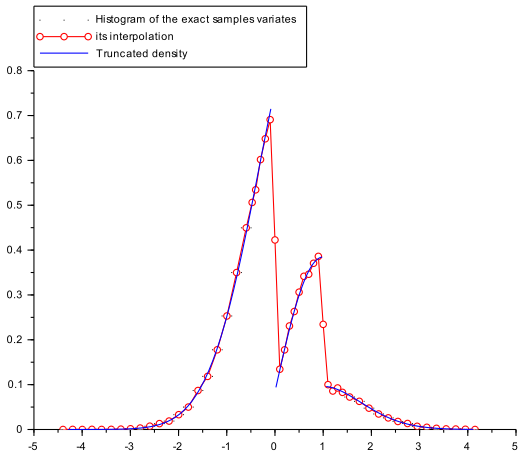

Figure 2.12: Comparison between the truncation at the $10-th$ term of the series expression of $y \mapsto p^{(-0.8,-0.6)}(1, 0.5, y)$ given in (2.2.6) and the histogram resulting from 50000 exact simulations obtained through generalized rejection sampling. The barriers are $z_1 = 0$ and $z_2 = 1$. The average acceptance number is $N_{ac} = 1.37$.

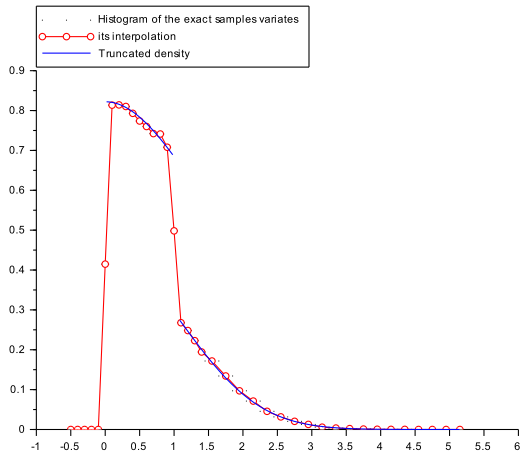

Figure 2.13: Comparison between the truncation at the $10-th$ term of the series expression of $y \mapsto p^{(1,-0.4)}(1, 0.5, y)$ given in (2.2.6) and the histogram resulting from 50000 exact simulations obtained through generalized rejection sampling. The barriers are $z_1 = 0$ and $z_2 = 1$. The average acceptance number is $N_{ac} = 1.27$.

Chapter 3

Brownian diffusions with drift admitting several jumps: an exact simulation

Outline of the chapter: The aim of this chapter is to provide an exact simulation algorithm for real valued Brownian diffusions whose drift admits a finite number of jumps. The method is based on the retrospective rejection sampling scheme introduced in [9] (in the case of regular coefficient) and generalized to coefficients with one finite jump in [20, 48]. We propose here a non trivial extension of this algorithm in the case where the drift admits several jumps. We treat explicitly and extensively the case of two jumps, providing numerical simulations. Our main contribution is to manage the technical difficulty due to the presence of *two* jumps thanks to the new explicit expression of the transition density of the skew Brownian motion with two semipermeable barriers and a constant drift proved in Chapter 2. We provide the pseudo-code of the retrospective rejection sampling. The content of this chapter is the object of a submitted preprint [15].

3.1 The framework

The aim of this chapter is to develop an exact simulation method for the following real-valued Brownian diffusion

$$\begin{cases} dX_t = dW_t + b(X_t)dt, & t \in [0,T],\ T < \infty \\ X_0 = x_0 & x_0 \in \mathbb{R}, \end{cases} \tag{3.1.1}$$

where the drift function b is a bounded regular map on $\mathbb{R}$ except on a finite set $J := \{z_1, \dots, z_n\} \subset \mathbb{R}$ where jumps occur.

The existence and uniqueness of $\mathbb{P}_b$, the weak solution of (3.1.1), is straightforward because the coefficients of the equation are measurable and bounded (Varadhan and Strook in [58]). Moreover the strong existence and uniqueness holds as well by Zvonkin and Yamada-Watanabe results (see [72, 66]) indeed pathwise uniqueness holds because the unit drift coefficient trivially satisfies the assumption (c) of Theorem 1.3 in Le Gall [32].
See also the results of Ariasova and Pilipenko (Theorem 1.1 in [6]) on strong existence and uniqueness of solutions for irregular drift b.

Beskos, Papaspiliopoulos and Roberts in [10, 8, 9] propose algorithms for simulating exactly the solution of (3.1.1) in the case where the drift b is regular everywhere. The method has been recently improved first by Étoré and Martinez [20] and then by Papaspiliopoulos, Roberts and Taylor [48, 62], in case of a drift with a unique jump ($n = 1$). We provide here a generalization of these results, proposing a theoretical exact simulation scheme in the case of a drift with *several jumps* ($n > 1$) and treating explicitly the case of two discontinuities ($n = 2$).

Our approach is inspired by the one in [20], and is based on the explicit representation of the transition density of a skew Brownian motion with constant drift and two semipermeable barriers (see Theorem 2.3.7).

3.1.1 The measures involved: definitions and notations

Consider $\mathcal{C} := \mathcal{C}([0,T],\mathbb{R})$ the canonical continuous path space and $\mathscr{C}$ the Borel σ-algebra on $\mathcal{C}$ induced by the supremum norm.

Let us fix $x_0 \in \mathbb{R}$ and denote by $\mathbb{P}$ the Wiener measure on $(\mathcal{C},\mathscr{C})$, law of a Brownian motion $(W_t)_t$ starting from x_0. $(X_t)_t$ always denotes the canonical process.

Let us introduce the various measures which are involved in this chapter.

- $\mathbb{P}_b$ denotes the law of the Brownian motion with drift b, weak solution of (3.1.1).
- For $0 \neq |\beta| \leq 1$ let $\mathbb{P}^{(\beta)}$ denote the law of the (β)-skew Brownian motion (SBM), solution of the stochastic differential equation (1.1.1).
- $\mathbb{P}_b^{(\beta)}$ will denote the law of the (β)-skew Brownian motion with drift b.
- Analogously $\mathbb{P}^{(\beta_1,\beta_2)}$ (respectively $\mathbb{P}_b^{(\beta_1,\beta_2)}$) is the law of the $(\beta_1,\beta_2)-$skew Brownian motion with two semipermeable barriers at z_1 and z_2, $z_1 < z_2$, (resp. with drift b).

The two-SBM is a particular case of the multi-SBM, whose law is denoted by $\mathbb{P}^{(\beta_1,\dots,\beta_n)}$. Let $J = \{z_1,\dots,z_n\}$ be an ordered set of n barriers (or jumps) with respective skewness coefficient $\beta_1,\cdots,\beta_n \in [-1,1]$. The law of the $(\beta_1,\dots,\beta_n)-$SBM with drift b, $\mathbb{P}_b^{(\beta_1,\dots,\beta_n)}$, is the weak solution of the following equation:

$$\begin{cases} X_t = X_0 + W_t + \displaystyle\int_0^t b(X_s)\,ds + \sum_{j=1}^{n} \beta_j L_t^{z_j}(X) \\ L_t^{z_j}(X) = \int_0^t \mathbb{1}_{\{X_s = z_j\}}\, dL_s^{z_j}, \quad j \in \{1,\cdots,n\} \end{cases} . \tag{3.1.2}$$

In conclusion we can arrange the above measures in a simple diagram:

$$\begin{array}{ccccccc} & & \text{skew } \beta_1 & & \text{more barriers} & & \\ \mathbb{P} & \longrightarrow & \mathbb{P}^{(\beta_1)} & \dots\longrightarrow\dots & \mathbb{P}^{(\beta_1,\dots,\beta_n)} & & \\ \text{drift } b \downarrow & & \downarrow & & \downarrow & & \text{drift } b \\ \mathbb{P}_b & \longrightarrow & \mathbb{P}_b{}^{(\beta_1)} & \dots\longrightarrow\dots & \mathbb{P}_b{}^{(\beta_1,\dots,\beta_n)}. & & \end{array}$$

3.1.2 Useful theorems

We are going to introduce here the Itô-Tanaka formula (see for example Kallenberg [28], theorem 22.5 for the statement and page 588 for the history of the result) and the occupation time formula (Meyer [43] and Wang [65]).

Occupation time formula

Let X be a continuous real-valued semimartingale. Almost surely for all functions f positive and Borel measurable,

$$\int_0^t f(X_s)\, d\langle X\rangle_s = \int_{\mathbb{R}} f(w)\, L_t^w(X)\, dw,$$

where $s \mapsto \langle X\rangle_s$ is the quadratic variation of the process.

The Itô-Tanaka formula

Let X be a continuous semimartingale with symmetric local time in y at time t, $L_t^y(X)$. Let $B : \mathbb{R} \to \mathbb{R}$ be difference of two convex functions, then

$$B(X_T) - B(X_0) = \int_0^T \frac{B'(X_t^+) + B'(X_t^-)}{2} dX_t + \frac{1}{2} \int_{\mathbb{R}} L_t^y(X) \mu_B(dy).$$

where $x \mapsto B'(x^-)$ (resp. $B'(x^+)$) is the left (resp. right) derivative of B, and μ_B is the measure defined by

$$\int_{\mathbb{R}} g(x) \mu_B(dx) = -\int_{\mathbb{R}} g'(x) \frac{1}{2} \left(B'(x^+) + B'(x^-) \right) dx \text{ for all } g \in \mathcal{C}_c^1(\mathbb{R}).$$

Let us check that this formula can be applied to the primitive of b, $B(x) := \int_0^x b(y)dy$. If b is of bounded variation on $\mathbb{R}$, then the primitive is well defined (since b is locally integrable) and it is indeed the difference of two convex functions.

Application to a particular case

Let us assume that b is a function of bounded variation that has a jump in z equal to 2θ but elsewhere it is continuous and has continuous derivative which admits a left and right limit at z. Let B be the primitive of b, then the measure μ_B is the measure

$$\mu_B(dw) = \mathbb{1}_{\{w \neq z\}} b'(w)\, dw + 2\theta\, \delta_z\,(dw).$$

The Itô-Tanaka formula yields

$$\begin{aligned} B(X_T) - B(X_0) &= \int_0^T \frac{1}{2} \left(B'(X_t^+) + B'(X_t^-) \right) dX_t + \frac{1}{2} \int_{\mathbb{R}} L_T^w(X) \mathbb{1}_{\{w \neq z\}} B''(w) dw \\ &\quad + \int_{\mathbb{R}} L_T^w(X) \frac{B'(z^+) - B'(z^-)}{2} \delta_z(dw) \\ &= \int_0^T \frac{1}{2} \left(b(X_t^+) + b(X_t^-) \right) dX_t + \frac{1}{2} \int_0^T b'(X_t) d\langle X \rangle_t + \theta\, L_T^z(X), \end{aligned}$$

where we recall $\theta := \dfrac{b(z^+) - b(z^-)}{2}$ is half of the jump height. In the last equality the second term is due to the *occupation time formula* and the third term comes from the continuity of b on $\mathbb{R} \setminus \{z\}$.
Let us define the function b and b' on the discontinuity as follows:

$$b(z) := \frac{1}{2} \left(b(z^+) + b(z^-) \right) \qquad b'(z) := \frac{1}{2} \left(b'(z^+) + b'(z^-) \right).$$

Let us explicit the Itô-Tanaka formula in two special cases.

Example 3.1.1. *Under $\mathbb{P}_\mu$, the law of the Brownian motion with constant drift μ, one has*

$$B(X_T) - B(X_0) = \int_0^T b(X_t) dW_t + \int_0^T b(X_t) \mu dt + \frac{1}{2} \int_0^T b'(X_t) dt + \theta\, L_T^z(X).$$

Example 3.1.2. *Under $\mathbb{P}_\mu^{(\beta)}$, the law of the (β)-skew Brownian diffusion with drift μ, one has*

$$B(X_T) - B(X_0) = \int_0^T b(X_t) dW_t + \int_0^T b(X_t) \mu dt + \frac{1}{2} \int_0^T b'(X_t) dt + (\theta + \beta\, b(z))\, L_T^z(X).$$

3.1.3 Assumptions on the drift

Let us now spell out the assumptions on the drift b in order to apply the exact algorithm.
Let J be the set $\{z_1 < \ldots < z_n\}$. Let b be a function, continous on $\mathbb{R} \setminus J$ of bounded variation on $\mathbb{R}$ and whose weak derivative is bounded, continuous on $\mathbb{R} \setminus J$ and admits left and right limits at every point of J. So there exist left and right derivative $\partial_\pm b(z_j)$ for $j = 1, \ldots, n$.
At each of the n discontinuity points $z_1, \ldots, z_n \in J$, b admits a jump with (half) height $(\theta_j)_{j=1,\ldots,n}$ defined by

$$\theta_j = \frac{b(z_j^+) - b(z_j^-)}{2}. \tag{3.1.3}$$

Since only the left and right limit values $b(z_i^-)$ and $b(z_i^+)$ (and not $b(z_i)$) do matter, for simplicity, we define the function b at each point z_i as the average value

$$b(z_i) := \frac{b(z_i^+) + b(z_i^-)}{2}, \quad z_i \in J. \tag{3.1.4}$$

Similarly, at the points of discontinuity, b' can be arbitrarily defined for example as

$$b'(z_i) := \frac{\partial_+ b(z_i) + \partial_- b(z_i)}{2}, \quad z_i \in J.$$

The primitive of b, $B(y) := \int_0^y b(w)\, dw$, is well defined since b is locally integrable (because bounded) and it is the difference of convex functions because b has bounded variation on $\mathbb{R}$. Therefore one can apply the Itô-Tanaka formula recalled before.
The boundedness of b and b' comes from the fact that we need $\frac{1}{2}\left(b^2 + b'\right)$ to be bounded. Moreover, since b is bounded, one can apply Girsanov Theorem.

3.2 Existing results for drifts admitting a unique jump

In this section we first recall the general retrospective rejection sampling scheme. Then we introduce the difficulties arising in case of a drift admitting one or more jumps. We finally propose two different solutions contained in the literature in the one-jump-case, and we discuss the possibility to extend them to the case of several discontinuities. Our main contribution is the extension, which is the object of Section 3.4

3.2.1 Retrospective rejection sampling scheme

We now recall briefly the main idea introduced in [10] which allows to *simulate exactly* the law of the diffusion $\mathbb{P}_b$ on the canonical continuous path space $\mathcal{C}$. The first key point is the following:

There should exist another probability measure $\mathfrak{Q}$ on $\mathcal{C}$, called instrumental measure, such that

- it is known how to sample from $\mathfrak{Q}$ (actually from its finite-dimensional distributions)
- $\mathbb{P}_b$ is absolutely continuous with respect to this instrumental probability measure and

$$\mathbb{P}_b(dX) \propto e^{-\Phi_b(X)}\, \mathfrak{Q}(dX) \text{ where } \Phi_b(X) := \int_0^T \phi_b^+(X_t)\, dt. \tag{3.2.1}$$

In other words, the log-density of $\mathbb{P}_b$ with respect to $\mathfrak{Q}$ has the form of an additive functional, whose integrand ϕ_b^+ is supposed to be positive and bounded (on $\mathbb{R} \setminus J$ in our framework). The proportionality sign $\propto$ indicates that there might be a renormalizing constant.
Once one has found an instrumental measure, it is possible to construct a rejection sampling scheme according to Proposition 1 in [10] and Theorem 1 in [8]: given a sample path ω from the instrumental

measure, one needs an event A with conditional probability with respect to ω equal to the Radon-Nikodym derivative $e^{-\Phi_b(\omega)}$. Then one accepts or rejects ω as a sample from the target measure depending on whether the event $A|\omega$ is satisfied or not.
In fact the desired event A is obtained as follows: let Ψ be an homogeneous Poisson point process of unit intensity on the rectangle $[0,T]\times[0,\|\phi_b^+\|_\infty]$, then one sets

$$A = \{\textit{all points of } \Psi \textit{ are above the graph of } t \mapsto \phi_b^+(\omega_t)\}.$$

The resulting procedure to accept a given path is called *retrospective* rejection method:

- First realize the random Poisson field Ψ, which yields M points
$$(\tau_1, x_1), \dots, (\tau_M, x_M) \in [0,T]\times[0,\|\phi_b^+\|_\infty].$$
- Then, for each time τ_j, sample X_{τ_j} under the law $\mathfrak{Q}$.
- Finally check if there is some point (τ_j, x_j) satisfying $x_j < \phi_b^+(X_{\tau_j})$. If this is not the case, accept $(\tau_j, x_j)_{j=1,\dots,M}$, else start again.

The algorithm returns a skeleton of a path $(X_t(\omega))_{t\in[0,T]}$ under $\mathbb{P}_b$: $\left(X_{\tau_1}(\omega), X_{\tau_2}(\omega), \dots, X_{\tau_M}(\omega), X_T(\omega)\right)$. The skeleton can be enlarged/completed adding the position of the process at any intermediary time $t\in[0,T]$, following a bridge dynamics. The pseudocode of this method is similar to Algorithm 2 in Section 3.5.2.
In conclusion, the main issue is to find in our context the appropriate instrumental measure $\mathfrak{Q}$ and the appropriate functional Φ_b to apply the retrospective rejection sampling scheme.

3.2.2 Looking for the instrumental measure $\mathfrak{Q}$

In the context of Brownian motion with drift admitting jumps, it is quite natural to apply Girsanov theorem, the Itô Tanaka-Formula and the occupation time formula to find an instrumental measure. One can proceed as follows:

Step 1. Apply Girsanov theorem to obtain the Radon-Nikodym derivative of $\mathbb{P}_b$ with respect to $\mathbb{P}$:

$$\mathbb{P}_b(dX) = \exp\Big(\int_0^T b(X_t)dX_t - \frac{1}{2}\int_0^T b^2(X_t)dt\Big)\mathbb{P}(dX).$$

To replace the Itô stochastic integral $\displaystyle\int_0^T b(X_t)dX_t$ by a Stieltjes one, introduce the function

$$B(x) := \int_0^x b(y)dy,$$

primitive of b, and apply the Itô-Tanaka formula (see Example 3.1.2)

$$B(X_T) - B(X_0) = \int_0^T \frac{b(X_t^+) + b(X_t^-)}{2}dX_t + \frac{1}{2}\int_{\mathbb{R}\setminus J} L_t^x(X)b'(x)dx + \sum_{j=1}^n \theta_j L_T^{z_j}(X)$$

where L_t^y is the symmetric local time in y at time t and $\theta_j, j=1,\cdots,n$, is the (half) $j-th$ jump height of b given by (3.1.3).

Step 2. Thanks to the occupation time formula, obtain the decomposition (3.2.1)

$$\mathbb{P}_b(dX) \propto \exp\left(-\Phi_b(X)\right) \underbrace{\exp\left(B(X_T) - B(X_0) - \sum_{j=1}^n \theta_j L_T^{z_j}(X)\right)\mathbb{P}(dX)}_{\propto\, \mathfrak{Q}(dX)}$$

where $\Phi_b(X) := \int_0^T \phi_b^+(X_t)\,dt$ with

$$\phi_b^+(x) := \frac{1}{2}\left(b^2(x) + b'(x) - \inf_{y\in\mathbb{R}\setminus J}\left(b^2(y) + b'(y)\right)\right). \tag{3.2.2}$$

In conclusion,

The instrumental measure is

$$\mathfrak{Q}(dX) \propto \exp\left(B(X_T) - B(X_0) - \sum_{j=1}^{n}\theta_j L_T^{z_j}(X)\right)\mathbb{P}(dX). \tag{3.2.3}$$

In the case of one discontinuity ($n = 1$), in the literature there are two possible approaches to sample from the finite-dimensional distributions of $\mathfrak{Q}$. We briefly illustrate them in the next two sections.

3.2.3 Sampling via a convergence of schemes for skew Brownian motions

In this section we summarize the ideas presented in Étoré and Martinez's publications [19, 20].

Let $\mathfrak{Q}$ be defined by (3.2.3). The canonical process X under this law, is a Brownian motion conditioned on $(X_T, L_T^0(X)) \sim h(y,\ell)dyd\ell$ with

$$h(y,\ell)dy\,d\ell \propto \exp\left(B(y) - B(x) - \theta\ell\right)\mathbb{P}(X_T \in dy, L_T^0(X) \in d\ell). \tag{3.2.4}$$

Since it is difficult to sample from the joint density of $(X_T, L_T^0(X))$ and the density of the joint bridges, the authors observe that one just needs to sample X_T under $\mathfrak{Q}$. Therefore they use a limit argument to provide the finite-dimensional distributions and sample under the measure $\mathfrak{Q}$. This approach is based on the following key points:

- There is weak convergence of a sequence of $\mathbb{P}_b^{(1/n)}$ towards $\mathbb{P}_b$ (see Theorem 3.1 in Le Gall [32]).
- It is possible to apply the retrospective rejection sampling method for the one-skew with discontinuous drift b: let $\beta \in [-1,1]$ there exists an instrumental law $\mathfrak{Q}^{(\beta)}$ such that it is easy to sample from its finite-dimensional distributions and
$$\mathbb{P}_b^{(\beta)}(dX) \propto e^{-\Phi_b(X)}\mathfrak{Q}^{(\beta)}(dX).$$
- The weak convergence implies convergence of the instrumental measure and of the exact algorithms to a limit algorithm which is exact as well.

We follow this approach and we show that the same limit argument is possible even if the drift admits several discontinuities, and it is not necessary to provide an exact simulation for any multi-SBM (see Section 3.3).
In addition we provide a parallel method to sample from the finite-dimensional distribution of the instrumental measure $\mathfrak{Q}$ (3.2.3).

3.2.4 Sampling from the joint distribution of Brownian motions and its local times

Papaspiliopoulos, Roberts and Taylor in [48] (extracted from Taylor PhD's thesis [62]) sample from $\mathfrak{Q}$ using the explicit expression of some conditional laws of the Brownian motion and its symmetric local time at *one* point.
$\mathfrak{Q}$ is interpreted as the law of the "local time tilted biased Wiener process". This is a disintegration of the

Brownian motion $\mathbb{P}$ conditioned at its marginals at the initial time $t = 0$ and at the final time T.
Their approach has two crucial steps: first simulating from the bivariate distribution at time T of the path and its local time $(X_T, L_T^0(X))$ and second sampling X_{t_i} and $L_{t_i}^0(X)$ at a finite number of times $(t_i)_{i=1,\dots,M}$ conditioning on $(X_0, 0)$ and $(X_T, L_T^0(X))$.
For (X_T, L_T^0) they jointly simulate if the unique jump θ is negative, else they decompose the joint law as the marginal of X_T and the conditional law of $L_T^0|X_T$. The latter approach is based on the observation that (3.2.4) can be interpreted as the joint distribution of the Brownian motion and its local time biased by the terms $e^{B(X_T)}$ and $e^{-\theta L_T^0(X)}$.
The authors need then to sample from the conditional laws of

$$(L_t^0(X)|X_s, X_t, L_s^0(X)) \text{ and of } (X_t, L_t^0(X)|X_s, X_u, L_s^0(X), L_u^0(X))$$

where $0 \leq s < t < u \leq T$. We refer to sections 2.1-2.4 of [48] for the explicit densities.

According to us this approach is not generalizable to the case of a drift with several discontinuities because the joint distribution of the Brownian motion and its local times at several points is not explicit. It seems quite complicated to obtain and probably difficult to handle as well.

3.3 On the way: the exact simulation scheme of a multi-skew Brownian diffusion whose drift admits jumps

The goal of the chapter is to provide an exact simulation of the brownian motion with drift b admitting a finite number of jumps, whose law is denoted by $\mathbb{P}_b$. Up to now we have found a measure $\mathfrak{Q}$, given by (3.2.3) such that the factorization (3.2.1) holds. This is the framework in which we can apply the retrospective rejection sampling scheme presented in Section 3.2.1. If one can sample from the finite-dimensional distribution of $\mathfrak{Q}$, then one has provided the desired exact simulation scheme for $\mathbb{P}_b$.

As announced we generalize the scheme presented in Section 3.2.3. We notice that we can provide the exact simulation of $\mathbb{P}_b$ by finding an exact simulation scheme for the multi-skew Brownian motion, of law $\mathbb{P}_b^{(\beta_1,\dots,\beta_n)}$, with *small* skewness parameters $(\beta_j)_{j=1,\dots,n}$ and then using a limit argument.
In fact we are able to find $\beta_1, \dots, \beta_n \in [-1, 1]$ (Lemma 3.3.1) which allow to develop the scheme presented in Section 3.2.1

1. there exists an instrumental measure $\mathfrak{Q}^{(\beta_1,\dots,\beta_n)}$ such that

$$\mathbb{P}_b^{(\beta_1,\dots,\beta_n)}(dX) \propto \exp\left(-\Phi_b(X)\right) \mathfrak{Q}^{(\beta_1,\dots,\beta_n)}(dX)$$

   where $\mathbb{P}_b^{(\beta_1,\dots,\beta_n)}$ is the law of the multi-SBM with drift defined by (3.1.2);

2. the weak convergence of $\mathbb{P}_b^{(\beta_1,\dots,\beta_n)}$ to the law of the Brownian motion with drift $\mathbb{P}_b$, when the β_j's tend to 0, implies the weak convergence of the instrumental measures $\mathfrak{Q}^{(\beta_1,\dots,\beta_n)}$ to $\mathfrak{Q}$ (see Lemma 3.4.1);

3. the exact simulation scheme *propagates* at the limit:

$$\begin{array}{ccccc} \mathbb{P}_b^{(\beta_1,\dots,\beta_n)}(dX) & \propto & \exp\left(-\Phi_b(X)\right) & \mathfrak{Q}^{(\beta_1,\dots,\beta_n)}(dX) & \\ \beta_j \to 0 \quad \downarrow & & & \downarrow & \beta_j \to 0 \\ \mathbb{P}_b(dX) & \propto & \exp\left(-\Phi_b(X)\right) & \mathfrak{Q}(dX) & \end{array} \tag{3.3.1}$$

   and the previous limit result provide also a method for sampling from the finite-dimensional distribution of $\mathfrak{Q}$. See Section 3.4.1 for the explanation and Section 3.4.4 for the simulation method.

Let us now present the retrospective rejection sampling scheme for the multi-SBM with drift b (i.e. the point 1 of this list).

3.3.1 The instrumental measure

One knows by Girsanov theorem, and Itô-Tanaka formula, that

$$\mathbb{P}_b^{(\beta_1,\dots,\beta_n)}(dX) \propto \exp\left(-\Phi_b(X)\right) \exp\left(B(X_T) - B(X_0) - \sum_{j=1}^{n} \beta_j C_{\beta_j} L_T^{z_j}(X)\right) \mathbb{P}^{(\beta_1,\dots,\beta_n)}(dX), \tag{3.3.2}$$

where $C_{\beta_j} = b(z_j) + \frac{\theta_j}{\beta_j}$, and $b(z_j)$ is defined in (3.1.4).
Except for the precise values $\beta_j = -\frac{\theta_j}{b(z_j)}, j = 1,\dots,n$ for which $C_{\beta_j} = 0$, the local time terms in (3.3.2) do not vanish, which makes the simulation hard. One can get around this difficulty choosing the coefficients β_j and a real number μ such that

$$\mathbb{P}_b^{(\beta_1,\dots,\beta_n)}(dX) \propto \exp\left(-\Phi_b(X)\right) \underbrace{\exp\left(B^{(\mu)}(X_T) - B^{(\mu)}(X_0)\right) \mathbb{P}_\mu^{(\beta_1,\dots,\beta_n)}(dX)}_{\propto\, \mathfrak{Q}^{(\beta_1,\dots,\beta_n)}(dX)}, \tag{3.3.3}$$

where $B^{(\mu)}(x) := B(x) - \mu x$ is a primitive of $b - \mu$. Indeed, for our purpose, we are free to let the coefficients $(\beta_j)_{j=2,\dots,n}$ depend from β_1, as long as $\lim_{\beta_1 \to 0} \beta_j = 0$ for $j = 2,\dots,n$.

Thus, knowing how to sample under the measure $\mathfrak{Q}^{(\beta_1,\dots,\beta_n)}$, it would be possible to simulate exactly $\mathbb{P}_b^{(\beta_1,\dots,\beta_n)}$ following the retrospective rejection sampling method described in Section 3.2.1.

In the next lemma, we show how to choose $\beta_1,\dots,\beta_n \in [-1,1]$ and $\mu \in \mathbb{R}$ in such a way that identity (3.3.3) holds.

Lemma 3.3.1. *The representation* (3.3.3) *holds as soon as the skewness parameters and the constant* μ *satisfy*

$$\beta_j = \beta_1 \frac{\theta_j}{\theta_1 + \beta_1\big(b(z_1) - b(z_j)\big)}, j = 2,\dots,n, \quad \text{and} \quad \mu = b(z_1) + \frac{\theta_1}{\beta_1}. \tag{3.3.4}$$

Proof. Girsanov theorem yields

$$\mathbb{P}_b^{(\beta_1,\dots,\beta_n)}(dX) \propto \exp\left(B^{(\mu)}(X_T) - B^{(\mu)}(X_0) - \Phi_b(X) - \sum_{j=1}^{n} \beta_j \Big(C_{\beta_j} - \mu\Big) L_T^{z_j}(X)\right) \mathbb{P}_\mu^{(\beta_1,\dots,\beta_n)}(dX).$$

To erase the coefficients in front of the local times, it is sufficient to set $\mu = C_{\beta_1} = \cdots = C_{\beta_n}$, which leads to the identities (3.3.4). □

Remark 3.3.2. Notice that, for the choice of $\beta_1,\dots,\beta_n$ and μ in Lemma 3.3.1, since $\beta_j\mu = b(z_j)\beta_j + \theta_j$ one has $\lim_{\beta_1\to 0} \beta_j\mu = \theta_j$ and also $\lim_{\beta_1\to 0} \beta_j = 0$ for any $j = 2,\dots,n$. The latter limit will be very useful in what follows.

Remark 3.3.3. Choosing appropriately a *piecewise constant* function μ, one can obtain the identity (3.3.3) for any choice of $\beta_1,\dots,\beta_n \subset [-1,1]$ not necessarily small. If all C_j's either vanish or are equal to an unique constant C, one considers the constant drift $\mu = C$. Otherwise assume there exist at least two indices j_1, j_2 such that $C_{\beta_{j_1}} \neq C_{\beta_{j_2}}$ and both do not vanish. One then defines the piecewise constant function $\mu = \sum_{j=1}^{n-1} C_{\beta_j} \mathbb{1}_{[z_j, z_{j+1})} + C_{\beta_n} \mathbb{1}_{[z_n,\infty)}$. In this case a retrospective rejection sampling for $\mathbb{P}_b^{(\beta_1,\dots,\beta_n)}$ is possible as soon as an explicit expression for the transition density of the skew Brownian motion with piecewise constant drift is known (see Section 1.4 or Chapter 4).

3.3.2 Simulation of $\mathfrak{Q}^{(\beta_1,\dots,\beta_n)}$

The simulation of $\mathfrak{Q}^{(\beta_1,\dots,\beta_n)}(dX)$, consist in sampling from the finite-dimensional marginals, i.e. giving a finite number of sample variates - called skeleton $(X(t_1),\dots,X(t_M),X_T)=(y_1,\dots,y_M,y)$ - from the density

$$h^{(\beta_1,\dots,\beta_n)}(y)\prod_{i=0}^{M-1} q_\mu^{(\beta_1,\beta_2,\dots,\beta_n)}(t_{i+1}-t_i,T-t_i,y_i,y,y_{i+1})dy_1\dots dy_M dy, \tag{3.3.5}$$

where $t_0:=0$, $y_0:=X_0=x_0$ and $q_\mu^{(\beta_1,\dots,\beta_n)}$ is the transition density of the bridge of $\mathbb{P}_\mu^{(\beta_1,\dots,\beta_n)}$. The density function $h^{(\beta_1,\dots,\beta_n)}(y)$ of the conditioned law of $X_T|X_0=x_0$ satisfies

$$h^{(\beta_1,\dots,\beta_n)}(y)\propto\exp\Big(B^{(\mu)}(y)-B^{(\mu)}(x_0)\Big)p_\mu^{(\beta_1,\dots,\beta_n)}(T,x_0,y),$$

where $p_\mu^{(\beta_1,\dots,\beta_n)}$ is the transition density of $\mathbb{P}_\mu^{(\beta_1,\dots,\beta_n)}$, as already introduced.
The relationship between $q_\mu^{(\beta_1,\dots,\beta_n)}$ and $p_\mu^{(\beta_1,\dots,\beta_n)}$ is, as usual for bridges of a Markov process, given by

$$q_\mu^{(\beta_1,\dots,\beta_n)}(t,T,x_1,x_2,y)=\frac{p_\mu^{(\beta_1,\dots,\beta_n)}(t,x_1,y)\;p_\mu^{(\beta_1,\dots,\beta_n)}(T-t,y,x_2)}{p_\mu^{(\beta_1,\dots,\beta_n)}(T,x_1,x_2)}.$$

Let us write for simplicity p_μ instead of $p_\mu^{(0,\cdots,0)}$ (resp. q_μ instead of $q_\mu^{(0,\cdots,0)}$) for the transition density of a Brownian motion with constant drift μ (resp. for the transition density of a Brownian bridge with constant drift μ). Recall also that in fact q_μ does not depend on the drift μ and is equal to q_0, the transition density of the Brownian bridge.

The challenge is therefore

- to obtain an explicit expression for the transition density $p_\mu^{(\beta_1,\dots,\beta_n)}$ involving an instrumental density from which it is known how to sample, namely p_μ the transition density of the Brownian motion with drift μ

$$p_\mu^{(\beta_1,\dots,\beta_n)}(t,x,y)=p_\mu(t,x,y)\;v_\mu^{(\beta_1,\dots,\beta_n)}(t,x,y). \tag{3.3.6}$$

- to bound uniformly the function $(x,y)\mapsto v_\mu^{(\beta_1,\dots,\beta_n)}(t,x,y)$.

In the case $n=2$ these facts are rigorously proved in Theorem 2.3.7 and Proposition 2.5.3. In Chapter 4 we discuss about the adaptability of this method to the case $n\geq 3$.
We assume these facts for $n\geq 2$ in the remainder of the section. Hence the densities involved in (3.3.5) are given by

$$q_\mu^{(\beta_1,\dots,\beta_n)}(t,T,x_1,x_2,y)=q_0(t,T,x_1,x_2,y)\frac{v_\mu^{(\beta_1,\dots,\beta_n)}(t,x_1,y)v_\mu^{(\beta_1,\dots,\beta_n)}(T-t,y,x_2)}{v_\mu^{(\beta_1,\dots,\beta_n)}(T,x_1,x_2)}, \tag{3.3.7}$$

$$\text{and}\quad h^{(\beta_1,\dots,\beta_n)}(y)\propto\exp\Big(B^{(\mu)}(y)-B^{(\mu)}(x_0)\Big)\;p_\mu(T,x_0,y)\;v_\mu^{(\beta_1,\dots,\beta_n)}(T,x_0,y).$$

One may then apply the generalized rejection sampling method thanks to the uniform boundedness of the function $v_\mu^{(\beta_1,\dots,\beta_n)}$. This important property also implies the integrability of $h^{(\beta_1,\dots,\beta_n)}$, as we prove in the next lemma.

Lemma 3.3.4. *Let $x_0\in\mathbb{R}$. Under our assumptions on the drift b, for any choice of $\beta_1,\dots,\beta_n\in[-1,1]$ and $\mu\in\mathbb{R}$, the density function $y\mapsto h^{(\beta_1,\dots,\beta_n)}(y)$ is integrable and therefore normalizable.*

Proof. The density $h^{(\beta_1,\dots,\beta_n)}(y)$ satisfies

$$h^{(\beta_1,\dots,\beta_n)}(y) \propto e^{B(y)-B(x_0)}\ p_0(T,x_0,y)\ v_\mu^{(\beta_1,\dots,\beta_n)}(T,x_0,y). \tag{3.3.8}$$

Since b is bounded, its primitive B satisfies $B(y)-B(x_0)\le \|b\|_\infty |y-x_0|$. We have

$$\begin{aligned}\int_{\mathbb{R}} e^{B(y)-B(x)}\ p_0(T,x,y)\ v_\mu^{(\beta_1,\dots,\beta_n)}(T,x,y)\ dy &\le \frac{\|v_\mu^{(\beta_1,\dots,\beta_n)}(T,x_0,\cdot)\|_\infty}{\sqrt{2\pi T}}\int_{\mathbb{R}} e^{\|b\|_\infty|y-x_0|}\ e^{-\frac{(y-x_0)^2}{2T}}\ dy\\ &= \|v_\mu^{(\beta_1,\dots,\beta_n)}(T,x_0,\cdot)\|_\infty\ e^{\frac{\|b\|_\infty^2}{2}T}.\end{aligned}$$

The integrability follows. □

Notice the reformulation (3.3.8) of the definition of $h^{(\beta_1,\dots,\beta_n)}$, which depends on μ only through $v_\mu{}^{(\beta_1,\dots,\beta_n)}$.

3.4 A drift with two or more jumps: exact simulation scheme for the associated Brownian diffusion

3.4.1 The exact simulation scheme of $\mathbb{P}_b$ as a limit scheme

In the entire section, we correlate the parameters $(\beta_j)_{j=1,\dots,n}$ and μ as in Lemma 3.3.1. The following convergence result provides a method for sampling under the measure $\mathfrak{Q}$, once $p_\mu^{(\beta_1,\dots,\beta_n)}$ is made explicit and uniformly bounded. This result yields the completion of the simulation scheme for $\mathbb{P}_b$.

Lemma 3.4.1. *Take $\beta_1=\frac{1}{\kappa}$ and define the other skewness parameters $\beta_j(\kappa), j=2,\dots,n$, by the relationship* (3.3.4)*: $\beta_j(\kappa)=\dfrac{\theta_j}{\kappa\theta_1+b(z_1)-b(z_j)}$ and $\mu(\kappa)=b(z_1)+\kappa\theta_1$. Then*

$$\mathbb{P}_b^{\left(\frac{1}{\kappa},\beta_2(\kappa),\dots,\beta_n(\kappa)\right)} \underset{\kappa\to\infty}{\longrightarrow} \mathbb{P}_b \quad \text{and} \quad \mathfrak{Q}^{\left(\frac{1}{\kappa},\beta_2(\kappa),\dots,\beta_n(\kappa)\right)} \underset{\kappa\to\infty}{\longrightarrow} \mathfrak{Q},$$

where the convergences hold in the weak topology.

Proof. First notice that even a stronger convergence holds in the following sense: If Y is the strong solution of equation (3.1.1) and $Y^{(\kappa)},\kappa\ge 1$, is the strong solution of equation (3.1.2) with skewness coefficients $\beta_1=\frac{1}{\kappa},\beta_2(\kappa),\cdots,\beta_n(\kappa)$, then the sequence $(Y^{(\kappa)})_\kappa$ converges in $L^1(\mathcal{C})$ to Y:

$$\lim_{\kappa\to\infty}\mathbb{E}\Big(\sup_{s\in[0,T]}|Y_s^{(\kappa)}-Y_s|\Big)=0.$$

This is due to Theorem 3.1 in [32], slightly extended in Theorem 5.1 in [20]. Strong convergence then implies the weak convergence of $(\mathbb{P}_b^{\left(\frac{1}{\kappa},\beta_2(\kappa),\dots,\beta_n(\kappa)\right)})_\kappa$ towards $\mathbb{P}_b$.
The weak convergence of the sequence $\mathfrak{Q}^{\left(\frac{1}{\kappa},\beta_2(\kappa),\dots,\beta_n(\kappa)\right)}$ is straightforward once one has noticed that the function defined on $\mathcal{C}$ by $X\mapsto\exp\left(\Phi_b(X)\right)$ is bounded and continuous in the topology of the sup-norm. □

As an immediate consequence one obtains the desired relationship (3.2.1), see the scheme 3.3.1. Therefore the retrospective rejection sampling for $\mathbb{P}_b$ is possible as soon as one can sample from $\mathfrak{Q}$. Moreover Lemma 3.4.1 yields also the sampling method for the instrumental measure $\mathfrak{Q}$. Indeed the weak convergence of $\mathfrak{Q}^{\left(\frac{1}{\kappa},\beta_2(\kappa),\dots,\beta_n(\kappa)\right)}$ ensures the convergence of the finite-dimensional distributions with density given by (3.3.5) to the finite-dimensional marginals of $\mathfrak{Q}$. And, if the sequences of density $(h^{\left(\frac{1}{\kappa},\beta_2(\kappa),\dots,\beta_n(\kappa)\right)})_\kappa$ and $(q^{\left(\frac{1}{\kappa},\beta_2(\kappa),\dots,\beta_n(\kappa)\right)}(t,T,x_1,x_2,\cdot))_\kappa$ admit pointwise limits $h^{(\theta_1,\dots,\theta_n)}$ and $q^{(\theta_1,\dots,\theta_n)}(t,T,x_1,x_2,\cdot)$ respectively (see (3.3.7) and (3.3.8)), then the limit of the expression (3.3.5) is given by

$$h^{(\theta_1,\dots,\theta_n)}(y)\prod_{i=0}^{M-1}q^{(\theta_1,\dots,\theta_n)}(t_{i+1}-t_i,T-t_i,y_i,y,y_{i+1})\,dy_1\dots dy_M dy. \tag{3.4.1}$$

Thanks to Scheffé's Lemma, one can easily conclude that (3.4.1) is the density of $(X_{t_1}, X_{t_2}, \dots, X_{t_M}, X_T)$ under $\mathfrak{Q}$.

We focus directly on the limits $h^{(\theta_1,\dots,\theta_n)}(y)dy$ and $q^{(\theta_1,\dots,\theta_n)}(t,T,x_1,x_2,y)dy$, providing a rejection sampling scheme for them with instrumental densities the transition density of the Brownian motion $p_0(\frac{T}{1-\delta}, x_0, y)$ (for some $\delta \in (0,1)$) and the transition density of the Brownian bridge $q_0(t,T,x_1,x_2,y)$ respectively.
It is necessary to find positive functions $f^{\mathcal{H}}_{\delta}$ and $f^{\mathcal{B}}_{x_1,x_2}$ smaller than 1 such that

$$\frac{h^{(\theta_1,\theta_2,\dots,\theta_n)}(y)}{p_0(\frac{T}{1-\delta}, x_0, y)} = C^{\mathcal{H}} \cdot f^{\mathcal{H}}_{\delta}(y), \quad \text{and } \frac{q^{(\theta_1,\theta_2,\dots,\theta_n)}(t,T,x_1,x_2,y)}{q_0(t,T,x_1,x_2,y)} = C^{\mathcal{B}} \cdot f^{\mathcal{B}}_{x_1,x_2}(y). \tag{3.4.2}$$

One introduces a parameter $\delta \in (0,1)$, for some reason that will be explained when we explicit the ratio $\frac{h^{(\theta_1,\theta_2,\dots,\theta_n)}(y)}{p_0(\frac{T}{1-\delta},x_0,y)}$, see (3.4.15). The normalizing constant $C^{\mathcal{H}}$ (resp. $C^{\mathcal{B}}$) depends only on the jumps $(\theta_1,\dots,\theta_n)$, the time T, the bound of the drift $\|b\|_\infty$, and δ (resp. on $(\theta_1,\dots,\theta_n), t,\ T,\ x_1,\ x_2$).

Assuming that the decomposition (3.3.6) holds and assuming that there exists a pointwise limit $v^{(\theta_1,\dots,\theta_n)}$ for $v^{(\frac{1}{\kappa},\beta_2(\kappa),\dots,\beta_n(\kappa))}_{\mu(\kappa)}$ when κ tends to ∞, one can pass to the limit in the equations (3.3.7 and 3.3.8) obtaining the relationships

$$\begin{aligned} q^{(\theta_1,\dots,\theta_n)}(t,T,x_1,x_2,y) &= q_0(t,T,x_1,x_2,y)\,\frac{v^{(\theta_1,\dots,\theta_n)}(t,x_1,y)v^{(\theta_1,\dots,\theta_n)}(T-t,y,x_2)}{v^{(\theta_1,\dots,\theta_n)}(T,x_1,x_2)}, \\ h^{(\theta_1,\dots,\theta_n)}(y) &\propto \exp\left(B(y)-B(x_0)\right)\, p_0(T,x_0,y)\, v^{(\theta_1,\dots,\theta_n)}(T,x_0,y). \end{aligned} \tag{3.4.3}$$

It is then sufficient to prove the existence of a uniform bound for $(x,y) \mapsto v^{(\theta_1,\dots,\theta_n)}(t,x,y)$ in order to develop the rejection sampling scheme from $h^{(\theta_1,\dots,\theta_n)}$ and $q^{(\theta_1,\dots,\theta_n)}$. Moreover this bound yields the integrability of $h^{(\theta_1,\dots,\theta_n)}$, analogously to Lemma 3.3.4.
In conclusion, Lemma 3.4.1 ensures that the exact simulation scheme for the skew Brownian motion with drift b is transposed to the desired exact simulation scheme for the Brownian diffusion with drift b.

3.4.2 The limit of the SBM

From now on we will consider the case of a drift with two discontinuities ($n=2$) at the points 0 and $z>0$, that is $J=\{0,z\}$. In this case the transition density of the (β_1,β_2)-SBM with drift μ admits the decomposition (3.3.6) (Theorem 2.3.7), and for any $t>0$ $(x,y) \mapsto v^{(\theta_1,\dots,\theta_n)}_{\mu}(t,x,y)$ is uniformly bounded (Proposition 2.5.3).

In fact we are mainly interested in the asymptotic regime for small skewness: κ large integer, $\beta_1 = \frac{1}{\kappa}$, $\beta_2(\kappa) = \frac{\theta_2}{\kappa\theta_1 + b(0) - b(z)}$ and $\mu(\kappa) = b(0) + \kappa\theta_1$ as in Lemma 3.4.1. Recall that $\lim_{\kappa\to\infty}\beta_2(\kappa) = 0$ and $\lim_{\kappa\to\infty}\beta_j(\kappa)\mu(\kappa) = \theta_j, j=1,2$ (see Remark 3.3.2).
The function $(t,x,y) \mapsto v^{(\beta_1,\dots,\beta_n)}_{\mu}(t,x,y)$ admits a pointwise limit $(t,x,y) \mapsto v^{(\theta_1,\theta_2)}(t,x,y)$ which is bounded from above uniformly on (x,y). This is the content of Proposition 3.4.2 and Proposition 3.4.3.

Let us define the polynomials $\tilde{c}_j(y;\xi) := \lim_{\kappa\to\infty} c_j(y,\mu(\kappa)\sqrt{t};\xi)$, $j=1,2,3,4$, where $c_j(y,\mu(\kappa)\sqrt{t};\xi)$ are given by (2.3.2). They satisfy

$$\begin{cases} \tilde{c}_1(y;\xi) = (\xi+\theta_1\sqrt{t})(\xi+\theta_2\sqrt{t}) \\ \tilde{c}_2(y;\xi) = -\theta_1\sqrt{t}\left(\xi - \left(2\mathbb{1}_{\{y>z\}}-1\right)\theta_2\sqrt{t}\right) \\ \tilde{c}_3(y;\xi) = -\theta_2\sqrt{t}\left(\xi + \left(2\mathbb{1}_{\{y>0\}}-1\right)\theta_1\sqrt{t}\right) \\ \tilde{c}_4(y;\xi) = -\left(1-2\mathbb{1}_{\{0\le y<z\}}\right)\theta_1\theta_2 t. \end{cases} \tag{3.4.4}$$

Their coefficients $\tilde{c}_{j,h}$, defined by the relationship $\tilde{c}_j(y;\xi) = \sum_{h=0}^{2}\tilde{c}_{j,2-h}(y)\xi^h$, satisfy

$$\begin{cases} \tilde{c}_{1,0}(y) = 1, \\ \tilde{c}_{2,0}(y) = 0 \\ \tilde{c}_{3,0}(y) = 0 \\ \tilde{c}_{4,0}(y) = 0 \end{cases}, \quad \begin{cases} \tilde{c}_{1,1}(y) = \theta_1\sqrt{t} + \theta_2\sqrt{t} \\ \tilde{c}_{2,1}(y) = -\theta_1\sqrt{t} \\ \tilde{c}_{3,1}(y) = -\theta_2\sqrt{t} \\ \tilde{c}_{4,1}(y) = 0 \end{cases}, \quad \begin{cases} \tilde{c}_{1,2}(y) = \theta_1\theta_2 t \\ \tilde{c}_{2,2}(y) = \left(2\mathbb{1}_{\{y\ge z\}}-1\right)\theta_1\theta_2 t \\ \tilde{c}_{3,2}(y) = -\left(2\mathbb{1}_{\{y>0\}}-1\right)\theta_1\theta_2 t \\ \tilde{c}_{4,2}(y) = -\left(1-2\mathbb{1}_{[0,z)}(y)\right)\theta_1\theta_2 t. \end{cases}$$

They are obtained as the limit for $\kappa \to \infty$ of $\mu(\kappa)^h\, c_{j,h}$, with $c_{j,h}$ given by (2.3.2). Finally, for any $\mathfrak{a}$, $\tilde{C}_{j,h}$ are defined, analogously to (2.3.3), by

$$\tilde{C}_{j,0} = \tilde{c}_{j,0}, \quad \tilde{C}_{j,1} = \tilde{c}_{j,1} + 2\tilde{c}_{j,0}\mathfrak{a}, \quad \tilde{C}_{j,2} = \tilde{c}_{j,2} + \tilde{c}_{j,1}\mathfrak{a} + \tilde{c}_{j,0}\mathfrak{a}^2, \quad j = 1,2,3,4. \tag{3.4.5}$$

Proposition 3.4.2. *Let $\theta_1, \theta_2 \in \mathbb{R}$. Let us denote by $v^{(\theta_1,\theta_2)}$ the pointwise limit for $\kappa \to \infty$ of the functions $(t,x,y) \mapsto v_{\mu(\kappa)}^{(1/\kappa,\beta_2(\kappa))}(t,x,y)$ defined by (2.3.10). Recall that $\omega_{j,k}$ is defined by (2.3.12) and $\tilde{c}_j$ by (3.4.4). Let $\mathfrak{a} \geq 0$ such that $\mathfrak{a} > \max(-2\theta_1, -2\theta_2)$. Then the following representation holds*

$$v^{(\theta_1,\theta_2)}(t,x,y) = \sum_{k=0}^{\infty} (-\theta_1\theta_2)^k t^k \sum_{j=1}^{4} \tilde{F}_{j,k}(\omega_{j,k}(x,y), \mathfrak{a}\sqrt{t}) \tag{3.4.6}$$

where $\tilde{F}_{j,k}$, which is actually a function of $(t,x,y,\mathfrak{a})$, satisfies

$$\tilde{F}_{j,k}(\omega_{j,k},\mathfrak{a}) = e^{\frac{1}{2}(\omega_{1,0}^2+\mathfrak{a}^2)} e^{-\mathfrak{a}\omega_{j,k}} \mathcal{F}\left(w \mapsto e^{-\frac{w^2}{2}} \tilde{c}_j(y; iw+\mathfrak{a}) \frac{-1}{(w-i\tilde{\mathfrak{a}}_1)^{k+1}(w-i\tilde{\mathfrak{a}}_2)^{k+1}} \right)(\omega_{j,k} - \mathfrak{a}) \tag{3.4.7}$$

where $\tilde{\mathfrak{a}}_{\mathfrak{i}} := \mathfrak{a}\sqrt{t} + \theta_{\mathfrak{i}}\sqrt{t}$.

Proof. Without loss of generality we can prove the statement for $t = 1$. To prove it, it is sufficient to pass to the limit into the integral (2.3.14). One then finds (3.4.6) and (3.4.7). Proposition 3.4.3 guarantees that integral and series can be exchanged.
Remark that $\tilde{F}_{j,k}$ can also be defined as the pointwise limit of the functions $F_{j,k}$ given in (2.3.11) and therefore

$$\tilde{F}_{j,k}(\omega_{j,k},\mathfrak{a}) = \begin{cases} \sum_{n=0}^{k} \left(\frac{(2k-n)!}{(k-n)!n!k!} \frac{e^{\frac{1}{2}\omega_{1,0}^2}}{(\theta_1-\theta_2)^{2k-n+1}} \sum_{h=0}^{2} \tilde{C}_{j,2-h}(y) \tilde{\mathscr{F}}_{h,n}(\omega_{j,k},\mathfrak{a}) \right), & \theta_1 \neq \theta_2; \\ \frac{(-1)^{k+1}}{(2k+1)!} \sum_{h=0}^{2} \tilde{C}_{j,2-h}(y) e^{\frac{1}{2}\omega_{1,0}^2} \mathscr{G}_{h,0,2k+1}(\omega_{j,k},\mathfrak{a},\theta_1), & \theta_1 = \theta_2, \end{cases} \tag{3.4.8}$$

where $\tilde{\mathscr{F}}_{h,n}(\omega,\mathfrak{a}) := \mathscr{G}_{h,0,n}(\omega,\mathfrak{a},\theta_2) - (-1)^n \mathscr{G}_{h,0,n}(\omega,\mathfrak{a},\theta_1)$ and the functions $\tilde{C}_{j,h}$ are given by (3.4.5). The function $\mathscr{G}_{h,0,n}$ is defined by (2.3.7).
Notice that, due to our appropriate choice of $\mathfrak{a}$, we can obtain the latter formula from (3.4.7) proceeding as for Theorem 2.3.7. Indeed, since $\mathfrak{a}$ is strictly larger than any pole of the limit expression, there exists κ_0 such that, for any $\kappa > \kappa_0$, $\mathfrak{a}$ is larger than $\max(-2\frac{1}{\kappa}\mu(\kappa), -2\beta_2(\kappa)\mu(\kappa))$. □

3.4.3 A uniform bound for $v^{(\theta_1,\theta_2)}$

The main result in this section is the following proposition.

Proposition 3.4.3 (Uniform bound for $(x,y) \mapsto v^{(\theta_1,\theta_2)}(t,x,y)$)**.** *Let θ_1, θ_2 be any real numbers. Let us denote by $\left(v^{(\theta_1,\theta_2)}\right)_k(t,x,y)$ the $k-$th term of the series $v^{(\theta_1,\theta_2)}(t,x,y)$ given by (3.4.6). There exists a positive constant C, depending only on θ_1, θ_2, such that*

$$\sup_{x,y} \left| \left(v^{(\theta_1,\theta_2)} \right)_k (t,x,y) \right| \leq\ C\, e^{-\frac{2z^2\, k}{t}}\,.$$

More precisely, one can take

$$C = \begin{cases} 1 + \max\{\psi(\theta_1,\theta_2), \psi(\theta_2,\theta_1)\} + \min\left\{1, \left|\frac{\theta_1\theta_2\sqrt{t}}{\theta_1-\theta_2}\right| \left|\varphi(\theta_1\sqrt{t}) - \varphi(\theta_2\sqrt{t})\right|\right\} & \text{if } \theta_1 \neq \theta_2, \\ 1 + 2\sqrt{t}|\theta_1|\varphi(\theta_1\sqrt{t}) + 3\theta_1^2 t & \text{if } \theta_1 = \theta_2, \end{cases} \tag{3.4.9}$$

where

$$\varphi(w) := \sqrt{2\pi} e^{\frac{w^2}{2}} \Phi^c(w) \tag{3.4.10}$$

and

$$\psi(\theta_1,\theta_2) := |\theta_1|\sqrt{t}\varphi(\theta_1\sqrt{t})+|\theta_2|\sqrt{t}\varphi(\theta_2\sqrt{t})+\min\left\{2, \left(\left|\frac{\theta_1+\theta_2}{\theta_1-\theta_2}\right|-1\right)|\theta_1|\sqrt{t}\varphi(\theta_1\sqrt{t}) + 2\left|\frac{\theta_1\theta_2\sqrt{t}}{\theta_1-\theta_2}\right|\varphi(\theta_2\sqrt{t})\right\}.$$

Moreover, there the sum of the series is uniformly bounded

$$\sup_{x,y}\left|v^{(\theta_1,\theta_2)}(t,x,y)\right| \leq \frac{C}{1-e^{-\frac{2z^2}{t}}}, \tag{3.4.11}$$

and if $R_N v^{(\theta_1,\theta_2)}$ denotes the remainder after the $(N+1)-th$ term of the series (3.4.6) *which represents $v^{(\theta_1,\theta_2)}$, then*

$$\sup_{x,y}\left|R_N v^{(\theta_1,\theta_2)}(t,x,y)\right| \leq \frac{C}{1-e^{-\frac{2z^2}{t}}} e^{-\frac{2z^2}{t}(N+1)}. \tag{3.4.12}$$

The proof is similar to the one of Proposition 2.5.3, nevertheless the combinations of the steps is different.
Considering formula (3.4.6), it is clear that the proof of (3.4.11) is complete as soon as one finds an appropriate bound for $\sup_{x,y}\tilde{F}_{j,k}(\omega_{j,k},\mathfrak{a}\sqrt{t})$ for each $j\in\{1,2,3,4\}$ and $k\in\mathbb{N}$. This is done in the next lemma.

Lemma 3.4.4. *Let us define $\tilde{F}_{j,k}$ by* (3.4.7) *and $\omega_{j,k}$ by* (2.3.12) *for any $j=1,2,3,4$ and $k\in\mathbb{N}$. Then there exists a positive constant C_j, depending on j and (θ_1,θ_2) but not on k, such that*

$$\sup_{x,y}|\theta_1\theta_2 t|^k\left|\tilde{F}_{j,k}(\omega_{j,k},\mathfrak{a}\sqrt{t})\right| \leq C_j\ e^{-\frac{2z^2}{t}k}.$$

Proof of Lemma 3.4.4. It becomes straightforward once one shows that, for each $j=1,\dots,4$ and $k\in\mathbb{N}$, there exists a positive constant C_j not depending on k such that

$$\sup_{x,y}|\theta_1\theta_2 t|^k\left|\tilde{F}_{j,k}(\omega_{j,k},\mathfrak{a}\sqrt{t})\right| \leq C_j\, e^{-\frac{(\omega_{j,k}^2-\omega_{1,0}^2)}{2}}. \tag{3.4.13}$$

Indeed, since $a_j(x,y)\geq 0$ for all $j=1,2,3,4$, the following estimate holds

$$\frac{1}{2}(\omega_{1,0}^2-\omega_{j,k}^2) \leq -\frac{1}{2t}\left(a_j(x,y)+2kz\right)^2 \leq -\frac{2z^2}{t}k.$$

Let us prove (3.4.13). To simplify the notation, in the rest of the proof, one take $t=1$.Then we define $\tilde{\mathfrak{a}}_{\mathfrak{i}}=\mathfrak{a}+\theta_{\mathfrak{i}}$ for $\mathfrak{i}=1,2$ and also

$$\tilde{p}_j(w) := \frac{-\tilde{c}_j(y;iw+\mathfrak{a})}{(w-i\tilde{\mathfrak{a}}_1)(w-i\tilde{\mathfrak{a}}_2)}$$

where the polynomials $\tilde{c}_j(y;w)$ are given by (3.4.4). Equations (3.4.6, 3.4.7) can be rewritten as

$$\begin{cases} v^{(\theta_1,\theta_2)}(1,x,y) = \sum_{k=0}^{\infty}(-\theta_1\theta_2)^k\sum_{j=1}^4\tilde{F}_{j,k}(\omega_{j,k},\mathfrak{a}), \\ \tilde{F}_{j,k}(\omega_{j,k},\mathfrak{a}) = -e^{\frac{1}{2}(\omega_{1,0}^2+\mathfrak{a}^2)}e^{-\mathfrak{a}\omega_{j,k}}\left(\frac{\mathcal{F}(\tilde{p}_j)}{\sqrt{2\pi}} * e^{-\frac{w^2}{2}}\right) * \frac{f_k(w,\tilde{\mathfrak{a}}_1,\tilde{\mathfrak{a}}_2)}{\sqrt{2\pi}}(\omega_{j,k}-\mathfrak{a}), \qquad j=1,2,3,4, \end{cases}$$

where f_k is defined in (2.3.6).

The rest of the proof of Lemma 3.4.4 is tricky and divided in several steps.
First one need to compute the convolution between the Fourier transform of $\tilde{p}_j$ and a Gaussian kernel: it will lead to the product between a Gaussian kernel and a linear combination of translations of the function φ defined by (3.4.10). Then one has to compute the convolution of this quantity with the function $f_k(\cdot,\tilde{\mathfrak{a}}_1,\tilde{\mathfrak{a}}_2)$, which is positive with support on $(-\infty,0)$. Its L^1-norm is computed in Lemma 3.4.5. We will complete the proof finding an estimate of the convolution which uses this latter information.

Let us compute now the convolution of a Gaussian kernel with the Fourier transforms $\mathcal{F}(\tilde{p}_j)$, $j = 1, 2, 3, 4$.
First we'll focus on the case $\theta_1 \neq \theta_2$ where

$$\begin{cases} \frac{1}{\sqrt{2\pi}}\mathcal{F}(\tilde{p}_1) * e^{-\frac{w^2}{2}} = e^{-\frac{\omega^2}{2}} \\ \frac{1}{\sqrt{2\pi}}\mathcal{F}(\tilde{p}_2) * e^{-\frac{w^2}{2}} = e^{-\frac{\omega^2}{2}} \left(-\theta_1 \frac{\theta_1 + (2\mathbb{1}_{\{y\geq z\}}-1)\theta_2}{\theta_1-\theta_2}\, \varphi(\omega+\tilde{\mathfrak{a}}_1) + 2\mathbb{1}_{\{y\geq z\}} \frac{\theta_1\theta_2}{\theta_1-\theta_2}\, \varphi(\omega+\tilde{\mathfrak{a}}_2)\right) \\ \frac{1}{\sqrt{2\pi}}\mathcal{F}(\tilde{p}_3) * e^{-\frac{w^2}{2}} = e^{-\frac{\omega^2}{2}} \left(-\theta_2 \frac{\theta_2 - \big(2\mathbb{1}_{\{y>0\}}-1\big)\theta_1}{\theta_1-\theta_2}\, \varphi(\omega+\tilde{\mathfrak{a}}_2) - 2\mathbb{1}_{\{y\leq 0\}} \frac{\theta_1\theta_2}{\theta_1-\theta_2}\, \varphi(\omega+\tilde{\mathfrak{a}}_1)\right) \\ \frac{1}{\sqrt{2\pi}}\mathcal{F}(\tilde{p}_4) * e^{-\frac{w^2}{2}} = e^{-\frac{\omega^2}{2}} \left(2\mathbb{1}_{[0,z)}(y) - 1\right) \frac{\theta_1\theta_2}{\theta_1-\theta_2}\, \left(\varphi(\omega+\tilde{\mathfrak{a}}_2) - \varphi(\omega+\tilde{\mathfrak{a}}_1)\right). \end{cases}$$

The Gaussian component is positive and decreasing on $(0, +\infty)$, and the function φ, defined by (3.4.10), is positive and decreasing on $\mathbb{R}$.
The bound of the convolutions $\left|\left(\frac{1}{\sqrt{2\pi}}\mathcal{F}(\tilde{p}_j) * e^{-\frac{w^2}{2}}\right) * \frac{f_k(w,\tilde{\mathfrak{a}}_1,\tilde{\mathfrak{a}}_2)}{\sqrt{2\pi}}\right|(\omega_{j,k} - \mathfrak{a})$ is then controlled by the convolutions

$$\left|\left(e^{-\frac{w^2}{2}}\varphi(\tilde{\mathfrak{a}}_{\mathfrak{i}} + w)\right) * f_k(w, \tilde{\mathfrak{a}}_1, \tilde{\mathfrak{a}}_2)\right|(\omega_{j,k} - \mathfrak{a}) = \left|\int_{\mathbb{R}} e^{-\frac{(\omega_{j,k}-\mathfrak{a}-y)^2}{2}} \varphi(\theta_{\mathfrak{i}} + \omega_{j,k} - y) f_k(y, \tilde{\mathfrak{a}}_1, \tilde{\mathfrak{a}}_2) dy\right|, \quad \mathfrak{i} = 1, 2.$$

Notice that f_k has support on $(-\infty, 0)$. Then

$$\begin{aligned} \left|\left(e^{-\frac{w^2}{2}}\varphi(w + \tilde{\mathfrak{a}}_{\mathfrak{i}})\right) * \frac{f_k(w, \tilde{\mathfrak{a}}_1, \tilde{\mathfrak{a}}_2)}{\sqrt{2\pi}}\right|(\omega_{j,k} - \mathfrak{a}) &\leq \varphi(\omega_{j,k} + \theta_{\mathfrak{i}}) e^{\mathfrak{a}\omega_{j,k}} e^{-\frac{\mathfrak{a}^2}{2}} \int_{-\infty}^{0} e^{-\frac{(\omega_{j,k}-y)^2}{2}} \left|e^{-\mathfrak{a}y} \frac{f_k(y, \tilde{\mathfrak{a}}_1, \tilde{\mathfrak{a}}_2)}{\sqrt{2\pi}}\right| dy \\ &\leq \varphi(\omega_{j,k} + \theta_{\mathfrak{i}}) e^{-\frac{(\omega_{j,k}-\mathfrak{a})^2}{2}} \frac{1}{\sqrt{2\pi}} \|e^{-\mathfrak{a}y} f_k(y, \tilde{\mathfrak{a}}_1, \tilde{\mathfrak{a}}_2)\|_{L^1(\mathbb{R}, dx)}. \end{aligned}$$

Suppose we knew that $\|e^{-\mathfrak{a}\cdot} f_k(\cdot, \tilde{\mathfrak{a}}_1, \tilde{\mathfrak{a}}_2)\|_{L^1(\mathbb{R}, dx)} = \frac{\sqrt{2\pi}}{|\theta_1\theta_2|^k}$, as we will prove in Lemma 3.4.5 below.
We can then complete the proof in the following way. Since $\omega_{j,k} \geq 0$, $\varphi(\omega_{j,k} + \theta_{\mathfrak{i}}) \leq \varphi(\theta_{\mathfrak{i}})$ and

$$|v^{(\theta_1,\theta_2)}(1, x, y)| = \sum_{k=0}^{\infty} |\theta_1\theta_2|^k \sum_{j=1}^{4} \left|\tilde{F}_{j,k}(\omega_{j,k}, \mathfrak{a})\right| \leq \sum_{k=0}^{\infty} \sum_{j=1}^{4} m_j\, e^{-\frac{\omega_{j,k}^2 - \omega_{1,0}^2}{2}}$$

where the coefficients m_j are given by

$$\begin{cases} m_1 = 1 \\ m_2 = |\theta_1|\varphi(\theta_1) + \mathbb{1}_{\{y\geq z\}} \min\left(2,\, 2\left|\frac{\theta_1\theta_2}{\theta_1-\theta_2}\right| \varphi(\theta_2) + |\theta_1| \left(\left|\frac{\theta_1+\theta_2}{\theta_1-\theta_2}\right| - 1\right) \varphi(\theta_1)\right) \\ m_3 = |\theta_2|\varphi(\theta_2) + \mathbb{1}_{\{y<0\}} \min\left(2,\, 2\left|\frac{\theta_1\theta_2}{\theta_1-\theta_2}\right| \varphi(\theta_1) + |\theta_2| \left(\left|\frac{\theta_1+\theta_2}{\theta_1-\theta_2}\right| - 1\right) \varphi(\theta_2)\right) \\ m_4 = \min\left(1,\, \left|\frac{\theta_1\theta_2}{\theta_1-\theta_2}\right| |\varphi(\theta_1) - \varphi(\theta_2)|\right). \end{cases}$$

The fact that $e^{-\frac{\omega_{j,k}^2 - \omega_{j,0}^2}{2}} \leq e^{-\frac{2z^2}{t}k}$ yields the conclusion.

If $\theta_1 = \theta_2$ then, analogously,

$$\begin{cases} \mathcal{F}(w \mapsto \tilde{p}_1(w)\, e^{-\frac{w^2}{2}})(\omega) \\ \frac{1}{\sqrt{2\pi}}\mathcal{F}(\tilde{p}_2) * (e^{-\frac{w^2}{2}})(\omega) = e^{-\frac{\omega^2}{2}} \left[-\theta_1\varphi(\omega+\tilde{\mathfrak{a}}_1) + 2\mathbb{1}_{\{y\geq z\}}\theta_1^2\,(1 - (\omega+\tilde{\mathfrak{a}}_1)\varphi(\omega+\tilde{\mathfrak{a}}_1))\right] \\ \frac{1}{\sqrt{2\pi}}\mathcal{F}(\tilde{p}_3) * (e^{-\frac{w^2}{2}})(\omega) = e^{-\frac{\omega^2}{2}} \left[-\theta_1\varphi(\omega+\tilde{\mathfrak{a}}_1) - 2\mathbb{1}_{\{y<0\}}\theta_1^2\,(1 - (\omega+\tilde{\mathfrak{a}}_1)\varphi(\omega+\tilde{\mathfrak{a}}_1))\right] \\ \frac{1}{\sqrt{2\pi}}\mathcal{F}(\tilde{p}_4) * (e^{-\frac{w^2}{2}})(\omega) = e^{-\frac{\omega^2}{2}} \left(2\mathbb{1}_{[0,z)}(y) - 1\right)\theta_1^2\,(1 - (\omega+\tilde{\mathfrak{a}}_1)\varphi(\omega+\tilde{\mathfrak{a}}_1)). \end{cases}$$

Following the same procedure as before, the conclusion comes from the fact that $0 \leq w\,\varphi(w) \leq 1$ for $w \geq 0$. □

Lemma 3.4.5. *Suppose $a \neq 0$, $a_1, a_2 > 0$ and $k \in \mathbb{N}^*$. Then*

$$\left\| \mathcal{F}\left(w \mapsto \frac{1}{(w-ia)^k}\right)(\omega) \right\|_{L^1(\mathbb{R},dx)} = \frac{\sqrt{2\pi}}{|a|^k} \quad \text{and} \quad \|f_k(\cdot,a_1,a_2)\|_{L^1(\mathbb{R},dx)} = \frac{\sqrt{2\pi}}{(a_1a_2)^k},$$

where f_k is defined in (2.3.6).

Proof. If $a > 0$, by Lemma 2.3.5, $\left|\mathcal{F}\left(w \mapsto \frac{1}{(w-ia)^{k+1}}\right)(\omega)\right| = \sqrt{2\pi}\mathbb{1}_{\mathbb{R}^-}(\omega)\frac{|\omega|^k}{k!}e^{a\omega}$.
Integrating by part,

$$\left\| \mathcal{F}\left(w \mapsto \frac{1}{(w-ia)^{k+1}}\right)(\omega) \right\|_{L^1(\mathbb{R},dx)} = \frac{\sqrt{2\pi}}{a\ k!}\int_{-\infty}^{0} a\ (-\omega)^k e^{a\omega}\, d\omega = \frac{1}{a}\left\| \mathcal{F}\left(w \mapsto \frac{1}{(w-ia)^{k}}\right)(\omega) \right\|_{L^1(\mathbb{R},dx)}.$$

So the first identity follows from the inductive hypothesis.
If $a < 0$ then $\mathcal{F}\left(w \mapsto \frac{1}{(w-ia)^{k+1}}\right)(\omega) = -i^{k+1}\sqrt{2\pi}\frac{(-\omega)^k}{k!}e^{a\omega}\mathbb{1}_{\mathbb{R}^+}(\omega)$ and the proof works as before.
To compute the second norm proceed as follows:

$$\begin{aligned}\|f_{k+1}(\cdot,a_1,a_2)\|_{L^1(\mathbb{R},dx)} &= \frac{1}{\sqrt{2\pi}}\int_{\mathbb{R}}\left|\mathcal{F}\left(\frac{1}{(w-ia_1)^{k+1}}\right) * \mathcal{F}\left(\frac{1}{(w-ia_2)^{k+1}}\right)(\omega)\right| d\omega \\ &= \int_{\mathbb{R}}\left|(-1)^k\sqrt{2\pi}(k!)^2\int_{\mathbb{R}}(-y)^k e^{a_1 y}\mathbb{1}_{\mathbb{R}_-}(y)(y-\omega)^k e^{a_2(\omega-y)}\mathbb{1}_{\mathbb{R}_-}(\omega-y)dy\right| d\omega\end{aligned}$$

Since the integrand is positive, we can exchange the integration order and then use the previous result to conclude:

$$\begin{aligned}\|f_{k+1}(\cdot,a_1,a_2)\|_{L^1(\mathbb{R},dx)} &= \sqrt{2\pi}(k!)^2\left(\int_{\mathbb{R}}(-y)^k e^{a_1 y}\mathbb{1}_{\mathbb{R}_-}(y)\,dy\right)\left(\int_{\mathbb{R}}(-y)^k e^{a_2 y}\mathbb{1}_{\mathbb{R}_-}(y)dy\right) \\ &= \frac{1}{\sqrt{2\pi}}\|\mathcal{F}\left(\frac{1}{(w-ia_1)^{k+1}}\right)\|_{L^1(\mathbb{R},dx)}\|\mathcal{F}\left(\frac{1}{(w-ia_2)^{k+1}}\right)\|_{L^1(\mathbb{R},dx)} = \frac{\sqrt{2\pi}}{a_1^{k+1}a_2^{k+1}}.\end{aligned}$$

□

3.4.4 Sampling from the instrumental measure $\mathfrak{Q}$

One can produce the skeleton of random variates from expression (3.4.1), (i.e. sample under $\mathfrak{Q}$) through generalized rejection sampling schemes (see Proposition 2.5.2) for both functions $h^{(\theta_1,\theta_2)}$ and $q^{(\theta_1,\theta_2)}$ defined in (3.4.3). The necessary assumptions for applying the Algorithm 1 are satisfied thanks to Proposition 3.4.3. Indeed $v^{(\theta_1,\theta_2)}(t,x,y)$ is a bounded series (see (3.4.6)) with bound (3.4.11) uniform in x and y. Let us denote the renormalized series, its truncation at the $(N+1)-th$ term and the bound for the remainder as

$$rv^{(\theta_1,\theta_2)}(t,x,y) := \frac{1-e^{-\frac{2z^2}{t}}}{C}v^{(\theta_1,\theta_2)}(t,x,y), \quad r_N v^{(\theta_1,\theta_2)}(t,x,y), \quad \mathfrak{R}_N v^{(\theta_1,\theta_2)}(t) = e^{-\frac{2z^2}{t}(N+1)}, \quad (3.4.14)$$

respectively, where z is the distance between the barriers and C is given in (3.4.9). For any fixed $\delta \in (0,1)$, the density $h^{(\theta_1,\theta_2)}(y)$ satisfies

$$\frac{h^{(\theta_1,\theta_2)}(y)}{p_0(\frac{T}{1-\delta},x_0,y)} = \underbrace{\frac{C_{\theta,x_0,T}}{\sqrt{1-\delta}}\ e^{M_B}\frac{C}{1-e^{-\frac{2z^2}{T}}}}_{C^{\mathcal{H}}}\ \underbrace{\frac{e^{-\frac{(y-x_0)^2}{2T}\delta}\ e^{B(y)-B(x_0)}}{e^{M_B}}\ rv^{(\theta_1,\theta_2)}(T,x_0,y)}_{f_\delta^{\mathcal{H}}(y)}, \quad (3.4.15)$$

where $C_{\theta,x_0,T}$ is the normalizing constant for the density $h^{(\theta_1,\theta_2)}$ and $M_B \leq \frac{\|b\|_\infty^2 T}{2\delta}$ is an upper bound for $B(y)-B(x)-\frac{(y-x)^2\delta}{2T}$. Indeed the parameter δ is introduced to control the possibly unbounded term

$e^{B(y)-B(x)}$ with $e^{-\frac{(y-x)^2}{2T}\delta}$ and an appropriate choice of δ, for each specific case, can make the bound sharper.
One obtains a decomposition of the density $y \mapsto q^{(\theta_1,\theta_2)}(t,T,x_1,x_2,y)$ as

$$\frac{q^{(\theta_1,\theta_2)}(t,T,x_1,x_2,y)}{q_0(t,T,x_1,x_2,y)} = \underbrace{\frac{(C)^2}{\left(1-e^{-\frac{2z^2}{t}}\right)\left(1-e^{-\frac{2z^2}{T-t}}\right)}\frac{1}{v^{(\theta_1,\theta_2)}(T,x_1,x_2)}}_{C^{\mathcal{B}}} \underbrace{rv^{(\theta_1,\theta_2)}(t,x_1,y)\ rv^{(\theta_1,\theta_2)}(T-t,y,x_2)}_{f^{\mathcal{B}}_{x_1,x_2}(y)}. \tag{3.4.16}$$

Remark 3.4.6. The probability to accept a simulation from the instrumental density is respectively the inverse of $\mathcal{C}^{\mathcal{H}}$ and $\mathcal{C}^{\mathcal{B}}$. Therefore, it is of great importance to get a bound as small as possible for M_B and $v^{(\beta_1,\beta_2)}$ as in Proposition 3.4.3.

Therefore (3.4.15) and (3.4.16) are on the form we expected, see (3.4.2). Let us show how to control the (finite sum) approximation of $f^{\mathcal{B}}_{x_1,x_2}$ and its vanishing rate of convergence, as well as the respective quantities for $f^{\mathcal{H}}_{\delta}$.

Lemma 3.4.7. *There exists a sequence of finite series $(f^{\mathcal{B}}_N)_N$ (resp. $(f^{\mathcal{H}}_N)_N$) that converges pointwise to $f^{\mathcal{B}}_{x_1,x_2}$ (resp. to $f^{\mathcal{H}}_{\delta}$) for $N\to\infty$ with an exponentially vanishing rate of convergence.*

Proof. One has to find functions $f^{\mathcal{H}}_N$ (resp. $f^{\mathcal{B}}_N$) and an exponentially decreasing sequence $\mathfrak{R}^{\mathcal{H}}_N$ (resp. $\mathfrak{R}^{\mathcal{B}}_N$) such that, for all $y\in\mathbb{R}$, $\left|f^{\mathcal{H}}_{\delta}(y)-f^{\mathcal{H}}_N(y)\right|\le\mathfrak{R}^{\mathcal{H}}_N$ (resp. $\left|f^{\mathcal{B}}_{x_1,x_2}(y)-f^{\mathcal{B}}_N(y)\right|\le\mathfrak{R}^{\mathcal{B}}_N$).

Proposition 3.4.3 yields the following choices of truncated densities and rest term

$$\begin{cases} f^{\mathcal{B}}_N := r_N v^{(\theta_1,\theta_2)}(t,x_1,y)\cdot r_N v^{(\theta_1,\theta_2)}(T-t,y,x_2) \\ \mathfrak{R}^{\mathcal{B}}_N := e^{-\frac{2z^2}{t}(N+1)} + e^{-\frac{2z^2}{T-t}(N+1)} - e^{-2z^2\left(\frac{1}{t}+\frac{1}{T-t}\right)(N+1)} \end{cases} \tag{3.4.17}$$

and

$$\begin{cases} f^{\mathcal{H}}_N := r_N v^{(\theta_1,\theta_2)}(T,x_0,y)\ \exp\left(B(y)-B(x_0)-\dfrac{(y-x_2)^2}{2T}\delta - M_B\right) \\ \mathfrak{R}^{\mathcal{H}}_N := \mathfrak{R}_N v^{(\theta_1,\theta_2)}(T). \end{cases} \tag{3.4.18}$$

where $r_N v$ and $\mathfrak{R}_N v$ are given in (3.4.14).

Notice that the series $f^{\mathcal{H}}_N$ contains $N+1$ terms, but $f^{\mathcal{B}}_N$ contains $(N+1)^2$ terms, since it is the product of two truncated series, each one with $N+1$ terms. Indeed, if $Rr_N v^{(\theta_1,\theta_2)}$ is the remainder of $r_N v^{(\theta_1,\theta_2)}$, one can write

$$\begin{aligned} f^{\mathcal{B}}_{x_1,x_2} &= \left(r_N v^{(\theta_1,\theta_2)}(t,x_1,y)+Rr_N v^{(\theta_1,\theta_2)}(t,x_1,y)\right)\left(r_N v^{(\theta_1,\theta_2)}(T-t,y,x_2)+Rr_N v^{(\theta_1,\theta_2)}(T-t,y,x_2)\right) \\ &= \left(r_N v^{(\theta_1,\theta_2)}(t,x_1,y)\cdot r_N v^{(\theta_1,\theta_2)}(T-t,y,x_2)\right)+\left(r_N v^{(\theta_1,\theta_2)}(t,x_1,y)\cdot Rr_N v^{(\theta_1,\theta_2)}(T-t,y,x_2)+\right. \\ &\quad \left.+r_N v^{(\theta_1,\theta_2)}(T-t,y,x_2)\cdot Rr_N v^{(\theta_1,\theta_2)}(t,x_1,y)+Rr_N v^{(\theta_1,\theta_2)}(t,x_1,y)\cdot Rr_N v^{(\theta_1,\theta_2)}(T-t,y,x_2)\right). \end{aligned}$$

□

The exact simulation scheme for $\mathbb{P}_b$ is now completed.

As one can see our approach is a variant of the one in [20]. The difference is that in that case the densities $h^{(\beta_1,\beta_2)}(y)$ and $q^{(\beta_1,\beta_2)}_{\mu}(t,T,x_1,x_2,y)$ were expressed as in (3.3.7 and 3.3.8). Moreover the bound in Proposition 2.5.3 was used to obtain a (generalized) rejection sampling method (analogously to (3.4.2))

for $h^{(\beta_1,\beta_2)}(y)$ and $q_\mu^{(\beta_1,\beta_2)}(t,T,x_1,x_2,y)$. The latter converged to a rejection sampling for the respective pointwise limit functions $h^{(\theta_1,\theta_2)}(y)$ and $q^{(\theta_1,\theta_2)}(t,T,x_1,x_2,y)$ once β_1 tends to 0 (Proposition 3.4.2).

In order to do an approach amenable to the case of more discontinuities ($n \geq 3$), we tried to reduce the use of the explicit knowledge of the transition density of the multi-skew Brownian motion, as we will discuss in Chapter 4. Nevertheless in the cases $n = 1$ and $n = 2$ one can do everything directly.

3.5 Simulations

In this section we provide some numerical simulations for $\mathbb{P}_b$, solution to (3.1.1). We also measure the performance of the exact simulation method in comparison with the classical Euler-Maruyama method, which has the disadvantage to *smooth* the effect of the discontinuous drift. The smaller is the discretization time step, the weaker is the effect and so the exact method becomes more and more competitive.

The section is organized as follows. First we recall the appropriate functions to use for applying the generalized rejection sampling method (see Proposition 2.5.2 and Algorithm 1) to sample from the instrumental measure. In particular we sample from the densities $h^{(\theta_1,\theta_2)}$ and $q^{(\theta_1,\theta_2)}(t,T,x_1,x_2,\cdot)$ given in (3.4.3). We devote the second part to the pseudo-code of the retrospective rejection sampling (see Section 3.2.1), which relies on the simulation from the finite-dimensional distributions of the instrumental measure $\mathfrak{Q}$ given by (3.4.1). In order to minimize the necessary CPU time we propose two different ways to apply the scheme. In the last part we illustrate our simulations.

We coded in Python 3 and executed the programs on a personal computer equipped with an Intel Core i5 processor, running at 2.5 Ghz.

3.5.1 The generalized rejection sampling for sampling under $\mathfrak{Q}$ (GRS)

In Algorithm 1 we have given the pseudo-code of the generalized rejection sampling (GRS), which allows to sample a random variable from an instrumental random variable once the bounded ratio between the densities is an *infinite* series whose remainder is vanishing. Let us recall the relevant quantities: if $g(x)$ and $h(x)$ are respectively the instrumental density (w.r.t. the Lebesgue measure) and the density from which one would like to sample, then let us denote by $f(x)$ the function ratio $\frac{1}{m}\frac{h(x)}{g(x)}$, where m is an upper bound of the function $\frac{h}{g}$. The Algorithm 1 requires the following quantities and functionals:

- g: instrumental density under which it is known how to sample,
- N_{max}: the maximal number of terms of the series one decides to consider,
- $(f_N)_{N=0,\dots,N_{max}}$: the partial sums of the series f,
- $(\mathfrak{R}_N^f)_{N=0\dots,N_{max}}$: decreasing sequence of bounds for the remainder $f - f_N$,
- $I_{\mathfrak{R}}^f$: a (piecewise constant) non decreasing function $(0,1) \to \{0,\dots,N_{max}\}$, inverse of $\mathfrak{R}_N^f$: $I_{\mathfrak{R}}^f(u) = \inf\{N \leq N_{max} : \mathfrak{R}_N^f \leq u\}$,

As we have seen in the Section 3.4.4, the **GRS** enables us to sample from the finite-dimensional distributions of $\mathfrak{Q}$ (3.4.1). In particular we sample from the densities $h^{(\theta_1,\theta_2)}(T,x_0,\cdot)$ and $q^{(\theta_1,\theta_2)}(t,T,x_1,x_2,\cdot)$ in (3.4.3) with instrumental densities the two Gaussian densities $p_0\left(\frac{T}{1-\delta},x_0,\cdot\right)$ and $q_0(t,T,x_1,x_2,\cdot)$ respectively.
The sequence $(f_N,\ \mathfrak{R}_N^f)_{N\leq N_{max}}$ for $h^{(\theta_1,\theta_2)}$ and $q^{(\theta_1,\theta_2)}$ are provided by (3.4.18) and (3.4.17) respectively. Both sequences $(\mathfrak{R}_N^f)_N$ considered in this section are exponentially decreasing, hence the piecewise constant functions $I_{\mathfrak{R}}^f$ are easy to compute explicitly. Moreover all simulations turn out to be exact (i.e. one takes the decision to accept or reject without the need to consider N_{max}, as explained at the end of Section 2.5.1).

Let us recall that we fix the integer $N_{max} = I^f_{\mathfrak{R}}(0.00005)$, such that the probability that for all $N \leq N_{max}$ one has not been able to accept or reject a sample, is smaller than twice the bound $\mathfrak{R}^f_{N_{max}}$, i.e. 0.0001.

3.5.2 The retrospective rejection sampling

The following algorithm describes the scheme that returns the pair $(T + t_0, X_T)$. X_T is a sample of the solution $\mathbb{P}_b$ on $[t_0, T + t_0]$ of (3.1.1) at the final time $T + t_0$. The sample is obtained through retrospective rejection sampling from the finite-dimensional distributions of the instrumental measure $\mathfrak{Q}$.

The algorithm needs some parameters derived from the given drift b, such as the (half) heights θ_1, θ_2 of the two jumps, the bounded non negative function ϕ_b^+ defined in (3.2.2) and its sup norm $\|\phi_b^+\|_\infty$. Moreover it recalls the external function **GRS**.

Algorithm 2: The retrospective rejection sampling **RRS**

Input : The starting point x_0 (at the time t_0), the time increment T;
Output: A sample of X_T at the final time $T + t_0$.
reject $\leftarrow$ True;
while reject **do**
  reject $\leftarrow$ False;
  simulate a Poisson Point Process on $[0, T] \times [0, \|\phi_b^+\|_\infty]$: $(\tau_k, x_{\tau_k})_{k=1,\dots,M}$;
  sample X_T from the density $h^{(\theta_1,\theta_2)}$ through **GRS**;
  $\tau_0 \leftarrow 0$, $y_0 \leftarrow x_0$;
  for $k = 1$ **to** M **do**
    sample y_k through **GRS** for the bridge density $q^{(\theta_1,\theta_2)}$ connecting (τ_{k-1}, y_{k-1}) and (T, X_T) ;
    if $\phi_b^+(x_{\tau_k}) > y_k$ **then**
      reject $\leftarrow$ True;
      exit from this cycle and start again;
return X_T.

The retrospective rejection sampling procedure is such that the output can actually be more rich: it can return the skeleton of the Brownian motion with drift b: the vectors $(t_0, \tau_1 + t_0, \dots, \tau_M + t_0, T + t_0), (x_0, y_1, \dots, y_M, X_T)$. One can then add to the skeleton the simulation at any time instance t in $(t_0, T + t_0)$ using the bridges dynamics.

In order to make the algorithm more efficient one notices that, if the time increment T is large, there will be a large number of Poisson points which slows down the algorithm since it can reject more often. One can improve the algorithm in two directions.
First, simulating the Poisson point process on the rectangle $[t_0, T + t_0] \times [0, \|\phi_b^+\|_\infty]$ progressively within the rejection procedure.
Second, using the Markov property of the considered process. One can split the time increment into congruent time intervals of length t smaller than a fixed value T_{el}. One then applies the **RRS** on the different time intervals of length t with new initial conditions given by the ending point on the previous interval. We will call **SRRS** the split RRS obtained choosing $T_{el} \leq \|\phi_b^+\|_\infty^{-1}$ in a convenient way in order to minimize the computational times. If T_{el} were $\|\phi_b^+\|_\infty^{-1}$, the Poisson process on the rectangle in **RRS** would have intensity 1. Therefore, with probability higher than e^{-1} (when the Poisson process on $[0, t] \times [0, \|\phi_b^+\|_\infty]$ has an empty realization), one avoids to apply **GRS** for bridges.
We are proposing the next pseudo-code whose inputs are the same as for the algorithm **RRS**.

Algorithm 3: The split retrospective rejection sampling **SRRS**

Input : The initial conditions $(t_0,\ x_0)$,
the time increment T,
the function ϕ_b^+ and its upper bound m (see (3.2.2));
Output: A sample of X_T at the final time $T + t_0$.
Split the interval $[0, T]$ in m' congruent intervals of length smaller than $T_{el} = m^{-1}$;
forall $j = 1, \dots, m'$ **do**
  obtain $X_{T_{el}*j}$ through the **RRS** with input the time interval T_{el} and the initial conditions $(T_{el} * (j-1), x_0)$;
return X_T

We compare in the next subsection the CPU times using the retrospective rejection sampling described above for some piecewise smooth drift b defined by (3.5.1), see Figure 3.1.

3.5.3 Numerical results

Let us consider two examples of Brownian diffusions starting from $x_0 = 0.5$ whose drift b_1 (resp. b_2) is piecewise smooth and admits two discontinuity points at 0 and $z = 1$:

$$\bar{b}_1(x) := \begin{cases} 0 & x < 0 \\ 1 & 0 < x < 1\ , \\ 0 & x > 1 \end{cases} \qquad \bar{b}_2(x) := \begin{cases} -2\cos(x) & x < 0 \\ \sin(x) & 0 < x < 1\ , \\ \cos(x - z) + sin(z) & x > 1 \end{cases} \tag{3.5.1}$$

and $\bar{b}_1(0) = \frac{1}{2}, \bar{b}_1(1) = \frac{1}{2}$ as in (3.1.4), and $\theta_1 = 1/2 = -\theta_2$ (resp. $\bar{b}_2(0) = -1, \bar{b}_2(1) = \frac{1}{2}$, and $\theta_1 = 1$ and $\theta_2 = 1/2$). (Figure 3.3 represents the drift $\bar{b}_2$.)

In each case we need to choose the time length T_{el} (to apply the **SRRS**, see Algorithm 3) and the parameter $\delta \in (0, 1)$ appearing in (3.4.15). In the first case we fixed $T_{el} = 0.55$ ($\leq \|\phi_{\bar{b}_1}^+\|_\infty^{-1} = 2$) and $\delta = 0.75$. In the second case we choose $T_{el} = 0.2$ and $\delta = 0.6$. Let us briefly explain how we took our decision.

Once T_{el} has been fixed, we choose δ such that the quantity $\frac{1}{2}\|\bar{b}_1\|_\infty^2 \frac{T_{el}}{\delta}$ is as small as possible (hence we can take M_B in (3.4.15) equal to it). Indeed the sharpness of this quantity and of the constant C in (3.4.11) determines the probability to accept a sample from the instrumental density as a sample from $h^{(\theta_1,\theta_2)}$. The latter probability is the inverse of the constant $C^{\mathcal{H}}$ given explicitly in (3.4.15). Let us recall that the constant C is a factor of the quantity $C^{\mathcal{B}}$ (see (3.4.16)) as well, hence determines the probability of accepting a sample of a Brownian bridge as a sample from the desired density.

The choice of T_{el} is more delicate and it is based on the computational time of the algorithm **RRS**. The algorithm **SRRS** splits the given interval $(0, T)$ into intervals of length between $\frac{1}{2}T_{el}$ and T_{el} and applies **RRS**. We choose T_{el} such that **RRS** is fastest on $(\frac{1}{2}T_{el}, T_{el})$.

The CPU time for the RRS does not grow linearly with the time, as one can easily notice from Figure 3.1. The Euler-Maruyama method and SRRS instead show an asymptotic linear growth of the CPU time as function of the time T. Sometimes the growth factor of SRRS is considerably faster, and sometimes slower as in the cases of the drift $\bar{b}_2$. This is due to the nature of the drifts and to the quality of the bounds.

Figure 3.2 shows that the Euler-Maruyama scheme needs a very small discretization step to be more precise at the discontinuities of the drift.

Considering the drift $\bar{b}_1$ which is a indicator function, our simulation of the 10^5 samples is exact and it is much faster than Euler-Maruyama with discretization step 10^{-5}. The average time for a single sample is respectively of 0.09 and 0.18 seconds. The Euler-Maruyama scheme with step 10^{-2} instead is faster (0.0002 seconds).

In the other considered case, the Euler-Maruyama method is faster. For the drift $\bar{b}_2$, the average CPU times for one simulation of $X_{0.6}$, is $0.29\,s$ and $0.1\,s$ for the exact simulation through the **SRRS** and the

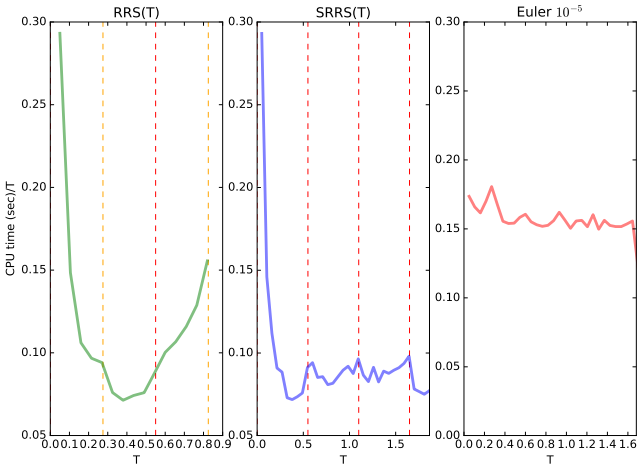

(a) X_T is the Brownian diffusion with drift $\bar{b}_1$ at time T

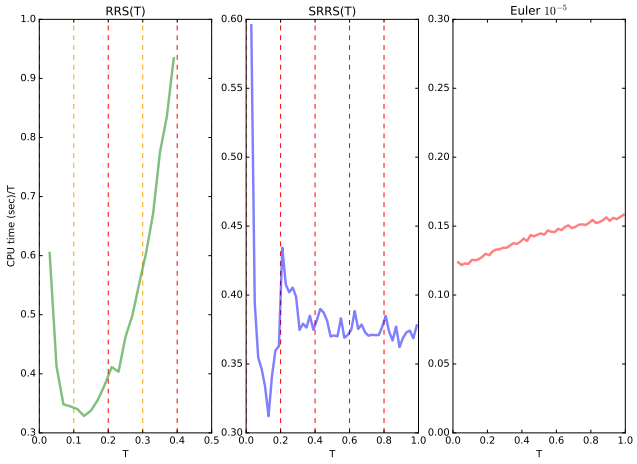

(b) X_T is the Brownian diffusion with drift $\bar{b}_2$ at time T

Figure 3.1: If X_T is the Brownian diffusion with drift $\bar{b}$ at time T, then the curves represent the ratio between the CPU times to sample X_T and the time T with the different methods. The (red) dashed lines represent the multiples of the maximal length for a split interval in the algorithm SRRS ($T_{el} \leq \|\phi_{\bar{b}}^{+}\|_{\infty}^{-1}$). The curve obtained through the RRS method reaches its minimum between the first two dashed lines (orange and red). We considered 1000 simulations and computed the average time.

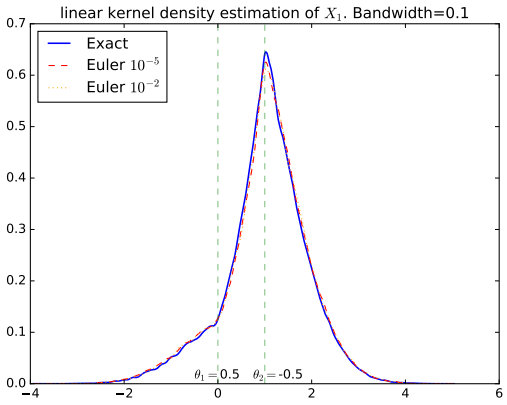

(a) The density of the Brownian diffusion $\mathbb{P}_{\bar{b}_1}$ at time 1. Bandwidth=0.1. $T_{el} = 0.55,\ \delta = 0.75$.

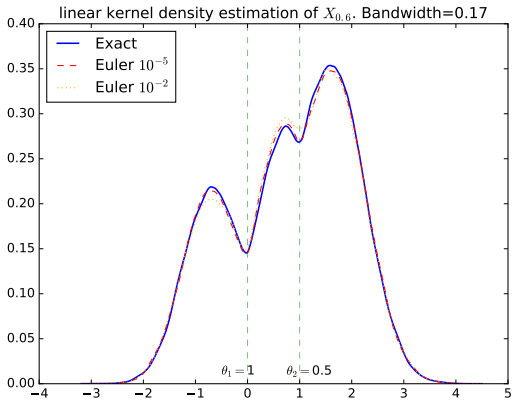

(b) The density of the Brownian diffusion $\mathbb{P}_{\bar{b}_2}$ at time 0.6. $T_{el} = 0.2$, $\delta = 0.6$.

Figure 3.2: The kernel density estimations of the density obtained from 10^5 samples with the Euler-Maruyama scheme (10^{-5} dashed line, and 10^{-2} dotted line) and the exact **SRRS** algorithm (with T_{el} and δ chosen above). The dashed vertical lines represent the points of discontinuity of the drift. The process has fixed initial condition $X_0 = 0.5$.

finest Euler-Maruyama respectively. To obtain $X_{0.6}$ the **SRRS** has applied three times **RRS** to intervals of length 0.2.

Let us quantify the average number of rejections for a single sample from the densities $h^{(\theta_1,\theta_2)}(y)$ (see (3.4.15)). For $\bar{b}_1$ with $T = T_{el} = 0.55$, it is around 5; indeed the probability of accepting a sample is the inverse of the constant $C^{\mathcal{H}}$ and it is about 0.196. For the densities $q^{(\theta_1,\theta_2)}(t, T, x_0, x_2, \cdot)$, $t < T$, the average number of rejections is around 2. Moreover, as expected, the number of terms of the series necessary to the decision (accept or reject) its rarely bigger than 1 and the average is around 1. This holds also in the case of the drift $\bar{b}_2$. Finally the average number of path rejection for each RRS in the SRRS is slightly larger than 5.

Let us consider the drift $\bar{b}_2$. In this case the average number of rejections for a single sample from the densities $h^{(\theta_1,\theta_2)}(y)$ and $q^{(\theta_1,\theta_2)}(t, T, x_0, x_2, \cdot)$, $t < T$ are respectively around 7 and 6. Finally the average number of path rejection for each RRS in the SRRS is slightly bigger than 9.

Figure 3.4 shows the realization of a path of the Brownian diffusion with drift $\bar{b}_1$. The path has been simulated as follows: given the skeleton with SRRS, it is sampled at each time of the discretization of step 10^{-3} following the bridges dynamics.

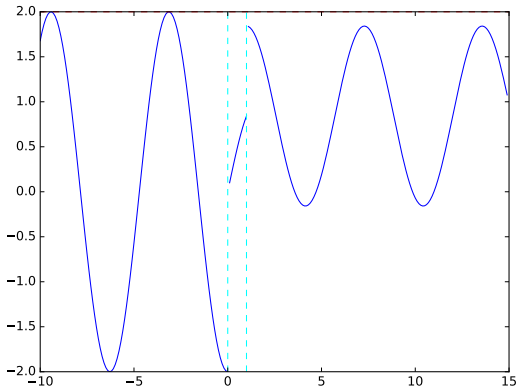

Figure 3.3: The drift $\bar{b}_2$.

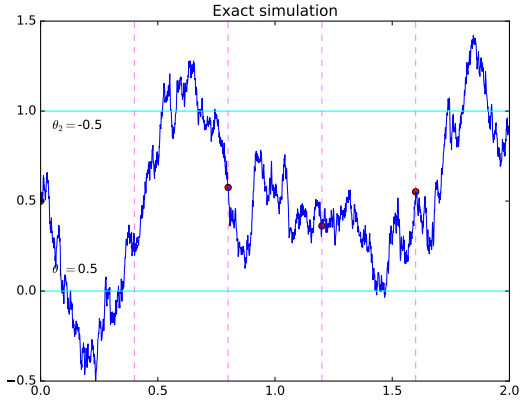

Figure 3.4: A realization of a path $t \mapsto X_t$ up to time $T = 2$ under $\mathbb{P}_{\bar{b}_1}$. The horizontal lines represent the points of discontinuity of the drift. The dots on the path are the skeleton of the process obtained by **SRRS** which splits $[0, 2]$ in five subintervals delimited by the dotted vertical lines.

Chapter 4

Possible extensions and open questions

Outline of the chapter: This chapter is devoted to some comments on possible extensions of the content of this document. At first we propose the natural extension of Sections 1.4 and 2.4. Then we discuss improvements and alternatives to the exact simulation method proposed in Chapter 3.

4.1 More on the transition density of general skew diffusions

4.1.1 Towards an explicit expression

Let us recall the main steps of the procedure we presented in Section 1.3 to obtain an explicit expression of the transition density of the SBM with constant drift. We continue here the discussion started in Sections 1.4 and 2.4 with the aim to treat the multi-skew case. The key steps are:

Step 1. the contour integral representation for the transition density (along a contour Γ) (1.3.6);

Step 2. the explicit computation of Green's function of the resolvent (Lemma 1.3.4);

Step 3. the regularity of Green's function of the resolvent on the half-plane of complex numbers with positive real part (after the *possible* change of variable through the complex square root ϕ). In particular

1. its holomorphy between the curve $\phi(\Gamma)$ and its continuous deformation to an appropriate curve $\mathfrak{a} + i\mathbb{R}$;
2. the localization of existing poles and therefore a criterion for choosing $\mathfrak{a}$ in an appropriate way;

Step 4. the reduction of the contour integral to an integral on the real line and the identification of a geometric sum;

Step 5. the identification of the result as a series of Fourier transforms and the explicit computations of them.

We discussed the **first step** in Section 1.4. We recall that Lejay, Lenôtre and Pichot [35] proved the extendibility of the contour integral representation for the transition density (1.3.6) for a class of skew diffusions with non constant diffusion coefficient. This class contains the multi-skew Brownian motion with discontinuous drift. They also proved that the zeros of Green's function are reals (partial answer to Step 2 and Step 3). In their paper, our Step 3-5 are replaced by computing the inverse Laplace transform when possible.

Consider first Step 2. Even in the case of a piecewise smooth drift with a finite number of discontinuities, it is difficult to find explicitly Green's function of the resolvent, i.e. to complete **Step 2**.

Let us focus on the multi-skew Brownian diffusion with piecewise constant drift.
Assume that the drift μ has a finite number of discontinuities at the skewness points $z_1 < z_2 < \ldots < z_n$ and satisfies:

$$\mu(w) := \mu_1 \mathbb{1}_{(-\infty,z_1)}(w) + \sum_{j=1}^{n-1} \mu_{j+1} \mathbb{1}_{[z_j,z_{j+1})}(w) + \mu_{n+1} \mathbb{1}_{(z_n,\infty)}(w), \quad \mu_1, \ldots, \mu_{n+1} \in \mathbb{R}\,.$$

As in Section 1.4, one can provide a self-adjoint infinitesimal generator and then show that its spectrum is contained in $(-\infty, 0]$ (partial Step 3). The associated Green's function satisfies Lemma 1.3.4 and is constructed from the functions $u_\pm^{(j)}(w) = e^{-\mu_j w \mp \sqrt{2\lambda+\mu_j^2}w}$ for $j = 1, \ldots, n+1$. It suffices to define the functions $U_\pm$ as in Figure 2.6 replacing $u_\pm$ with the functions $u_\pm^{(j)}$ on the $j-th$ interval. The required conditions on $U_\pm$ are continuity and the transmission conditions at the barriers:

$$k(z_j^-)\left(G_j^- \frac{d}{dw}u_-^{(j)}(z_j) + G_j^+ \frac{d}{dw}u_+^{(j)}(z_j)\right) = k(z_j^+)\left(G_{j+1}^- \frac{d}{dw}u_-^{(j+1)}(z_j) + G_{j+1}^+ \frac{d}{dw}u_+^{(j+1)}(z_j)\right).$$

These conditions are clearly more complicated, but it remains possible to compute the functions $U_\pm$. Therefore in case of a multi-skew Brownian diffusion with piecewise constant drift **Step 2** is doable.

Once Green's function is explicit, one considers **Step 3**.

> Let J be the union of the set of discontinuity points of the drift and the set of skewness points. For any $x, y \notin J$ we claim that $\lambda \mapsto G(x, y; \lambda)$ is holomorphic on the resolvent set. This should be a consequence of the holomorphy of the resolvent there.

We have not been able to find an explicit proof of this assertion in the literature.
In the case of a piecewise constant drift Green's function includes non trivial combinations of functions of $\phi_j(\lambda) := \sqrt{2\lambda + \mu_j^2}$ for different $j \in \{1, \ldots, n\}$. These are biholomorphisms between $\mathbb{C} \setminus (-\infty, -\frac{1}{2}\mu_j^2]$ and $\{\xi \in \mathbb{C};\, \Re e(\xi) > 0\}$. Let us define by ϕ the $\phi_{\hat{\jmath}}$ associated to the smallest $|\mu_{\hat{\jmath}}|$. This function induces a change of variable in the contour integral (1.3.6). In particular Green's function is transformed into $\xi \mapsto \bar{G}(x, y; \xi)$ such that $\xi := \sqrt{2\lambda + \mu_j^2}$ which, if the above claim is true, is holomorphic on $\{\xi \in \mathbb{C};\, \Re e(\xi) > 0\} \setminus [0, |\mu_{\hat{\jmath}}|]$. The possible singularities are poles (because the function is meromorphic) and are contained in $[0, |\mu_{\hat{\jmath}}|]$. Therefore the integrand is holomorphic between the curves $\phi(\Gamma)$ and $\mathfrak{a} + i\mathbb{R}$ as soon as $\mathfrak{a} > |\mu_{\hat{\jmath}}|$.
If our claim about holomorphy is true, one **could check the analogous of Lemma 2.3.3**, and this would complete **Step 3**.
As indication, in the case of the three-SBM without drift ($\mu \equiv 0$), we can prove that the denominator of Green's function does not have any real zero, but for the moment we cannot show that, for any choice of the parameters, there are no complex zero with positive real part. However we believe it is true, see Section 2.4. We also think that the analogous of Lemma 2.3.3 holds, but up to now we do not have a general proof.

Let us consider now **Step 4**. Once one is integrating on a line $\mathfrak{a} + i\mathbb{R}$, then a change of variable provides an integral on $\mathbb{R}$. We foresee difficulties in proving in general that the denominator gives rise to a geometric series. We think it does, at least if one chooses the constant $\mathfrak{a}$ big enough (think about the case of the three-SBM without drift).

Let us assume we can rewrite the transition density as a series of Fourier transforms using the previous step. The difficulty consists in dealing with the non trivial combinations of functions of the kind $\sqrt{w^2 + (\mu_{j_1}^2 - \mu_{\hat{\jmath}}^2)}e^{-i\,\omega\sqrt{w^2+(\mu_{j_2}^2-\mu_{\hat{\jmath}}^2)}}$ for some $\omega \in \mathbb{R}$ and $j_1 \neq j_2 \in \{1, \ldots, n+1\}$. This is similar to the problem encountered in Section 1.4, and makes treating **Step 5** in full generality not yet feasible. We think that those Fourier transforms will be made of transcendental functions such as the cumulative distribution function of a Gaussian or other kinds.

4.1.2 Its Gaussian bound

As we underlined in Section 3.3.2, the ratio between the transition densities of the multi-skew Brownian motion with constant drift μ and the Brownian motion with constant drift μ should be uniformly bounded. Recall that we prove this result in Proposition 2.5.3 for $n = 2$ semipermeable barriers. We believe to be able to extend this result in some particular cases with $n \geq 3$ (probably under some conditions on the parameters). Such results seem more complicated to obtain in the case of piecewise constant drift coefficients. New ideas need to be developed.
Note that for skew diffusions, there already exist Gaussian upper and lower bounds (see Stroock [57] who extended results by Aronson [5] and Nash [44]). But, to the best of the author's knowledge, these bounds are not explicit and can not be exploited in the exact simulation scheme presented in Chapter 3.

4.1.3 The Brownian motion with piecewise constant drift

Following the ideas developed in Chapter 2, we believe that the explicit computation of the transition density of the Brownian motion with piecewise constant drift in the case of two discontinuities (that is a three-valued drift) is achievable. This result would have at least two interesting applications.

First we could make a comparison between this explicit transition density and the empirical one obtained through the exact simulation algorithm plotted in Figure 3.2 (see Section 3). Obviously the non exact simulation provided by the Euler scheme already confirms that our exact algorithm is correct. But a comparison with the exact transition density is all the more convincing.

A second application involves an extreme setting when both barriers merge and the drift between the barriers goes to infinity. This extreme regime is related to many models in geophysics when heterogeneous medium contains thin slices of different matters. We suspect that the process converges to a one-SBM with two-valued drift. It seems likely that the proof could probably be done considering directly Green's function and checking that it converges to the one we expect. Another proof using the scale function and the speed measure is possible as well.

4.2 Exact simulation of skew diffusions

There are some alternatives to the exact simulation scheme provided in Chapter 3 for some skew diffusions with discontinuous drift. If the diffusion coefficient is discontinuous and the drift $b \neq 0$, to the best of our knowledge, no exact simulation scheme have been provided. However there is a recent "quasi-exact" method which uses the explicit expression of Green's function of the resolvent (see Lenôtre [40]).

In the next subsections we present some possible extensions of the algorithms in this document and some new exact algorithms we would like to develop in the future.

4.2.1 The multi-skew Brownian motion, a new method for drawing a path

The multi-skew Brownian motion behaves as a Brownian motion everywhere except when it reaches the barriers $z_1 < \ldots < z_n$, i.e. the effect of the barriers is purely local. Based on this observation we propose a theoretical scheme for sampling at the time T. The method, not yet completed, does not need the explicit knowledge of the transition densities but it relies on knowing how to simulate the one-SBM starting from its barrier, say z, and conditioned to stay in a symmetric band $(z - l, z + l)$, with $l > 0$. This task seems to be achievable using the Itô-McKean representation via the flipping excursions. To the best of our knowledge, this is still unknown but it should be similar to the Brownian case.

Let us present briefly the scheme of the algorithm. Let x_0 be the starting point of the process. The aim is to provide an exact simulation of the process at time T. If x_0 is not (respectively is) a barrier, we start the algorithm at Step 1 (respectively at Step 2).

Step 1. The initial point $x_0 \in \mathbb{R}$ is not a barrier. Let us denote by $\bar{z}$ the distance from x_0 to the closest barrier z_i. Let us consider $x_0 - \bar{z}$ and $x_0 + \bar{z}$; at least one of them is the barrier z_i. Let us sample the first time τ such that a Brownian motion starting from x_0 hits the levels $x_0 \pm \bar{z}$. One flips a fair coin to decide

whether it is $x_0 - \bar{z}$ or $x_0 + \bar{z}$. Then one repeats Step 1 until, either the motion reaches a barrier, or τ is greater than T. In the latter case we simulate a Brownian motion starting from x_0 conditioned on staying in the band $(x_0 - \bar{z}, x_0 + \bar{z})$. The value of this process at time T provides the expected exact simulation. If the process reaches a barrier, we simulate the rest of the process from this barrier using the Step 2.

Step 2. The starting point x_0 is at the barrier z_j, the process is a β_j-SBM. Let $\bar{z}$ be the distance from the closest other barrier (it is either $z_j - z_{j-1}$ or $z_{j+1} - z_j$). As before, one samples the first time τ that a Brownian motion starting from x_0 reaches one of the levels $x_0 \pm \bar{z}$. Thanks to the Itô-McKean representation, this stopping time is also the first time such that the β_j-SBM reaches $x_0 \pm \bar{z}$. If it surpasses the time horizon T, we conclude the algorithm with Step 3. Otherwise one flips a biased coin to choose the final point equal to $x_0 \pm \bar{z}$ with probability $\frac{1 \pm \beta}{2}$. Then one goes back to Step 1 or 2 depending on whether the result is a barrier or not.

Step 3. If τ is beyond T and the initial point x_0 is a barrier, say z_j. One samples a β_j-skew Brownian motion conditioned on staying between $x_0 - \bar{z}$ and $x_0 + \bar{z}$. Using again the Itô-McKean representation, we simulate first a Brownian motion starting from x_0 conditioned on staying between $x_0 - \bar{z}$ and $x_0 + \bar{z}$ and we flip a biased coin to choose the final point.

Notice that to apply this simulation scheme one needs in addition to be able to sample exactly from the θ-function giving the density of τ. If so, the method is exact and works for any discrete number of barriers. This algorithm cannot be extended in the drift case because of its strong dependence on the Itô-McKean trajectorial representation.

4.2.2 Possible improvements of the exact simulation of the Brownian motion with discontinuous drift

The main challenge of the exact simulation method for the Brownian motion with drift admitting several discontinuities consists in sampling from the finite-dimensional distribution of the instrumental measure. The solution we proposed in this document is based on the generalized rejection sampling method of some densities for which one knows an approximation and an estimate of the error.

We believe that the retrospective rejection sampling method can be extended to the case of a possibly infinite discrete set of discontinuities. Moreover, even in the case of a finite number of discontinuities, it might profit from some simplifications. For example, we think it is possible to sample under $\mathfrak{Q}$ even without the explicit expression of the function $v_\mu^{(\beta_1,\dots,\beta_n)}(t,x,y)$ (and therefore without $h_\mu^{(\beta_1,\dots,\beta_n)}$ and $q_\mu^{(\beta_1,\dots,\beta_n)}$).

In fact, in the context of the two-SBM with constant drift, we provided an alternative proof of Proposition 3.4.2 passing directly to the limit inside the contour integral. Unfortunately we don't have a general result in this direction but we believe that this way could be explored.

Similarly, we expect the limit $v^{(\theta_1,\dots,\theta_n)}$ to be a series of Fourier transforms. But we also could try to approximate the integral, with a bound on the error, and to apply the generalized rejection sampling method (Algorithm 1) without an explicit expression of these functions.

4.2.3 Skew Brownian diffusions with discontinuous drift

In Remark 3.3.3 we have seen that the explicit knowledge of the transition density of the multi-SBM with piecewise constant drift would provide an exact simulation for all multi-SBM with drift b as in Section 3.3.2. The most difficult part of this approach is to sampling under the instrumental measure. In particular the challenge is to find explicit appropriate Gaussian bounds needed in the rejection sampling procedure.

4.2.4 Numerical comparisons with other recent methods

In the five last years, several new simulation schemes (exact or not) and results have been developed for skew diffusions.

It would therefore be useful to compare them. One work in this direction is done by Lejay and Pichot in [38], but there is still a lot to be done. For instance the exact simulations methods can be explored,

improved and compared with the non-exact ones, especially when they are supposed to deal with several discontinuities in the coefficients.

4.3 ... and other unexplored dimensions!

Another direction of generalization of the modest present study is to consider multi-dimensional skew processes.
There have been some older work for defining these processes, see for example Portenko [49, 50], Takanobu [61, 60] and some more recent ones e.g. Zaitseva[69] and the very recent Atar and Budhiraja [7]. In the latter paper the authors provide a new proof of the weak existence and uniqueness for the $n-$dimensional SBM.
Apparently the unique existent simulation scheme in the multi-dimensional case is provided by Lejay [34]. Lenôtre in his PhD thesis [39] propose some way to extend these results. Anyway the (exact) simulation of multi-dimensional skew processes is a conceptually difficult question and there is much to be done, for simple barrier and for exotic barrier shapes...

Appendix A

Codes

Generalized rejection sampling method

The following class contains the implementation of Algorithm 1.

Listing A.1: GRS.py

```
import matplotlib.pyplot as plt

from numpy.random import random
from numpy import arange

class GRSVariable:

  # Samples a value according to the instrumental density
  def IDS(self):
    raise NotImplementedError
  def IDF(self,y):
    raise NotImplementedError

  # Computes the N-th term of the series in y
  def Term(self,y,N):
    raise NotImplementedError

  # Computes a bound for the remainder of the series
  def BRS(self,N):
    raise NotImplementedError
  # Inverse Bound Remainder: finds the first N such that BRS(N) < d
  def IBR(self,d):
    raise NotImplementedError

  # Returns the bound for the complete series v
  def Boundv(self):
    raise NotImplementedError

  ''' INPUT:
    *) Nmax is the maximal number of terms of the series
       we are going to consider.
    OUTPUT:
    *) y the sample from the goal random variable
```

```
34      *) False if it is not an exact sample and True if it is'''
35    def GeneralizedRejectionSampling(self,Nmax=None):
36      if Nmax is None:
37        Nmax=min(self.IBR(0.00005),10)
38      while (1):
39        y=self.IDS()    # Sample from the instrumental density
40        u=random()      # Sample a uniform
41
42        N=0 # we start considering the first term of the series
43        partial_series=self.Term(y,N)
44        while abs(partial_series-u)<self.BRS(N) and N<=Nmax:
45          # Chooses wisely the next value of N
46          newN=max(N+1,min(self.IBR(abs(partial_series-u)),Nmax))
47          while N<newN: # Computes the series up to newN
48            N+=1
49            partial_series+=self.Term(y,N)
50        if N>Nmax:
51          print('The rest at N=%s is %s' %(N,self.BRS(N)))
52          return (y,False) # Return the nonexact value y
53          '''This happens only with probability smaller than
54          2*self.BRS(Nmax+1), which is:
55          - smaller than 0.0001 if self.IBR(0.00005) is smaller than 10,
56          - else smaller then 2*self.BRS(10) which is a bit bigger'''
57        elif (partial_series > u):
58          # Return the value y and signals it is an exact simulation
59          return (y,True)
```

Transition density functions

We will apply Algorithm 1 to sample from the following densities.

Two-Skew Brownian motion without drift

This class contains the implementation of the functions needed to simulate the two-SBM (see (2.5.2)).

Listing A.2: TDFTwoSkew.py

```
1  from GRS import GRSVariable
2
3
4  from math import ceil
5  from math import sqrt
6  from math import log
7  from math import exp
8  from math import pi
9
10 from numpy import sign
11 from numpy.random import normal
12
13 import matplotlib.pyplot as plt
14
15 from scipy.stats import norm
16
```

```
17 from scipy.special import factorial
18 from scipy.special import binom
19
20
21 class TwoSkew(GRSVariable):
22
23   def __init__(self,b1=None,b2=None,it=None,x0=None,z=None):
24     if b1 is None or b2 is None or it is None or x0 is None or z is None:
25       print("""Please insert the right inputs:
26                first and second skewness parameters,
27                t, the starting point and the second barrier $z$""")
28     self.beta1=b1
29     self.beta2=b2
30     self.t=it     # time increment
31     self.x=x0     # starting point
32     self.z=z      # barriers distance (one barrier is 0, the other is z)
33
34   def IDS(self):
35     return normal(self.x,sqrt(self.t))
36
37   def IDF(self,y):
38     return norm.pdf(y,self.x,sqrt(self.t))
39
40   def Boundv(self):
41     return (1+abs(self.beta1)) * (1+abs(self.beta2)) /\
42            (1-abs(self.beta1*self.beta2)*exp(-2*(self.z**2)/self.t))
43
44   def Term(self,y,N):
45     if self.beta1*self.beta2==0 and N !=0:
46       return 0
47     c=[]
48     c.append(1)
49     c.append(sign(y)*self.beta1)
50     c.append(sign(y-self.z)*self.beta2)
51     c.append(sign(y*(y-self.z))*self.beta1*self.beta2)
52
53     a=[]
54     a.append(0)
55     a.append(abs(y)+abs(self.x)-abs(y-self.x))
56     a.append(abs(y-self.z)+
57              abs(self.x-self.z)-
58              abs(y-self.x))
59     a.append(2*max(self.z-max(self.x,y,0),0) +
60              2* max(min(self.x,y,self.z),0))
61     S=0
62     for i in range(0,4):
63       S+= c[i]*exp(-(a[i]+2*self.z*N)**2/(2*self.t))*\
64           exp(-(a[i]+2*self.z*N)*abs(y-self.x)/(self.t))
65     return (-self.beta1*self.beta2)**N*S/self.Boundv()
66
67   def BRS(self,N):
68     return (abs(self.beta1*self.beta2)*
69             exp(-2*self.z**2/self.t))**(N+1)
```

```
70
71    def IBR(self,d):
72      return ceil( log(d)/log(abs(self.beta1*self.beta2)*
73                   exp(-2*self.z**2/self.t)) )
```

Auxiliary functions

The file contains the functions given by (2.3.7). It contains also (3.4.10) and (3.4.11) of Proposition 3.4.3.

Listing A.3: vTermElem.py

```
1  from math import sqrt
2  from math import exp
3  from math import pi
4
5  from scipy.stats import norm
6
7  from scipy.special import factorial
8  from scipy.special import factorial2
9  from scipy.special import binom
10
11
12 def J(q,omega,arg):
13   J0= sqrt(2*pi)*exp(((omega+arg)**2)/2 + norm.logsf(omega+arg))
14   J1= -exp(-(omega**2)/2)
15   J0= -J0*J1
16   if q==0:
17     return J0
18   elif q==1:
19     return J1
20   elif q%2==0:
21     SumJ=0
22     for k in range(0,q//2):
23       SumJ+=(factorial2(q-1,True)/factorial2(q-2*k-1,True))*\
24              (omega+arg)**(q-2*k-1)
25     return J0*(factorial2(q-1,True))-J1*SumJ
26   else:
27     SumJ=0
28     for k in range(0,q//2+1):
29       SumJ+= (2**k)*(factorial(q//2,True))/(factorial(q//2-k,True))*\
30              (omega+arg)**(q-1-2*k)
31     return SumJ*J1
32
33
34 def S(L,n,omega,alpha,arg):
35   Sum=0
36   for k in range(0,n+1):
37     factor1=binom(n,k)*(omega+arg)**(n-k)
38     for l in range(0,L+1):
39       factor2=binom(L,l)*(arg+alpha)**(L-l)
40       Sum+= factor1*factor2*J(k+l,omega,arg)
41   return Sum
42
```

```
43
44 def G(K,m,n,omega,alpha,arg):
45   Su=0
46   for l in range(0,1+(K+m)//2):
47     Su+= ((-1)**(l))*S(K+m-2*l,n,omega,alpha,arg)/\
48          (2**l * factorial(l,True)*factorial(K+m-2*l,True))
49   return ((-1)**K)* factorial(K+m,True)*Su
50
51
52 def F(arg1,arg2,K,m,n,omega,alpha):
53   return G(K,m,n,omega,alpha,arg2)-(-1)**n * G(K,m,n,omega,alpha,arg1)
54
55
56 ''' Useful for h and q'''
57 def varphi(theta):
58   return sqrt(2*pi)*exp((theta)**2 /2 +norm.logsf(theta))
59
60
61 def Ctheta(theta1,theta2):
62   S1= abs(theta1)*varphi(theta1) + abs(theta2)*varphi(theta2)
63   if abs(theta1-theta2)<exp(-10):
64     return 1 + S1+3 * theta1**2
65   coeff1= (abs(theta1+theta2)-abs(theta1-theta2))
66   coeff2= 2*abs(theta1*theta2)
67   psi1= min(2*abs(theta1-theta2),
68             coeff1*abs(theta1)*varphi(theta1)+coeff2*varphi(theta2))
69   psi2= min(2*abs(theta1-theta2),
70             coeff1*abs(theta2)*varphi(theta2)+coeff2*varphi(theta1))
71   S2=max(psi1,psi2)
72   S3=min(abs(theta1-theta2),coeff2 * abs(varphi(theta1)-varphi(theta2))/2)
73   return 1+S1+ (S2+S3)/(abs(theta1-theta2))
74
75
76 def Bound_v(theta1,theta2,t,z):
77   return min(Ctheta(theta1,theta2)/(1-exp(-2*(z**2)/t)),3)
```

Two-Skew Brownian motion with drift

This class contains the implementation of the functions needed to simulate the two-SBM with drift, see (2.5.4).

Listing A.4: TDFTwoSkewDrift.py

```
1 from GRS import GRSVariable
2 from vTermElem import *
3
4 from math import ceil
5 from math import sqrt
6 from math import log
7 from math import exp
8 from math import pi
9
10 from numpy import sign
```

```
11 from numpy.random import normal
12
13 import matplotlib.pyplot as plt
14
15 from scipy.stats import norm
16
17 from scipy.special import factorial
18 from scipy.special import binom
19
20
21
22 class TwoSkewDrift(GRSVariable):
23
24   def __init__(self,b1=None,b2=None,mu=None,it=None,x0=None,z=None):
25     if b1 is None or b2 is None or mu is None or\
26        it is None or x0 is None or z is None:
27       print("""Please insert the right imputs:
28                first and second skewness parameters, the constant drift,
29                t, the starting point and the second barrier $z$""")
30     self.beta1=b1
31     self.beta2=b2
32     self.mu=mu*sqrt(it)  # constant drift
33     self.t=it            # time increment
34     self.x=x0            # starting point
35     self.z=z             # barriers distance
36
37   def IDS(self):
38     return normal(self.x+self.mu*self.t,sqrt(self.t))
39
40   def IDF(self,y):
41     return norm.pdf(y,self.x+self.mu*self.t,sqrt(self.t))
42
43   def Boundv(self):
44     return 4 / (1-exp(-2*(self.z**2)/self.t))
45
46   def Term(self,y,N):  # The N-th term of the normalized series v
47     if abs(self.beta1*self.beta2)<exp(-10) and N>0:
48       return 0
49
50     # The vectors of the coefficients of the polynomials
51     c1=[
52         1,
53         (self.beta1+self.beta2)*self.mu,
54         self.beta1*self.beta2*self.mu**2
55         ]
56     c2=[
57         self.beta1*sign(y),
58         -self.beta1*self.mu-sign(y*(y-self.z))*self.beta1*self.beta2*self.mu
   ↪ ,
59         self.beta1*self.beta2*(self.mu**2)*sign(y-self.z)
60         ]
61     c3=[
62         self.beta2*sign(y-self.z),
```

```
63          -self.beta2*self.mu+sign(y*(y-self.z))*self.beta1*self.beta2*self.mu
    ↪ ,
64          -self.beta1*self.beta2*(self.mu**2)*sign(y)
65          ]
66      c4=[
67          sign(y*(y-self.z))*self.beta1*self.beta2,
68          0,
69          -sign(y*(y-self.z))*self.beta1*self.beta2*(self.mu)**2
70          ]
71      # construct the matrix of the c[j,h]
72      c=[c1,c2,c3,c4]
73
74      alpha=min(abs(self.mu),
75                max(0,-2*self.beta1*self.mu,-2*self.beta2*self.mu))
76
77      C1=[c1[0],c1[1]+2*alpha*c1[0],c1[2]+alpha*c1[1]+(alpha**2) * c1[0]]
78      C2=[c2[0],c2[1]+2*alpha*c2[0],c2[2]+alpha*c2[1]+(alpha**2) * c2[0]]
79      C3=[c3[0],c3[1]+2*alpha*c3[0],c3[2]+alpha*c3[1]+(alpha**2) * c3[0]]
80      C4=[c4[0],c4[1]+2*alpha*c4[0],c4[2]+alpha*c4[1]+(alpha**2) * c4[0]]
81      C=[C1,C2,C3,C4]
82
83      a=[]
84      a.append(0)
85      a.append(abs(y)+abs(self.x)-abs(y-self.x))
86      a.append(abs(y-self.z)+abs(self.x-self.z)-abs(y-self.x))
87      a.append(2*max(self.z-max(self.x,y,0),0) +\
88               2* max(min(self.x,y,self.z),0))
89
90      omega=[]
91      for i in range(0,4):
92        omega.append((a[i]+2*N*self.z+abs(y-self.x))/sqrt(self.t))
93
94      if abs((self.beta1-self.beta2)*self.mu)<exp(-10):
95        Su=0
96        for m in range(0,N+1):
97          factor1= binom(N,m)
98          for s in range(0,N-m+1):
99            factor2= binom(N-m,s)*((-2*alpha)**(N-m-s))*\
100                     (self.mu**2-alpha**2)**s
101           for i in range(0,4):
102             for h in range(0,3):
103               factor3=C[i][2-h]*\
104                       G(N+h-s,m,2*N+1,omega[i],alpha,self.beta1*self.mu)
105               Su+= factor1* factor2 * factor3
106       return exp((self.x-y)**2/(2*self.t))*(-(self.beta1*self.beta2)**N)/\
107                  (factorial(2*N+1,True)) *Su/self.Boundv()
108
109     Su=0
110     for n in range(0,N+1):
111       factor0=  binom(2*N-n,N)/(factorial(n,True)*\
112                 ((self.beta1-self.beta2)*self.mu)**(2*N+1-n))
113       for m in range(0,N+1):
114         factor1=binom(N,m)
```

```
115         for s in range(0,N-m+1):
116           factor2= binom(N-m,s)*((-2*alpha)**(N-m-s))*\
117                    (self.mu**2-alpha**2)**s
118           for i in range(0,4):
119             for h in range(0,3):
120               factor3=C[i][2-h]*exp((self.x-y)**2/(2*self.t))*\
121                       F(self.beta1*self.mu,
122                         self.beta2*self.mu,
123                         N+h-s,
124                         m,
125                         n,
126                         omega[i],
127                         alpha)
128               Su+= factor0 * factor1* factor2 * factor3
129     return ((-1)**N)*(self.beta1*self.beta2)**N *Su/self.Boundv()
130
131   def BRS(self,N):
132     if abs(self.beta1*self.beta2)<exp(-10):
133       return 0
134     return (exp(-2*self.z**2/self.t))**(N+1)
135
136   def IBR(self,d):
137     if abs(self.beta1*self.beta2)<exp(-10):
138       return 0
139     return ceil( log(d)/(-2*self.z**2/self.t) )
```

For sampling under the instrumental measure

This class contains the functions needed to compute the series in Proposition 3.4.2

Listing A.5: vTerm.py

```
1  from vTermElem import *
2
3  from math import ceil
4  from math import sqrt
5  from math import log
6  from math import exp
7  from math import pi
8
9  from numpy import sign
10 from numpy.random import normal
11
12 import matplotlib.pyplot as plt
13
14 from scipy.stats import norm
15
16 from scipy.special import factorial
17 from scipy.special import factorial2
18 from scipy.special import binom
19
20
21
22 # the term N of the series in (3.4.6), (3.4.8)
```

```
23 def V(N,theta1,theta2,alpha,t,x,y,z):
24         # vector of the coefficients c_{j,h}=c[j][h] in (3.4.6)
25         c1=[1,(theta1+theta2), theta1*theta2]
26         c2=[0, -theta1, theta1*theta2*sign(y-z)]
27         c3=[0, -theta2, -theta1*theta2*sign(y)]
28         c4=[0,0,-sign(y*(y-z))*theta1*theta2]
29         c=[c1,c2,c3,c4]
30 
31         # vector of the functions in (3.4.7)
32         C1=[c1[0],c1[1]+2*alpha*c1[0],c1[2]+alpha*c1[1]+(alpha**2) * c1[0]]
33         C2=[c2[0],c2[1]+2*alpha*c2[0],c2[2]+alpha*c2[1]+(alpha**2) * c2[0]]
34         C3=[c3[0],c3[1]+2*alpha*c3[0],c3[2]+alpha*c3[1]+(alpha**2) * c3[0]]
35         C4=[c4[0],c4[1]+2*alpha*c4[0],c4[2]+alpha*c4[1]+(alpha**2) * c4[0]]
36         C=[C1,C2,C3,C4]
37 
38         # vector in (2.3.1)
39         a=[]
40         a.append(0)
41         a.append(abs(y)+abs(x)-abs(y-x))
42         a.append(abs(y-z)+abs(x-z)-abs(y-x))
43         a.append(2*max(z-max(x,y,0),0) + 2* max(min(x,y,z),0))
44 
45         # vector of the omega_{j,k} in (2.3.12)
46         omega=[]
47         for i in range(0,4):
48                 omega.append((a[i]+2*N*z+abs(y-x))/sqrt(t))
49 
50         if abs(theta1-theta2)<exp(-10):
51                 Su=0
52                 for i in range(0,4):
53                         for h in range(0,3):
54                                 Su+=C[i][2-h]*G(h,0,(2*N+1),
55                                 omega[i],alpha,theta1)
56                 return -exp((y-x)**2/(2*t))*((theta1*theta2)**N)/\
57                 (factorial(2*N+1,True))*Su
58 
59         Su=0
60         for n in range(0,N+1):
61                 factor1=binom(2*N-n,N)/\
62                 (factorial(n,True)*(theta1-theta2)**(2*N-n+1))
63                 for i in range(0,4):
64                         for h in range(0,3):
65                                 factor2=C[i][2-h]*exp((y-x)**2/(2*t))*\
66                         F(theta1,theta2,h,0,n,omega[i],alpha)
67                                 Su+= factor1 * factor2
68         return (-1)**N *(theta1*theta2)**N *Su
```

This class contains the implementation of the functions in (3.4.18), which allow to sample from the reference measure $\mathfrak{Q}$ as in Section 3.4.4.

Listing A.6: TDFh.py

```
1 ''' This file contains the class of the density h necessary for GRS
2 in order to sample from the finite dimensional distributions
3 of the reference measure Q defined in the RRS method.'''
```

```
4
5
6  # The class in which to find the functions for the GRS
7  from GRS import GRSVariable
8  from vTermElem import *
9  from vTerm import V
10
11 from math import ceil
12 from math import sqrt
13 from math import log
14 from math import exp
15 from math import pi
16
17 from numpy import sign
18 from numpy.random import normal
19
20 import matplotlib.pyplot as plt
21
22 from scipy.stats import norm
23
24 from scipy.special import factorial
25 from scipy.special import factorial2
26 from scipy.special import binom
27
28
29
30 #The density h of X_it starting at x0
31 class EDh(GRSVariable):
32
33   def __init__(self,
34                boundb=None,
35                primitive=None,
36                theta1=None,
37                theta2=None,
38                it=None,
39                x0=None,
40                z=None,
41                factorbound=None,
42                delta=0.5):
43     if boundb is None or primitive is None or theta1 is None or\
44        theta2 is None or it is None or x0 is None or z is None:
45       print("""Please insert: the bound for the drift, its primitive,
46                the jumps half heights, t, the starting point
47                and the second barrier $z$.""")
48       theta1=0
49       theta2=0
50     if factorbound is None:
51       # bound M_b in formula (3.4.18)
52       self.Bbound=exp((boundb**2) * it /(2*delta))
53     else:
54       self.Bbound=factorbound(x0)
55     self.boundb=boundb
56     self.primitive=primitive
```

```
57      self.delta=delta  # parameter that improves the efficiency
58      self.theta1=theta1*sqrt(it)  # half of the jump in 0 of the drift
59      self.theta2=theta2*sqrt(it)  # half of the jump in z of the drift
60      self.t=it           # time increment
61      self.x=x0           # starting point at the starting time
62      self.z=z
63
64    # Functions for GRS
65
66    def IDS(self):
67      return normal(self.x,sqrt(self.t/(1-self.delta)))
68
69    def IDF(self,y):
70      return norm.pdf(y,self.x,sqrt(self.t/(1-self.delta)))
71
72    '''Introduce some functions for each case'''
73    def Boundv(self):
74      return self.Bbound * Bound_v(self.theta1,self.theta2,self.t,self.z)
75
76    def Term(self,y,N):
77      if abs(self.theta1*self.theta2)<exp(-10) and N >0:
78        return 0
79
80      # The parameter a in Proposition 3.4.2
81      alpha=max(0,-2*self.theta1,-2*self.theta2)
82      Prim=exp(self.primitive(y)-self.primitive(self.x)-self.delta*(y-self.x)
        ↪ **2/(2*self.t))
83      return V(N,self.theta1,self.theta2,alpha,self.t,self.x,y,self.z)*Prim/
        ↪ self.Boundv()
84
85
86    def BRS(self,N):  # Bound remainder series
87      if self.theta1*self.theta2==0:
88        return 0
89      return (exp(-2*self.z**2/self.t))**(N+1)
90
91
92    def IBR(self,d):  # Inverse of BRS
93      if self.theta1*self.theta2==0:
94        return 0
95      return ceil( log(d)/(-2*self.z**2/self.t) )
```

This class contains the implementation of the functions needed to simulate the reference measure $\mathfrak{Q}$, see formula 3.4.17.

Listing A.7: TDFq.py

```
1  from GRS import GRSVariable
2  from vTermElem import *
3  from vTerm import V
4
5
6  from math import ceil
7  from math import sqrt
8  from math import log
```

```
9  from math import exp
10
11 from numpy.random import normal
12
13 import matplotlib.pyplot as plt
14
15 from scipy.stats import norm
16
17 from scipy.special import factorial
18 from scipy.special import factorial2
19 from scipy.special import binom
20
21 '''The density q for sampling at time t knowing that (t1,x1) and (t2,x2)
22 that is the limit of the bridges density of the skew BM
23 with paticular drift and semipermeability coefficients beta1, beta2
24 such that beta1*mu and beta2*mu converge to theta1 and theta2'''
25
26 class EDbridge(GRSVariable):
27
28   def __init__(self,
29                t=None,
30                t1=None,
31                t2=None,
32                x1=None,
33                x2=None,
34                theta1=None,
35                theta2=None,
36                z=None):
37     if t is None or t1 is None or t2 is None or x1 is None or\
38        x2 is None or theta1 is None or theta2 is None or z is None:
39       print("""Please insert the parameters t, starting time,
40                ending time, starting point, ending point,
41                jumps half heights, second barrier""")
42     self.t=t # time t between t1 and t2
43     self.t1=t1
44     self.t2=t2
45     self.x1=x1 # X_(t1)
46     self.x2=x2 # X_(t2)
47     self.theta1=theta1
48     self.theta2=theta2
49     self.z=z
50
51   def IDS(self):
52     return normal(self.x1+(self.x2-self.x1)*\
53                   (self.t-self.t1)/(self.t2-self.t1),
54                 sqrt((self.t2-self.t)*(self.t-self.t1)/\
55                   (self.t2-self.t1)))
56
57   def IDF(self,y):
58     m=self.x1+(self.x2-self.x1)*(self.t-self.t1)/(self.t2-self.t1)
59     sigma=(self.t2-self.t)*(self.t-self.t1)/(self.t2-self.t1)
60     return norm.pdf(y,m,sqrt(sigma))
61
```

```
62
63    def Boundv(self):
64      B1=Bound_v(self.theta1*sqrt(self.t-self.t1),
65                 self.theta2*sqrt(self.t-self.t1),
66                 self.t-self.t1,self.z)
67      B2=Bound_v(self.theta1*sqrt(self.t2-self.t),
68                 self.theta2*sqrt(self.t2-self.t),
69                 self.t2-self.t,self.z)
70      return B1*B2
71
72
73    def Term(self,y,N):
74
75      if abs(self.theta1*self.theta2)<exp(-10) and N >0:
76        return 0
77
78      # The parameter a in Proposition 3.4.2
79      alpha=max(0,-2*self.theta1,-2*self.theta2)
80      alpha1=sqrt(self.t-self.t1)*alpha
81      alpha2=sqrt(self.t2-self.t)*alpha
82      theta11=self.theta1*sqrt(self.t-self.t1)
83      theta21=self.theta2*sqrt(self.t-self.t1)
84      theta12=self.theta1*sqrt(self.t2-self.t)
85      theta22=self.theta2*sqrt(self.t2-self.t)
86
87      CompleteSu1=V(N,theta11,theta21,alpha1,self.t-self.t1,self.x1,y,self.z)
88      CompleteSu2=V(N,theta12,theta22,alpha2,self.t2-self.t,y,self.x2,self.z)
89      S=CompleteSu1*CompleteSu2
90      for j in range(0,N):
91        S+=CompleteSu1*V(j,
92                         theta12,
93                         theta22,
94                         alpha2,
95                         self.t2-self.t,
96                         y,
97                         self.x2,
98                         self.z)
99        S+=CompleteSu2*V(j,
100                         theta11,
101                         theta21,
102                         alpha1,
103                         self.t-self.t1,
104                         self.x1,
105                         y,
106                         self.z)
107     return S/self.Boundv()
108
109   def BRS(self,N):
110     if self.theta1*self.theta2==0:
111       return 0
112     R1=exp(-2*self.z**2 /(self.t-self.t1))
113     R2=exp(-2*self.z**2 /(self.t2-self.t))
114     return R1**(N+1)+R2**(N+1)-(R1*R2)**(N+1)
```

```
115
116
117   def IBR(self,d):
118     '''since we don't have an exact inverse, for the remainder
119     we consider as if there was only the product of the remainder.
120     We lost efficiency'''
121     if self.theta1*self.theta2==0:
122       return 0
123     # since BRS(N)<= 2*max(R1,R2)**(N+1) we have given it's inverse
124     return ceil( -log(d/2)/(2*(self.z**2)/\
125                 max((self.t-self.t1),(self.t2-self.t))) )
```

Retrospective rejection sampling scheme

The following class implements Algorithm 2 and Algorithm 3 explained in Section 3.5.2.

Listing A.8: RetroRS.py

```
1  from math import sqrt
2  from math import ceil
3  from math import floor
4  from math import pi
5
6  import matplotlib.pyplot as plt
7
8  from numpy.random import normal
9  from numpy import arange
10 from numpy import newaxis
11 from numpy import linspace
12 from numpy import exp
13 from numpy import asarray
14 from numpy import sign
15
16 import pickle
17
18 from random import expovariate
19 from random import uniform
20
21 from scipy.stats import norm
22
23 from TDFh import EDh
24 from TDFq import EDbridge
25
26
27 class SimBDDriftDisc:
28   # Simulate Brownian Diffusion with Discontinuous Drift
29
30   def x0(self):
31     raise NotImplementedError
32   def t0(self):
33     raise NotImplementedError
34   def theta(self):
35     raise NotImplementedError
```

```
36    def IT(self):
37      raise NotImplementedError
38    def T(self):
39      raise NotImplementedError
40    def z(self):
41      raise NotImplementedError
42    def b(self,x):
43      raise NotImplementedError
44    def phi_b(self,x):
45      raise NotImplementedError
46    def B(self,x):
47      raise NotImplementedError
48    def Bound_b(self):
49      raise NotImplementedError
50    def Bound_phi(self):
51      raise NotImplementedError
52    def delta(self):
53      raise NotImplementedError
54    def CleverBound(self,x):
55      raise NotImplementedError
56
57
58    ''' The retrospective rejection sampling
59      provides the simulation of (1.1)=BM+b*t
60      at the time self.t0+self.IT
61      INPUT:
62      *) T: length of interval
63      *) x0: starting point of the simulation
64      *) CB: if True uses the clever bound
65      OUTPUTS
66      *) The function returns the skeleton X_T:
67         the process at time t0+T'''
68    def RRS(self,T=None,x0=None,CB=True):
69      if T is None:
70        T=self.IT()
71      # initial conditions
72      if x0 is None:
73        x0=self.x0()
74
75      reject=True
76      while reject is True:
77
78        # simulation of X_T=X_{T+t0} with the GRS for the density h
79        if CB==True:
80          P=EDh(self.Bound_b(),
81                self.B,self.theta()[0],
82                self.theta()[1],
83                it=T,
84                x0=x0,
85                z=self.z(),
86                factorbound=self.CleverBound,
87                delta=self.delta())
88        else:
```

```
89          P=EDh(self.Bound_b(),
90                self.B,
91                self.theta()[0],
92                self.theta()[1],
93                it=T,
94                x0=x0,
95                z=self.z(),
96                delta=self.delta())
97        [X_T,ex]=P.GeneralizedRejectionSampling()
98        if ex is False:
99          print('h is not exact')
100
101       # Starting creating the Poisson points on the rectangle
102       AreaRectangle=T*self.Bound_phi()
103       if AreaRectangle < exp(-10):
104         return X_T
105
106       ''' Retrospective rejection for the Poisson times tau:
107       sample X_tau from q with GRS between the previous known point
108       and the final (T+t0,X_T)'''
109       reject=False
110       former_tau=0
111       x_tau=x0
112       covered_area=expovariate(AreaRectangle)
113       while(covered_area<AreaRectangle):
114         tau=covered_area/self.Bound_phi()
115         y_tau=uniform(0,self.Bound_phi())
116         P=EDbridge(
117              tau,
118              former_tau,
119              T,
120              x_tau,
121              X_T,
122              self.theta()[0],
123              self.theta()[1],
124              z=self.z())
125         (x_tau,ex)=P.GeneralizedRejectionSampling()
126         # Condition for the rejection-acceptance
127         if self.phi_b(x_tau)>y_tau:
128           reject=True
129           break
130         elif ex is False:
131           print('Not exact q')
132         former_tau=tau
133         covered_area+=expovariate(AreaRectangle)
134     return X_T
135
136
137   ''' The split retrospective rejection sampling for X_IT,
138   that splits the time interval of length self.IT into smaller intervals
139   of length smaller than self.T to whom RRS is applied
140   and pastes the skeletons'''
141   def SRRS(self,Ti=None):
```

```
142
143       if Ti is None:
144         Ti=self.IT()
145
146       if Ti<=self.T():
147         X_T= self.RRS(Ti,self.x0())
148         return X_T
149
150       # we simulate at intervals of length smaller than self.T()
151       k=ceil(Ti/self.T())
152
153       # the length of the small intervals
154       deltaT=Ti/k
155
156       # the starting positions
157       X_T=self.x0()
158       for h in range(0,k):
159         X_T=self.RRS(deltaT,X_T)
160
161       return X_T
```

The next functions contain the informations about the drifts (3.5.1).

Listing A.9: Drifts.py, first part

```
1  class Step(SimBDDriftDisc):
2    # Piecewise constant drift
3    def __init__(self,T=1,z=1):
4      self.fT=T
5      self.dz=z # the second barrier, the first is in zero
6      print("""The time %s has been chosen, we consider
7                time intervals smaller than %s""" % (self.fT,self.T()))
8
9    # initial conditions
10   def x0(self):
11     return 0.5
12   def t0(self):
13     return 0
14
15   # time interval
16   def IT(self):
17     return self.fT
18   # elementary time interval
19   def T(self):
20     return 0.55 #<(1/self.Bound_phi())
21   # distance between the barriers
22   def z(self):
23     return self.dz
24
25   # Jumps' intensities and drift
26   def theta(self):
27     return (0.5,-0.5)
28
29   # The drift
30   def b(self,x):
```

```
31      if (x<=0):
32        return 0
33      elif (x<=self.z()):
34        return self.theta()[0]-self.theta()[1]
35      else:
36        return 0
37
38    # The non negative function phi_b = (b**2+der_b-inf(b**2+der_b))/2
39    def phi_b(self,x):
40      if (x<=0):
41        return 0
42      elif (x<=self.z()):
43        return (self.b(x)**2)/2
44      else:
45        return 0
46
47    # The primitive of the drift b
48    def B(self,x):
49      if (x<=0):
50        return 0
51      elif (x<=self.z()):
52        return self.b(x)*x
53      else:
54        return self.b(self.z())*self.z()
55
56    # The upper bounds
57    def Bound_b(self):
58      return self.theta()[0]-self.theta()[1]
59    def Bound_phi(self):
60      return 1/2
61
62    def delta(self):
63      return 0.75
64
65    def CleverBound(self,x):
66      return exp((min(self.IT(),self.T())*self.Bound_b()**2)/(2*self.delta()))
```

Listing A.10: Drifts.py, second part

```
1  class DiscD(SimBDDriftDisc):
2
3    def __init__(self,T=1,z=1):
4      self.fT=T
5      self.dz=z # the second barrier, the first is in zero
6      print("""The time %s has been chosen, we consider time intervals
7               smaller than %s""" % (self.fT,self.T()))
8
9    # initial conditions
10   def x0(self):
11     return 0.5
12   def t0(self):
13     return 0
14
15   # time interval
```

```
16    def IT(self):
17      return self.fT
18    # elementary time interval
19    def T(self):
20      return 0.2 #<(1/self.Bound_phi())
21    # distance between the barriers
22    def z(self):
23      return self.dz
24
25    # Parameters and drift
26    # jumps' intensities
27    def theta(self):
28      return (1,0.5)
29
30    # The drift
31    def b(self,x):
32      if (x<0):
33        return -2*self.theta()[0]*cos(x)
34      elif (x==0):
35        return -self.theta()[0]
36      elif (x==self.z()):
37        return sin(self.z())+self.theta()[1]
38      elif (x<=self.z()):
39        return sin(x)
40      else:
41        return 2*self.theta()[1]*\
42               cos(x-self.z())+sin(self.z())
43
44    # The non negative function phi_b = (b**2+der_b-inf(b**2-der_b))/2
45    def phi_b(self,x):
46      m=-max(2*self.theta()[0],2*self.theta()[1],1)
47      if (x<=0):
48        return ((-2*self.theta()[0]*cos(x))**2+\
49                2*self.theta()[0]*sin(x)-m)/2
50      elif (x<=self.z()):
51        return (sin(x)**2+cos(x)-m)/2
52      else:
53        return ((2*self.theta()[1]*cos(x-self.z())+sin(self.z()))**2-\
54                 2*self.theta()[1] * sin(x-self.z())-m)/2
55
56    # The primitive of the drift b
57    def B(self,x):
58      if (x<=0):
59        return -2*self.theta()[0]*sin(x)
60      elif (x<=self.z()):
61        return 1-cos(x)
62      else:
63        return 1-cos(self.z())+sin(self.z())*(x-self.z())+\
64               2*self.theta()[1]*sin(x-self.z())
65
66    # The upper bounds
67    def Bound_b(self):
68      return max(abs(sin(self.z()))+2*abs(self.theta()[1]),
```

```
69                  1,
70                  2*abs(self.theta()[0]))
71
72    def Bound_phi(self):
73      m=-max(2*self.theta()[0],
74             2*self.theta()[1],
75             1)
76      M=max(5/4,
77            2*self.theta()[0],
78            (2*self.theta()[0])**2+1/4,
79            1,
80            2*self.theta()[1]+(abs(sin(self.z()))+2*self.theta()[1])**2)
81       return (M-m)/2
82
83    def delta(self):
84      return 0.6 #>=2*self.T()
85
86    def CleverBound(self,x):
87      return exp(min(self.IT(),self.T())*self.Bound_b()**2/(2*self.delta()))
```

Bibliography

[1] Stefan Ankirchner, Thomas Kruse, and Mikhail Urusov. "Numerical approximation of irregular SDEs via Skorokhod embeddings". In: *Journal of Mathematical Analysis and Applications* 2.440 (2016), pp. 692–715.

[2] Thilanka Appuhamillage and Daniel Sheldon. "First passage time of skew Brownian motion". In: *J. Appl. Probab.* 49.3 (2012), pp. 685–696. ISSN: 0021-9002. DOI: 10.1239/jap/1346955326.

[3] Thilanka Appuhamillage, Vrushali Bokil, Enrique Thomann, Edward Waymire, and Brian Wood. *Corrections for "Occupation and local times for skew Brownian motion with applications to dispersion across an interface"*. Sept. 2010. arXiv: 1009.5410 [math.PR].

[4] Thilanka Appuhamillage, Vrushali Bokil, Enrique Thomann, Edward Waymire, Brian Wood, et al. "Occupation and local times for skew Brownian motion with applications to dispersion across an interface". In: *The Annals of Applied Probability* 21.1 (2011), pp. 183–214.

[5] Donald G. Aronson. "Non-negative solutions of linear parabolic equations". eng. In: *Annali della Scuola Normale Superiore di Pisa - Classe di Scienze* 22.4 (1968), pp. 607–694.

[6] Olga V. Aryasova and Andrey Y. Pilipenko. "On properties of a flow generated by an SDE with discontinuous drift". In: *Electron. J. Probab.* 17 (2012), no. 106, 20. ISSN: 1083-6489. DOI: 10.1214/EJP.v17-2138.

[7] Rami Atar and Amarjit Budhiraja. "On the multi-dimensional skew Brownian motion". In: *Stochastic Process. Appl.* 125.5 (2015), pp. 1911–1925. ISSN: 0304-4149. DOI: 10.1016/j.spa.2014.12.001.

[8] Alexandros Beskos, Omiros Papaspiliopoulos, and Gareth O. Roberts. "Retrospective exact simulation of diffusion sample paths with applications". In: *Bernoulli* 12.6 (2006), pp. 1077–1098. ISSN: 1350-7265. DOI: 10.3150/bj/1165269151.

[9] Alexandros Beskos, Omiros Papaspiliopoulos, and Gareth O. Roberts. "A factorisation of diffusion measure and finite sample path constructions". In: *Methodol. Comput. Appl. Probab.* 10.1 (2008), pp. 85–104. ISSN: 1387-5841. DOI: 10.1007/s11009-007-9060-4.

[10] Alexandros Beskos and Gareth O. Roberts. "Exact simulation of diffusions". In: *Ann. Appl. Probab.* 15.4 (2005), pp. 2422–2444. ISSN: 1050-5164. DOI: 10.1214/105051605000000485.

[11] Alexei-N. Borodin and Paavo Salminen. *Handbook of Brownian Motion: Facts and Formulae*. Operator Theory, Advances and Applications. Birkhäuser Basel, 2002. ISBN: 9783764367053.

[12] Marc Decamps, Ann De Schepper, and Marc Goovaerts. "Applications of δ-function perturbation to the pricing of derivative securities". In: *Physica A: Statistical Mechanics and its Applications* 342.3 (2004), pp. 677–692. DOI: 10.1016/j.physa.2004.05.035.

[13] Marc Decamps, Marc Goovaerts, and Wim Schoutens. "Asymmetric skew Bessel processes and their applications to finance". In: *Journal of computational and applied mathematics* 186.1 (2006), pp. 130–147. DOI: 10.1016/j.cam.2005.03.067.

[14] Marc Decamps, Marc Goovaerts, and Wim Schoutens. "Self exciting threshold interest rates models". In: *International Journal of Theoretical and Applied Finance* 9.07 (2006), pp. 1093–1122. DOI: dx.doi.org/10.1142/S0219024906003937.

[15] David Dereudre, Sara Mazzonetto, and Sylvie Rœlly. *Exact simulation of Brownian diffusions with drift admitting jumps*. Accepted for publication by SIAM J. Sci. Comput. arXiv: 1605.08275 [math.PR].

[16] David Dereudre, Sara Mazzonetto, and Sylvie Rœlly. "An explicit representation of the transition densities of the skew Brownian motion with drift and two semipermeable barriers". In: *Monte Carlo Methods Appl.* 22.1 (2016), pp. 1–23. ISSN: 1569-3961. DOI: 10.1515/mcma-2016-0100.

[17] Luc Devroye. "The series method for random variate generation and its application to the Kolmogorov-Smirnov distribution". In: *American Journal of Mathematical and Management Sciences* 1.4 (1981), pp. 359–379.

[18] Pierre Étoré. "Approximation of one-dimensional diffusion processes with discontinuous coefficients and applications to simulation". PhD thesis. IECN, University of Nancy, France, 2006.

[19] Pierre Étoré and Miguel Martinez. "Exact simulation of one-dimensional stochastic differential equations involving the local time at zero of the unknown process". In: *Monte Carlo Methods Appl.* 19.1 (2013), pp. 41–71. ISSN: 0929-9629. DOI: 10.1515/mcma-2013-0002.

[20] Pierre Étoré and Miguel Martinez. "Exact simulation for solutions of one-dimensional stochastic differential equations with discontinuous drift". In: *ESAIM Probab. Stat.* 18 (2014), pp. 686–702. ISSN: 1292-8100. DOI: 10.1051/ps/2013053.

[21] E. Robert Fernholz, Tomoyuki Ichiba, and Ioannis Karatzas. "Two Brownian particles with rank-based characteristics and skew-elastic collisions". In: *Stochastic Processes and their Applications* 123.8 (2013), pp. 2999–3026.

[22] Masatoshi Fukushima, Yoichi Oshima, and Masayoshi Takeda. *Dirichlet Forms and Symmetric Markov Processes*. De Gruyter Studies in Mathematics. De Gruyter, 2010. ISBN: 9783110218091.

[23] Alexander Gairat and Vadim Shcherbakov. "Density of Skew Brownian motion and its functionals with application in finance". In: *Mathematical Finance* (2016).

[24] Bernard Gaveau, Masami Okada, and Tatsuya Okada. "Second order differential operators and Dirichlet integrals with singular coefficients. I. Functional calculus of one-dimensional operators". In: *Tohoku Math. J. (2)* 39.4 (1987), pp. 465–504. ISSN: 0040-8735.

[25] J.-Michael Harrison and Larry-A. Shepp. "On skew Brownian motion". In: *Ann. Probab.* 9.2 (1981), pp. 309–313. ISSN: 0091-1798.

[26] Martin Hutzenthaler and Arnulf Jentzen. "Numerical approximations of stochastic differential equations with non-globally Lipschitz continuous coefficients". In: *Mem. Amer. Math. Soc.* 236.1112 (2015), pp. v+99. ISSN: 0065-9266. DOI: 10.1090/memo/1112.

[27] Kiyoshi Itō and Henry-P. McKean. *Diffusion Processes and Their Sample Paths*. Grundlehren der mathematischen wissenschaften in einzeldarstellungen, bd. 125. Academic Press, 1965.

[28] Olav Kallenberg. *Foundations of Modern Probability*. Applied probability. Springer, 2002. ISBN: 9780387953137.

[29] Ioannis Karatzas and Steven E. Shreve. "Trivariate density of Brownian motion, its local and occupation times, with application to stochastic control". In: *The Annals of Probability* (1984), pp. 819–828.

[30] Alexei M. Kulik. "On the solution of a one-dimensional stochastic differential equation with singular drift coefficient". In: *Ukrainian Mathematical Journal* 56.5 (2004), pp. 774–789.

[31] Jean-François Le Gall. "Applications du temps local aux équations différentielles stochastiques unidimensionnelles". In: *Seminar on probability, XVII*. Vol. 986. Lecture Notes in Math. Springer, Berlin, 1983, pp. 15–31. DOI: 10.1007/BFb0068296.

[32] Jean-François Le Gall. "One-dimensional stochastic differential equations involving the local times of the unknown process". In: *Stochastic analysis and applications (Swansea, 1983)*. Vol. 1095. Lecture Notes in Math. Springer, Berlin, 1984, pp. 51–82. DOI: 10.1007/BFb0099122.

[33] Antoine Lejay. "On the constructions of the skew Brownian motion". In: *Probab. Surv.* 3 (2006), pp. 413–466. ISSN: 1549-5787. DOI: 10.1214/154957807000000013.

[34] Antoine Lejay. "Simulation of a stochastic process in a discontinuous layered medium". In: *Electron. Commun. Probab.* 16 (2011), pp. 764–774. ISSN: 1083-589X. DOI: 10.1214/ECP.v16-1686.

[35] Antoine Lejay, Lionel Lenôtre, and Géraldine Pichot. *One-dimensional skew diffusions: explicit expressions of densities and resolvent kernel*. 2015. URL: https://hal.inria.fr/hal-01194187.

[36] Antoine Lejay and Miguel Martinez. "A scheme for simulating one-dimensional diffusion processes with discontinuous coefficients". In: *Ann. Appl. Probab.* 16.1 (2006), pp. 107–139. ISSN: 1050-5164. DOI: 10.1214/105051605000000656.

[37] Antoine Lejay and Géraldine Pichot. "Simulating diffusion processes in discontinuous media: a numerical scheme with constant time steps". In: *Journal of computational physics* 231.21 (2012), pp. 7299–7314. DOI: 10.1016/j.jcp.2012.07.011.

[38] Antoine Lejay and Géraldine Pichot. "Simulating diffusion processes in discontinuous media: benchmark tests". In: *Journal of Computational Physics* 314 (2016), pp. 384–413.

[39] Lionel Lenôtre. "Étude et simulation des processus de diffusion biaisés". PhD thesis. Universit'e de Rennes 1, 2015.

[40] Lionel Lenôtre. *Two numerical schemes for the simulation of skew diffusions using their resolvent kernel*. 2015. URL: https://hal.inria.fr/hal-01206968v2.

[41] Vadim Linetsky. "On the transition densities for reflected diffusions". In: *Advances in Applied Probability* (2005), pp. 435–460.

[42] Gunter Lumer and Ralph S. Phillips. "Dissipative operators in a Banach space". In: *Pacific Journal of Mathematics* 11.2 (1961), pp. 679–698.

[43] Paul-André Meyer. "Un cours sur les intégrales stochastiques (exposés 1 à 6)". In: *Séminaire de probabilités de Strasbourg* 10 (1976), pp. 245–400.

[44] John Nash. "Continuity of solutions of parabolic and elliptic equations". In: *American Journal of Mathematics* 80.4 (1958), pp. 931–954.

[45] John von Neumann. "Various techniques used in connection with random digits. Monte Carlo methods". In: *Nat. Bureau Standards.* 12 (1951), pp. 36–38.

[46] Youssef Ouknine. "Le "Skew-Brownian motion" et les processus qui en dérivent". In: *Teor. Veroyatnost. i Primenen.* 35.1 (1990), pp. 173–179. ISSN: 0040-361X. DOI: 10.1137/1135018.

[47] Youssef Ouknine, Francesco Russo, and Gerald Trutnau. "On countably skewed Brownian motion with accumulation point". In: *Electron. J. Probab.* 20.82 (2015), pp. 1–27. ISSN: 1083-6489. DOI: 10.1214/EJP.v20-3640.

[48] Omiros Papaspiliopoulos, Gareth O. Roberts, and Kasya B. Taylor. *Exact sampling of diffusions with a discontinuity in the drift*. to appear in Festschrift for N. H. Bingham. 2016. eprint: 1511.04112.

[49] Mikola-I. Portenko. "Diffusion processes with a generalized drift coefficient". In: *Teor. Veroyatnost. i Primenen.* 24.1 (1979), pp. 62–77. ISSN: 0040-361X.

[50] Mykola-I. Portenko. *Generalized diffusion processes*. Vol. 83. Translations of Mathematical Monographs. Translated from the Russian by H. H. McFaden. American Mathematical Society, Providence, RI, 1990, pp. x+180. ISBN: 0-8218-4538-1.

[51] Jorge-M. Ramirez. "Multi-skewed Brownian motion and diffusion in layered media". In: *Proc. Amer. Math. Soc.* 139.10 (2011), pp. 3739–3752. ISSN: 0002-9939. DOI: 10.1090/S0002-9939-2011-10766-4.

[52] Jorge-M. Ramirez, Enrique-A. Thomann, Edward-C. Waymire, Juliette Chastanet, and Brian-D. Wood. "A note on the theoretical foundations of particle tracking methods in heterogeneous porous media". In: *Water Resources Research* 44.1 (2008). W01501. ISSN: 1944-7973. DOI: 10.1029/2007WR005914.

[53] Michael Renardy and Robert C. Rogers. *An Introduction to Partial Differential Equations*. Texts in Applied Mathematics. Springer New York, 2006. ISBN: 9780387216874.

[54] Sheldon-M. Ross. *Simulation*. Academic Press, 2013. ISBN: 9780124158252.

[55] Damiano Rossello. "Arbitrage in skew Brownian motion models". In: *Insurance: Mathematics and Economics* 50.1 (2012), pp. 50–56. DOI: 10.1016/j.insmatheco.2011.10.004.

[56] Shiyu Song, Suxin Wang, and Yongjin Wang. "On some properties of reflected skew Brownian motions and applications to dispersion in heterogeneous media". In: *Physica A: Statistical Mechanics and its Applications* 456 (2016), pp. 90–105.

[57] Daniel W. Stroock. "Diffusion semigroups corresponding to uniformly elliptic divergence form operators". In: *Séminaire de Probabilités XXII*. Ed. by Jacques Azéma, Marc Yor, and Paul André Meyer. Berlin, Heidelberg: Springer Berlin Heidelberg, 1988, pp. 316–347. ISBN: 978-3-540-39228-6. DOI: 10.1007/BFb0084145.

[58] Daniel W. Stroock and S.-R.-Srinivasa Varadhan. *Multidimensional Diffussion Processes*. Grundlehren der mathematischen Wissenschaften in Einzeldarstellungen mit besonderer Berücksichtigung der Anwendungsgebiete. Springer, 1979. ISBN: 9783540903536.

[59] Lars E.O. Svensson. "The term structure of interest rate differentials in a target zone: Theory and Swedish data". In: *Journal of Monetary Economics* 28.1 (1991), pp. 87–116.

[60] Satoshi Takanobu. "On the uniqueness of solutions of stochastic differential equations with singular drifts". In: *Publ. Res. Inst. Math. Sci.* 22.5 (1986), pp. 813–848. ISSN: 0034-5318. DOI: 10.2977/prims/1195177258.

[61] Satoshi Takanobu. "On the existence of solutions of stochastic differential equations with singular drifts". In: *Probab. Theory Related Fields* 74.2 (1987), pp. 295–315. ISSN: 0178-8051. DOI: 10.1007/BF00569995.

[62] Katarzyna B. Taylor. "Exact Algorithms for simulation of diffusions with discontinuous drift and robust Curvature Metropolis-adjusted Langevin algorithms". PhD thesis. University of Warwick, UK, 2015.

[63] Dirk Veestraeten. "The Conditional Probability Density Function for a Reflected Brownian Motion". In: *Computational Econ.* 24.2 (2004), pp. 185–207. ISSN: 0927-7099.

[64] John B. Walsh. "A diffusion with a discontinuous local time". In: *Astérisque* 52.53 (1978), pp. 37–45.

[65] Albert T. Wang. "Generalized Ito's formula and additive functionals of Brownian motion". In: *Zeitschrift für Wahrscheinlichkeitstheorie und Verwandte Gebiete* 41.2 (1977), pp. 153–159.

[66] Toshio Yamada and Shinzo Watanabe. "On the uniqueness of solutions of stochastic differential equations." In: *J. Math. Kyoto Univ.* 11 (1971), pp. 155–167. ISSN: 0023-608X.

[67] Kôsaku Yosida. "On Titchmarsh-Kodaira's formula concerning Weyl-Stone's eigenfunction expansion". In: *Nagoya Mathematical Journal* 1 (1950), pp. 49–58.

[68] Ludmila L. Zaitseva. "Wiener process with two partly reflecting membranes". In: *International Gnedenko conference, Kyiv, June 3-7, 2002. Abstracts - p.24* (2002).

[69] Ludmila L. Zaitseva. *On stochastic continuity of generalized diffusion processes constructed as the strong solution to an SDE*. Sept. 2006. arXiv: math/0609305 [math.PR].

[70] Ludmila L. Zaitseva. *On the Markov property of strong solutions to SDE with generalized coefficients*. Sept. 2006. arXiv: math/0609307 [math.PR].

[71] Ludmila L. Zaitseva. *On a multidimentional brownian motion with partly reflecting membrane on a hyperplane*. Oct. 2012. arXiv: 1210.8015 [math.PR].

[72] Alexander K. Zvonkin. "A transformation of the phase space of a diffusion process that removes the drift". In: *Mathematics of the USSR-Sbornik* 22.1 (1974), p. 129.